

# Image Processing and Informatics Laboratory

**2000-2002 Biennial Report**

*February 2002*



Image Processing and Informatics Laboratory  
Childrens Hospital Los Angeles/USC  
Department of Radiology, MS #81  
4650 Sunset Boulevard  
Los Angeles, California 90027  
Ph: (323)671-3899  
Fax: (323)671-3217

## SUMMARY

Dr. Marvin Nelson, Chairman of Radiology, Childrens Hospital Los Angeles/ University of Southern California recruited Dr. Huang and Dr. Fei from UCSF to join the department in early 2000. Together they developed the Image Processing and Informatics Laboratory (IPI). During the process, former colleagues including Gilsanz, Pietka, Sayre, Zhang, Liu, Erberich, and Brookes joined the IPI staff. New recruits during the past two years also include Mogel, Law, M. Zhang, and Dey.

Image informatics has been the focus of research and development at IPI during the past two years. Some major accomplishments are:

- PACS Fault-Tolerant Server
- PACS Simulator
- The Next Generation Internet
- PACS and Image-Based CAD
- Image Data Integrity
- PACS-Based Radiation therapy Server Concept
- PACS-Based Neurosurgical Command Module Concept

This report summarizes the current status in the development of these research areas. It contains preprints to appear in the *Proceedings of the International Society for Optical Engineering, and SPIE Medical Imaging 2002*, San Diego, California, February 23-28. It also contains selected reprints from other journals and proceedings that appeared during the past two years, as well as the abstracts and presentations from the RSNA, November 24-30, 2001.

Our research is supported by:

- US Army Medical R&D contract DAMD17-99-P-3732
- NIH 8 R01-EB 00298-06
- NLM Grant 1T15LM07356-01
- Reliance Health Care, Inc.
- Array Corporation, Japan
- MD OnLine, Inc.

## TABLE OF CONTENTS 2000-2002

SUMMARY .....	i
Table of Contents .....	ii
Title Page .....	1
Image Processing and Informatics Laboratory (IPI) Staff .....	2
IPI CHLA/USC Facility, Network Architecture and Posters .....	3
 <b>PREPRINTS FROM SPIE</b>	
1. <b>S. G. Erberich, K. Willmes, A. Thron, W. Oberschelp, H. K. Huang</b> Knowledge-based Approach for Functional MRI Analysis by SOM Neural Network Using Prior Labels from the Talairach Stereotaxic Space [4683-41] .....	13
2. <b>G. T. Mogel, H. K. Huang, F. Cao, Z. Zhou, P. Dey, M. Gill, B.J. Liu</b> NGI Performance for Teleradiology Application [4685-04] .....	24
3. <b>B. J. Liu, L. Document, D. A. Sarti, H. K. Huang, J. Donnelly</b> PACS Archive Upgrade and Data Migration: Clinical Experiences [4685-14] .....	30
4. <b>B. J. Liu, H. K. Huang, F. Cao, L. Document, D. A. Sarti</b> Fault-Tolerant Back-up Archive Using an ASP Model for Disaster Recovery [4685-15] .....	36
5. <b>Z. Zhou, H. K. Huang, B. J. Liu, F. Cao, J. Zhang, G. T. Mogel, J. Zhuang, X. Zhang</b> PACS Simulator: A Standalone Educational Tool [4685-21] .....	43
6. <b>M. Y. Law, X. Zhang, J. Zhang, H. K. Huang</b> PACS and Imaging Informatics-based Radiation Therapy (RT) Server [4685-25] .....	52
7. <b>F. Cao, B. J. Liu, Z. Zhou, H. K. Huang, J. Zhang, X. Zhang, G. T. Mogel</b> Fault-tolerant PACS Server [4685-44] .....	60
8. <b>J. Zhang, R. Han, D. Wu, X. Zhang, J. Zhuang, F. Jie, M. Wang, G. Zhang, C. Wang</b> Managed PACS Operation with an Automatic Monitoring Tool [4685-45] .....	70
9. <b>J. Zhang, R. Han, D. Wu, X. Zhang, J. Zhuang, H. K. Huang</b> Automatic Monitoring System for PACS Management and Operation [4685-49] .....	77
10. <b>J. Zhuang, D. Wu, W. Xie, J. Zhang,</b> <b>R. Moats, M. D. Nelson, F. Cao, Z. Zhou, H. K. Huang</b> Integrating a DICOM Acquisition and Distribution Gateway for Micro-CT Imaging in a PACS Environment [4685-51] .....	85

## SELECTED REPRINTS

1. **Stahl JN, Zhang J, Zeller C, Pomerantsev EV, Lou SL, Chou TM, Huang HK.** 2000. Teleconferencing with Dynamic Medical Images. *IEEE Trans Inform Tech Biom V.* 4, No.1, 88-96. ....87
2. **Zhang J, Stahl JN, Huang HK, Zhou X, Lou, SL, Song KS.** 2000. Real-time Teleconsultation with High-Resolution and Large-Volume Medical Images for Collaborative Healthcare. *IEEE Trans Inform Tech Biom V.*4, No.1, 178-185. ....96
3. **Yu F, Hwang K, Gill M, Huang HK.** 2000. Some Connectivity and Security Issues of NGI in Medical Imaging Applications. *J High Speed Networks.* 9, 3-13.....104
4. **Cao X, Huang HK.** 2000. Current Status and Future Advances of Digital Radiography and PACS. *IEEE Eng Med & Bio.* Vol 19, No.5, 80-88. ....115
5. **Stahl JN, Zhang J, Chou TM, Zellner C, Pomerantsev EV, Huang HK.** 2000. A New Approach to Tele-conferencing with Intravascular Ultrasound and Cardiac Angiography in a Low-Bandwidth Environment. *RadioGraphics.* 20:1495-1503.....124
6. **Cao F, Huang HK, Pietka E, Gilsanz V.** 2000. Digital Hand Atlas and Web-based Bone Age Assessment: System Design and Implementation. *J Comp Med Imag & Graphics.* Vol 24, 297-307. ....133
7. **Huang HK, Cao F, Zhang JG, Liu BJ, Tsai ML.** 2000. Fault tolerant Picture Archiving and Communication System and Teleradiology Design. In Reiner B, Siegel EL, Dwyer SJ: *Security Issues in the Digital Medical Enterprise, SCAR, Chapter 8, 57-64.* ....144
8. **Johannes N. Stahl JN, Tellis W, Huang HK.** 2000. Network Latency and Operator Performance in Teleradiology Applications. *J Digital Imag.* V. 13, No. 3, 119-123.....152
9. **Wang J, Huang HK.** 2000. Three-dimensional Image Compression with Wavelet Transform. In *Handbook of Medical Imaging*, Editor-in-chief, IN Bankman, Section Editors RM Rangayyan, RP Woods, RA Robb, HK Huang, Academic Press. Chapter 52, 851-862.157
10. **Pietka E, Gertych A, Pospeich S, Cao F, Huang, HK, Gilsanz V.** 2001. Computer Assisted Bone Age Assessment: Image Preprocessing and Epiphyseal/Metaphyseal ROI Extraction. *IEEE Trans. Medical Imaging*, Aug Vol 20, No 8, 715-729. ....169
11. **Zhou X, Huang HK.** 2001. Authenticity and Integrity of Digital Mammography Image. *IEEE Trans. Medical Imaging*, Vol 20, No. 8, 784-791.....184
12. **Huang HK.** 2001. Radiography and Information Technology (IT). (Invited) *Hong Kong Radiographers J.* Vol 5, 18-20. ....192
13. **Huang HK.** 2001. Book Review. Handbook of Medical Imaging. Vol 1-3. *Physics Today*, Sept. 2001, 57. ....195
14. **Huang HK.** 2001. PACS, Informatics, and the Neurosurgery Command Module. *J. Mini Invasive Spinal Technique.* Vol 1, 62-67. ....196
15. **Law YY, Huang HK.** 2001. Serving up Integrated Therapy. *Advance for Imaging and Oncology Administrator.* November 2001, Vol.11, No.11. 46-53. ....202
16. **Huang HK.** 2000. Advances in Radiological Informatics.*J. Hong Kong College Radiologist.* Vol. 3, 9-16 Supplement 2000 .....206

**RSNA 2001 ABSTRACTS AND PRESENTATIONS (Radiology Vol. 221P 2001) .....214**

**IMAGE PROCESSING AND INFORMATICS LABORATORY**

**Childrens Hospital Los Angeles/University Of Southern California**

**2000-2002 Biennial Report**

## IMAGE PROCESSING AND INFORMATICS (IPI) LABORATORY STAFF

### *Faculty and Administration*

---

**H.K. Huang, D.Sc., FRCR(Hon.)**  
Professor and Director, IPI

**Marvin Nelson, M.D., M.B.A.**  
Professor and Chairman, Dept of Radiology  
CHLA

**Fei Cao, Ph.D.**  
Assistant Professor

**Vincente Gilsanz, M.D.**  
Professor

**Greg T. Mogel, M.D.**  
Assistant Professor

**Stephan G. Erberich, Ph.D.**  
Assistant Professor

**Rex Moats, Ph.D.**  
Assistant Professor

**Loretta Brookes**  
Administrative Officer

**Ewa Pietka, Ph.D.**  
Professor  
University of Silesia, Poland  
Consultant

**Jianguo Zhang, Ph.D.**  
Professor, Shanghai Institute of Technical  
Physics, The Chinese Academy of Science  
Consultant

**Brent Liu, Ph.D.**  
PACS System Administrator  
St. John's Hospital, LA  
Consultant

**Maria YY Law, MPhil, BRS,**  
TeachDip(Ed), Assistant Professor  
The Hong Kong Polytechnic University  
Consultant

**James Sayre, Ph.D.**  
Professor of Biostatistics and Radiological Science  
UCLA  
Consultant

### *Graduate Students*

---

**Michael Zhou, M.S.**  
Ph.D. Student

**Partha Sarathi Dey, B.S.**  
Master Student

### *IPA Fellow*

---

**Richard Satava, M.D.**  
TATRC, Army Medical Research and  
Materiel Command

# **IPI CHLA/USC Facility, Network Architecture and Posters**

## **List of Figures**

1. IPI laboratory Layout.....	4
2. IPI office Layout.....	5
3. IPI Network Switch and Archive Server Racks.....	6
4. IPI NGI Network.....	7
5. IPI/CHLA Imaging Research Network.....	7
6. PACS Simulator: A Training Tool .....	8
7. Fault-Tolerant Archive Server .....	9
8. Hand Image Processing and Bone Age Assessment.....	10
9. Web-based CAD Application Server for Digital Hand Atlas.....	11
10. ASP back-up server.....	12

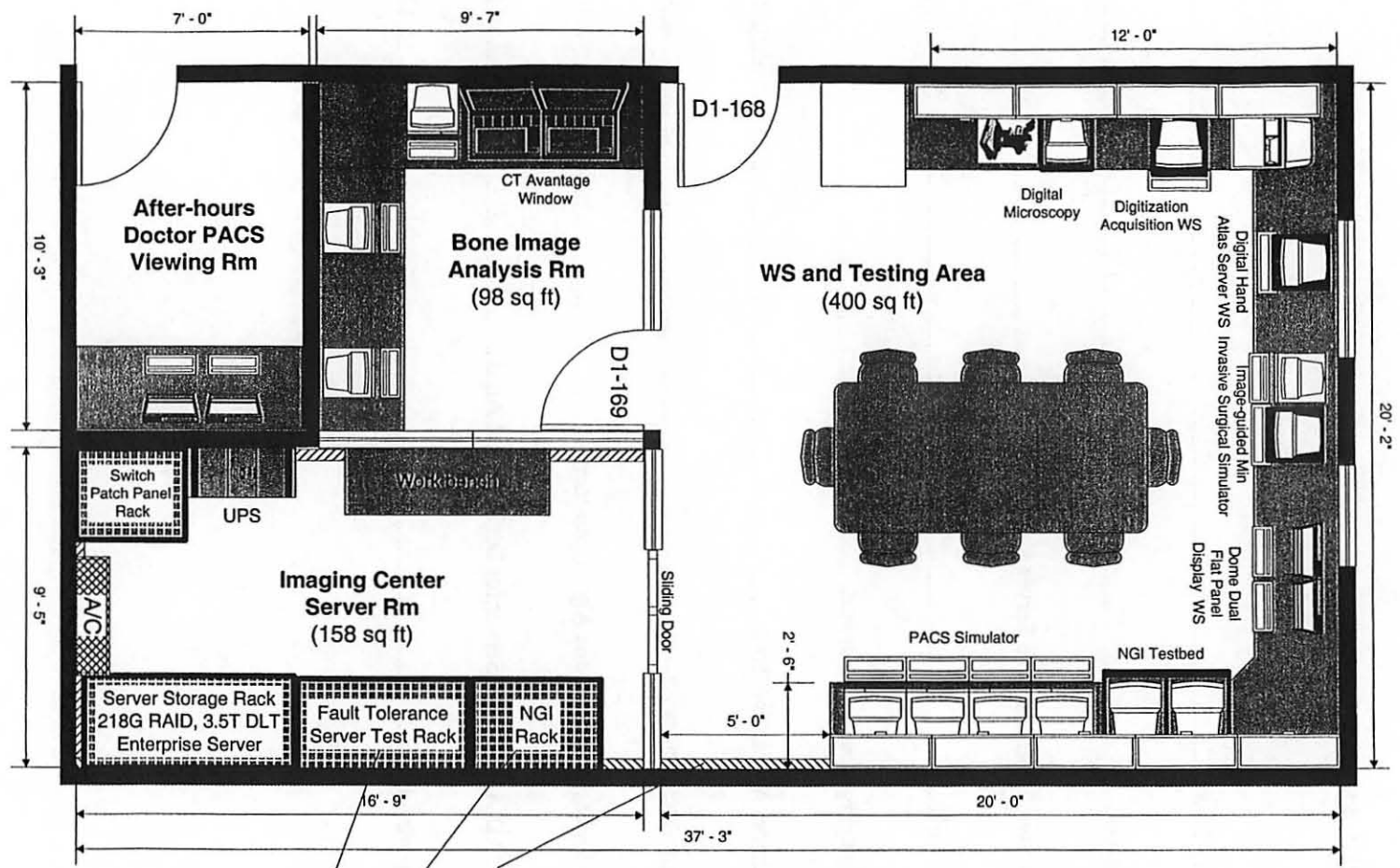
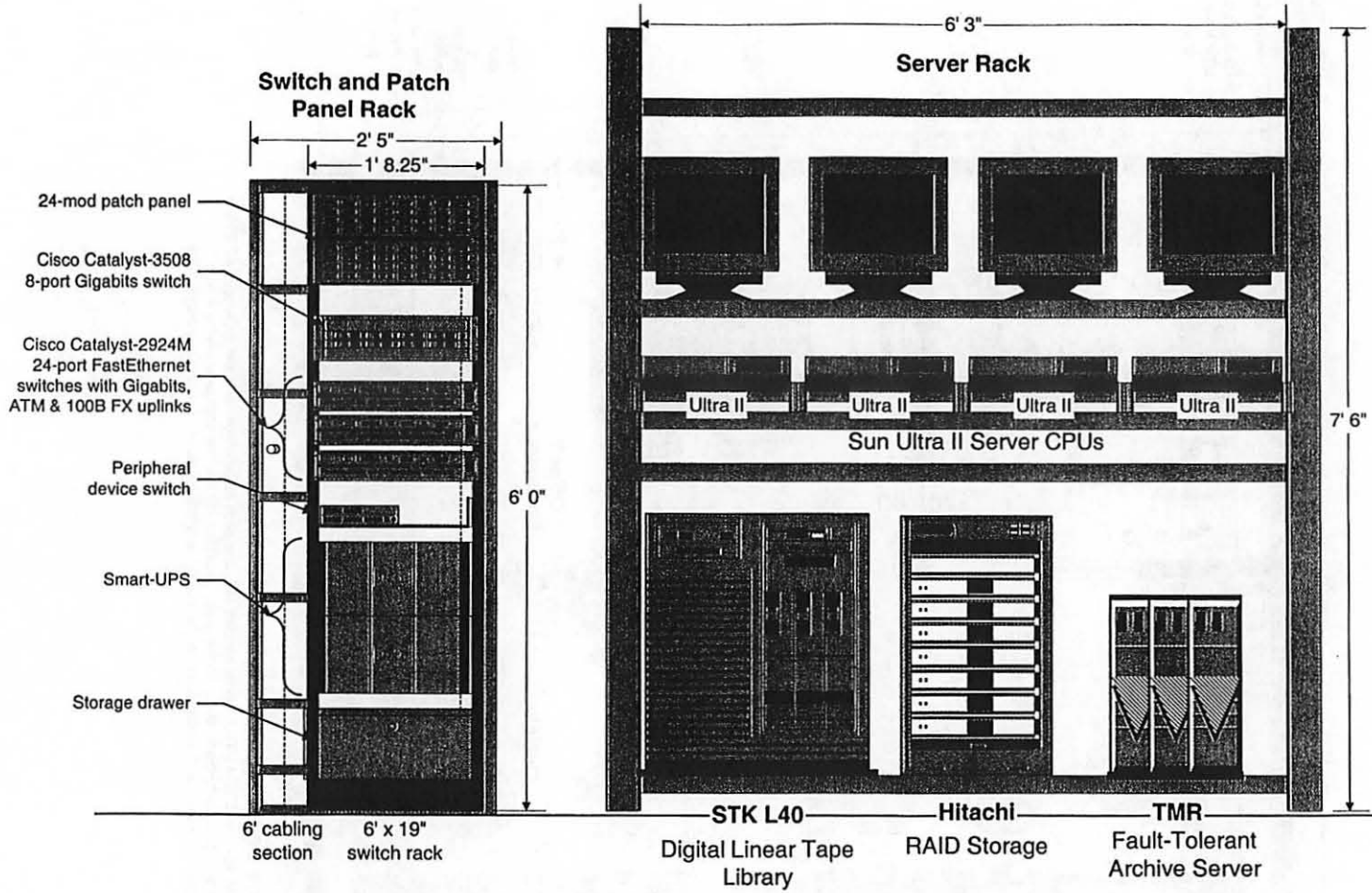


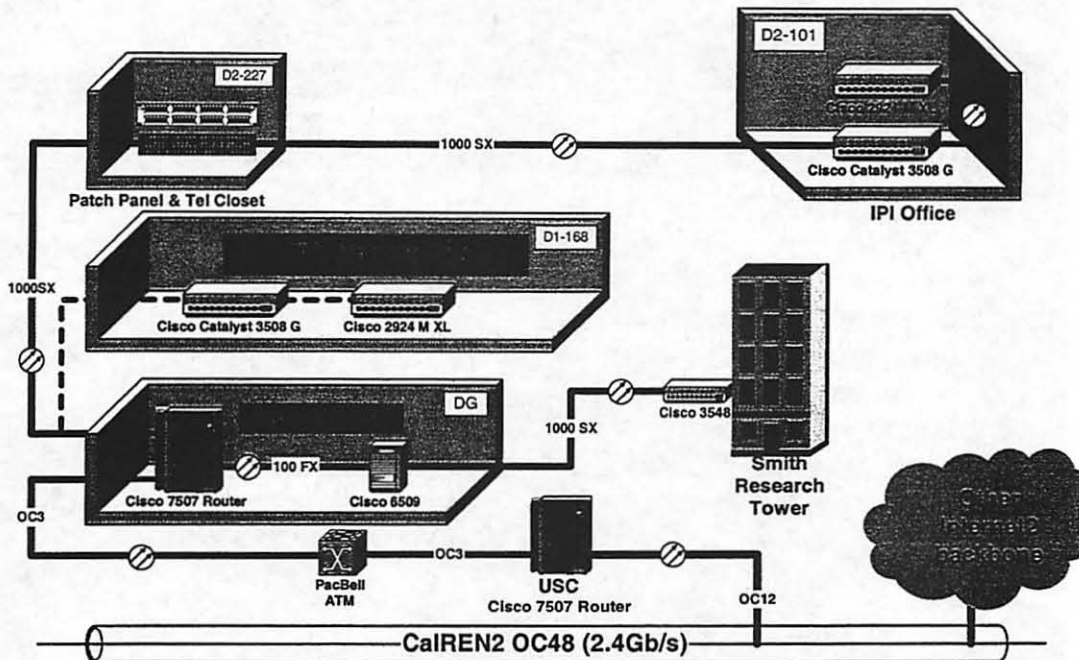
### Image Processing and Informatics (IPI) Lab

- FT Machine, PACS controller and 3 servers, Fuji PACS Gateway
- Network, Security Equipment
- Under-Table Cable Tray 4'Dx6'H

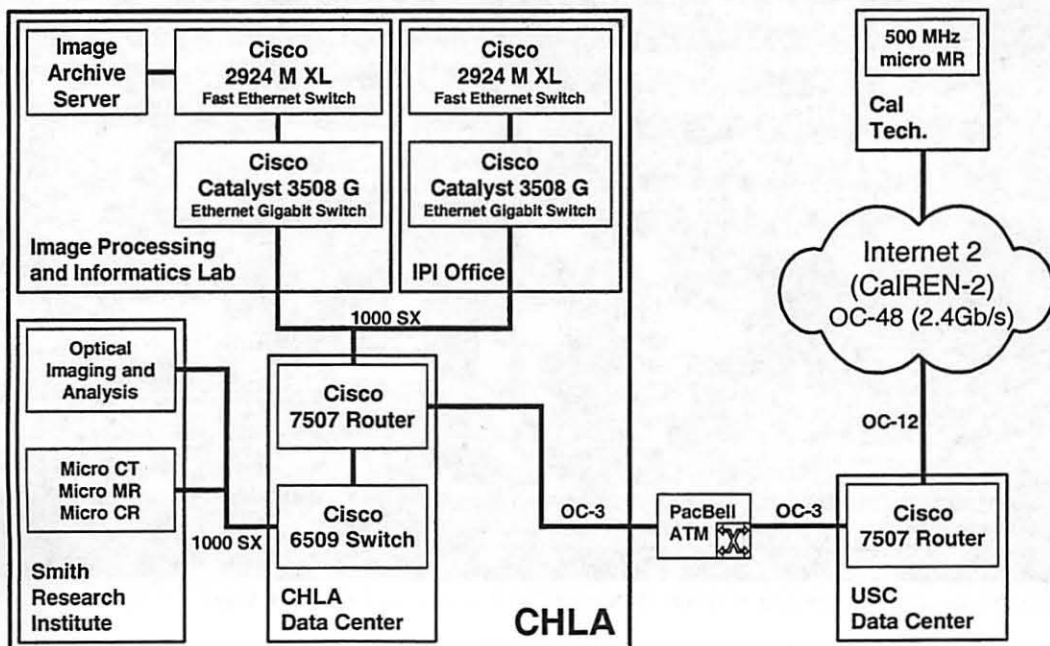




## A Second Internet 2 Testbed

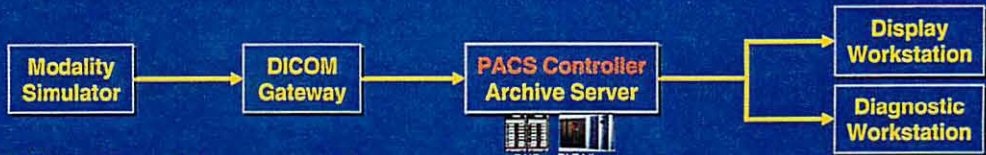


## CHLA Imaging Research Network Design



# PACS Simulator

Department of Radiology, Childrens Hospital Los Angeles/USC



## PACS Simulator Components:

- Modality Simulator and RIS Simulator
- Acquisition Gateway
- PACS Controller - Archive Server
- Display and Diagnostic workstations
- Networking
- Automatic system monitoring software



## PACS

- Is not a single modality
- Is not an examination
- Is not only to display images
- **It is a system integration & workflow**

**Need a New Training Tool for Learning PACS**

# A Training Tool to Learn

- Functions of each component
- Connectivity between components
- Dataflow between components
- Dataflow of the complete PACS
- Identify system bottle necks
- Error detection and correction
- System monitoring

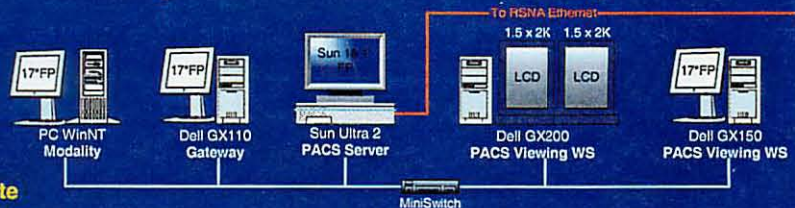
## Modality Simulator

contains a collection of multi-modality images. A software program takes these images in random and feeds to the Acquisition Gateway, simulating continuous image data input in clinical environment.

**Also Acting As a Remote Archive Server for InfoRAD #9114, #9617 and #9504**

**To Participate in a one day hand-on training, please write**

Dr. H.K. Huang, Professor and Director of Informatics, Childrens Hospital of Los Angeles/University of Southern California, Department of Radiology, Mailstop #81, 4650 Sunset Boulevard, Los Angeles, California 90027.  
Tel: (323) 671-3847 ; Fax: (323) 671-1588; E-mail: HKHuang@aol.com



# Fault-Tolerant PACS Server

*Department of Radiology, Childrens Hospital Los Angeles/USC*

**Fault-tolerant PACS server provides a CA (continuous available, 99.999%) hardware uptime in PACS operation.**

## IN THIS DEMONSTRATION:

### We will Review

Clinical PACS Workflow

- Archiving
- Querying/Retrieving

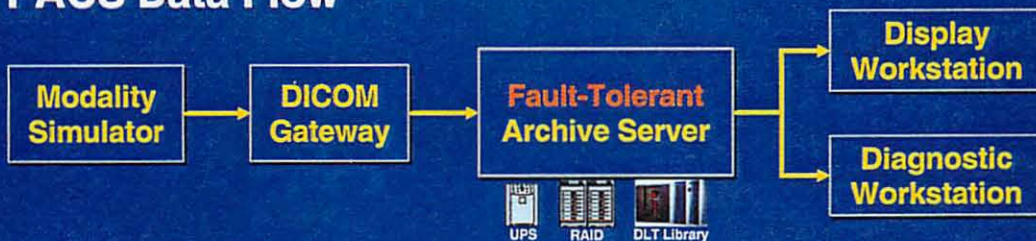
### We will Demonstrate

Fault-Tolerant Scenarios

- Ethernet Failure
- CPU Module Failure
- Disk Failure

For further information: **H.K. Huang, D.Sc., Prof.**; Tel: (323) 671-3847 ; Fax: (323) 671-1588; E-mail: HKHuang@aol.com

## PACS Data Flow



## Fault-Tolerant Design

### Triple Modular Redundant Hardware

CPU, memory, controller, power supply

### Continuous Availability I/O

Ethernet, disk, RAID & DLT with failover

	Synchronous	Bridging	Asynchronous
<b>C</b>	CPU and Memory	Bridge	I/O Devices
<b>B</b>	CPU and Memory	Bridge	I/O Devices
<b>A</b>	CPU and Memory	Bridge	I/O Devices

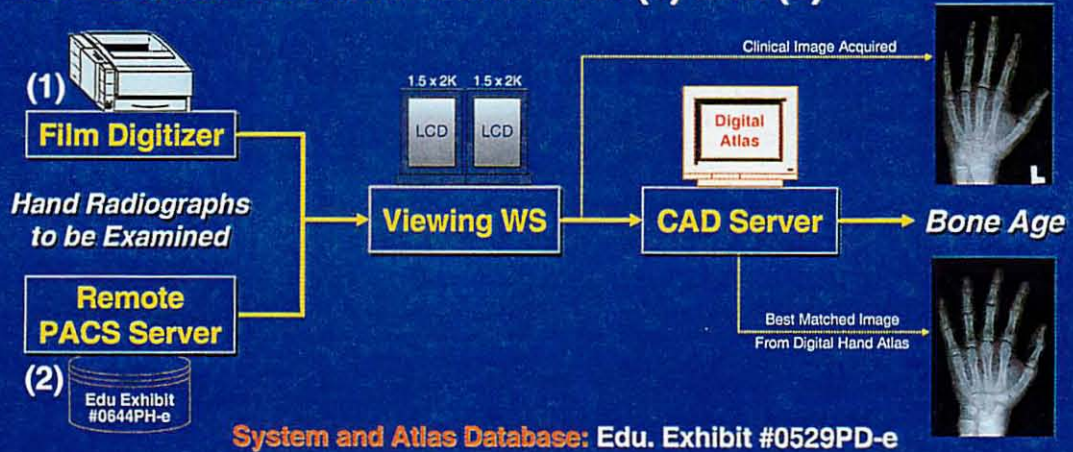
**Fault-Tolerant PACS Server runs uninterrupted with no downtime or data loss should any hardware component fail.**

# Computer-aided Assessment of Skeletal Maturity Using Digital Hand Atlas

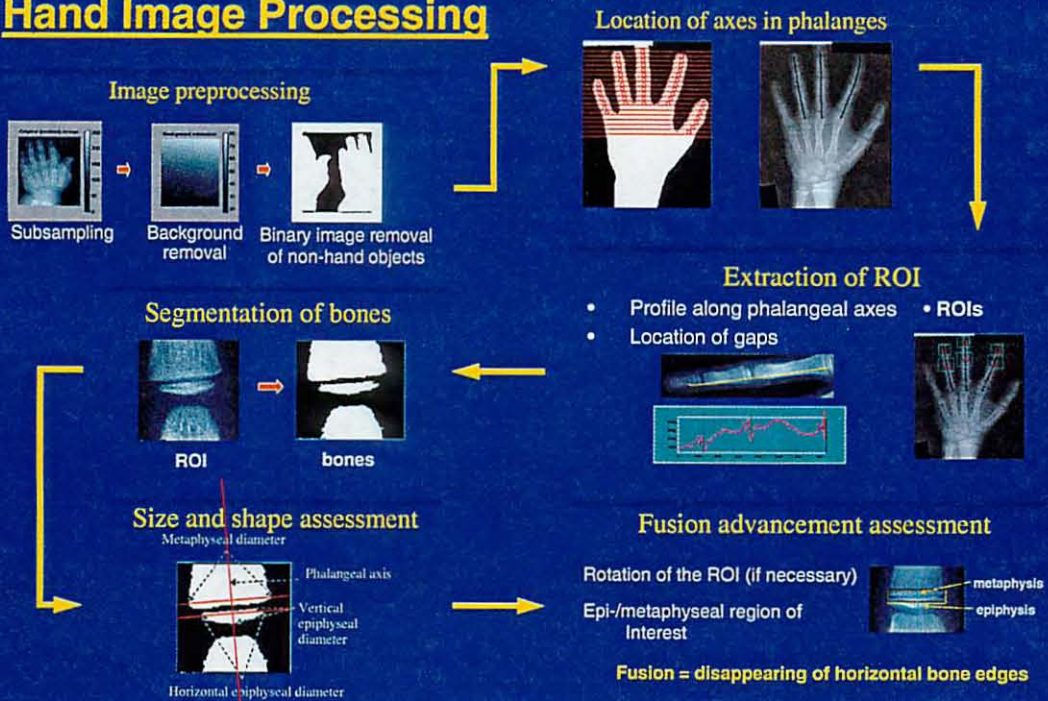
E. Pietka PhD, A. Gertych MS, S. Pospiech MS  
Div. of Medical Electronics, Silesian Univ. of Tech.

P. S. Dey MS, F. Cao PhD, H. K. Huang DSc, V. Gilsanz MD  
Dept of Radiology, Childrens Hospital Los Angeles/USC

## Live Demonstration Workflows: (1) and (2)



## Hand Image Processing



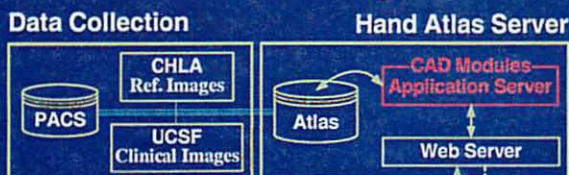
# Digital Hand Atlas for Web-based Bone Age Assessment

F. Cao PhD, H. K. Huang DSc, P. S. Dey MS, V. Gilsanz MD,  
Department of Radiology, Childrens Hospital Los Angeles/USC

E. Pietka PhD, A. Gertych MS, S. Pospiech MS  
Div. of Medical Electronics, Silesian Univ. of Tech.

The bone age assessment method currently used in radiological diagnosis is based on atlas matching with a small reference set of old Greulich-Pyle atlas<sup>[1]</sup>, which was developed in 1950s and is not fully applicable for children of today. We have developed a new digital hand atlas with a large set of clinically normal hand images of diverse ethnic groups and also implemented a CAD system for Web-based bone age assessment.

## System Architecture



- CAD: Computer-aided Diagnosis
- PACS: Picture Archive and Communication System
- Atlas: Hand Atlas Database
- CHLA: Childrens Hospital LA
- UCSF: University of California at San Francisco

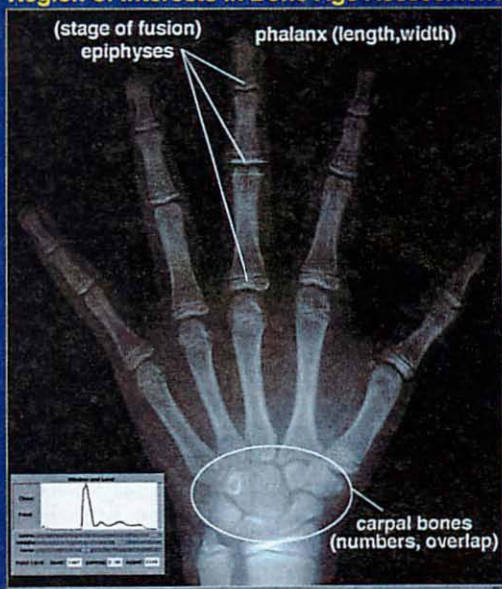
### Data Collection

- 1,120 Reference images collected at CHLA from new born to 18 years old evenly distributed among race, age & sex.  
Race: European, African, Hispanic and Asian descent.
- 800 Clinical Images collected at UCSF for comparison study.

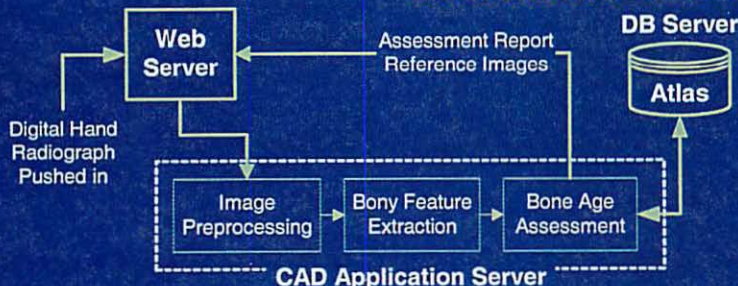
### Hand Atlas CAD Server<sup>[2]</sup>

- Oracle DB Server for accessing atlas image database.
- Web Server serving a client's request through Web.
- Application Server as an integrated platform for CAD software and its interfaces to Web and the atlas database.

### Region of Interests in Bone Age Assessment



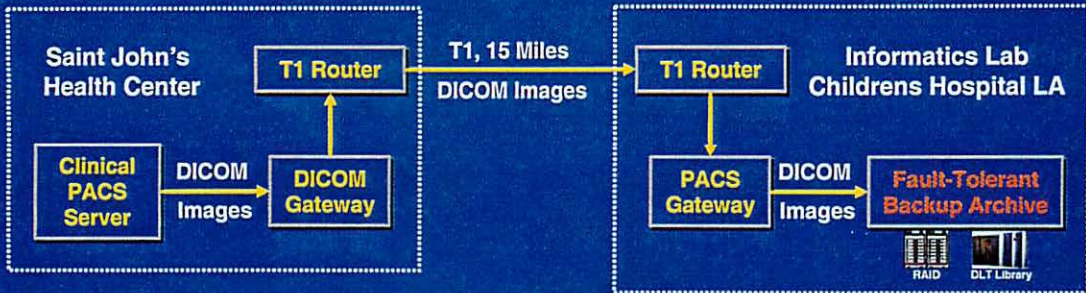
## Web-based Assessment



A work-up sequence for a Web-based bone age assessment and the role that the CAD server plays between the Web server and the digital hand atlas database. A patient hand image to be examined will be pushed in via the Web server. The image is passed on to the CAD server for preprocessing and feature extraction. The radiological findings associated with the extracted bony features are then compared with corresponding values from the hand atlas database and therefore to determine the patient's bone age. An assessment report along with relevant hand images is then sent back to the client's browser through the Web server.

# Backup ASP PACS Archive

Dept of Radiology, Saint John's Health Center & Childrens Hospital LA/USC



## Components:

- Clinical PACS Server
- Gateway Workstations
- T1 Routers
- Fault-Tolerant Backup Archive
- Networking

**ASP: Application Service Provider**

**Backup ASP PACS Archive** can provide storage of crucial clinical PACS data at a secondary site and recover this PACS data in the event of a disaster directly into the clinical PACS. In this display, you will see an example of the ASP model along with the recovery procedure.

## PACS Archive Disaster & Recovery

**CHALLENGE:** What Happens if Online SJHC PACS Data is Lost During a Disaster?

• Surrounding Issues At SJHC:

- 1) Future Regulations May Require PACS Data Backup. No More Films Will be Stored.
- 2) Disaster Recovery Solutions are Scarce In the PACS Environment.
- 3) New Archive Upgrade Allows for Disaster Recovery BUT Solution is not Turnkey to Match PACS Workflow.

**CONCLUSION:** A Disaster Recovery Solution is Necessary for SJHC!

### Tape Archiving & Retrieval Management of New Archive

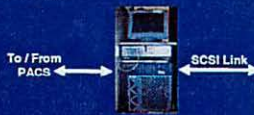
SERVER/JUKEBOX PACS DATA MGMT

- Relates PACS Exam to the Tape to be Retrieved
- Manages Backup Tape Copies (3 Copies Made)
- Updates Server Database When Tapes Are Loaded/Unloaded.

Tape Jukebox: 384 Slots For Tapes (7.9 TB)



- Server System Data (3 Tapes)
- Server DB Backup (8 Tapes)
- Copy1 Image Data (365 Tapes max)
- Copy2 & Copy3 Image Data (4 Each - 8 Tot)



•Three Tape Drives Available for Multiple Reading/Writing.

•One Drive has First Priority for Study Retrievals to Accomodate for Faster Responses to Queries.

•One Tape Can Hold 5 Days Worth of PACS Exams Currently and Will DOUBLE When Tape Density Doubles in the Near Future. If Copy2 Backup Tape is Still in Tape Jukebox At Time of Disaster...

**POSSIBLY UP TO 10 DAYS OF DATA COULD BE LOST!**

## SJHC PACS Archive Disaster Recovery Procedure



- 1) PACS Exam Arrives and Three Copies Written to Three Separate Tapes. Copy1 is Primary Copy and Always Resides In Tape Jukebox.
- 2) At 10 AM Every Day, Copy2 Tape is Checked.
  - 2a) If Copy2 Tape is 95% Full, it is Ejected (Occurs Approx Every 5 Days) and Sent Offsite.
  - 2b) A New Copy2 Tape is Loaded Into Jukebox From Copy2 Tape Pool.
- 3) Copy3 Tape(s) Replaced Daily: Coverage for Period When Copy2 Tape Reaches 95% Full.
  - 3a) Copy3 Tapes Ejected 10AM Every Day and Sent Offsite. If Copy2 Tapes 95% Full, Copy3 Tapes of That Specific Day are Returned to Copy3 Tape Pool for Re-Use.
  - 3b) Two New Copy3 Tapes Loaded Into Jukebox From Copy3 Tape Pool.
- 4) Data Vault Storage Service Picks Up Tapes to Transfer to Secure Location. Copy2 Tapes Stored Permanently for Disaster Recovery. Copy3 Tapes Stored Temporarily.
- 5) When a Copy2 Tape Arrives at Data Vault Storage Facility, All Copy3 Tapes Stored are Returned to SJHC and Returned to the Copy3 Tape Pool.
- 6) When a Copy3 Tape is 95% Full, Copy3 Tape Contents are Erased and Ready for Re-Use.

RSNA2001, InfoRAD 9617, Back-up Archive Using an ASP Model for Disaster Recovery, B.J. Liu, H.K. Huang, F. Cao, L. Documet, D. A. Sarti. RSNA2001, Certificate of Merit Award. Exhibit 0664PH, PACS Archive Upgrade and Data Migration. B. J. Liu, L. Documet, D. A. Sarti, H.K. Huang, J. Donnell

# Knowledge-Based Approach for functional MRI Analysis by SOM Neural Network using Prior Labels from Talairach Stereotaxic Space

Stephan G. Erberich<sup>acc</sup>, Klaus Willmes<sup>b</sup>, Armin Thron<sup>c</sup>, Walter Oberschelp<sup>d</sup>, H.K. Huang<sup>e</sup>

<sup>a</sup>Neurofunctional Imaging Laboratory, <sup>b</sup>Department of Neuropsychology, <sup>c</sup>Department of Neuroradiology, <sup>d</sup>Department for Computer Science VII, University of Technology (RWTH), Aachen, Germany

<sup>d</sup>Image Processing and Informatics Laboratory, Department of Radiology, Childrens Hospital Los Angeles, University of Southern California (USC), Los Angeles, U.S.A.

## ABSTRACT

Among the methods proposed for the analysis of functional MR we have previously introduced a model-independent analysis based on the self-organizing map (SOM) neural network technique. The SOM neural network can be trained to identify the temporal patterns in voxel time-series of individual functional MRI (fMRI) experiments. The separated classes consist of *activation*, *deactivation* and *baseline* patterns corresponding to the task-paradigm. While the classification capability of the SOM is not only based on the distinctness of the patterns themselves but also on their frequency of occurrence in the training set, a weighting or selection of voxels of interest should be considered prior to the training of the neural network to improve pattern learning. Weighting of interesting voxels by means of autocorrelation or F-test significance levels has been used successfully, but still a large number of *baseline* voxels is included in the training. The purpose of this approach is to avoid the inclusion of these voxels by using three different levels of segmentation and mapping from Talairach space: (1) voxel partitions at the lobe level, (2) voxel partitions at the gyrus level and (3) voxel partitions at the cell level (Brodmann areas). The results of the SOM classification based on these mapping levels in comparison to training with all brain voxels are presented in this paper.

**Keywords:** fMRI, non-linear regression, self-organizing map (SOM), time series analysis, un-supervised classification, Talairach stereotaxic space

## 1. INTRODUCTION

Functional Magnetic Resonance Imaging (fMRI) is a technique to map regional neural activity of the brain. Changes in the regional metabolism, the blood oxygen level level dependent (BOLD) effect [<sup>1</sup>] [<sup>2</sup>] and regional cerebral blood flow (rCBF) from neural activity results in an increased MR signal in a well circumscribed brain region. Using a BOLD sensitive gradient echo planar imaging (GR-EPI) MR sequence, one can measure the temporal neural state changes from the acquired brain volumes in time.

These stage changes can be induced by functional tasks performed by the subject in the magnet while images of the brain are taken, e.g. sensory-motor, word/language or visual tasks. The task paradigm defines control/resting epochs and activation epochs for the investigated function. Box-car paradigms consist of alternating periods (some ten seconds) of permanent control/rest and activation, e.g. hand-clenching or finger-tapping. More sophisticated paradigm designs use event-related stimulus presentation with a previously defined inter stimulus interval (ISI) between two events.

The acquired  $n$  3D brain volumes in time for each scan represent time series for each voxel which are compared to the temporal distribution or pattern of the performed task paradigm. After spatial preprocessing,

---

\*Correspondence: E-mail: serberich@chla.usc.edu; Phone: (323)-671-3897; Fax: (323)-671-1588

motion correction, transformation into Talairach space and spatial smoothing, the fMRI data is analyzed based on the time series of each voxel.

(1) Model-based analysis compares the distributions of control/rest and activation for each voxel time series based on the model of the paradigm. For instance the commonly used Statistical Parametric Mapping (SPM) [3] uses a general linear model (GLM) to describe the variance in each time series. The descriptor or regressor for the variance is a model of the task paradigm convolved by an empirical observed hemodynamic response function (HRF). Additional regressors for smoothing and scaling or other covariates can also be applied to refine the variance model. SPM estimates the optimal coefficients for the model by fitting the data to the model using a least-squares minimization approach. From the estimated data, t-test and F-test scores between control/rest and activation distribution for each time series are obtained and mapped onto the structural brain volume.

(2) In contrast to the model-based approaches the model-independent methods do not compare the distributions of control/rest and activation in the time series, but try to differentiate temporal patterns, periodicity and features among all voxel time series. The different patterns found by the applied discrimination process, e.g. principle and independent component analysis [4], fuzzy-cluster analysis [5] [6] or neural networks [7] are used for later interpretation.

The advantage of the model-independent methods is, that they do not rely on one static model for the whole brain which is indeed not correct [8], but can depict individual *activation* or even *deactivation* (inhibition of rCBF) patterns. Among the model-independent methods we have previously introduced the self-organizing map (SOM) neural network for box-car [7] and event-related paradigms [9].

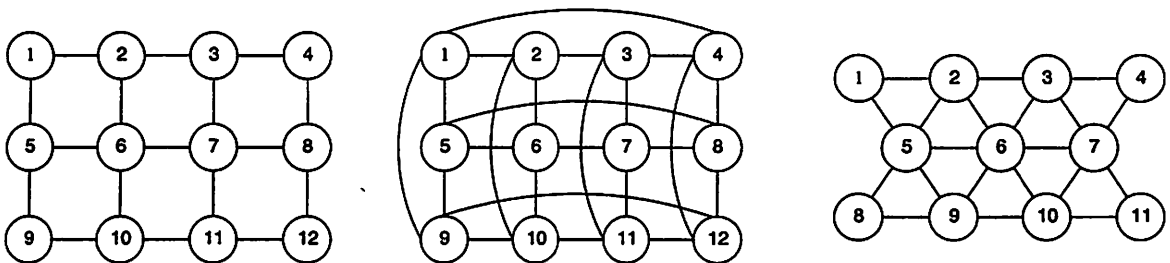


**Figure 1.** 2D SOM neural network topologies: Left: Standard rectangular grid topology. Center: Rectangular grid with toroidal extension. Right: Hexagonal grid.

The SOM is a 2D topology of interconnected artificial neurons which can be either rectangular, toroidal rectangular or toroidal rectangular (Figure 1) which we used in this study. Hyper-cube SOM (3D) also exist but have not been investigated by this study. Each of the neurons in the network carry a weight or reference vector of the same dimensionality like the voxel time series. Through successive presentation of the voxel time series to the network, called training of the network, the reference vectors of the network adapt to the time series. By updating not only one, but a region in the network around the neuron selected for adaption, clusters of similar patterns are developed over the network structure. This clustering process supports the layout of the major pattern features of the time series, e.g. *activation*, *deactivation* and *baseline*. After the training the neurons reference vectors are overlaid onto the structural MR image to inspect the mapping for each neuron along with its trained feature pattern.

As the SOM represents the major disjunct features of the time series the classification results depend on the neural networks feature memory, the capacity. A previous study using the SOM approach [7] outlined that non-brain voxels and *baseline* voxels have to be removed prior to the training, or very large networks of some hundred neurons have to be used which are too computational intensive for single processor systems. The capacity of the neural network is limited and is directly related to the number of features being stored in the network. The features stored in the network them-self represent the distributions size. During training the SOM's feature memory is fitted to the input features content. If this content has too many features for the

given capacity of the neural network, less prominent features will be removed by more prominent features and thus are lost. This is the case with fMRI data. There are only 3 major features in the time series, *activation*, *deactivation* and *baseline* patterns, but the majority of the time series are *baseline* patterns. Typically fMRI experiments activate 2-15% of the brain voxels. Therefore the *baseline* patterns dominate the SOM, leaving very little capacity for the interesting features of *activation* and *deactivation*.

One strategy to remove *baseline* is to preprocessing the time series in a way, that voxels were selected based on their periodic features similar to the task paradigm, using auto-correlation function or Fourier spectrum analysis [10]. A priori selection of non-baseline voxels by this method is a successful approach, but still a threshold based method. If the threshold is too stringent, important *activated* voxels can be lost. One can also use the periodicity measure as a weight during the training of the SOM to achieve improved patterning, without removal of voxels, but still the non-activated voxels will be stored in the network consuming 30-50% of the capacity.

In this paper we would like to introduce another method to optimize the neural network for fMRI data analysis. Instead of weighting potential activated voxel time series we select a priori a region of interest (ROI). Only voxel time series of this ROI are selected for classification by the SOM. These regions are chosen from the standard brain atlas defined by Talairach and Tournoux [11] which are known to be involved in the functional task, e.g. occipital lobe for visual experiments. Once the knowledge-based ROIs have been defined, the corresponding voxel time series are selected for training and classification by the SOM. Two task paradigms, a visual and a word/language paradigm, each with four different sized ROIs have been investigated in this study and compared to analyzing without knowledge-based ROIs.

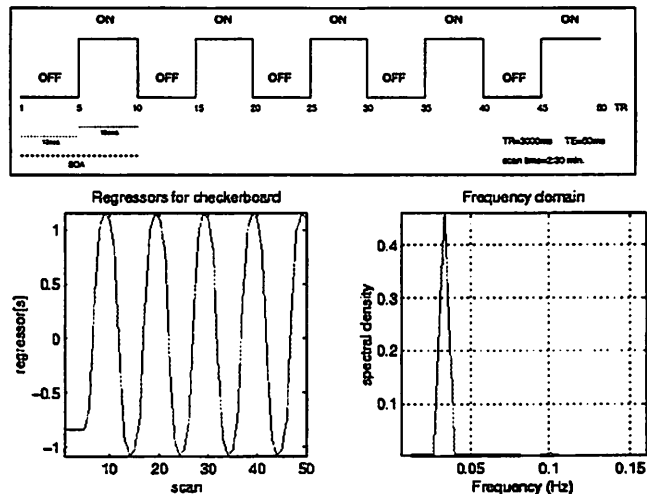


Figure 2. Visual box-car paradigm: Top: Task paradigm with 5 alternating control/rest and activation epochs for a total of 2:30 minutes. Lower left: Model of the expected hemodynamic response. Lower right: Fourier spectrum of the hemodynamic response model.

## 2. METHODS

### 2.1. Task Paradigms

Two paradigms, a visual and an auditory task, have been investigated with 20 adult volunteers, age between 20 and 30 year, in this study.

The visual task was a passive perception task where the subject looked at a checkerboard (red/black on black background) flickering at 8Hz during the activation epochs. During the resting epochs a fixation marker

(small cross) in the center of the view area was displayed. The paradigm consists of 5 epochs for each condition with an equal duration of 15 seconds each with a fixed stimulus onset asynchrony (SOA) of 30 seconds (Figure 2). The total of 50 volumes were acquired in 2:30 minutes.

The auditory task was a language experiment where the subjects listened during each activation epoch to German words and reversed German words having the same frequency spectrum. The subjects had to decide internally, if each word is a real word or not. Silence was used as control during the control/rest epoch. The paradigm consists of 3 alternating epochs, each lasts for 44 seconds (Figure 3). The overall scan time was 4 minutes and 4 seconds for a total of 66 brain volumes.

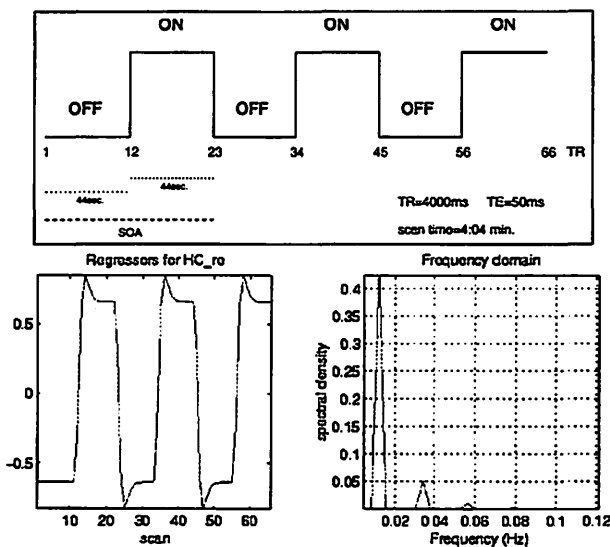


**Figure 3. Auditory box-car paradigm:** Top: Task paradigm with 3 alternating control/rest and activation epochs for a total of 4:04 minutes. Lower left: Model of the expected hemodynamic response. Lower right: Fourier spectrum of the hemodynamic response model.

## 2.2. Data Acquisition

Image acquisition was done on the Inera 1.5 Tesla whole-body MRI scanner (Philips, Best, Netherlands) using the standard birdcage head-coil. Head movement was reduced by fixing the subject's head with foam pads and velcro straps. Acoustic instructions and auditory stimuli were given using the scanner's integrated sound system using a headset covering both ears. For BOLD imaging we used a T2\*-weighted gradient echo planar imaging (GR-EPI) MR sequence with the following parameters:

**visual task:** TR=3000ms, TE=50ms, FA=85 deg, matrix  $64 \times 64$ , in-plane resolution  $3 \times 3mm^2$ , FOV= $192mm^2$ , 50 volumes comprising the whole brain.

**auditory task:** TR=4000ms, TE=40ms, FA=40 deg, matrix  $64 \times 64$ , in-plane resolution  $4 \times 4mm^2$ , FOV= $256mm^2$ , 66 volumes comprising the whole brain.

In addition a T1-weighted structural scan (spin-echo, TR=550ms, TE=20ms, matrix  $256 \times 256$ , FOV= $192mm^2$  visual and FOV= $256mm^2$  auditory) using the same slice angulation as the functional images was set according to the bi-commissural line (anterior and posterior commissure AC-PC), with a scan volume from apical to pontomesial. Three pre-saturation gradient RF pulses preceded the actual data acquisition to approach tissue steady state magnetization.

Prior to functional data collection, T1-weighted scout images and in-plane anatomic scans were taken. According to the study design, the functional scans were conducted during performance of the task conditions.

Stimuli were generated using a Inspiron5000e PC notebook computer (Dell Inc.) and were rear-projected onto a screen located in front of the head-coil. We used a LCD data projector (VPL-S500, Sony Corp.) and a custom-made collimator lens (Buhl Inc.) to focus the visual stimuli onto an opaque screen. Participants viewed the screen through a mirror located above the head-coil in direct visual pathway with an eye to screen distance of approximately 250mm. Maximum projection area was  $104 \times 79mm^2$ . Image reconstruction was performed automatically by the Intera system, the images were archived locally and transferred via DICOM protocol to the analysis workstation (SUN Ultra80, Dual Ultrasparc2, Sun Systems Inc., Palo Alto, CA) and parallel cluster [12] system (48 Pentium-III 500MHz distributed system running Linux and parallel virtual machine PVM software) for image processing.

### 2.3. Preprocessing

Preprocessing consists of spatial 3D preprocessing based on the brain volumes and 1D temporal preprocessing based on the time series vectors.

Spatial preprocessing includes motion correction, Talairach atlas Co-registration and spatial smoothing (Figure 4). First the acquired brain volumes have to be corrected for head motion of the subject during the scan. This can be accomplished by Co-registering each volume of the dynamic series to the first volume of the series used as reference volume. Motion correction was performed by an optimized parallel rigid-body parameter estimation and transformation algorithm suggested by Schmidt [13] et al. were optimal transformation parameters are determined for different minimization strategies by parallel evaluation on a data probe using a parallel cluster computer system.



**Figure 4. Spatial preprocessing:** Left: Original brain volume, coronar, sagittal and transversal aspects. Center: Volume after *rigid body* motion correction and transformation in Talairach atlas space. Right: Volume after 3D Gaussian smoothing.

The next step is to transform the motion corrected brain volumes into Talairach space. This can be archived when Co-registering each brain volume of the series with a brain volume (template) which is in the Talairach atlas coordinate system. For this purpose Ashburner [14] suggests a full 3D affine transformation with non-linear optimization from parameters derived from Co-registering the Talairach template and the first volume of the series. We followed Ashburners approach and used a template averaged from 152 individual brains, the MNI brain template (MNI version of ICBM brain), with  $2 \times 2 \times 2mm^3$  voxel resolution. After MNI space transformation all brain volumes were spatially smoothed using as 3D Gaussian filter with a filter kernel of 3-times the  $x, y, z$ -resolution in millimeters.

Because the MNI template is not exactly in Talairach space, we used a coordinate correction (Table 1) for each voxel. After spatial preprocessing the time series vectors of the brain volumes were temporally smoothed with a 1D Gaussian filter in time direction and thresholded at ray value 100, to segment brain tissue from background.

Above the AC, $z \geq 0$	Below the AC, $z < 0$
$x_{\text{tal}} = 0.99 \cdot x_{\text{MNI}}$	$x_{\text{tal}} = 0.99 \cdot x_{\text{MNI}}$
$y_{\text{tal}} = 0.9688 \cdot y_{\text{MNI}} + 0.0460 \cdot z_{\text{MNI}}$	$y_{\text{tal}} = 0.9688 \cdot y_{\text{MNI}} + 0.0420 \cdot z_{\text{MNI}}$
$z_{\text{tal}} = -0.0485 \cdot y_{\text{MNI}} + 0.9189 \cdot z_{\text{MNI}}$	$z_{\text{tal}} = -0.0485 \cdot y_{\text{MNI}} + 0.8390 \cdot z_{\text{MNI}}$

**Table 1.** Conversion from MNI coordinates into Talairach coordinates as suggested by the MRC Cognition and Brain Sciences Unit, Cambridge, England.

## 2.4. Region of Interest from Talairach Atlas

The next step in our approach foresees the selection of ROIs in correspondents to the functional task. To determine the region in the Talairach brain we used the automated Talairach atlas labels proposed by Lancaster [15]. We transformed the atlas labels associated with each coordinate into region labels suitable for marking the brain volumes. Lancaster used five level of refinement, the hemisphere, the lobe, the gyrus, the tissue and the cell level.

For our approach we choose four levels of selection associated with the functional task performed by the subjects:

**No regional selection:** This includes all brain voxel after preprocessing to compare the results with the ROI results.

**Lobe level:** Voxels were selected on the lobe level of the Talairach labels, occipital lobe for the visual experiment and temporal lobe for the auditory experiment.

**Gyrus level:** Voxels are being selected on the gyrus level of the Talairach labels, lingual and cuneus gyrus for the visual experiment and superior temporal and middle temporal gyrus for the auditory experiment.

**Cell level:** Voxel were selected on the cell level out of the Talairach labels, Brodmann areas 17 and 18 for the visual experiment and Brodmann areas 21 and 22 for the auditory experiment.

For each of these ROIs an individual SOM was trained and used for classification.

## 2.5. SOM Training and Classification

Finally these selected voxel partitions were used for training of SOM maps. For the all voxel case we used a large  $6 \times 4$  neuron map, for the ROIs the much smaller  $3 \times 3$  maps. Training and classification was done according to [16] in 2 phases: 1. 20.000 repetitions with a learning rate of  $\alpha = 0.9$  and a large neighborhood radius  $r = (\text{SOM}_w \cdot \text{SOM}_h)/2$ , 2. 100.000 repetitions with a learning rate of  $\alpha = 0.02$  and a smaller neighborhood radius  $r = (\text{SOM}_w \cdot \text{SOM}_h)/4$ .

After the training of the neural networks, the classification results for each neuron were individually overlaid onto the structural image. Each voxel is colored by the quantization error (QE), the Euclidean distance between the voxel’s time series and the corresponding neuron’s reference weight vector. Yellow color coding means low QE up to red for high QE. The selected ROI voxels, the structural and QE labeled image and the reference weight vector are displayed for interpretation.

## 3. RESULTS

Table (2) lists the average number of voxels selected for all 20 subjects for the four cases. One can observe that by selecting ROIs, the number of training voxels drops dramatically to only a fraction compare to all brain voxels.

For the illustration of the findings, we choose exemplarily only one slice which had the average maximum number of voxels (Table 2) and present the SOMs for all cases of the visual experiment (Figures 5 to 9).

Talairach Label Level	Visual Experiment		Auditory Experiment	
all voxels	$z = +5$	2378/3339 (72%)	$z = -2$	2463/3339 (74%)
	$z = [-37 \dots + 74]$	81980/153594 (54%)	$z = [-37 \dots + 74]$	69875/153594 (46%)
lobe level	$z = +5$	480/3339 (15%)	$z = -2$	456/3339 (14%)
	$z = [-37 \dots + 74]$	6177/153594 (5%)	$z = [-37 \dots + 74]$	n.a./153594 (n.a.)
gyrus level	$z = +5$	197/3339 (6%)	$z = -2$	198/3339 (6%)
	$z = [-37 \dots + 74]$	2972/153594 (2%)	$z = [-37 \dots + 74]$	2952/153594 (2%)
cell level	$z = +5$	84/3339 (3%)	$z = -2$	134/3339 (5%)
	$z = [-37 \dots + 74]$	1237/153594 (1%)	$z = [-37 \dots + 74]$	1144/153594 (1%)

Table 2. Averaged selected voxels for training for both experiment and all levels. For each case the slice with the maximum number of selected voxels and all selected voxel of the whole volume are listed.

Figure (5) shows the results from training a large  $6 \times 4$  SOM with all 2378 brain voxels in the slice. One can observe, that the 5 alternating epochs of control/rest and visual checkerboard (Figure 2) were learned by the neurons 21 and 22, and more noisy by neuron 20, 15 and 16 - the surrounding neurons. The corresponding voxel classification is in the primary visual cortex, as expected from the functional task. In result, less than 17% of the neurons carry *activation* patterns, but more than 83% of the SOM's capacity is occupied by *baseline*. If we lower the number of neurons to nine (Figure 6), only one neuron (7) carries the *activation* pattern, but local differentiation inside the calcarine cortex is impossible.

Figure (7) shows the same slice as before, but this time the voxel have been selected only if they were in the occipital lobe (left). The training with these 480 voxels results in 6 neurons (4-9) carrying the *activation* pattern and local pattern characteristics like amplitude and onset variations are observable (center and left).

In Figure (8) the ROI for training is decreased to only the lingual and cuneus gyrus (left). The total number of voxels in this ROI is 197, only less than half of the occipital lobe ROI. Now all reference weight vectors show only variations of the *activation* pattern, no *baseline* is trained (center and left).

The last ROI is on the cell level, combining Brodmann areas 17 and 18 (Figure 9). Only 84 voxels of all 3339 voxels in this slice have been selected for SOM training. Again one can observe, that only the *activation* pattern are trained, but pattern variance among the neuron weight vectors (right) is diminished due to the small number of input vectors.

#### 4. CONCLUSIONS

In summary it is obvious that by reducing the number of non-activated *baseline* voxels, one can dramatically improve the patterning quality of the neural network. Along with the reduced number of voxels being trained by the SOM, we conclude from our experiments, that one can also reduce the size of the neural network. Both, the reduced voxel size, e.g. only 2% of all brain voxels for the gyrus level in the visual experiment, and the reduce network size increase the calculation time by a factors of ten.

Beside calculation enhancement and thus usefulness of the approach, it also improves patterning quality. The results also emphasize the use of ROIs, because amplitude or temporal characteristics in conjunction with the regional extent of the BOLD effect are valuable additional information for the neuroscience investigator.

ROI selection has also its limits, because only whole brain images of healthy subjects can be considered for Talairach Co-registration. As this is usually the case for basic neuroscience questions which will benefit from the additional regional informations delivered by the SOM, this disadvantage is only of fair concern. Useful comparison like left and right hemispheric evaluation for specific activation patterns are possible.

From the results we conclude that the knowledge-based ROI selection using prior labels from Talairach stereotaxic space enhance the SOM approach greatly. It seems that the most favorable ROI will be the gyrus level, because the BOLD effect is not limited to the cortex surface, but does not extent into the deeper lobe level regions.

## ACKNOWLEDGMENTS

We wish to thank Philips Medical Systems (MRI Division Best Holland) for the kind support with the Philips Gyroscan NT 1.5T MRI system. The work is funded by the research grant *TV25*, Interdisciplinary Center for Clinical Research in the Neurosciences, University Hospital, University of Technology RWTH Aachen and the Department for Research and Education of the State of North-Rhine Westfalia.

## REFERENCES

1. S. Ogawa and T. Lee, "Magnetic resonance imaging of blood vessels at high fields: In vivo and in vitro measurements and image simulation," *Magnetic Resonance in Medicine* 16(1), pp. 9–18, 1990.
2. S. Ogawa, T. Lee, A. Kay, and D. Tank, "Brain magnetic resonance imaging with contrast dependent on blood oxygenation," in *Proceedings of the National Academy of Science USA*, 3, pp. 9868–9872, 1990.
3. K. Friston, A. Holmes, K. Worsley, J.-P. Poline, C. Frith, and R. Frackowiak, "Statistical parametric maps in functional imaging: a general linear approach," *Human Brain Mapping* 2, pp. 189–210, 1995.
4. P. Common, "Independent component Analysis: A new concept?," *Signal Processing* 36, pp. 11–20, 1994.
5. C. Goutte, P. Toft, E. Rostrup, F. Nielsen, and L. Hansen, "On clustering fMRI time series," *NeuroImage* 9, pp. 298–310, 1999.
6. C. Goutte, L. Hansen, M. Liptrot, and E. Rostrup, "Feature-space clustering for fMRI meta-analysis," *Human Brain Mapping* 13, pp. 165–183, 2001.
7. S. Erberich, M. Fellenberg, T. Krings, S. Kemeny, W. Reith, K. Willmes, and W. Oerschelp, "Unsupervised Time course analysis of functional magnetic resonance imaging (fMRI) using self-organizing maps (SOM)," in *Medical Imaging: Physiology and Function for Multi-Dimensional Images*, 3660, pp. 19–25, SPIE, SPIE, 1999.
8. M. Samuel, S. Williams, P. Leigh, A. Simmons, S. Chakraborti, C. Andrew, K. Friston, L. Goldstein, and D. Brooks, "Exploring the temporal nature of hemodynamic responses of cortical motor areas using functional mri," *Neurology* 51, pp. 1567–1575, 1998.
9. S. Erberich, M. Liebert, K. Willmes, A. Thron, and W. Oerschelp, "Analysis of event-related fMRI using a non-linear regression self-organizing map neural network," in *Medical Imaging: Physiology and Function from Multi-Dimensional Images*, p. in press, SPIE, SPIE, March 2001.
10. S. Erberich, S. Weis, S. Kemeny, K. Willmes, and W. Oerschelp, "Preprocessing strategies for fMRI data analysis by self-organizing map (SOM) neural network," *NeuroImage* 9 20, 1999.
11. J. Talairach and Tournoux, *Coplanar stereo-tactic atlas of the human brain*, Thieme Medical, New York, 1988.
12. S. Erberich, M. Hoppe, C. Jansen, T. Schmidt, A. Thron, and W. Oerschelp, "Hospital-integrated parallel cluster for fast and cost-efficient image analysis - clinical experience and research evaluation," in *Medical Imaging: PACS Integrated Medical Information Systems: Design and Evaluation*, p. in press, SPIE, SPIE, 2001.
13. T. Schmidt, S. Erberich, M. Hoppe, C. Jansen, A. Thron, and W. Oerschelp, "Optimized knowledge-based motion correction of fmri time-series using parallel algorithms," in *Physiology and Function from Multidimensional Imaging, Medical Imaging*, SPIE, 03 2001.
14. J. Ashburner and K. Friston, "Nonlinear Spatial Normalization Using Basis Functions," *Human Brain Mapping* 7, pp. 254–266, 1999.
15. J. Lancaster, M. Woldorff, L. Parsons, M. Liotti, C. Freitas, L. Rainey, P. Kochunov, D. Nickerson, S. Mitkiten, and P. Fox, "Automated Talairach atlas labels for functional brain mapping," *Human Brain Mapping* 10, pp. 120–131, 2000.
16. T. Kohonen, *Self-Organizing Maps*, Springer, Berlin, 2 ed., 1997.

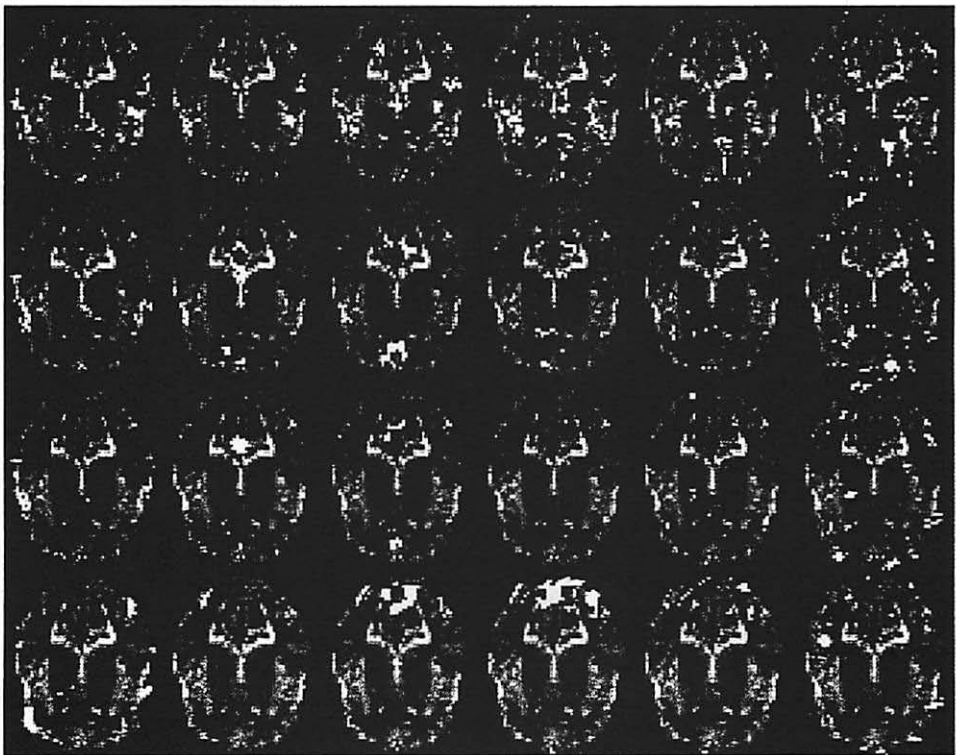
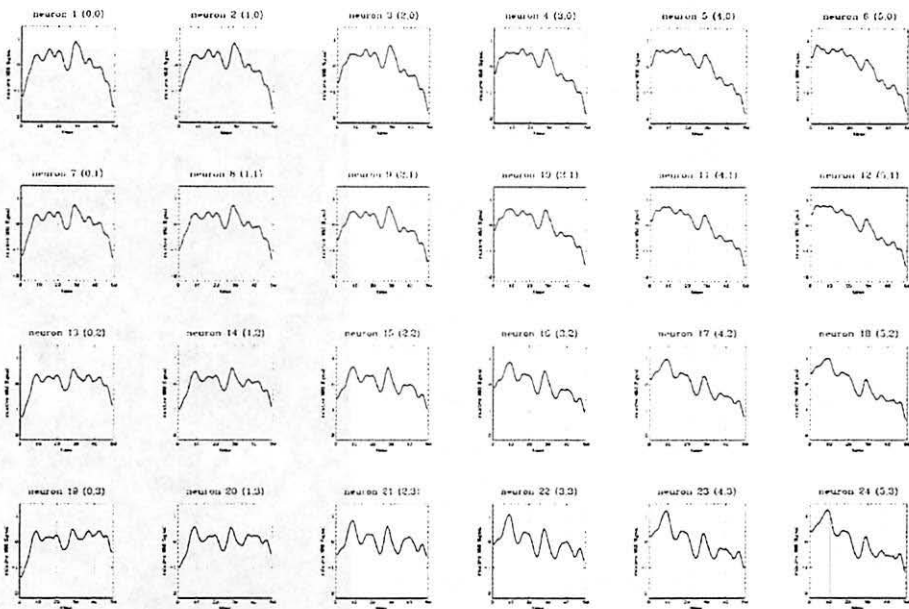


**Figure 5. Visual Experiment:**  $6 \times 4$  SOM trained with all voxels of the slice at Talairach coordinate  $z = +5$ . **Top:** Map of the reference weight vectors for each neuron in the SOM grid. **Bottom:** Voxels classified by the corresponding neurons in the SOM, colored by its quantization error.

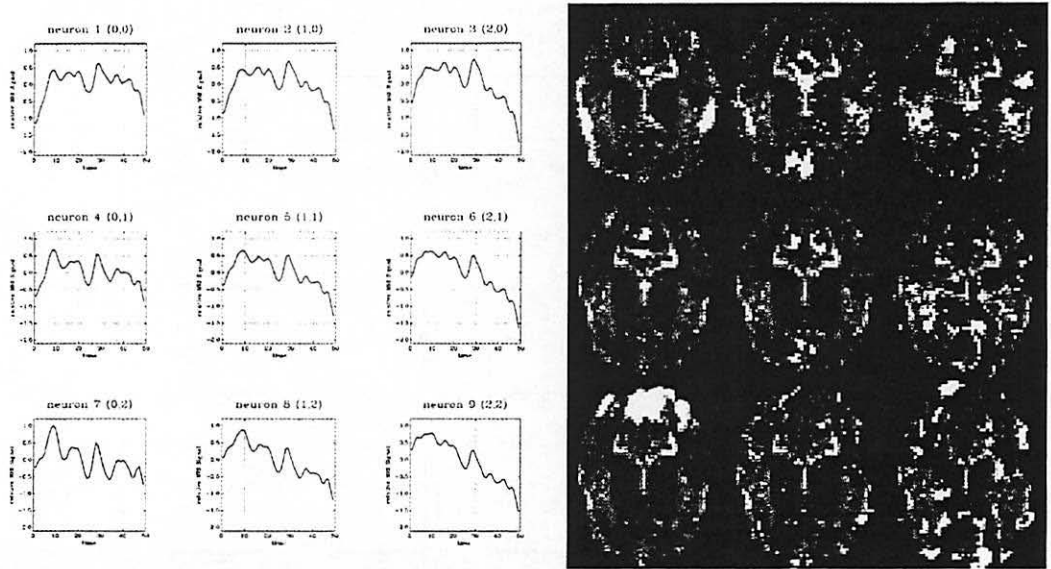


**Figure 6. Visual Experiment:**  $3 \times 3$  SOM trained with all voxels of the slice at Talairach coordinate  $z = +5$ . **Left:** Map of the reference weight vectors for each neuron in the SOM grid. **Right:** Voxels classified by the corresponding neurons in the SOM, colored by its quantization error.

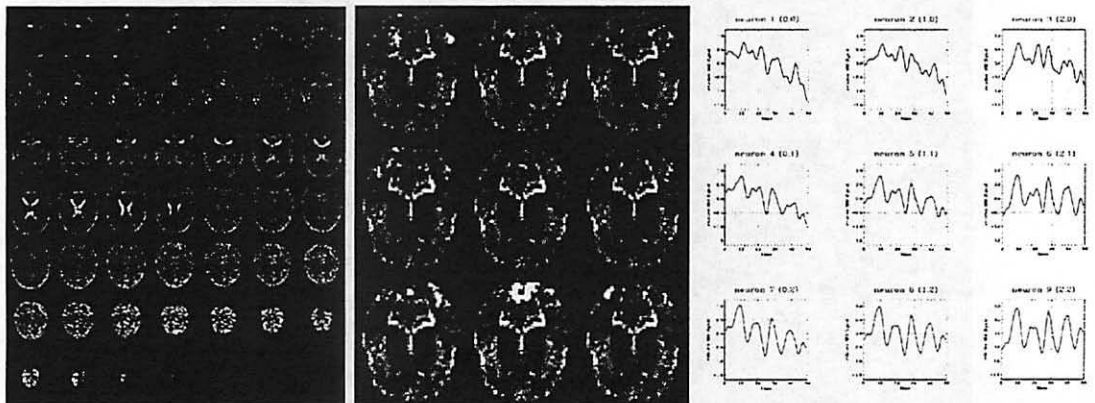


**Figure 7. Visual Experiment:**  $3 \times 3$  SOM trained with voxels selected on the lobe level in the slice at Talairach coordinate  $z = +5$ . **Left:** All voxels of the occipital lobe (red) selected from Talairach database. **Center:** Voxels classified by the corresponding neuron in the slice at Talairach coordinate  $z = +5$  using its quantization error color map. **Right:** Map of the reference weight vector for each neuron in the SOM grid.

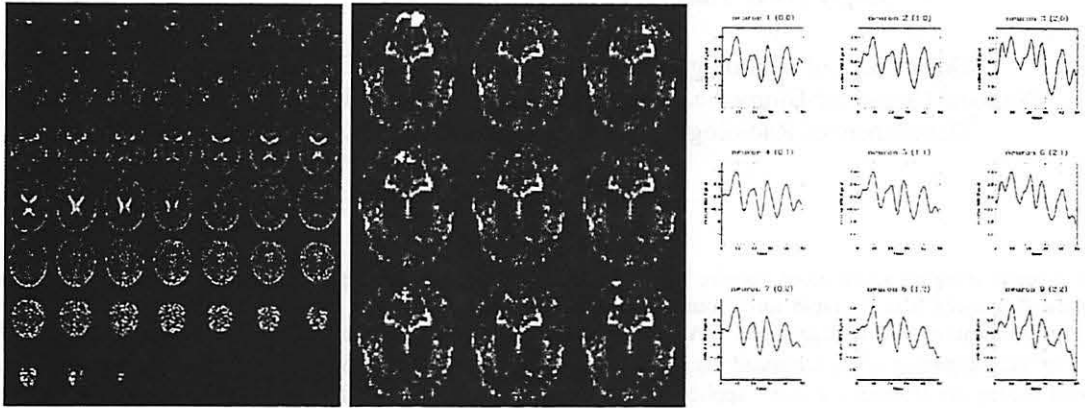


**Figure 8. Visual Experiment:**  $3 \times 3$  SOM trained with voxels selected on the gyrus level in the slice at Talairach coordinate  $z = +5$ . **Left:** All voxels of the lingual and cuneus gyrus (red) selected from Talairach database. **Center:** Voxels classified by the corresponding neurons in the slice at Talairach coordinate  $z = +5$  using its quantization error color map. **Right:** Map of the reference weight vector for each neuron in the SOM grid.

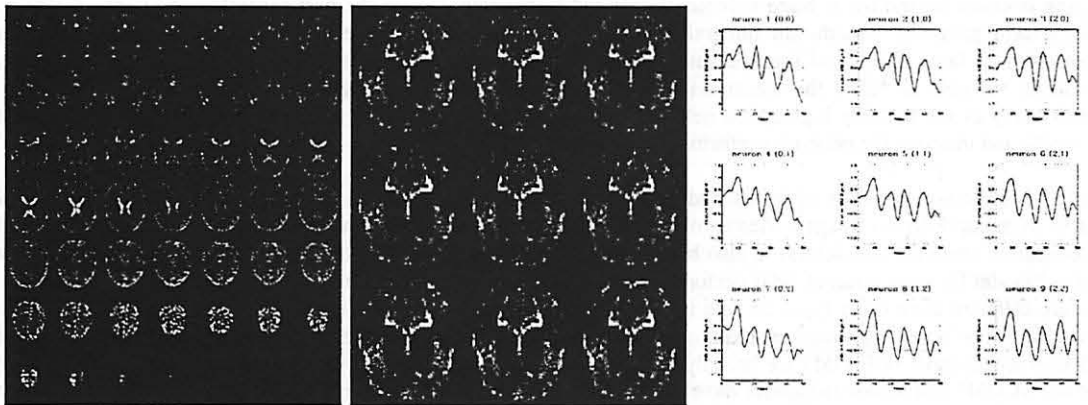


**Figure 9. Visual Experiment:**  $3 \times 3$  SOM trained with voxels selected on the cell (Brodmann area) level in the slice at Talairach coordinate  $z = +5$ . **Left:** All voxels of the Brodmann areas 17 and 18 (red) selected from Talairach database. **Center:** Voxels classified by the corresponding neurons in the slice at Talairach coordinate  $z = +5$  using its quantization error color map. **Right:** Map of the reference weight vector for each neuron in the SOM grid.

# NGI Performance for Teleradiology Applications

G. Mogel<sup>1</sup>, H.K. Huang<sup>1</sup>, F. Cao<sup>1</sup>, Z. Zhou<sup>1</sup>, P. Dey<sup>1</sup>, M. Gill<sup>2</sup>, B. J. Liu<sup>3</sup>

<sup>1</sup>Department of Radiology, Childrens Hospital LA/USC, Los Angeles, CA 90027

<sup>2</sup>National Center for Biomedical Communications, National Library of Medicine, MD 20894

<sup>3</sup>Department of Radiology, Saint John's Health Center, Santa Monica, CA 90404

## ABSTRACT

Tele-medical imaging applications require low cost, and high-speed backbone wide area networks (WAN) to carry large amount of imaging data for rapid turn around interpretation. Current low cost commercially WAN is too slow for medical imaging applications, while high speed WAN is too costly. The next generation Internet (NGI) or Internet2 is federal initiatives for the integration of higher speed backbone communication networks (up to 2.4 Gbits/sec) as a means to replace the current inadequate Internet for many applications including medical imaging. This paper describes our preliminary experience of connecting to Internet2 for teleradiology application. A case study is given for the NGI WAN connection between Childrens Hospital Los Angeles and National Library of Medicine. NGI WAN performance for different image modalities, measured in throughput rate and application response time, were obtained and then compared to the T1 WAN connection between Childrens Hospital Los Angeles and Saint John's Health Center Santa Monica.

**Keywords:** Internet, Next Generation Internet, Internet2, Medical Images, Teleradiology, Telemedicine.

## 1. INTRODUCTION

The next generation internet (NGI) or Internet2 is an initiative for the integration of higher speed backbone communication networks as a means to replace the current inadequate Internet for many applications including medical imaging. The medical imaging is characterized by its huge volume of data and image size. During the past several years, telemedicine and teleradiology have gradually become an integral part in the US health care delivery system. But the problem of high-speed transmission of large volume of medical images over a wide area network (WAN) has become an issue since the standard Internet is not able to fulfill the transmission bandwidth requirement for teleradiology applications. The NGI initiative utilizes many of the existing high-speed network backbones (capable of up to 2.4Gbits/sec), and promises to increase the bandwidth and improve the network performance.

Of all the potential application of broadband networks in healthcare, the current model that is most widely in practice is the transfer of medical digital images. Meanwhile, the promise of future applications that support intervention (robotic surgery) and education (medical simulators) is also being pursued by extensive funding in those areas. In this case study, we find a practical model for evaluation of NGI performance for these medical applications. The characteristics of radiologic imaging files, are different from other types of data in some important aspects: file size is very large with the DICOM Standard file format [3], some image examinations require near real-time transmission for practical use, and finally, mature but technically burdensome standards (DICOM) are broadly accepted across manufacturers as well as borders. For this reason, the public Internet, ".COM" and movie industries have not been able to fulfill the need in routine daily clinical application. Simultaneously, due to the health care reform, telemedicine and teleradiology are gradually becoming an integral part in healthcare delivery with the assumption that the problem of high-speed transmission of large volume medical images will be solved by the non-medical communications industry.

In this case study, we use our established NGI testbed at Image Processing and Informatics (IPI) lab, CHLA to test the current NGI WAN performance. Our goal is to measure the NGI WAN performance for teleradiology applications using the T1

---

GM: Email: [Xrad2@alltel.net](mailto:Xrad2@alltel.net)

H.K.H: Email: [hkhuang@aol.com](mailto:hkhuang@aol.com)

F.C.: Email: [fcao@pacbell.net](mailto:fcao@pacbell.net)

WAN performance as a benchmark. Since DICOM is the standard communication protocol in medicine. We would like to see what's the DICOM performance overhead over the standard TCP/IP when medical images are transferred over NGI. The purposes of the study are:

- 1) Obtaining the two key NGI performance indicators:
  - Throughput rate for transferring typical medical Images
  - Response time for short transaction-type applications
- 2) Comparing NGI WAN performance with T1
- 3) Comparing the DICOM performance with non-DICOM applications

## 2. NGI TESTBED SETUP

### 2.1. Test Sites

#### Sites 1: IPI Lab at Childrens Hospital LA

Figure 1 shows the Internet2 connection at Image Processing and Informatics (IPI) laboratory, Childrens Hospital Los Angeles (CHLA), which was established in early 2000. The NGI site at IPI has the OC3 (155 mbit/sec) connection to the Internet2 through the CalREN2 GigPos at USC.

#### Site 2: NLM. Center of Biomedical Communications

National Center of Biomedical Communicatons, National Library of Medicine connections to the MAX aggregation point at OC-3 (155 mbit/sec).

#### Site 3: Saint John's Health Center (SJHC)

SJHC, Santa Monica has been collaborating with IPI, Childrens Hospital/USC in developing a novel short-term, automatic, fault-tolerant solution for disaster recovery of PACS data based on the Application Service Provider (ASP) model using a T-1 line. This ASP off-site archive server will be used to test the T1 WAN performance as a benchmark for nation wide NGI performance.

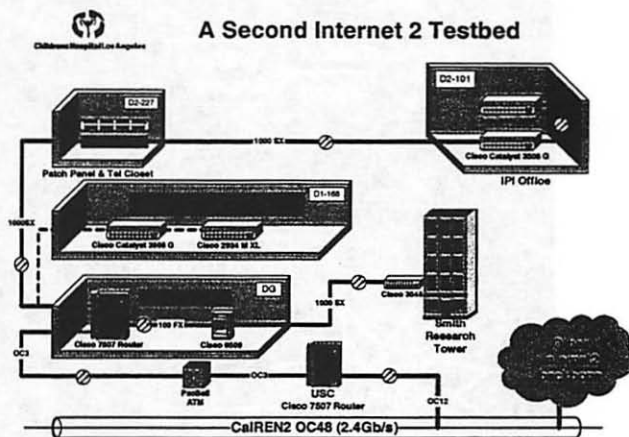


Figure 1. Internet 2 at Image Processing and Informatics (IPI) lab, CHLA/USC

Figure 2 shows the network and testbed setup. The network performance tests were conducted for

- NGI WAN between IPI Lab and NLM
- T1 WAN between IPI Lab and SJHC

#### PACS Simulator

To measure the DICOM performance in real time under clinical environments, the PACS Simulator Software developed at IPI Lab for research and teaching purposes has been used. It is a DICOM compliance PACS Simulator, consisting of five key components simulating a typical clinical PACS: acquisition modality Simulator (AMS), DICOM gateway, PACS Controller (archive server), clinical viewing workstations (WS), and a network connecting these components. Generic PACS DICOM compliant software runs on these components simulating normal clinical data flow. We have successfully used this Simulator as a standalone PACS training tool 24 hours a day and 7 days a week for half year to simulate clinical PACS operation. The Modality Simulator is connected to the CHLA/USC clinical PACS and contains thousands of CT, MRI, US, CR, and digitized film examinations (with patient's ID stripped off). These images are replenished continuously in loop through the clinical PACS connection. Image examinations are fed from AMS to the DICOM gateway simulating the continuous clinical environment. From there they are pushed to the PACS server for archive and workstations for review.

In our NGI WAN tests, the Modality Simulator was installed in NLM site and it continuously feeds the DICOM images to

the remote archive site at IPI Lab. The NGI DICOM performance is measured between the Modality Simulator at NLM and the DICOM Gateway at IPI Lab.

The existing off-site archive system from SJHC to IPI Lab has been used in T1 WAN testing. A fault-tolerant (FT) back-up archive server and storage device is implemented at CHLA/USC offsite from the SJHC PACS archive. Clinical PACS data from SJHC is sent to this FT storage server as a disaster recovery in parallel to the exams being archived in the main server. The T1 WAN performance was measured between the two gateways at SJHC and IPI Lab.

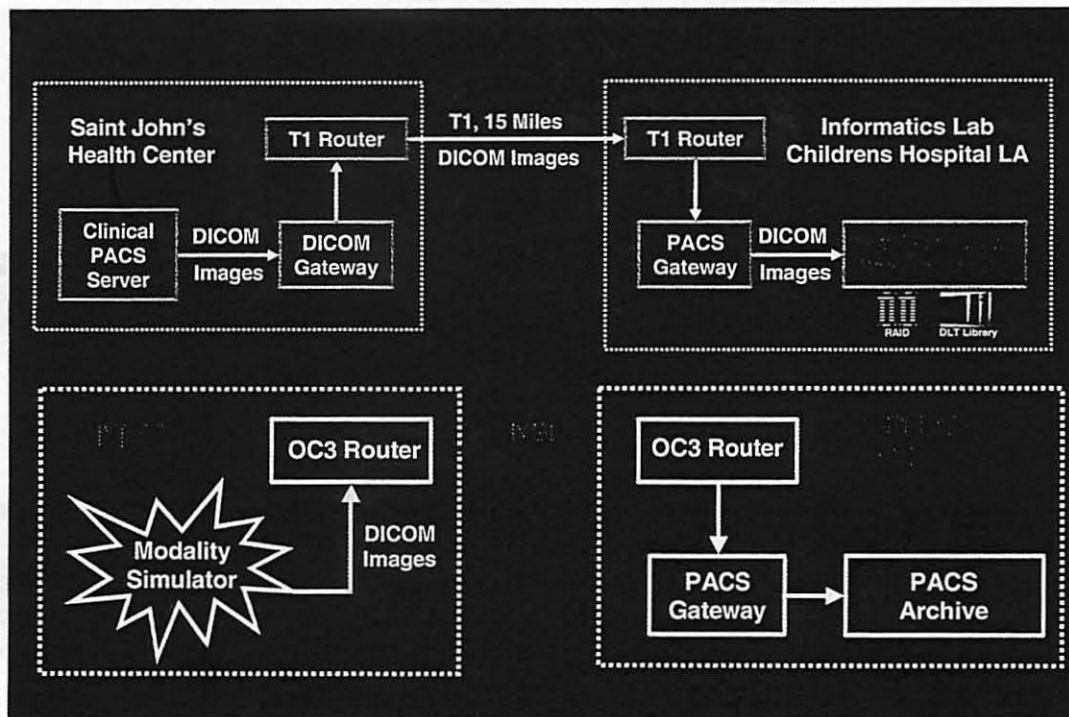


**Figure 2.** NGI and T1 WAN Setup. T1 WAN: The DICOM compliance off-site ASP (Application Service Provider) archive server for St. John's Health Center developed at IPI lab. NGI WAN: The Modality Simulator feeds variety of DICOM test images to IPI Lab, continuously through NGI WAN.

### 3. TESTING PROTOCOLS

To measure the NGI WAN performance for teleradiology applications, we are interested in two key performance indicators:

- Throughput rate for transferring typical medical Images
- Response time for short transaction-type applications

To evaluate DICOM performance and overhead, we compared the DICOM performance with non-DICOM applications. Two TCP/IP utilities were used as the non-DICOM applications. The common TCP/IP file transfer tool, FTP is used to measure the throughput rate while TCP/IP network utility **QCheck**, a software from NetIQ, (Web site: [www.qcheck.net](http://www.qcheck.net)), is used to measure the response time.

To measure the throughput rate, patient exams of different modalities (Digital mammography, CT and MR section images, CR) were selected and sent through NGI and T1 WAN. To measure the application response time, a small data package, 25Kbytes DICOM header, was used to send over the network.

Table 1 summarizes types of medical exams, network protocols and test tools used in our NGI and T1 WAN performance tests.

Network Performance NGI and T1 WAN	Testing Tools TCP and DICOM	Protocols	Medical Data
Throughput	FTP	FTP	Digital Mammo: ~4 x 40MB Section images: ~200 x 0.5MB X-Ray: 2 x 10MB
	PACS Simulator	DICOM	
Response Time	Ping/QCheck	ICMP/TCP	Short commands, transactions and Instructions: 1-32,000Bytes
	PACS Simulator	DICOM	DICOM Image Header

Table 1 Medical exams, network protocols and test tools used in NGI and T1 WAN performance tests

**NGI:** Next Generation Internet, **WAN:** Wide Area Network

**CHLA:** Childrens Hospital Los Angles, **NLM:** National Library of Medicine

**SJHC:** Saint John's Health Center, Santa Monica, CA

**PACS Simulator:** a PACS software packages developed at IPI, CHLA including image modality simulator, DICOM gateway, archive server and display workstations.

**QCheck:** a software utility from NetIQ; **ICMP:** Internet Communication Management Protocol, **MB:** Megabytes

#### Data path between IPI Lab and NLM

Hop	Latency	IP Address	Node Name
1	1 ms	128.125.76.33	128.125.76.33 (CHLA router)
2	1 ms	128.125.251.174	128.125.251.174
3	1 ms	128.125.251.86	chl-gw.usc.edu
4	1 ms	128.125.254.43	rtr-gw-43.usc.edu
5	1 ms	128.125.251.65	c2-12008.usc.edu
6	2 ms	198.32.248.86	Abilene--USC.ATM.calren2.net
7	33 ms	198.32.8.22	hstn-losa.abilene.ucaid.edu
8	52 ms	198.32.8.34	atla-hstn.abilene.ucaid.edu
9	67 ms	198.32.8.66	wash-atla.abilene.ucaid.edu
10	67 ms	206.196.177.1	wash-abilene-oc48.maxgigapop.net
11	68 ms	206.196.178.46	clpk-so3-1-0.maxgigapop.net
12	68 ms	206.196.177.34	wash-nlm.maxgigapop.net
13	68 ms	130.14.38.196	130.14.38.196
14	68 ms	130.14.60.91	whistler.nlm.nih.gov

#### Data path between IPI Lab and SJHC: Point-to-Point T1

#### 4. PRILIMINARY RESULTS

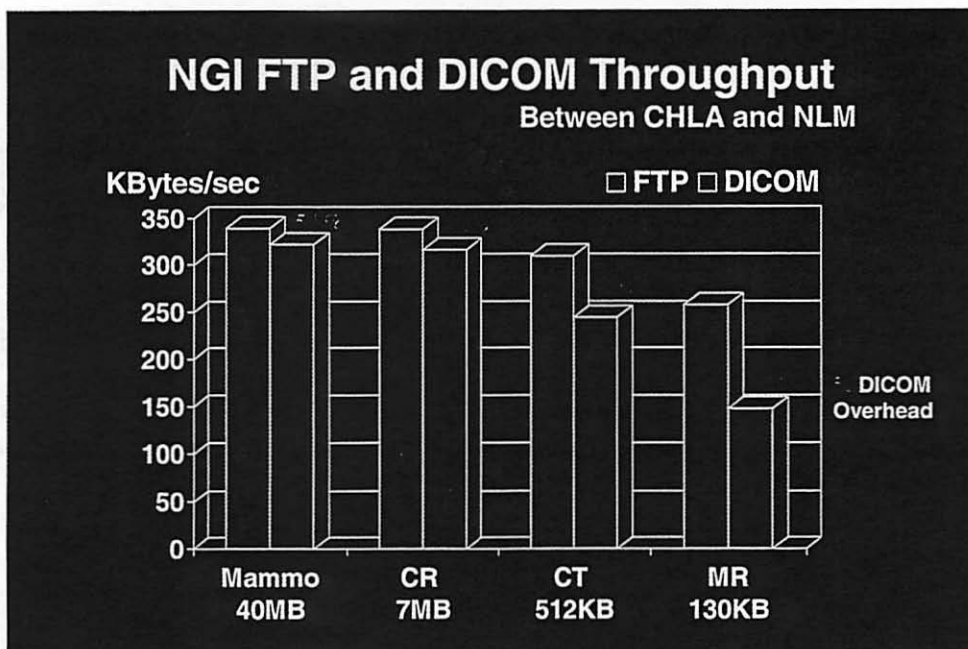


Figure 3 NGI FTP and DICOM performance between IPI Lab and NLM.

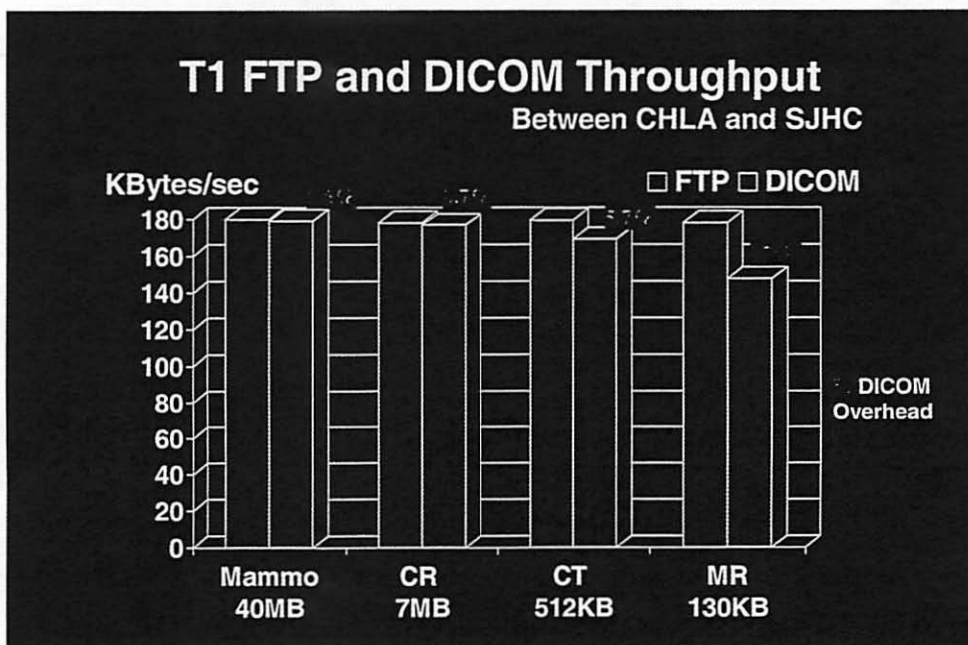


Figure 4 T1 FTP and DICOM performance between IPI Lab and SJHC.

## Roundtrip Response Time

NGI: CHLA-NLM		T1: CHLA-SJHC	
TCP	DICOM	TCP	DICOM
0.18s	0.53s		0.27s

Data Size: 25KByte DICOM header

Figure 5 Roundtrip TCP and DICOM response times for NGI and T1 WAN.

### ACKNOWLEDGMENT

This work is partially supported by the US Army Medical Research and Materiel Command Contract No. DAMD17-99-P-3732 and NIH Grant No. N01-LM-9-3538.

# PACS ARCHIVE UPGRADE AND DATA MIGRATION: CLINICAL EXPERIENCES

Brent J. Liu<sup>1</sup>, Luis Documet<sup>1</sup>, Dennis Sarti<sup>1</sup>, H.K. Huang<sup>2</sup>, John Donnelly<sup>3</sup>

<sup>1</sup>Department of Radiology, Saint John's Health Center, Santa Monica, CA 90404;

<sup>2</sup>Department of Radiology, Childrens Hospital LA/USC, Los Angeles, CA 90027;

<sup>3</sup>IntePro Solutions Inc., Colonia, NJ

## ABSTRACT

Saint John's Health Center PACS data volumes have increased dramatically since the hospital became filmless in April of 1999. This is due in part of continuous image accumulation, and the integration of a new multi-slice detector CT scanner into PACS. The original PACS archive would not be able to handle the distribution and archiving load and capacity in the near future. Furthermore, there is no secondary copy backup of all the archived PACS image data for disaster recovery purposes. The purpose of this paper is to present a clinical and technical process template to upgrade and expand the PACS archive, migrate existing PACS image data to the new archive, and provide a back-up and disaster recovery function not currently available. Discussion of the technical and clinical pitfalls and challenges involved in this process will be presented as well. The server hardware configuration was upgraded and a secondary backup implemented for disaster recovery. The upgrade includes new software versions, database reconfiguration, and installation of a new tape jukebox to replace the current MOD jukebox. Upon completion, all PACS image data from the original MOD jukebox was migrated to the new tape jukebox and verified. The migration was performed during clinical operation continuously in the background. Once the data migration was completed the MOD jukebox was removed. All newly acquired PACS exams are now archived to the new tape jukebox. All PACS image data residing on the original MOD jukebox have been successfully migrated into the new archive. In addition, a secondary backup of all PACS image data has been implemented for disaster recovery and has been verified using disaster scenario testing. No PACS image data was lost during the entire process and there was very little clinical impact during the entire upgrade and data migration. Some of the pitfalls and challenges during this upgrade process included hardware reconfiguration for the original archive server, clinical downtime involved with the upgrade, and data migration planning to minimize impact on clinical workflow. The impact was minimized with a downtime contingency plan.

**Keywords:** PACS, Archive Upgrade, and Disaster Recovery

## 1. INTRODUCTION

Saint John's Hospital has a filmless PACS that acquires approximately 130,000 Radiological exams annually. Saint John's began the PACS process in April 1999 by implementing PACS with CR for all critical care areas. This was considered Phase I of the PACS process. Phase II comprised of the integration of MR, CT, US, Digital Fluorography, and Digital Angiography within the PACS. Phase II was completed in April 2000. Since then Saint John's PACS volumes have increased steadily. Figure 1 shows exam volumes for three specific modality types, CT, MR, and US. As shown in the figure, each of the modality types has increased annually with CT showing the largest growth. In addition, the number of CR exams has increased by approximately 900 since the previous year. In the spring of 2001, Saint John's Health Center integrated a multi-sliced detector CT scanner, a digital angiography unit, and an additional digital fluorography unit with PACS. The multi-sliced detector CT exams can comprise of over 600 images (300MB of data). Currently, Saint John's is archiving 9.8 GB/day, which amounts to 3.5 TB/yr. In addition, distribution of PACS data has increased as CT, MR, and US exam numbers increased which requires an archive server that can handle the necessary performance criteria. Currently, the maximum storage capacity of the PACS archive implemented in April 1999 is 3.0 TB, which would mean that older PACS exams would have to remain offline before a year is over. The current archive storage device is a Magneto Optical Disk (MOD) Jukebox with only a single copy of the PACS data. Therefore, should Saint John's encounter a disaster there is potential for all the PACS data to be lost because there is no

backup of the data. With these considerations, it was determined that Saint John's need for an archive server upgrade, data storage expansion, and data backup was becoming increasingly urgent.

With the archive upgrade, all new PACS exams are archived through a Sun Enterprise 450 platform server with a 270 GB RAID. The exams are then archived to a network attached digital tape storage system comprising of an additional Sun Enterprise 450 with a 43 GB RAID and a 7.9 TB storage capacity digital tape library. The storage capacity of the tape library is scheduled to double in the next few years as the tape density doubles eventually making it a 16 TB tape library. All older PACS exams are still distributed via the original archive server but the exams have been successfully migrated to the tape library as well. See Figure 3 for more details.

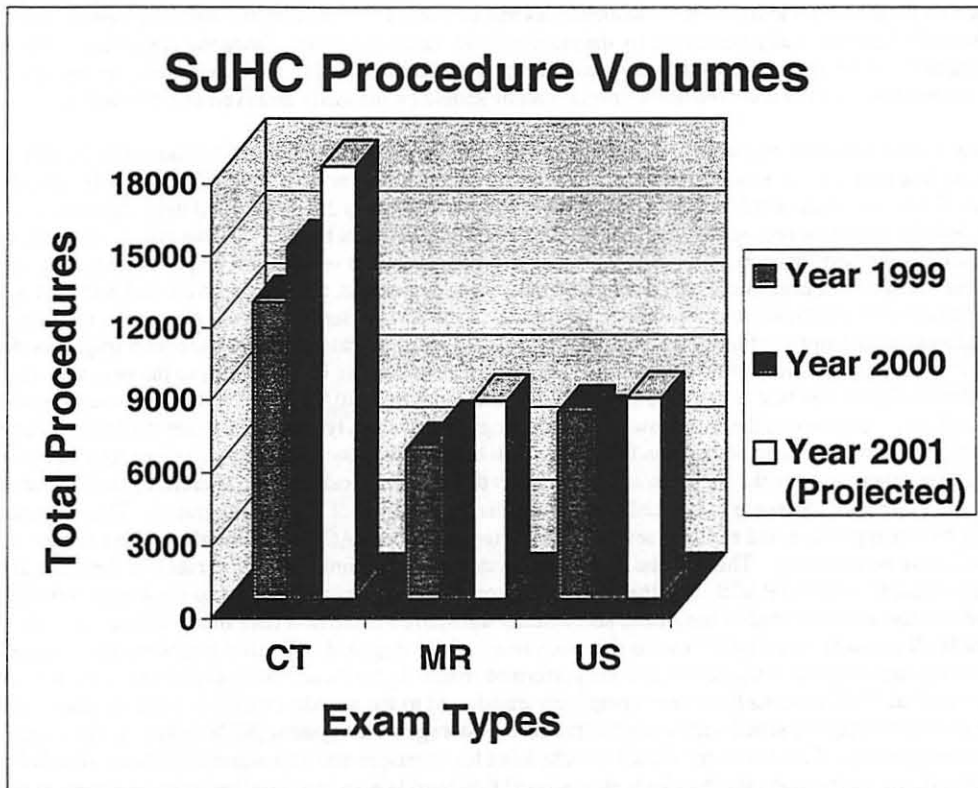


Figure 1: Saint John's Health Center PACS Exam Volumes for Three Modalities

## 2. METHODS AND MATERIALS

There are three major challenges facing Saint John's Health Center with regards to successfully implementing an upgraded archive system. The first challenge is how to upgrade to a new PACS archive server during a live clinical setting. The second challenge is how to migrate 2.5 years of PACS data from optical disk media (MOD) to a new digital tape media during a live clinical setting. The third and final challenge is developing a disaster recovery solution for the hospital for all current data stored once the new archive has been implemented. It comes as no surprise that these three challenges evolved into the three major milestones for this archive upgrade process.

Some of the issues surrounding the upgrade to a new archive server include the fact that the current archive server required a software version upgrade in order to be compatible with the new archive server. In addition, the archive databases needed to be reconfigured to include the new archive server as well. All of these issues pointed to the fact

that substantial downtime of the original PACS archive server was necessary in order to perform the software upgrade and configure the new databases. Since this downtime was scheduled, a procedural plan could be developed to minimize the affect of the downtime on PACS clinical workflow for the radiologists and the hospital. The first step is to determine the start time for the archive upgrade that would have the least impact. Therefore, the downtime was scheduled for Friday evening to Saturday evening. Once the downtime has been scheduled, the next step is to notify all staff and begin removing all unnecessary previous exams on local workstation to allow for space for new PACS exams that will not be immediately archived. The next step is to obtain the weekend schedule for CT and MR modalities and prefetch any previous like-modality exams from the archive so that the radiologists will have comparison studies when the new PACS exam arrives at the workstations. All auto-archiving rules are removed so that the workstation will not continue to attempt to send during the downtime and affect the performance. During the downtime period, no queries or retrievals should be made by the local workstations and any new PACS exams are manually distributed to the ward areas instead of automatically performed by the archive server since it is down. Once the upgrade is complete and the new archive is online, then all workstations need to be configured to archive to the new archive server. At this point, all PACS exams that were not archived during the downtime should be manually archived and verified.

Once the archive has been upgraded and is stable, the next challenge is to migrate the previous PACS data that resides on optical disk media to the new digital tape media during a live clinical setting. For Saint John's Health, the volume of data was almost 2.5 years worth of PACS data, which was approximately 2.5 TB of total data. Some of the issues that surrounded the migration procedure were that the data migration must not hamper the live clinical workflow in anyway and reduce system performance. With any migration, it is important that verification be performed to prevent any data loss. Once the data has been successfully migrated to the new data media, the original data media storage system should be removed which may incur additional downtime of the archive server. Development of a migration plan was key to addressing the surrounding issues and insuring a data migration that would have the least impact on the live clinical PACS. First, it is important to determine the best times to migrate PACS exams to the new archive. For Saint John's Health Center, the best times were from 9 PM to 6AM and from 10AM to 3PM daily. These times were determined, in part, based on the workflow of the Radiologists as well as typical daily exam volumes. Even though these times were initially estimated, some fine-tuning will be necessary because these estimates may not be accurate. This is a very crucial step as this step can adversely affect the entire clinical PACS. Therefore, careful attention to the archive and system performance is especially important during the onset of the data migration. The migration of PACS data may be too aggressive and result in severely hampering the entire PACS including the archive server. In that case, scale back may be necessary. This may be an iterative cycle until an optimal migration rate is achieved that does not adversely affect the clinical PACS. Another important aspect of the migration process to implement verification tools to insure that the migrated studies have been successfully transferred to the new data media storage system. A database log records all transactions of PACS exams that were successfully migrated. The first migration run was performed automatically and successive migration runs are performed manually for those PACS exams that were not successfully migrated until all PACS exams have been completely transferred to the new data media storage system. Finally, another downtime must be scheduled to remove the current storage media system (MOD jukebox) from the PACs archive configuration. The downtime should be scheduled for overnight and downtime procedures should be implemented in case there are any problems encountered that would delay bringing the archive back online as initially scheduled.

With the new digital tape archive storage system, the third and final milestone was to implement a disaster recovery procedure for all new PACS data acquired. Since Saint John's Health Center is a filmless institution, future regulations may require a PACS data backup solution because film will no longer be stored. However, disaster recovery solutions are scarce in the PACS environment. In addition, although the new archive upgrade and digital tape storage system allows for a disaster recovery solution, it is still not a turnkey solution to match hospital PACS workflow. For Saint John's Health Center, it was estimated that one digital tape media could hold approximately 5 days worth of PACS data. In the near future this figure will double when the tape density doubles. Therefore, even if a second copy of the PACS data is made and stored on a tape and a disaster scenario occurs, the hospital could still lose up to 10 days of data in the worst case. Because of this a disaster recovery procedure that includes a daily third copy of the PACS data is necessary to cover this turnover period. Figure 2 shows the disaster recovery procedure developed at Saint John's Health Center that includes vaulting all tape media to an offsite vault service. The following are the procedure steps described in more detail:

- 1) PACS exam arrives and three copies are written to three separate tapes. Copy1 is primary copy and always resides in tape jukebox.
- 2) At 10AM every day, Copy2 tape is checked.
  - a. If Copy2 tape is 95% full, it is ejected (occurs approximately every 5 days) and sent offsite.
  - b. A new Copy2 tape is loaded into the jukebox from the Copy2 tape pool.
- 3) Copy3 tape(s) replaced daily: Coverage for period when Copy2 tape reaches 95% full.
  - a. Copy3 tapes ejected 10AM every day and sent offsite. If Copy2 tape is 95% full, Copy3 tapes of that specific day are returned to Copy3 tape pool for re-use.
  - b. Two new Copy3 tapes are loaded into the jukebox from the Copy3 tape pool. Two tapes are loaded in case the first tape fills to capacity during the day and overflows onto the second tape.
- 4) Data vault storage service picks up tapes to transfer to a secure location daily. Copy2 tapes stored permanently for disaster recovery. Copy3 tapes stored temporarily.
- 5) When a Copy2 tape arrives at the data vault storage facility, all Copy3 tapes stored are returned to hospital and returned to the copy3 tape pool.
- 6) When a Copy3 tape is 95% full, Copy3 tape contents are erased and ready for re-use.

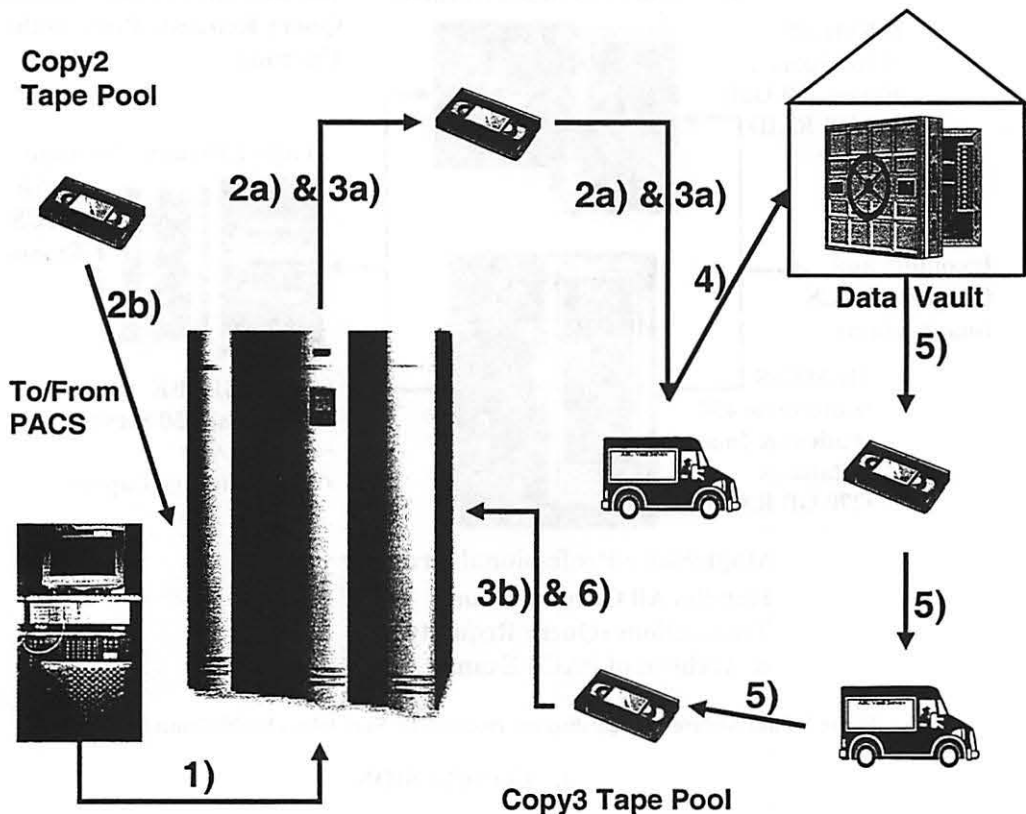


Figure 2: Disaster Recovery Procedure for Saint John's Health Center PACS data

### 3. RESULTS AND DISCUSSION

Figure 3 shows the final configuration and processes of the new archive upgrade that was implemented at Saint John's Health Center. Each of the three challenges and milestones were completed with success. Currently, the original

archive server is used to distribute any query/retrieval requests on all previous PACS exams even though the old PACS exams were successfully migrated to the new digital tape library. The new archive server handles all distribution as well as provide query/retrieval and archival of all current and future exams. PACS system performance has improved in many functions including query/retrieval of PACS exams as well as distribution of exams to the hospital wards with the new more powerful Sun Enterprise 450 platform archive server as compared to the original Sun Ultra 2 platform archive server. Transition to the new archive was performed with minimal effect on the clinical workflow due to the contingency plans developed. Data migration of previous exams from the optical disk (MOD) jukebox to the new digital tape jukebox was successful with no loss of PACS data. However, careful attention should be paid when executing any data migration to assure that it is not too aggressive so as to hamper the performance of the clinical PACS during live operation. All new and old PACS exams are archived on the digital tape library and the optical disk (MOD) jukebox has been removed from the archive system as a deep archive solution. With the new digital tape jukebox, the hospital has online storage capacity for over 5 years of PACS data. Finally, a disaster recovery plan was successfully implemented using the procedures developed and a successful rotation of digital tape media has been established with an offsite vault storage vendor.

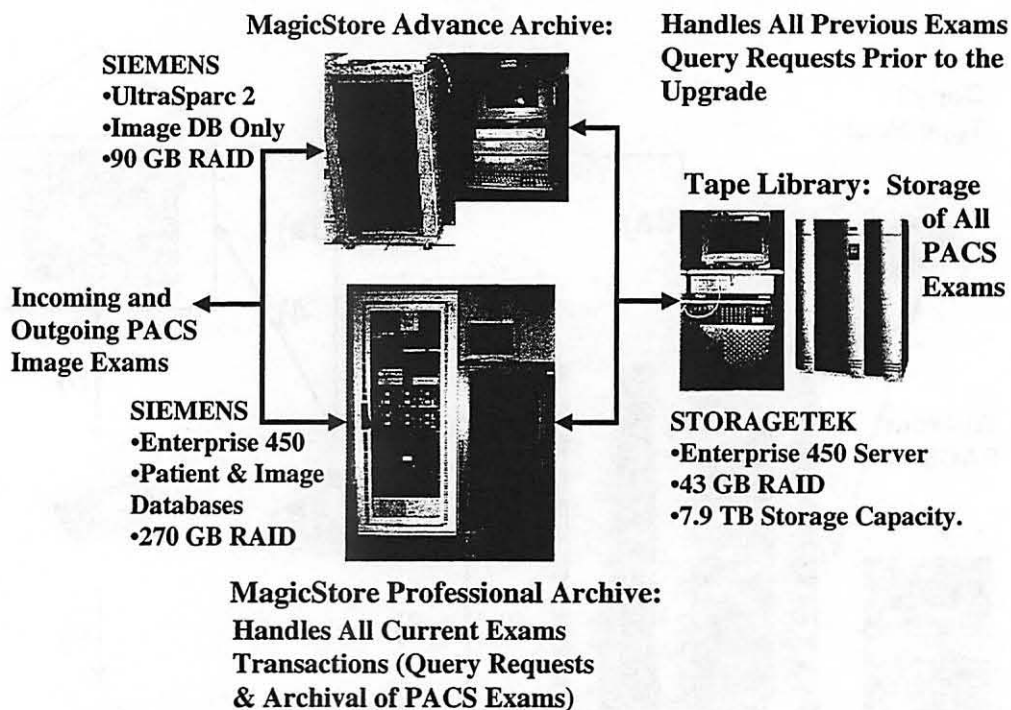


Figure 3: Final Archive Configuration and Processes for Saint John's Health Center PACS

#### 4. CONCLUSION

Due to the growth of a hospital's PACS volumes, it is necessary to upgrade and expand the archive, migrate the existing data, and provide a data back-up solution for disaster recovery process. With proper planning and contingency procedures, the amount of downtime necessary for the upgrade is reduced with very little impact on the clinical workflow and no loss of PACS data. In addition, a disaster recovery plan was developed to provide protection against loss of PACS data due to any potential disaster scenarios, which is crucial as more hospitals make the transition to a filmless institution.

In the future, Saint John's plans to remove the original archive server from the archive configuration so that the new archive server will handle all PACS exams requests. In addition, new options are being considered for a disaster recovery solution since the current solution is quite cumbersome and involves training of an operator to perform the daily tasks. Furthermore, should a disaster occur today, previous PACS exams would not be available until new hardware has arrived and been installed which may take a few weeks and possibly months. A new solution is currently being considered that will provide faster uptime for access to previous PACS exams and is presented in a paper titled "A Fault-Tolerant Back-Up Archive Using an ASP Model for Disaster Recovery" located in the same SPIE Proceedings [1].

#### REFERENCES

1. A Fault-Tolerant Back-Up Archive Using an ASP Model for Disaster Recovery, B.J. Liu, H.K. Huang, F. Cao, L. Documet, D.A. Sarti, *SPIE Medical Imaging*, Feb. 2002.

# A FAULT-TOLERANT BACK-UP ARCHIVE USING AN ASP MODEL FOR DISASTER RECOVERY

Brent J. Liu<sup>1</sup>, H.K. Huang<sup>2</sup>, Fei Cao<sup>2</sup>, Luis Documet<sup>1</sup>, Dennis Sarti<sup>1</sup>

<sup>1</sup>Department of Radiology, Saint John's Health Center, Santa Monica, CA 90404;

<sup>2</sup>Department of Radiology, Childrens Hospital LA/USC, Los Angeles, CA 90027

## ABSTRACT

A single point of failure in PACS during a disaster scenario is the main archive storage and server. When a major disaster occurs, it is possible to lose an entire hospital's PACS data. Few current PACS archives feature disaster recovery, but the design is limited at best. These drawbacks include the frequency with which the back-up is physically removed to an offsite facility, the operational costs associated to maintain the back-up, the ease-of-use to perform the backup consistently and efficiently, and the ease-of-use to perform the PACS image data recovery. This paper describes a novel approach towards a fault-tolerant solution for disaster recovery of short-term PACS image data using an Application Service Provider model for service. The ASP back-up archive provides instantaneous, automatic backup of acquired PACS image data and instantaneous recovery of stored PACS image data all at a low operational cost. A back-up archive server and RAID storage device is implemented offsite from the main PACS archive location. In the example of this particular hospital, it was determined that at least 2 months worth of PACS image exams were needed for back-up. Clinical data from a hospital PACS is sent to this ASP storage server in parallel to the exams being archived in the main server. A disaster scenario was simulated and the PACS exams were sent from the offsite ASP storage server back to the hospital PACS. Initially, connectivity between the main archive and the ASP storage server is established via a T-1 connection. In the future, other more cost-effective means of connectivity will be researched such as the Internet 2. A disaster scenario was initiated and the disaster recovery process using the ASP back-up archive server was success in repopulating the clinical PACS within a short period of time. The ASP back-up archive was able to recover two months of PACS image data for comparison studies with no complex operational procedures. Furthermore, no image data loss was encountered during the recovery.

**Keywords:** PACS, Archive Backup, Disaster Recovery, ASP

## 1. INTRODUCTION

In a clinical PACS one single point of failure during a disaster scenario is the main archive storage and server. During a major disaster, it is possible to lose an entire hospital's PACS data. Some common disaster scenarios include earthquake, fire, flood, sabotage, or any combination of these that results in the complete destruction of the archive storage and server. With the increasing presence of fully filmless hospitals it becomes more and more crucial to provide procedures to protect the PACS data. Some reasons for this include the fact that in a filmless environment, only one data copy of the PACS exam may be available in PACS. In addition, future HIPAA (Health Insurance Portability and Accountability Act of 1996) requirements may necessitate a disaster recovery solution for PACS data. Other factors include the importance of previous PACS exams for accurate diagnosis of the current exam. Even though new PACS exams can be acquired during a disaster scenario, previous exams may not be accessible if the archive storage and server has been destroyed. The overall damages and costs associated with a destroyed PACS archive storage and server is comparable to losing the entire onsite film archive of the hospital department. Because of these factors, procedures should include both data redundancy as well as PACS data recovery.

### 1.1 Current PACS Disaster Recovery Solutions

Current general disaster recovery solutions vary in the approach towards creating redundant copies of PACS data. For some PACS sites, there is no disaster recovery solution in which case the PACS data is extremely vulnerable to a catastrophic loss. However, other solutions include creating a secondary copy of each new PACS exam acquired. This secondary copy can be stored in a variety ways. First, the secondary copy can be held within PACS. This is usually not

recommended since the likelihood of it being destroyed is the same as the primary copy. A second option is to create the secondary copy and store the data media somewhere onsite in a fireproof safe or storage compartment. While this decreases the possibility of data loss, should the disaster be widespread throughout the local area, the PACS data is still susceptible to destruction. A third option is to store the data media offsite in a storage vault, a strategy adopted by most data centers. This third option is the best solution among the three previously mentioned for a disaster recovery solution.

PACS archives with large data media storage capacities such as digital tape usually have large data media elements that can store PACS data. These tape media can hold up to a few week's worth of PACS data. In this case, a secondary copy may not be enough to protect against a large catastrophic incident. This is due to the fact that should a disaster occur right when the most recent tape is being filled to capacity and has not been sent offsite, then the hospital could lose up to a few weeks' worth of PACS exams. Therefore, in these cases, it is necessary to create a third copy to cover the turnover period between secondary copy tapes. As with the secondary copy, there are a few options for the management of the third copy of PACS exams. The first is to store the third copy tapes onsite. The disadvantages to this option include the high likelihood of damage similar to the primary copy. Also, there must be recyclable data media for each day of the coverage period and must involve an operator to perform the daily backup cycle procedure. Even though this solution will provide proper redundancy of all acquired PACS data, the hospital must logistically still wait for new hardware to replace the damaged components in order to import the data media after a disaster. This could take another week to a few weeks depending on availability of hardware. In the meantime, Radiologists are dependent on the previous exams for an accurate diagnosis, which will not be available until the replacement hardware arrives and is installed. A second option is to store the third copy tapes offsite in a data storage vault. Although this option removes the likelihood of damage similar to the primary copy of the PACS exam, it still has the same issues as discussed previously with the first option as well as having to arrange for daily pickup of the data media that will be stored offsite. A third option is to create a third copy of the PACS exam and store the copy on a backup archive server offsite. With this option, a copy can be stored automatically and does not need operator to perform the daily backup cycle. In addition, the backup storage capacity is easily configurable based on the needs of the hospital. Some of the downsides of this option include the logistics of purchasing, maintaining, and supporting a backup archive server offsite by the hospital. During a disaster, there is a high likelihood that the network connection may be down and therefore access to the backup copies of the PACS exams would be very difficult. Saint John's Health Center PACS currently uses the method where a daily third copy backup tape is created and stored offsite.

This paper describes a novel approach towards a fault-tolerant solution for disaster recovery of short-term PACS image data using an Application Service Provider model for service. The ASP backup archive provides instantaneous, automatic backup of acquired PACS image data and instantaneous recovery of stored PACS image data all at a low operational cost because it utilizes the ASP business model. In addition, should the disaster render the network communication inoperable, a portable solution is available using a Data Migrator. The Data Migrator is a portable laptop with a large capacity hard disk that contains DICOM software for exporting and importing PACS exams. Currently, a laptop is utilized as the solution; however, in the future an even more portable solution may be offered where hot-swappable large capacity hard disks are used to physically transport the PACS data while the Data Migrator remains stationary at both sites. The Data Migrator can populate PACS exams that were stored on the backup archive server directly onto the clinical PACS within hours to allow the Radiologists to continue to read with previous PACS exams until new replacement hardware arrives and is installed.

## **2. METHODS AND MATERIALS**

### **2.1 General Architecture**

Figure 1 shows the General Architecture of how the ASP backup archive would integrate with a clinical PACS. The separate sites would be connected via some broadband connection. Currently, a T1 line can be established. However, as newer connectivity solutions become cost-effective and available (eg, wireless, Next Generation Internet or NGI), they can potentially replace the current T1 connection. On the hospital side, any new exam acquired and distributed in the PACS is sent from the clinical PACS Archive server to a DICOM Gateway. This DICOM Gateway is crucial towards maintaining the clinical workflow since it provides a buffer and manages the transfer of the exams should the connectivity traffic between the two sites becomes congested by queuing the PACS exams within the DICOM Gateway.

The DICOM Gateway proceeds to transfer an exam in its queue through the T1 router across the T1 line to a receiving T1 router at the offsite area. At the PACS storage site another PACS gateway receives the PACS exams and queues these exams to be stored into a Fault-Tolerant Backup Archive. This fault-tolerant backup is a continuously available (CA) archive has 99.999% availability utilizing triple modular redundancy architecture [1]. It is interesting to note that all PACS data transmitted throughout this architecture conform to the DICOM protocol standard.

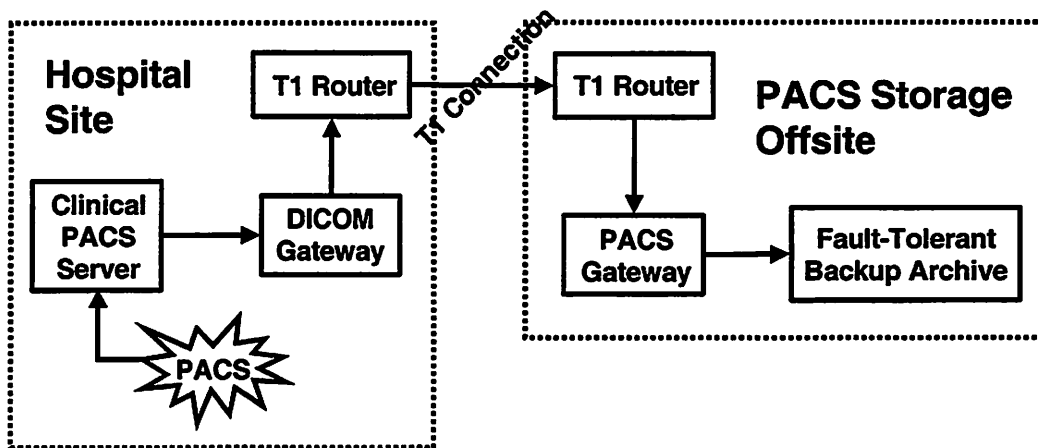


Figure 1: General Architecture of the ASP Backup Archive

## 2.2 Disaster Recovery Procedure

Figure 2 shows the recovery procedure of the PACS data should a hospital encounter a disaster scenario. If the connectivity between the two sites is still live, then the stored PACS exams can be migrated over to the hospital using DICOM compliant network protocols. At this point, the radiologist will have previous and current PACS exams to continue reading until the new hardware is replaced and the hospital archive is brought back online. However, in most disaster scenarios, there is likelihood that the connectivity between the two sites is not functional in addition to the damage to the hospital PACS archive. In this case, the PACS exams are imported into the hospital PACS from the fault-tolerant backup archive server using a portable Data Migrator. The portable data migratory will export the PACS exams from the fault-tolerant archive server. Then, it is physically brought to the hospital where the PACS exams can be imported directly into a workstation or server so that the radiologists will have previous cases to read. Since the portable data migrator is DICOM compliant the PACS exams can be directly imported into the hospital PACS without any additional software or translation. This recovery procedure can serve as an interim solution until the hospital PACS archive has been brought back online. The Data Migrator contains up-to-date PACS data since it is always synchronized with the clinical PACS workflow.

## 2.3 Key Features

- 1) Copy of PACS exam is created and stored automatically
- 2) Backup archive server is CA fault-tolerant with 99.999% availability
- 3) No need for operator intervention
- 4) Backup storage capacity easily configurable and expanded based on requirements and needs
- 5) Data recovered and imported back into hospital PACS within one day using a portable Data Migrator
- 6) DICOM-compliant and ASP model-based
- 7) System does not impact normal clinical workflow
- 8) Radiologists can read with previous exams until hospital PACS archive is recovered.

The next few paragraphs will describe a general step-by-step procedure of building this particular system. Included will be suggestions of potential resources within the hospital as well as any necessary ancillary personnel that should be involved in each of the procedures.

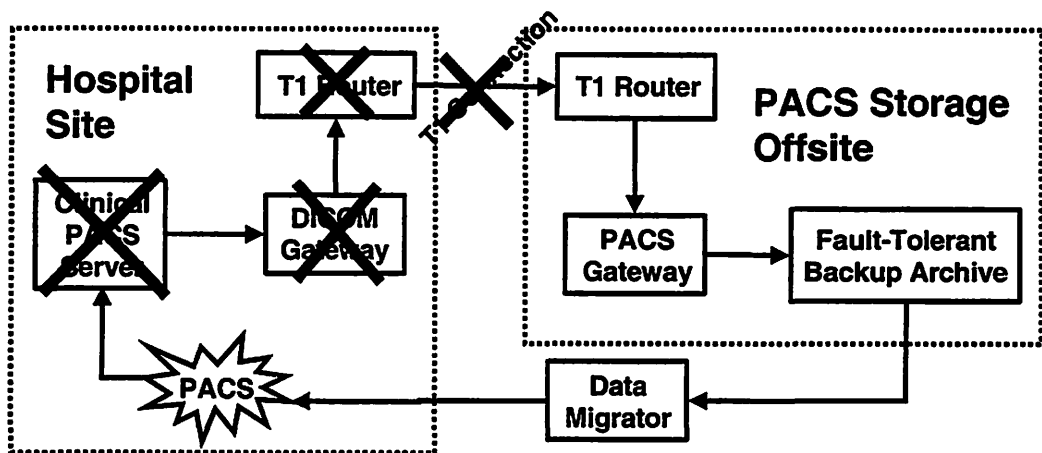


Figure 2: Disaster Recovery Procedure

#### 2.4 General Setup Procedures

Since this system will integrate with a clinical PACS, an important first step for implementing this system is to determine the configuration that will have the least impact on the hospital clinical workflow. The PACS system administrator and a clinical staff representative would help in this initial procedure since they are aware of the day-to-day operations involved with the hospital PACS.

The next few procedures center on establishing the connectivity between the hospital site and the backup archive server site. First, it should be determined the best connectivity bandwidth and configuration based on cost and availability. There currently are a variety of different options that range in costs. Some connectivity solutions may involve a continuous operational fee while others may involve a one-time initial cost for installation. The cost and availability also depends on the distance between the two sites. Because this is a complex decision, it is important to involve any resource that can provide information on options such as an information technology (IT) hospital staff member. In addition, it is important to involve the Radiology administrator, as there will be budget constraints that may factor into the decision-making process. Once the connectivity choice has been made, the next steps involve ordering hardware and installing it. This can be accomplished through a vendor but should also involve the IT and telecommunications staff members of both the hospital and the offsite location. Once the connectivity has been established, some testing should be performed to verify that the two sites are connected. Once again, this can be accomplished with the vendor as well as input from both an IT and telecommunications staff member.

At this point, the hospital and the offsite location have connectivity established. Testing of the clinical PACS workflow and the transmission of PACS exams to the backup archive server is necessary not only to verify that the PACS exams are received without any data loss but also to observe how this workflow will impact the clinical PACS. This is a crucial step in the procedure because the backup archiving procedure should appear seamless in terms of performance and usability to the clinical PACS user. The PACS system administrator may play a key role in determining the effects of the system on the clinical workflow. In addition, any testing of PACS data transmissions should be coordinated with an operator at the offsite location. If the new workflow is successfully integrated with the hospital PACS, the final step is to perform trial runs of disaster scenario simulations as well as test and verify the PACS data recovery process. These simulations should be coordinated with the PACS system administrator and an operator at the offsite location to insure that any results are observed as well as documented. Once all the tests are complete and verified, then the new workflow can become live in the clinical setting.

## RESULTS AND DISCUSSION

Saint John's Hospital has a filmless PACS that acquires approximately 130,000 Radiological exams annually. Although the hospital has a disaster recovery procedure implemented, the current procedures must involve an operator to perform daily tasks. In addition, should the archive encounter a disaster, the hospital would still be unable to provide previous PACS exams for the radiologists until new hardware has been shipped and installed. This could be an extended period of time. A more automatic and quick turn-round time solution is definitely desired. Using the procedural steps described above a system was implemented between the hospital site and the Image Processing and Informatics Laboratory (IPI) at Childrens Hospital/USC. The two sites are approximately 13 miles apart. First, a workflow with the least clinical impact was determined. Within Saint John's PACS, there is a workstation located within the Radiation Therapy Department that provides PACS exams to the treatment planning systems. It was determined that this workstation had the least impact on the overall clinical workflow since it is used on a sporadic basis. The new workflow was implemented where any PACS exams status marked "read" by the Radiologist is automatically sent to the workstation for storage offsite. Next, it was determined that a T1 connection would be the most feasible and cost-effective connectivity choice between the two sites. Since the backup is performed in the background, there was no need to speed up the network performance at the sacrifice of higher cost. A vendor was contacted to order the T1 connection and was installed connecting both sites. At this time, hardware for the T1 connectivity was ordered and installed as well. For each site, some physical connectivity inhouse was necessary to bridge between the vendor's T1 line installation and the inhouse network and was performed by the proper IT staff at each site. Once the hardware was in place, the next step was the configuration of the hardware and verification of the T1 connectivity. After the T1 connection had been established, PACS exams were sent from the hospital workstation to a PACS gateway workstation located at the backup archive offsite area. This gateway serves as a buffer prior to archival on the fault-tolerant backup archive. It is interesting to note, that a similar gateway on the hospital side would be desirable as well. Figure 3 shows the current Saint John's configuration to the ASP Backup Archive at the Informatics Laboratory located at Childrens Hospital LA/USC.

Table 1 shows the number of PACS exams that were tested on this system. A total of approximately 447 PACS exams comprising of 29,000 DICOM images of various modality types or 9 GB of total data were tested. Each exam was verified as successfully sent from the Saint John's PACS workstation to the fault-tolerant backup archive. The average T1 performance bandwidth was measured as 179 Kbytes/sec using the FTP protocol and 168 Kbytes/sec using the DICOM transfer protocol. In addition, disaster scenarios were performed with both the T1 connectivity alive as well as down. In both cases, PACS exams were successfully exported from the fault-tolerant backup server and imported directly into the PACS workstation at Saint John's using either the T1 connection or the portable Data Migrator.

During the implementation of this system, there were some pitfalls and challenges that occurred. The biggest issue was determining an appropriate PACS device to transmit exams to the offsite backup server that would have the least impact on the clinical PACS workflow. Initially, it was determined that the archive server at Saint John's would transmit all PACS exams across the T1 connection to the offsite backup server. However, the archive server performance would be affected since the T1 network performance bandwidth cannot support the large daily volumes of PACS exams. Therefore, the hospital archive server would have to queue all the daily PACS exams which would then affect the performance of other network functions that need to be performed within the hospital PACS. Another option was to use the fileroom workstation to perform the daily backup. However, this workstation is a highly used workstation especially since the film librarians perform a lot of functions with that specific workstation. The final decision was then to use the PACS workstation located in the Radiation Therapy department since it had the least clinical impact. The ultimate solution is to implement a DICOM gateway workstation that will receive the daily PACS exams from the hospital PACS and perform the network transmission across the T1 connection to another gateway workstation located offsite where the backup archive server resides. In addition, should the T1 network traffic become congested, the gateway has its own queue to manage the PACS data transmissions. These gateway workstations act as a buffer for the two separate systems and creates the least impact on the hospital PACS workflow. Because this system utilizes resources from various areas like IT, Telecommunications, PACS, Radiology for both the hospital and the offsite location, another challenging aspect of the implementation was to clearly define the roles that each of the resources would play assisting with the implementation. Careful attention to the installation of the T1 connection is most challenging as it involves the vendor as well as all the other resources listed above. The best solution is to define roles

for the connectivity, hardware, and software portions of the connectivity between the two sites as well as identifying the appropriate software vendor support. Finally, although all components within the system utilize the DICOM protocol, a key issue is to thoroughly test and verify the entire workflow prior to going live since there are different software products involved in the integration of this system by transmitting PACS exams of multiple modality types.

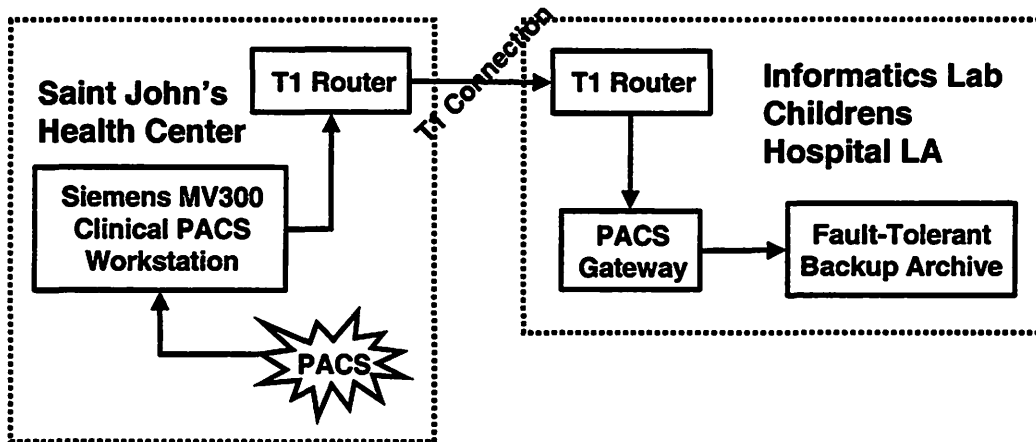


Figure 3: Saint John's Health Center/Childrens Hospital LA Configuration

	CT Exams	MR Exams	CR Exams	US Exams	RF/Angio Exams	Total
<b>No. of Exams</b>	111	110	109	61	56	447
<b>Total Images</b>	10,385	15,977	164	1,981	497	29,004
<b>Avg No. Of Images Per Exam</b>	93.6	145	1.5	32.5	8.9	
<b>Data Size (MB)</b>	5192.5	998.6	1312	495.3	994	8992.4

Table 1: Results of PACS Exams Stored Using the ASP Backup Archive

### CONCLUSION

The system has been implemented successfully and PACS exams from Saint John's Health Center are backed up to an offsite fault-tolerant archive server. Future plans include further burn-in testing for a specific length of time. Another plan is to add an additional DICOM gateway on the hospital side to handle extreme PACS volume loads. The current backup storage capacity is configured for two months. After burn-in testing is complete, it may be necessary to review the current capacity configuration and make any necessary changes. Once everything has been finalized, the system can be turned over to full operational status.

In summary, it is possible to provide a short-term fault-tolerant back-up archive server using the ASP model that is instantaneous in archiving and recovering PACS image data. In addition, there is little or no manual operator intervention in the archiving and recovery procedures. During a disaster scenario, the ASP back-up archive server can repopulate a clinical PACS quickly with the majority of studies available for comparison during the interim until the main PACS archive is fully recovered. The solution is both cost-effective because it is based on the ASP business model, as well as elegant as a disaster recovery solution, which will become even more crucial as the filmless environment expands.

## **ACKNOWLEDGMENT**

This work is partially supported by the US Army Medical Research and Materiel Command Contract No. DAMD17-99-P-3732, NIH National Library of Medicine Contract No. N01-LM-9-3538, and Reliant Care, Inc.

## **REFERENCES**

1. Fault-Tolerant PACS Server Design, H.K. Huang, F. Cao, B. J. Liu, J. Zhang, Z. Zhou, A. Tsai, G. Mogel, *SPIE Medical Imaging*, Vol 4323-14, Feb. 2001.

# PACS SIMULATOR

## A STANDALONE EDUCATIONAL TOOL

Z. Zhou<sup>1</sup>, H.K. Huang<sup>1</sup>, F. Cao<sup>1</sup>, B. Liu<sup>2</sup>, J. Zhang<sup>3</sup>, G. Mogel<sup>1</sup>, J. Zhuang<sup>3</sup>, X. Zhang<sup>3</sup>

<sup>1</sup>Department of Radiology, Childrens Hospital LA/USC, Los Angeles, CA 90027

<sup>2</sup>Department of Radiology, Saint John's Health Center, Santa Monica, CA 90404

<sup>3</sup>Shanghai Institute of Technical Physics, Shanghai, China

### ABSTRACT

Many educational courses have been designed for training radiologists and allied healthcare providers to operate PACS workstations. There are yet tools available for training of PACS concepts and workflow analysis. We have designed and implemented a PACS Simulator for this purpose. The PACS Simulator consists of five key components that simulates a typical clinical PACS: acquisition modality Simulator (AMS), DICOM gateway, a continuous available (CA) fault-tolerant (FT) PACS server (UNIX-based), two clinical viewing workstations, and the network infrastructure with a 100 mbits/sec Ethernet switch connecting all the PACS components. A generic DICOM compliant PACS software package is used to simulate normal clinical data flow. Using this simulator, trainees can:

1. Observe clinical PACS operation component by component
2. Trace image flow through each component
3. Query and retrieve images from workstations and observe the image flow
4. Review images from workstations
5. Identify PACS data flow bottle neck,
6. Induce failure in a component to observe its impact on the PACS workflow and operation

The PACS simulator is a valuable tool for participants to gain knowledge towards the complexity of PACS data flow with hand-on experience. The next version of the PACS Simulator will be an addition of an HIS Simulator connected to the AMS and PACS server for simulating the input of patient related information.

**Key words:** PACS, DICOM, Simulator, Acquisition modality simulator, Gateway, Fault-tolerant PACS controller, Viewing workstation

### 1. INTRODUCTION

A picture archiving and communication system (PACS) [1] is a medical imaging management system for the healthcare enterprise. It consists of images and textual data of various imaging modalities (such as CT, CR, MR, and US images) and storage and display subsystems connected by various digital networks. As a concept that began in the early 1980s [1], PACS is widely used in hospitals and imaging institutions now. Since PACS is a digital radiology management system, it changes the traditional radiologists' workflow. Therefore, to learn and master how to utilize, manage and support a PACS becomes an important process for radiologists and PACS administrators within a clinical site. Many educational courses have been designed for training radiologists and new residents in learning how to operate PACS workstations, as an example, a PACS training course offered by The Department of Radiology, University of Pennsylvania Health System [2] or at the RSNA (Radiological Society of North America) conference. However, they are either lecture format or focus only on the end-user workstations. There are yet tools available for training of concept and workflow analysis throughout the entire PACS. We have developed a PACS Simulator as a stand-alone tool for trainees to understand the overall PACS concept and image dataflow. It gives participants valuable hand-on experience of PACS data flow. The PACS simulator consists of five key components simulating a typical clinical PACS: acquisition modality simulator (AMS), DICOM [3] gateway, continuous available (CA) fault-tolerant (FT) [4]

PACS server (UNIX-based), two clinical viewing workstations, and the network infrastructure with a 100 mbits/sec Ethernet switch connecting all the PACS components. A DICOM compliant PACS software package is running on the PACS components to simulate a typical clinical PACS workflow. The AMS (Acquisition Modality Simulator) is connected to a clinical PACS and contains thousands of CT, MR, US, CR, and digitized film examinations. These images are replenished continuously throughout the clinical PACS network. Image exams are fed from the AMS to the DICOM gateway continuously in a loop simulating the continuous clinical environment. From the DICOM gateway they are pushed to the PACS server for archival and to the workstations for review.

We have successfully used this Simulator as a standalone PACS training tool 24 hours/day, 7 days/week for four months to simulate a clinical PACS operation. Therefore, this PACS Simulator becomes a very good standalone PACS training tool for radiologists, residents and healthcare providers.

## 2. PACS SIMULATOR SYSTEM DESIGN AND IMPLEMENTATION

A typical PACS (Picture Archiving and Communication System) consists of image and data modalities, acquisition gateways, a PACS controller and archive, display workstations and a network infrastructure connecting all these components [1]. To simulate a typical PACS, the PACS simulator consists of five key components: acquisition modality Simulator (AMS), DICOM gateway, CA FT PACS server (UNIX-based), two clinical viewing workstations, and a network infrastructure with a 100 mbits/sec Ethernet switch connecting to all these components. Figure 1 shows the architecture of the components of PACS simulator. The AMS randomly generates DICOM compliant exams and sends the exams to the DICOM gateway automatically or manually. Upon receiving the exams from the AMS, the DICOM gateway automatically sends the exams to the PACS controller. Once the PACS controller receives the exams, the controller stores them in the database and archive device for long-term storage. It also distributes the exams to two viewing workstations either automatically or by query/retrieve function. The viewing workstations put the exams into a local database and hard disk ready for clinical diagnosis.

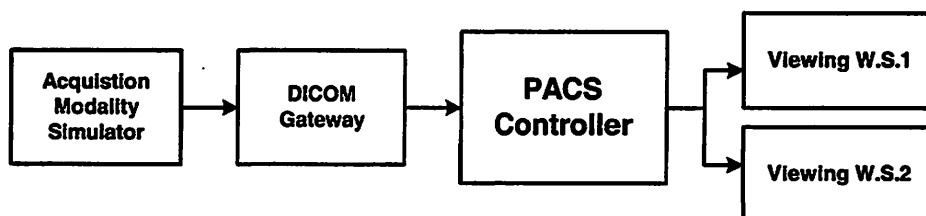


Figure 1. Architecture of the components of PACS simulator

### 2.1 Acquisition modality simulator

There are various imaging modalities (e.g., CR, CT, MRI, etc.) in clinical PACS and they generate thousands of images everyday. Though the functionality of these modalities is different, their basic workflow is almost same. They generate images and send them to the DICOM gateway automatically or manually. We developed an acquisition modality simulator (AMS) to simulate the basic workflow of these modalities. To simulate clinical modalities, we first studied how clinical modalities work. Suppose there are 2 CT, 1 CR and 3 MR modalities in a clinical PACS. These modalities generate hundreds of examinations and thousands of images everyday. These exams are generated in a random time order. For example, there are 2 CT exams, 2 CR exams, and 2 MR exams generated at 10 o'clock, while there may be 3 CT exams, 1 CR exam, and 1 MR exam generated at 11 o'clock. The order these exams are sent to the DICOM gateway is also random since they are sent to the DICOM gateway separately. To simulate such kind situation, the AMS is connected to a clinical PACS and contains thousands of CT, MRI, US, CR, and digitized films

examinations in its local hard disk. The images are replenished continuously through the clinical PACS connection. AMS can randomly generate 4-6 (User can set the number of examinations) exams each time and automatically send them to the DICOM gateway. This process is a continuous loop to simulate the continuous clinical environment. Since most clinical modalities have the function to manually select and send exams, the AMS also allows users to manually select examinations from a list of Patient/Series exams or a list of exam modalities and send them manually to DICOM gateway. By using the AMS, the radiologists can easily understand the workflow of clinical modalities while at the same time it is not necessary to physically go to the clinical modalities to observe the characteristics since modalities are usually busy with patients and not used for demonstration or training.

The AMS is a simulation software running under WINDOWS 98/NT4/2000 environment. It consists of three sub-modules and one user interface. The first module is to receive the various exams from clinical PACS. It acts as a simple DICOM Storage SCP. It receives all kinds of DICOM-compliant exams and stores the exams in the local hard disk. The second module manually loads the exams from local disk to the local database. The third module is a simple DICOM Storage SCU. It sends the exams to the DICOM gateway. Figure 2 shows the flow chart of these three sub-modules. There is a main user interface (Figure 3) of the AMS for the user to generate and send the exams. The user can set the number of random exam generation and send option (automatic or manual). The user can also select exams from a worklist using 'Patient View' or 'Modality View' and manually send the exams to the DICOM gateway. The user interface also shows statistical information of the exams and the send process data/results.

The AMS requires a common PC with large capacity hard disks. We use a Dell PIII 600 MHz with a 20 Gbytes hard disk.

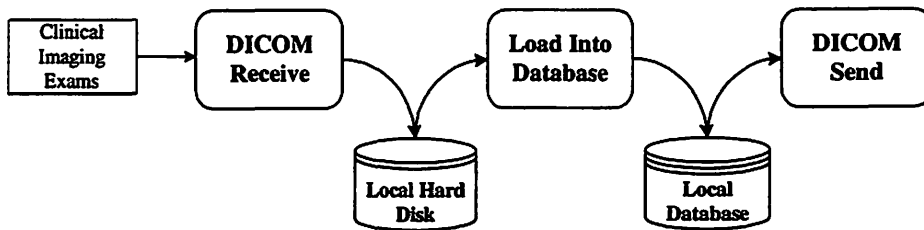


Figure 2. Work Flow Chart of the AMS (Acquisition Modality Simulator)

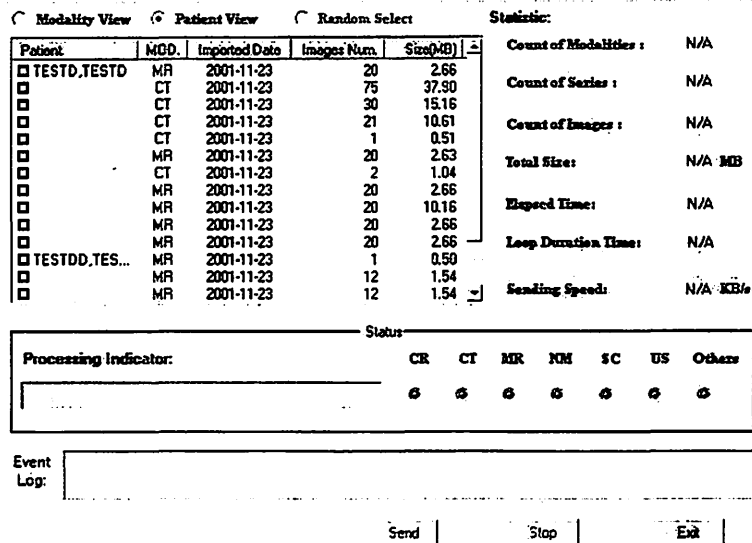


Figure 3. User Interface of the AMS (Acquisition Modality Simulator)

## 2.2 DICOM gateway

The DICOM gateway receives a DICOM exam of any modality type and sends the exams to a PACS device node (e.g., PACS controller). It performs three functions. First, it receives images from different imaging modalities for the PACS controller to archive [1]. There are various imaging modalities in clinical PACS and these modalities come from different vendor/manufacturers. Even though these modalities are DICOM compliant, each has their own DICOM conformance statements. The DICOM gateway has to communicate with all these different modalities and receive all the exams. Second, it verifies the image format and reformats images into the DICOM format if they are not standard DICOM-compliant. There may be some legacy non-DICOM compliant modalities in hospitals. The DICOM gateway has to receive the exams from these modalities and convert them into DICOM format. Thirdly, it performs the transmission automatically and verifies whether the transfer of the exam was complete without image loss – an important task that most modalities currently do not perform. Most of the DICOM gateway is transparent to the users and it automatically sends the exams from various modalities. It also verifies whether any image is lost during the transmission of the exam, which is a very important issue of a successful PACS.

We developed a generic DICOM gateway that supports most of the DICOM compliance modality exams and also some non-DICOM compliant modality formats, like TIFF and MPEG. It can convert the non-DICOM compliant modality exams to the standard DICOM format. The DICOM gateway receives the exams from the AMS and automatically sends them to the PACS controller for archival. Since the exams in the AMS are already DICOM compliant, they don't need to be reformatted. However, this feature enables the PACS simulator to support non-DICOM compliant modalities as well. The DICOM gateway is a software running under WINDOWS NT4/2000. It consists of three sub-components in a sequential processing chain with a first-in-first-out (FIFO) model [5] as shown in Figure 4. The first component is a DICOM/non-DICOM receive program. It receives DICOM-compliant exams from the AMS and put the exams into Queue1. Then, the second component retrieves the exams from Queue1 and loads them into a local database and puts the DICOM compliant exams (the non-DICOM compliant exams have to be converted into DICOM format first) into Queue2. Finally, the third component retrieves the exams from Queue2 and sends them to a PACS node (e.g., PACS controller). From this sequential process, the DICOM gateway assures that every exam sent to the PACS controller is DICOM-compliant and makes the whole process flow quickly and efficiently. The DICOM gateway provides three user interfaces for users to understand the above workflow. The user can watch the data flow

through these interfaces, and can even induce the failure of the data flow by simply stopping one of these three components.

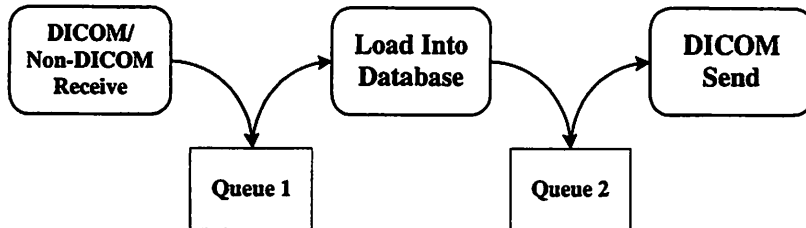


Figure 4. Data flow of DICOM gateway

### 2.3 PACS controller

The PACS controller can be considered the engine of the PACS [1]. It receives and archives DICOM exams of various modalities. It is responsible for the automatic or on-demand distribution of exams to a PACS node (e.g., diagnostic workstation). It is also responsible for the short-term and long-term storage of all modality type exams. We developed a generic CA FT UNIX-based PACS controller that supports standard DICOM Storage and Query/Retrieve services. It receives exams from the DICOM gateway and stores them in the local hard disk. It can automatically send the exams to two viewing workstations based on a simple routing mechanism. Users at the viewing workstation can also query/retrieve exams from the PACS controller by patient/study information.

The PACS Controller software is running on the UNIX (Solaris) environment. It consists of six processes. Figure 5 shows the data flow of PACS Controller: The PACS controller waits for incoming request. If the incoming request is a storage request from the DICOM gateway, the 'dicom\_storage' process receives the exam and puts one task (new exam) to the Queue1. The 'Insert into database' process takes the task from Queue1 and inserts the patient/exam data into the PACS database and puts a new task to the Queue2. The 'Routing' process takes the task and adds the routing information of this exam to Queue 3 with a new task if automatic send is enabled. The 'dicom\_send' process takes the task from Queue3 and automatically sends the exam to a destination such as a viewing workstation. If it is a Query/Retrieve request from a viewing workstation, the 'query/retrieve' process searches the PACS database and puts a new task (retrieval result) to Queue 4. The 'Q/R\_send' process executes the task and sends the retrieval result exams to the requesting viewing workstation. The PACS database was developed using a DICOM-compliant model built on ORACLE database system. The queues, 'Queue 1' to 'Queue 4' are structured tables built in ORACLE database. With this FIFO model, PACS controller processes DICOM Storage and Query/Retrieve in a pipeline manner, which has been proven to be quick and efficient.

Most of the PACS training courses do not provide training in the data workflow of a PACS controller because the PACS controller is complex and usually connected to a high-end archive device. We separated the archive device from the PACS controller since the archive device will not affect the basic workflow of the PACS controller. The user can understand better the workflow of the PACS controller by using the developed software. They can even manually induce failure to the data workflow of the PACS controller by stopping any of the above processes.

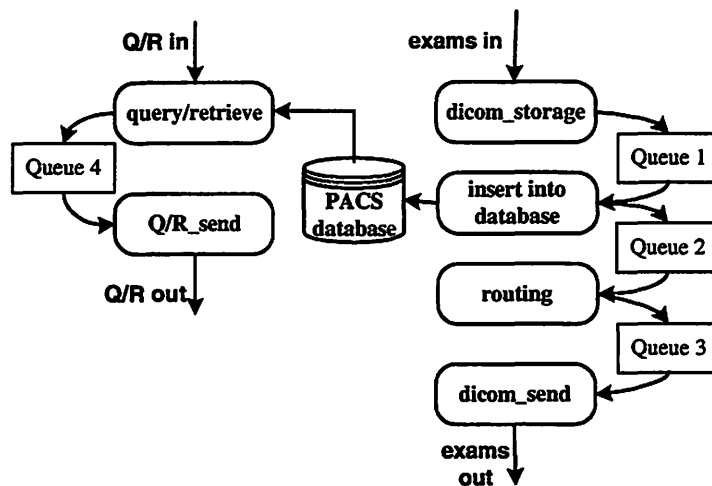


Figure 5. Data flow of PACS controller

## 2.4 Viewing workstation

The viewing workstation is the last component in the PACS workflow [1]. The user can view the exams with relevant data and generate the diagnostic report. It receives exams either automatically, or on-demand through query/retrieval from the PACS controller. The viewing workstation includes three main components: a computer, a user-friendly viewing software, and a high-resolution display hardware. Because the quality of the display monitor can affect the viewing or diagnostic result, a very high-resolution monitor is usually required for clinical usage. The viewing software includes an image receive module and an image display module. The image receive module is a very simple DICOM-compliant program. It receives any type of modality exams from the PACS controller. The image display module must be very user-friendly and tailored to the radiologists' workflow. Radiologists have special requirements for display software for diagnostic purpose, which usually translates into retrieving the image from PACS controller as quickly as possible with some image processing tools to produce the final result easily and quickly.

To make the PACS simulator applicable for clinical training, we used a dual 2K\*2K DOME C3 digital flat-panel display system [6], almost the most advanced product available now, as the viewing monitor for one viewing workstation. The viewing software (VR Read 4.0 [7]) is from Cedara Software Corporation. By using the viewing workstation, the user can not only watch the data workflow during query/retrieval of exams from the PACS controller, but also receive training on how to view clinical image data on state-of-the-art high-resolution monitor. Figure 6 shows a screen shot of CR chest images displayed by VR Read 4.0 on the dual DOMC C3 digital flat panel monitors.

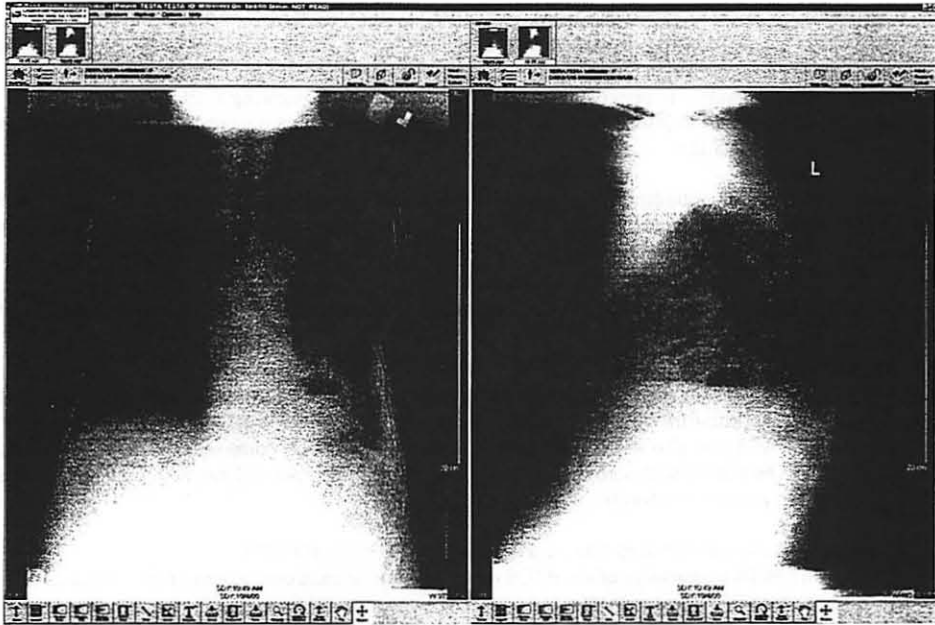


Figure 6. A screen shot of CR chest images in a dual 2K\*2K DOME C3 digital flat-panel display system with a viewing software (VR Read 4.0) from Cedara

### 3. TRAINING PROTOCOLS OF PACS SIMULATOR

#### 3.1 Attendee Requirements

The PACS simulator is specially designed for training of radiologists, residents, new PACS administrators and related PACS management and support personnel. Before the onset of any training protocol for the PACS simulator, the attendees must have some knowledge of the basic concept of PACS. Therefore, it is expected that the attendants have read and familiarized themselves with material on PACS. Additional clinical experience within the Radiology department can be a benefit as well.

#### 3.2 Training Curriculum

The training curriculum is divided into two levels based on the fact that attendees may have different levels of technical and clinical expertise as well as different requirement of training. The two levels of training are:

- 1) Basic PACS Concepts and Data Workflow
- 2) Advanced PACS Technical Concepts and Data Workflow Training and Troubleshooting

##### 3.2.1 Curriculum Level I: Basic PACS Concept and Data Workflow

This introductory training is geared primarily for radiologists, residents and those that only need to learn the basic concepts and data workflow of PACS. Their training requirements are more centered on the basic concepts and data workflow of PACS. In addition, they would require some limited hand-on training on specific PACS components (e.g., Viewing workstation). The training session includes 5 components:

- (1) Introduction of the concept and data workflow of a typical clinical PACS.
- (2) Explanation and Demonstration of the PACS data workflow of each component of the PACS simulator by operating on each component.
- (3) Training of the attendees to operate on a specific workstation, e.g., viewing workstation.
- (4) Attendees are required to provide answers to some questions based on the concept and data workflow of PACS.
- (5) Visit a clinical PACS site.

An experienced PACS system administrator of a filmless PACS site will perform components 1, 4 and 5. A PACS technician will be responsible for leading components 2 and 3. The training period can be one or two days based on the availability of the attendees. Therefore it is feasible to complete the training session in any weekend.

### **3.2.2 Curriculum Level II: Advanced PACS Technical Concepts and Data Workflow Training and Troubleshooting**

This training session is for new PACS administrators and related PACS management and support personnel, and is designed as a continuation of the introductory course. The attendees will not only learn the basic concepts and data workflow of PACS, but also will receive hand-on experience of every component of the PACS simulator. In addition, attendees will be trained with some ability to analyze and troubleshoot failures within the PACS data workflow. The training session involves 6 components:

- (1) Introduction of the concepts and data workflow of a typical clinical PACS.
- (2) Explanation and Demonstration of the PACS data workflow of each component of the PACS simulator by operating on each PACS component.
- (3) Training of the attendees to operate on each component of the PACS simulator.
- (4) Training the attendees to manually induce failures to each of the PACS component and observe the results and its effects on the entire PACS data workflow.
- (5) Training of the attendees to analyze and recognize some common failures within the PACS simulator as an operator manually induces them.
- (6) Visit a clinical PACS site.

An experienced PACS system administrator of a filmless PACS site will perform components 1, and 6. A PACS technician will be responsible for leading components 2 through 5. Similar to level I, the training period can be two or more days based on the availability of the attendees, which means that it can be scheduled within a weekend as well.

## **4. CONCLUSION**

We have successfully developed a PACS simulator as a standalone training tool for radiologists and new PACS administrators and support personnel as well as relevant healthcare providers. The same simulation also has been successfully performed in the Educational Exhibit at RSNA 2001. Furthermore, the PACS simulator has been successfully applied to test our Fault-Tolerant PACS server [4].

A by-product of the PACS Simulator is to be used as a standalone testing bed for any new PACS related components, including both software and hardware. Since the PACS simulator supports most of the DICOM compliant device or software, user can test whether a new component complies with the DICOM in an existing PACS system before it is connected to a clinical PACS system.

Since most PACS are connected to a Radiology Information System (RIS) or a Hospital Information System (HIS), we are in the process of building a HIS/RIS connected PACS simulator based on the concept of IHE (Integrating of Healthcare Enterprise) [8]. Then a complete training tool which can be available for not only radiologists but other relevant healthcare providers and support personnel.

## ACKNOWLEDGEMENT

This work is partially supported by the US Army Medical Research and Materiel Command Contract No. DAMD 17-99-P-3732, NLM Training Grant Contract No 1T15LM07356-01, and Reliant Health Care, Inc.

## REFERENCES

1. Huang HK. *PACS: Basic Principles and Applications*, Wiley & Sons, 1999.
2. Department of Radiology, University of Pennsylvania Health System <http://www.rad.upenn.edu/PACSWeb.html>.
3. Digital Imaging and Communication in Medicine (DICOM) PS 3.1-2000, National Electrical Manufacturers Association
4. Fault-Tolerant PACS Server Design, H.K. Huang, F. Cao, B. J. Liu, J. Zhang, Z. Zhou, A.Tsai, G. Mogel, *SPIE Medical Imaging*, Vol 4323-14, Feb. 2001.
5. Zhang J., Andriole, K., and Huang, H.K., Computed Radiographic Image Post-Processing in Picture Archiving and Communication System. *SPIE Medical Imaging*, Vol. 3035, 1997.
6. DOME imaging systems, C3 digital flat-panel display system, <http://www.dome.com>
7. Cedara Software Corporation, VR Read 4.0, <http://www.cedara.com>
8. IHE Technical Framework Year 3, <http://www.rsna.org/IHE>

# **A PACS and Imaging Informatics-based Radiation Therapy (RT) Server**

Maria Y.Y. Law \*<sup>1</sup>, Xiaoyan Zhang<sup>2</sup>, Jianguo Zhang \*\*<sup>2</sup>, H.K. Huang \*\*\*<sup>1,3</sup>

<sup>1</sup>Dept. of Optometry and Radiography, The Hong Kong Polytechnic University; <sup>2</sup>Shanghai Institute of Technical Physics, Chinese Academy of Sciences; <sup>3</sup>Childrens Hospital Los Angeles/University of Southern California

## **ABSTRACT**

Radiation therapy (RT) is an image intensive treatment. It requires images from projection X-rays, CT, MR, PET for tumor localization, treatment planning and verification of treatment plans. It also needs patient information, images and their processing for tumour localization and dose computation to ensure the delivery of uniform high dose to the target but avoidance of sensitive structures. In these processes, PACS and imaging informatics technologies are used extensively. However, they are not integrated with these technologies as a complete radiation treatment system. Currently RT treatment still relies mostly on tedious manual image and data transfer methods because the community as a whole has not championed the concept of system integration heavily. System integration of RT treatment has many benefits including lower equipment and operation costs, streamline treatment procedures, and better healthcare delivery to the patient. In this paper, we discuss the concept of a PACS and imaging informatics-based RT server as an attempt to integrate diverse healthcare information systems, imaging modalities and RT equipment into one seamless treatment system.

**Keywords:** PACS, imaging informatics, radiation therapy, server

## **1. INTRODUCTION**

Picture archiving and communication system (PACS) is an image management system. It combines both imaging modalities and related patient information systems. PACS integrates images of a patient from magnetic resonance, computed tomography, ultrasonic, computed and digital radiography, digital subtraction angiography, nuclear medicine, and endoscopy images, archives them into a database, and distributes selectively to designated workstations for review and diagnosis. PACS has been integrated into daily clinical operation by many healthcare centers and clinics since 1992. Although it has not been stated formally, PACS was developed for diagnostic purpose. However, it can be extended to applications for other purposes. The image-based radiation therapy (RT) server we discuss below is such an example. Figure 1 shows the generic PACS architecture and its connection to different application servers, RT server to be discussed here is one of them. PACS uses DICOM as image format and communication standard and HL-7 as textual information standard. [1]

Radiation therapy (RT) is an image intensive treatment. Images are not only required from diagnostic modalities but also from treatment equipment. The treatment requires images from projection X-rays, CT, MR, PET for tumor localization, treatment planning and verification of treatment plans. These processes need patient information to plan a treatment; image registration to identify regions to be treated, and markers to align images; image fusion to delineate pathological structures from various imaging modalities, anatomy to identify the shape, size, and location of the targets and radio-sensitive vital organs; and dose computation to ensure the delivery of uniform high dose to the target but avoidance of sensitive structures. In addition, carefully monitoring treatment optimization and dose calculation are essential for successful patient outcome. In these processes, PACS and imaging informatics technologies can play an extensive role. However, they are not used to integrate various radiation treatment information into a complete system. Currently RT still relies mostly on tedious manual

image and data transfer methods because the community as a whole has not championed the concept of system integration heavily. System integration of RT has many benefits including lower equipment and operation costs, streamline treatment procedures, and better healthcare delivery to the patient. This paper attempts to discuss the concept of system integration in radiation therapy through the PACS and an image-based RT server.

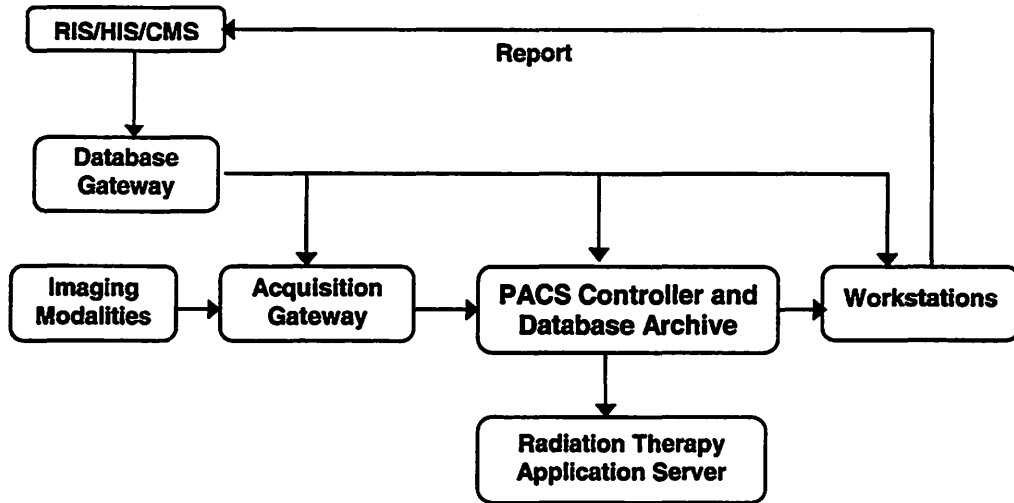


**Fig. 1 Basic PACS architecture and connection to application server**  
 RIS: Radiological Information System; HIS: Healthcare Information System;  
 CMS: Clinical Management System

## 2. METHODOLOGY

Setting standard is the key to system integration. While DICOM format is the standard for imaging informatics in PACS for integrating radiological modalities from different vendors, DICOM RT is the standard used for integrating radiation therapy images, treatment plans and records. DICOM RT and its objects are explained in the paragraphs below. When the standard is in place, the workflow in radiation therapy is reviewed to enable the design of the dataflow of radiation therapy images.

### DICOM Standard and DICOM RT

DICOM is the de facto standard in medical imaging format and communication and has been used by PACS users and vendors for many years [2]. RT uses radiological images and images from the simulator and linear accelerator for planning, treatment, and verification. It is therefore advantageous to use DICOM as its image and data communication standard [3]. Between 1994-97, DICOM Working Group 7 was formed under the auspices of NEMA (National Electrical Manufacturers' Association) to define the DICOM standard for RT. As of 1999, seven RT-specific DICOM objects were ratified [4]:

- RT Structure Set (97) contains information related to patient structures, markers, isocenter and related data.

- RT Plan (97) refers to information contained in a treatment plan such as beam angles, collimator openings and beam modifiers
- RT Image (97) includes all images taken using radiotherapy equipment such as conventional simulators, digitizers for simulator films or electronic portal imagers
- RT dose (97) contains dose data such as dose distribution generated by treatment planning system, DVH (Dose Volume Histogram), dose points etc.
- The remaining 3 objects are RT Beams Treatment Record (99), RT Brachy Treatment Record (99), and RT Treatment Summary Record (99).

When the DICOM RT standard is complied, informatics in the RT Server can be standardized. To illustrate RT information stored in the image informatics-based RT server using the DICOM RT objects, the example of a conventional radiation treatment for prostate cancer is used.

The patient undergoes CT and MR diagnostic examinations (DICOM Standard) of the pelvis, images of which are archived in the PACS server. If fusion needs be done to the pelvic images from different modalities, images can be retrieved from the PACS server for fusion of images at a fusion application workstation. The radiation therapy treatment planning system (TPS) or the virtual simulator (VS) workstation can also retrieve the relevant CT/MR images or the CT-MR fused images for treatment planning. The diagnostic images as well as the fused images are *RT Image* objects of the DICOM RT. In the TPS or virtual simulator, the tumor in the prostate gland is outlined as well as critical organs such as the urinary bladder and rectum. These are the *RT Structure Set* objects. With such information, an *RT Plan* is designed with all the treatment parameters such as beam size, gantry angle, and collimator angle. The resultant treatment plan should deliver uniform dose to the target volume of the prostate tumor while avoid dose to critical organs such as the urinary bladder and the rectum. Digital reconstruction can also be performed in either the TPS or Virtual Simulation workstation when the radiation fields are inserted. The images so produced are *RT image* objects. Dose calculation will be done in the TPS and a plan with isodose distribution is generated. Using the DVH (Dose Volume Histogram), the resultant plan can be evaluated. All such dose related information is in the arena of *RT Dose*.

Information of the treatment plan (*RT Plan* object) of the prostate tumor from the TPS can be exported to a Linear Accelerator (LINAC) to initiate the treatment. A portal image of the treatment region, *RT Image* object is taken in the LINAC and be compared with the DRR generated from the TPS/Virtual Simulation workstation or a digitized simulator image (when no virtual simulation facility is available), another *RT image* object. The LINAC will generate the daily treatment record or summary record (both are *Treatment Records* objects) for each patient.

When the RT objects are stored in the RT Server, the diagnostic and treatment information of the same patient can be easily retrieved and distributed for evaluation and confirmation. This is particularly advantageous when treatment progress needs to be assessed and at times of follow-up for reviewing patients' progress. It also reduces a lot of efforts in searching for old clinical files and treatment files when retrospective studies are called for. The data stored in the Image-based RT Server can also be retrieved for enriching teaching materials.

### Workflow of RT Images

In this section, we review the conventional workflow of RT images. Based on this workflow and making use of the DICOM RT Objects described, we can design the dataflow for the RT server. Figure 2 shows the workflow of image-based conventional radiation therapy.

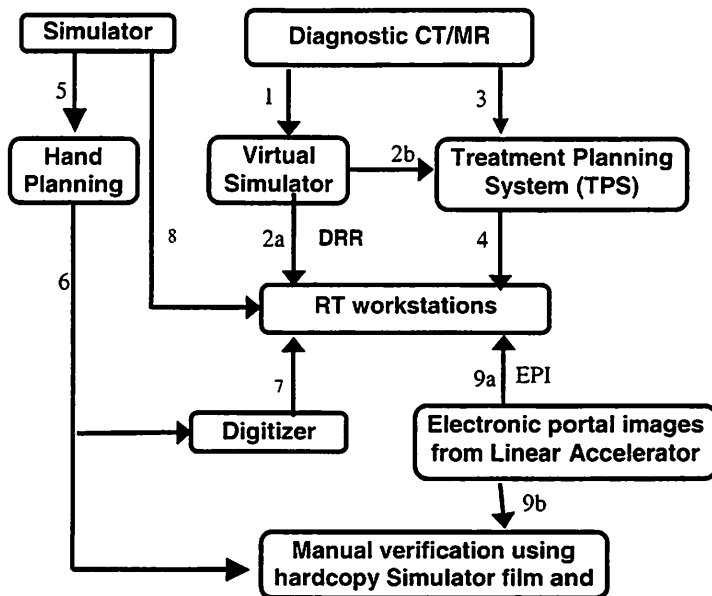


Figure 2. Workflow of image-based Conventional Radiation Therapy  
 DRR: Digital reconstructed radiograph

With reference to Figure 2, the workflow can be described in the following routes:

Route 1

- i. CT or MR scans of the region of the body for radiation treatment planning can be acquired from a diagnostic CT or MR scanner or a CT simulator.
- ii. The CT/MR images can be sent either to:
  - a. The Virtual Simulator when only beam positioning and shielding are required or
  - b. The Treatment Planning System (TPS) when radiation distribution isodose plans need to be generated in addition to what is done in a.

Route 2 a

- i. At the Virtual Simulator (VS), digital reconstructed radiographs (DRRs) are generated for field planning, i.e. input the appropriate beam sizes, collimator angle, gantry angle and beam blockings. The rough target volume and treatment volume can also be visualized on the DRR.
- ii. The plans in the VS can later be retrieved for comparison with the verification portal images from the Linear Accelerator

Route 2b and 3 (For plans requiring dose computation)

- i. CT scans of the region of the body for radiation treatment planning can be acquired from a diagnostic CT scanner or a CT simulator. The CT images are then input into the TPS for treatment planning and dose computation.

- ii. Plans from VS that require dose computation will also be sent to TPS for dose computation
- iii. DRRs can also be generated from the TPS.

#### Route 4

- i. The finished treatment plans can be retrieved at remote stations by radiation oncologists for reviewing and approval.
- ii. If the plan is unsatisfactory, the planning radiographer/radiation therapist/dosimetrist will be informed to replan it.

#### Route 5

- i. This is for situations when only plain films were done using a treatment simulator. Hand planning is done on the hardcopy film.

#### Route 6 & 7

- i. After hand planning the hardcopy film can be digitized by the digitizer or be kept as it is for later comparison with the treatment portal film.

#### Route 8

- i. For Simulator with direct capture of electronic image facility, images from the Simulator can be sent to the appropriate RT workstations when verification with treatment portal film is required.

#### Route 9a (For Linear Accelerator with electronic portal imager)

- i. Electronic portal image (EPI) of the treatment region is acquired on the Linear Accelerator
- ii. The EPI is sent to RT workstation for comparison with DRR or digitized Simulator images

#### Route 9b (For manual procedure of verification)

- i. Hard copy portal image of the treatment region is acquired on the Linear Accelerator
- ii. The hardcopy portal film so acquired is compared with the hardcopy Simulator film acquired at the planning stage for treatment verification purpose.

### **3. RESULTS**

Based on the concept of the RT Server, procedures in the radiation treatment of a head and neck cancer found common in Southeast Asia, the nasopharynx carcinoma (NPC), are used as a dataflow example to illustrate the imaging informatics integration of images and pertinent information in radiology and radiation treatment equipment. The workflow in radiation therapy is rescheduled so that images can eventually take home in the image-based RT server (Figure 3). The dataflow of the images is described below:

#### **Route 1**

- i. Acquire images of the region of the body for diagnosis or treatment planning from modalities such as CT, MR, and PET before treatment and also other images for evaluation of treatment results after radiation therapy.
- ii. Store the images in PACS server.
- iii. Select the relevant images and send the images to the image-based RT Server.

#### **Route 2**

- i. Retrieve acquired CT images from the PACS server at the Virtual Simulation (VS) workstation or Treatment Planning System (TPS) for treatment planning.
- ii. Generate digital reconstructed radiographs (DRR) from VS workstation or TPS.
- iii. Perform treatment field planning.

- iv. Treatment plans from VS workstation can be sent to TPS for dose computation if required.
- v. Send resultant RT Plans together with DRR from VS workstation or TPS to Image-based RT Server. Each treatment plan consists of the following files: CT image file (DICOM RT-image object), Structure set file (DICOM RT-structure object), Plan setup file (DICOMRT-plan object) and Dose file (from TPS only, DICOM RT-dose object).

**Route 3a (When no isodose plan is required and Virtual Simulation workstation is available)**

- i. Retrieve CT simulator images at the Virtual Simulation Workstation.
- ii. DRR is reconstructed from the CT Simulator images
- iii. Field planning is performed using Virtual Simulation.
- iv. The path from VS workstation will then follow steps ii to v in Route 2.

**Route 3b (When isodose plan is required)**

- i. Retrieve CT simulator images at the TPS.
- ii. Field planning and dose computation are performed in the TPS.
- iii. When virtual simulation is available and field planning has been done in the VS workstation, the plans are forwarded to the TPS for dose computation.
- iv. The path from TPS will then also follow steps ii to v in Route 2.

**Route 4**

- i. For cases that do not require CT for planning, acquire conventional simulator film image for treatment planning.
- ii. Treatment fields are drawn manually on hard copy simulator film and then digitized.
- iii. Send digitized image to Image-based RT server.

**Route 5**

- i. Acquire portal image from Linear Accelerator either manually or using the Electronic Portal Imager.
- ii. Send digitized or electronic portal image to the Image-based RT Server.

**Route 6**

- i. Retrieve the relevant images from the Image-based RT Server at the RT workstations for evaluation of treatment plans or for verification purposes.
- ii. In the former, the radiation oncologist can confirm a treatment plan.
- iii. In the latter, simulator image (reference image) of a patient can be compared with his portal image from the Linear Accelerator whereby verification is confirmed or modification is ordered.

**Route 7**

- i. The written confirmation or comments of the treatment plan or the verification of treatment by the radiation oncologists can be sent back to the Image-based RT Server.
- ii. An Electronic Patient Record (EPR) is generated at the RT Server.

**Route 8**

- i. If the treatment plan is not satisfactory, the oncologist can request the plan to be modified or redone.

**Functions of the RT server**

To summarize, the Image-based RT server contains the diagnostic and therapy images and related information of patients undergoing radiation therapy all in DICOM-RT standards. It also contains organized treatment summaries.

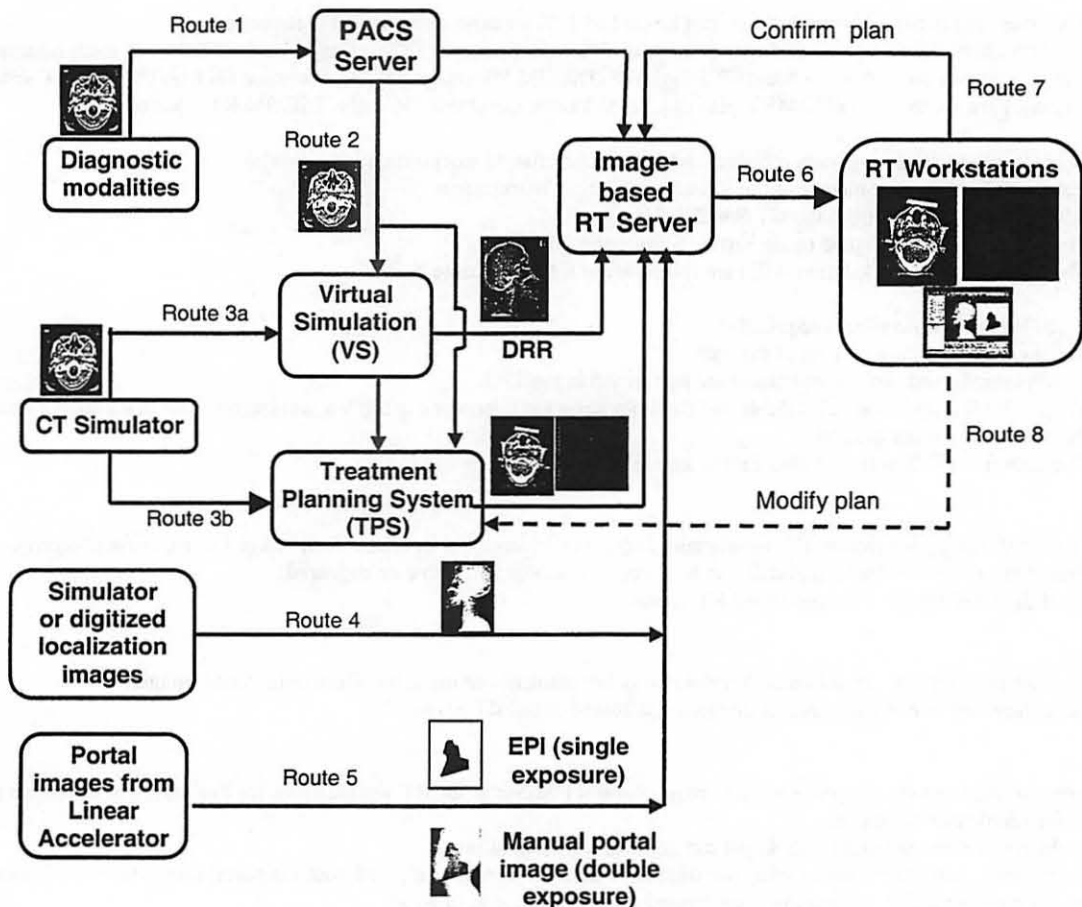


Figure 3. Dataflow of the PACS and imaging informatics-based RT Server. DRR: Digital reconstructed radiograph; EPI: Electronic Portal Image

#### 4. DISCUSSION

This paper is the first attempt to introduce the concept of a PACS and imaging informatics-based RT server as a means for a total workflow system integration of radiation treatment. Radiation therapy is an image intensive treatment. Images are not only required from diagnostic modalities but also from treatment equipment. Currently RT treatment still relies mostly on tedious manual image and data transfer methods because the community as a whole has not championed the concept of system integration heavily. System integration of RT treatment has many benefits including lower equipment and operation costs, streamline treatment procedures, and better healthcare delivery to the patient. We discuss the concept of a PACS and imaging informatics-based server as an attempt to integrate diverse healthcare information systems, imaging modalities and RT equipment into one seamless treatment system. The workflow and dataflow from various pieces of equipment to the server are depicted, and the use of DICOM standard and DICOM RT should be emphasized in each step.

As to date, DICOM RT standards are in existence waiting for manufacturers' incorporation into their products. Except for receiving diagnostic images from PACS or modalities where DICOM is used, other DICOM objects are not normally offered in radiation therapy equipment.

Experience of system integration of diagnostic images in PACS has highlighted the importance of the concept of scheduled workflow of Integrating of the Healthcare Enterprise (IHE). IHE is to define protocols for scheduled workflow in radiation therapy and manufacturers are to participate in connectivity between products from different manufacturers [5]. "Proprietary" is no longer the norm in the PACS era. In order to move forward to the next level of operation effectiveness and efficiency, IHE is a must for the RT community to consider and to participate.

## 5. CONCLUSION

Radiation therapy is an image-based treatment. It requires information and images from both diagnostic and treatment equipment. The RT server concept is based on DICOM RT and PACS-based imaging informatics. We use two clinical examples to illustrate steps in achieving the total information integration in RT treatment.

### REFERENCES:

1. H.K. Huang, *Picture Archiving and Communication Systems: Principles and Applications*, p.521, Wiley & Sons, NY, 1999
2. *Digital Imaging and Communications in Medicine (DICOM)*. National Electrical Manufacturers' Association. Rosslyn, VA: NEMA, 1996; PS 3.1
3. C. Borrás. Automation in Precision Radiotherapy: From Image Acquisition to Dose Computation—Existing and Needed Standards. In NZ Xie, *Medical Imaging and Precision Radiotherapy*. Guangzhou, China: The Foundation of International Scientific Exchange, 2000, p. 168-169.
4. Michael Neumann. The Impact of DICOM in Radiotherapy. Lecture 5<sup>th</sup> Biennial ESTRO Meeting on Physics for Clinical Radiotherapy, Gottingen, April 8, 1999. <http://www.sgsmp.ch/null983b.htm>.
5. [www.rsna.org/IHE](http://www.rsna.org/IHE)[www.rsna.org/IHE](http://www.rsna.org/IHE)

---

\* ormaria@polyu.edu.hk; phone 852 2766-6106; fax 852 2764-6051  
\*\* jzhang@mail.sitp.ac.cn  
\*\*\* hkhuang@aol.com

# Fault-Tolerant PACS Server

F. Cao<sup>1</sup>, B. J. Liu<sup>2</sup>, H.K. Huang<sup>1</sup>, M. Z. Zhou<sup>1</sup>, J. Zhang<sup>3</sup>, X. Zhang<sup>3</sup>, G. Mogel<sup>1</sup>

<sup>1</sup>Department of Radiology, Childrens Hospital LA/USC, Los Angeles, CA 90027

<sup>2</sup>Department of Radiology, Saint John's Health Center, Santa Monica, CA 90404-2091

<sup>3</sup>Shanghai Institute of Technical Physics, Shanghai, China

## ABSTRACT

Failure of a PACS archive server could cripple an entire PACS operation. Last year we demonstrated that it was possible to design a fault-tolerant (FT) server with 99.999% uptime. The FT design was based on a triple modular redundancy with a simple majority vote to automatically detect and mask a faulty module. The purpose of this presentation is to report on its continuous developments in integrating with external mass storage devices, and to delineate laboratory failover experiments. An FT PACS Simulator with generic PACS software has been used in the experiment. To simulate a PACS clinical operation, image examinations are transmitted continuously from the modality simulator to the DICOM gateway and then to the FT PACS server and workstations. The hardware failures in network, FT server module, disk, RAID, and DLT are manually induced to observe the failover recovery of the FT PACS to resume its normal data flow. We then test and evaluate the FT PACS server in its reliability, functionality, and performance.

**Keywords:** PACS, Computer, Technology Assessment, Fault Tolerance.

## 1. INTRODUCTION

A picture archiving and communication system (PACS) [1] is a system integration consisting of medical image and data acquisition of many imaging modalities (such as CT, CR, MR and ultrasonic images) and storage and display subsystems all integrated by various digital networks. A PACS is widely used in hospitals and is considered a mission critical system for around-the-clock daily clinical operation. While failure of individual workstations or acquisition machines will affect the local functions and data flow in the PACS local branch, failure of the PACS controller or the main PACS archive server would cripple the entire PACS operation. Operational reliability of the PACS server is always a major concern in a filmless hospital environment. It also becomes vitally important, as more digital techniques have been employed on critical tasks in hospitals. Nowadays, reliability is a necessary requirement for the systems. Design and implementation of a reliable PACS is to have maximum uptime for end users while ensuring transactional integrity. What this means is that, in the event of a PACS component failure, users might notice a minimal performance impact without interruption of clinical data flow or loss of data.

Currently many PACS, especially medium and small size ones, do not have a fault-tolerant (FT) design or an adequate backup system for the main archive server due to complexity of FT design and significant cost of FT implementation. Larger PAC systems, however, utilizes a mix of software and hardware redundant approaches in addressing PACS fault tolerance. To insure no loss of clinical data, multiple copies of an image are always in existence in various components at one time until the image is archived in the long-term storage. A second copy of the archived image is stored off line but not necessary in a library system because of the expense involved. In the area of no interruption of PACS data flow, larger PACS usually have a backup system for its main archive server, or use distributed server architecture with a mirrored PACS database. They also have certain software design implemented for each of PACS components, like queuing mechanisms for image-processing tasks, to automatically resume the PACS data flow once the backup system kicks in to take over the failed server. But the fail over of workload to the backup system usually requires the applications and the workflow to be restarted with the loss of all processing states (current transactions and history) not already committed to disk. The transfer is often a labor-intensive ac-

---

H.K.H: Email: [hkhuang@aol.com](mailto:hkhuang@aol.com)

F.C.: Email: [fcdo@pacbell.net](mailto:fcdo@pacbell.net)

BJL: Email: [Brent.Liu@stjohns.org](mailto:Brent.Liu@stjohns.org)

tivity.

Fault Tolerance is the implementation of redundant systems, such that in the event of a system failure, maximum availability and reliability - without the loss of transactional data - can be achieved. The requirements for a FT PACS server are to support

1) High reliable PACS Operations

- No loss of data,
- No workflow interruptions

PACS server reliability tests server uptime and fault tolerance. In the event of a server hardware failure, users might notice a minimal performance impact during server failover process but all PACS server functions, such as image archive/retrieval/distribution, must be continuously available. No loss of data and no work interruptions are permitted. All current PACS processes and transactions should automatically resume with no interruptions.

2) Acceptable system performance.

- No performance degradation in daily PACS operations
- Occasional glitches in an acceptable amount of time.

Performance inclusively measures how well hardware, operating systems, network, and PACS software perform together. Ultimately, PACS server performance affects the end users and the response time of the applications they are using on display, diagnostic and modality acquisition workstations. For FT PACS servers, the redundant server hardware once taking over the failed hardware should be able to handle the same workload in network speed, CPU power and archive storage as in normal PACS operations so that the user will not notice any performance degradation. PACS operations and user sessions halt until the FT server successfully fails over and resumes in the event of a system glitch. PACS users are usually tolerable to an occasional delay of 10-30 seconds so long as the delay would not interrupt their interactive PACS operation sessions. A longer delay in minutes is acceptable for non-interactive background processes such as image archiving.

3) Low cost and easy implementation

- Portable
- Scalable
- Affordable

Portability means that current PACS software should be able to run on the FT server without any major changes. Scalability tests how additional hardware, system and PACS software work with the FT server, and impact its ability to handle the workload. High-end million-dollar FT machines such as the Tandem system, which utilizes a sophisticated system design and can recover from system failure in milliseconds, is still too expensive for most hospitals and is often used for short transaction types of applications in banking, security and stock exchange, and telecommunication industries. Meanwhile, as hardware costs go down rapidly in recent years, a simply designed FT server such as the triple-module-redundancy (TMR) UNIX server become affordable which costs about three times the amount of a comparable Unix server but has much longer failover times in seconds.

As a proof of concept [2], last year we demonstrated that it was possible to design a fault-tolerant (FT) PACS server to meet with 99.999% uptime, which is affordable in most PACS implementations. The FT design was based on the triple modular redundancy with a simple majority vote to automatically detect and mask a faulty module. PACS software was executed concurrently on highly replicated hardware. In the event of a failure, work continues without interruption on the remaining and still fully functional hardware. The proof-of-concept testing determined that an affordable and cost effective FT solution could be designed and implemented for a PACS server to meet its operational criteria of continuous availability.

This paper is to report on the continuous developments of FT server, and to delineate laboratory failover experiment. Specifically

1) Implementation of external FT devices with the PACS controller

- Network

- External mass storage devices of RAID and DLT library
- UPS power backup

A truly fault tolerant server is only as good as the weakest link in the whole integrated environment including networking and mass storage. For networks, this includes multiple connectivity points for data communications to the hospital network. For external mass storage, both RAID and DLT library are directly attached to the FT PACS server with multiple connections and dynamic port monitoring software routes data automatically to the redundant paths in the event of a hardware failure. Meanwhile, the whole system is backed up by UPS, which with a feedback link to the server can automatically and gracefully shut down the PACS system whenever the UPS battery drains out during an extensive period of power outage.

## 2) Generic PACS Software Development for FT evaluation

- PACS Simulator---Modality, DICOM Gateway, PACS Controller and Display Workstation
- Monitoring Software

The PACS Simulator with generic PACS software has been developed and used in the experiment to simulate PACS clinical data flow to and from the FT server [3]. The hardware failures in network, FT server module, disk, RAID and DLT are then manually induced to observe the failover recovery of the FT PACS to resume its normal data flow. In simulator component design, the use of common PACS technologies such as DICOM and Job Queuing in communication between clients and the PACS server is to provide the ability to wait, roll-back transactions, or queue them until such a time that they can be processed. Monitoring services are used to assure that a PACS is functioning and stable 24 hours a day, 7 days a week. Proper monitoring will help to resolve many issues immediately and with as little downtime as possible.

## 3) FT Testing

FT testing tests the continuous availability of the FT PACS server, in terms of

- Reliability test--- no loss of data and no interruption of workflow by monitoring PACS data flow and insuring the data integrity.
- Functionality test--- To find how each of the PACS components and functions work with the FT Server. It is used to find errors and compatibility issues between all components.
- Performance test --- To measure the failover time needed for FT system recovery as well as the application response time.

Our goal is to implement and evaluate the affordable FT PACS server, which leads to 24x7 availability by reducing planned downtime as well as unplanned downtime. Our performance measurement provides a benchmark and reference standard for future FT implementation in Hospital PACS.

## 2. SYSTEM ARCHITECTURE FOR FAULT TOLARANT PACS SERVER

The FT PACS server developed at the IPI (Image Processing and Informatics) Laboratory, Childrens Hospital/University of Southern California is the first low-cost implementation of a continuous availability (CA) FT architecture. It uses a triple modular redundant (TMR) system with a high level of integration and an elegantly simple voting mechanism to achieve the continuous availability of PACS server. The server has been implemented recently with external mass storage devices of RAID and DLT tape library.

### 2.1. Triple Modular Redundant (TMR) Architecture for FT PACS Controller [2]

The FT PACS controller uses Triple Modular Redundancy (TMR) to achieve fault tolerance at the CPU/memory level. Figure 1 shows the core of the TMR PACS controller system made up of three identically configured UltraSPARC-based modules (Sun Microsystems, CA). The three modules are tightly synchronized and interconnected through a high-speed back-plane for inter-module communications. Each module is a complete, operational computer running Sun's Solaris Unix OS server, with its own UltraSPARC CPU, memory, I/O interfaces, bridge logic, and power supply. More details about the system configuration have been described in [2].

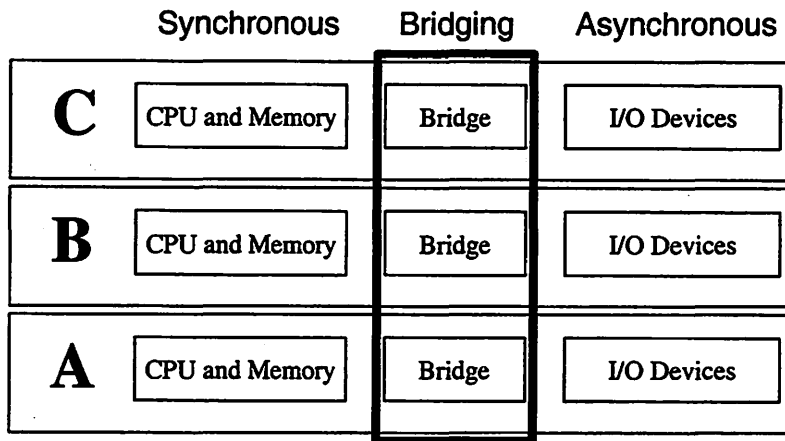


Figure 1. Fault Tolerance Triple Modular Redundancy Design.

To the UltraSPARC core, a programmable-ASIC (Application-Specific Integrated Circuit) technology is used to build TMR bridge logic that keeps the three modules synchronized, continuously monitors and compares their operation, and exchanges I/O data among the three modules. The bridge logic reads Sbus transactions within each module and compares them across the modules. If the logic detects a variation between transactions, it assumes an error. Then, the system pauses (typically for 5-30 seconds depending on memory size) while the diagnostic software determines the faulty module and disables it. Next, the memories of the two remaining modules are synchronized by performing a full memory copy. Once the copy is complete, the system resumes processing by using the remaining two modules.

The hardware in the bridge compares all data that comes into, or goes out of the synchronous part of the system to diagnose any problems. The hardware voting ASIC built into Bridge unit provides real-time fault detection and masking functions that are transparent to the application program. The TMR voting system uses a simple majority voting logic to mask the failed module that comes with minor vote. This is a conceptually simple model, since the logic that compares the operation of the three modules need not know what faulty behavior looks like; only that deviant module should be regarded as faulty. Since the comparisons occur within the hardware, there is no overhead to the operating system and performance is not affected.

The system responds in a totally automatic, seamless manner, allowing uninterrupted operation of the system. The system administrator is notified of any failure within a module, so the module can be replaced as needed, but there is no need to shut down the system.

### 2.1.1 Limitation of TMR Voting System

The TMR voting system currently implemented is a passive (static) one that uses fault masking to hide occurrence of fault without further system action (active) to diagnose the failed module. A hybrid approach, which is expensive but better to achieve higher availability, could be used that implements a feature that automatically distinguishes between hard (repeatable) or transient (not repeatable) failures and then responds appropriately. Our current system responds to all errors as if they were hard by disabling the affected module. A hard error in a computer system is reproducible and will occur every time the same component attempts the same operation. The module with a hard error must be replaced. If the failure was transient, then the system should automatically re-synchronize the module back into operation. However, if the number of transient errors exceeds a set threshold, the module is taken out of service for replacement.

The hardware-based voting approach to FT does not address software failures that are due to bugs in the application program or operating system itself since the data from the three modules are the same and will be voted without error. If the operating system fails, all execution entities fail simultaneously. This event requires a reboot. Application failures need a restart. Automatic restart of failed applications may be implemented on FT systems with the addition of even management software.

The TMR configuration with the three modules is the minimum redundancy requirement in which the majority voting logic

can identify a faulty module. After a single module fails, a TMR configuration will fall back to operate as a DMR (Double Modular Redundancy) configuration until the third module is repaired. In a DMR configuration, the system can still detect a fault by comparing but voting fails to determine which of the two modules is faulty. Therefore, a DMR configuration requires, in general, use of additional algorithms to perform self-diagnoses and determine the faulty module. The low-cost TMR controller implemented in our lab does not support self-diagnosis in the DMR configuration.

## 2.2. FT I/O and Storage Subsystem

Operating I/O devices such as SCSI or Ethernet interfaces in TMR synchronization is not only extremely difficult, it does not achieve the required system-wide continuous availability. Each I/O subsystem must be regarded individually, with continuous availability implemented in a manner appropriate to each subsystem.

### 2.2.1 Ethernet.

Each of the three modules contain its own 10/100baseT Ethernet interface, each of which is connected, preferably via independent paths, to the local network backbone. The three interfaces form a single software interface (one IP and MAC address). One interface acts as the active interface, while the others stand by. Should the module containing the active interface fail, or some element of its connection to the backbone fail, that interface is disabled and a standby unit becomes active in its place. Normal network retry mechanisms hide the failure from applications.

### 2.2.2 Fault-Tolerant Storage system

#### RAID as a short-term storage

Each of the three modules contains its own fast/wide SCSI interface. The SCSI interfaces, unlike the CPUs, do not run in synchronization, but rather appear as three independent host adapters. To automatically survive a single disk failure, all storage must be RAID (Redundant Arrays of Independent Disks) configured. Storage management software is used to implement two different fault-tolerance strategies. The first strategy is disk mirroring for system boot and applications storage where identical external disk drives are attached to two or three modules and the same data is written to each drive. If a disk drive or a module fails, a redundant drive attached to a working module is used for system or application operation until the faulty unit is replaced.

The second strategy is to use RAID subsystem for non-boot storage, but not all RAID systems are able to support the fault-tolerance storage. The RAID system must be cluster-ready as commonly called, in which two or more modules are given their own direct link to the storage system and the RAID system can be detached from the failed module and automatically reattached to a healthy module with a functional path to the data. It must have at least dual ports to which multiple modules can attach. Ideally, the RAID system should also be designed with a split bus. The split bus design allows dual ports to be segmented on the bus, providing channel redundancy. To be fully fault tolerant, a second RAID hardware controller is also required. In a typical configuration, two modules are connected to a dual-controller RAID subsystem, preferably with a split bus for each controller as shown in Figure 2. If a module fails, the other module takes over. Disk drive or RAID controller failures are handled by the RAID mechanism. The four redundant connections in Figure 2 provide a full FT storage solution, which guarantees the system survival in an even of failure of one module, one RAID controller or both at the same time.

A Hitachi 9200 RAID with Veritas Volume manager software has been implemented with the FT PACS controller. The 325Gbytes Hitachi 9200 RAID with dual hardware controllers connected to the module A and B, provides the two paths to TMR PACS controller while Veritas software dynamically monitors the two paths and switches automatically from one to another in case one path is disconnected.

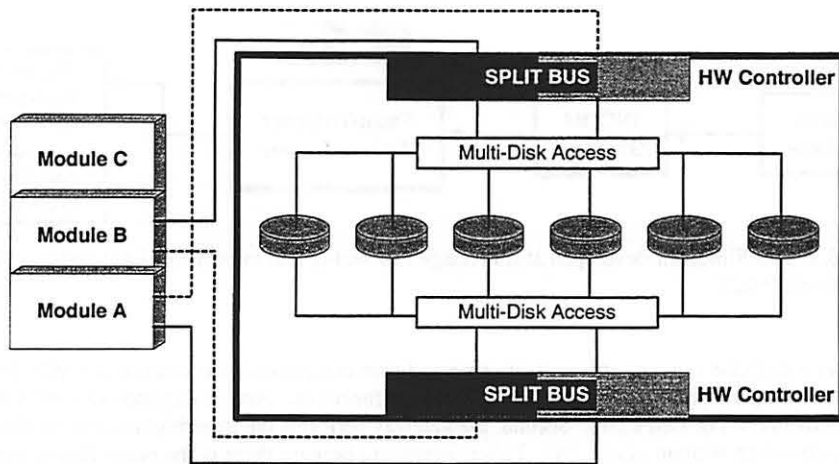


**Figure 2.** A RAID subsystem with two HW controllers and split bus. The Module-A SCSI port connects to one controller and the Module B SCSI port connects to the other controller. The dash lines show the optional SCSI direct connections to the RAID's split bus ports, providing additional link redundancy for system reliability.

### DLT Tape Library for Long-term Archive

For PACS long-term archive, we use StorageTek L30 DLT tape library with storage capacity of 3.2TB. The library comes with two drives, each of which is connected to one of the TMR controller modules, providing the redundant paths to FT PACS server. Meanwhile, Veritas Netbackup and Migrator software are installed to automatically migrate the data from short-term RAID to long-term tape library archive. The Veritas Migrator software comes with a built-in feature to monitor the multiple paths and to fail over from one to another. The FT tape library implementation in our lab is a still works-in-progress and has yet to be fully tested.

## 3. GENERIC PACS SOFTWARE FOR FT EVALUATON

In order to evaluate the robustness and effectiveness of a Fault-Tolerance PACS server design, a testbed environment has been developed to allow for observation and results gathering.

### 3.1. The PACS Simulator [2]

A system that simulates key components of a typical clinical PAC System as well as the normal operating clinical data flow was developed to evaluate the Fault-Tolerant PACS design. This system, called a PACS Simulator, is comprised of :

- 1) Acquisition Modality
- 2) Gateway
- 3) PACS Controller
- 4) Two Clinical Viewing Workstations
- 5) Network Infrastructure.

The acquisition modality simulates a modality scanner by transmitting exams in DICOM format into the PACS. The modality simulator can send any modality type exam including Computed Radiography (CR), Computed Tomography (CT), Magnetic Resonance (MR), Ultrasound (US), Digital Fluorography (DF), and Digital Angiography (DS). Transmission of the exams is executed only once without verification of exam completeness which is similar to most image acquisition modalities.

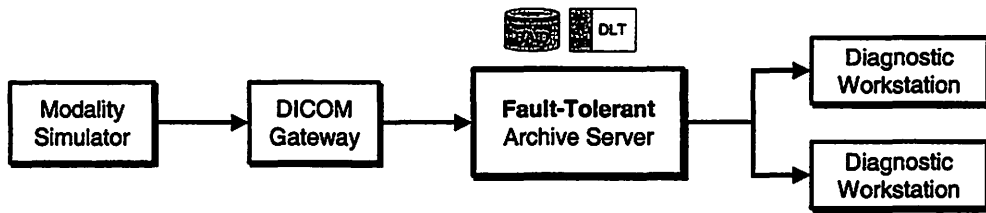


**Figure 3.** PACS Simulator developed at IPI (Image Processing and Informatics Lab) and connected to the clinical PACS.

The gateway receives a DICOM exam of any modality type and then in turn sends the exam to a PACS device node – usually the PACS controller. The gateway performs a couple of possible functions. First, it can receive exams that are not DICOM compliant and reformat into a DICOM exam. Second, the gateway performs the transmission and verifies whether the transfer of the exam was complete without image loss. This is important because there is the possibility of image loss during the transmission of a large image number DICOM exam. Because current modality acquisition scanners do not have the ability to verify that the exam is complete, the gateway performs this very important function.

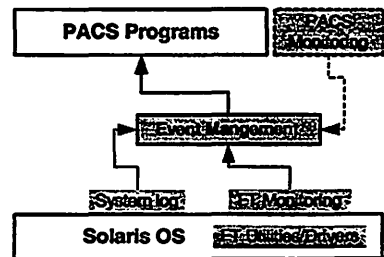
The PACS controller receives and archives DICOM exams of multiple modalities. It is also responsible for the distribution of exams to a PACS node. The exam distribution is either performed automatically or on-demand by a requesting PACS node. It is also responsible for short-term and long-term storage of all modality type exams. The PACS controller supports the following DICOM services: Image storage, Image query and Image retrieval.

The clinical viewing workstations display multiple modality type DICOM exams for diagnostic viewing and review. These workstations can receive DICOM exams automatically. Additionally, the workstations can initiate a query and retrieval of specific exams on demand. The workstations can also send DICOM exams to another PACS node as well as store exams locally for short-term storage within its own database.

### 3.2. FT Monitoring and Management Software

To be developed is Event Management software that can help resolve many issues immediately with as little downtime as possible such as handling application software failures and automatic recovery of the application programs.

- Monitoring Failures in an Application Program
- Interface to the existing FT system event monitoring programs
- Collection, filtering and logging messages from the FT, applications, and OS
- Executing predefined processes, such as restart of failed applications
- Test and Evaluate the event management software for PACS server



## 4. FT TESTING AND PERFORMANCE MEASUREMENT

### 4.1. Evaluation Protocol for FT Server Reliability and Functionality Tests

#### 4.1.1 Define and Create Clinical Test scenarios for FT Testing

Development of an evaluation protocol for the fault-tolerant testing and evaluation is anchored around creating clinical situations with which a hardware failure can occur. In addition, simulations of hardware failures are created within these clinical scenarios to test the fault-tolerant abilities of the FT PACS server. Clinical scenarios simulated in the evaluation can be bro-

ken down into types based upon the perspective of the end-user. This is important since ultimately the success of the fault-tolerance of the system benefits the end-user the most. The two types of scenarios are: 1) Clinical background or “passive” scenarios, and 2) Clinical On-Demand or “active” scenarios.

Clinical background or “passive” scenarios are basically automatic functions of the PACS Controller. These include storage and archival of PACS exams and automatic distribution of PACS exams to the viewing workstations. To create an effective clinical simulation, the PACS Controller should perform these background functions on a continuous basis 24 hours a day, seven days a week. However, for testing purposes it is not feasible for an operator to continuously send PACS exams to the PACS Controller for archival and storage. In addition, there are not enough test case exams to continuously send to the PACS Controller for archival and storage for long periods of time. An automatic loop was created to continuously simulate the background scenarios for long periods of time. The loop involves the acquisition gateway that automatically sends a selected number of PACS exams to the PACS controller that in turn automatically distributes the PACS exams to the viewing workstations. Then, after a set amount of time elapses, the PACS controller automatically deletes the PACS exams from its archive and database and the PACS exams are sent again by the acquisition gateway and the loop begins again. This loop can be executed continuously for extended periods of time to simulate the clinical environment. This clinical scenario was simulated in the evaluation procedure of the Fault-Tolerant PACS design and any hardware failure occurrences were noted and recorded.

Clinical on-demand or “active” scenarios are functions of the PACS Controller executed based on requests made by a PACS component. For example, a viewing workstation can query the archive for a specific patient exam. Once the specific exam has been located, a retrieve request is initiated for the exam to be sent from the PACS controller to the requesting viewing workstation. This clinical scenario is simulated in the same manner with the fault-tolerant PACS Simulator. Failover procedures are described in greater detail in the forthcoming paragraphs.

#### *4.1.2 Failover Procedures for Evaluation*

Two types of hardware failures were simulated on the PACS controller running on the fault-tolerant server. The first simulated hardware failover is the failure of network devices either in the PACS controller component or the network switch connected to the PACS controller. The second simulated hardware failover is the failure of the CPU, memory, or entire motherboard of the PACS controller component.

Determination of what type of failover during which type of clinical scenario is dependent on the ability to verify results, the ability to repeat the test procedure indefinitely, the feasibility of the evaluation procedure, and the impact of the failure to the end-user. Ultimately, it is the scenario with the most severe detrimental effects to users of a PACS that should be tested for fault-tolerance even if the probability for such an occurrence is extremely low. In this way, the evaluation can cover the largest spectrum of scenarios – from the least probable but most crucial scenario to the most probable and least crucial scenario. It is important to note that least and most crucial type scenarios are relative in the true clinical environment since all scenarios utilized in the evaluation process are mission critical events for PACS.

The first failover procedure that was evaluated was initiated during the query and retrieval of a PACS exam from the Fault-Tolerant PACS controller to the viewing workstation. As the PACS exam is received by the viewing workstation, the Ethernet cable connected to the Fault-Tolerant PACS controller is pulled apart from the port located on the network switch. This simulates a failure of any of the network devices involved as well as the scenario of an accidentally cut cable. The PACS exam is verified as being transmitted to the viewing workstation by the updates to the worklist of the viewing workstation. The number of images of the PACS exam is displayed on the worklist and that number is dynamically updated as each image arrives. The evaluator can confirm that the images are being transmitted to the viewing workstation if the number continues to increase until the entire exam has been transmitted. Once the cable is pulled apart, the number of images is frozen on the worklist with the last image number prior to pulling the cable. This shows that there is a broken transmission due to a possible network device failure. However, the images should continue to transfer to the viewing workstation after a few seconds once the Fault-Tolerant PACS controller has completed its Ethernet failover. This once again can be confirmed, as the image numbers will continue to increase. The final confirmation is to open the PACS exam to display on the viewing workstation in order to confirm that all image data is correctly transmitted without any loss of images and/or image corruption.

The second failover procedure that was evaluated was again initiated during the query and retrieval of a PACS exam from the Fault-Tolerant PACS controller to the viewing workstation. However, this time the failover simulated is the hardware failure

of the CPU, memory, the entire motherboard, or the power supply. To accomplish this, the power to one of the three modules is shut off during the transmission of the PACS exams from the PACS controller to the viewing workstation. Once again, the operator verifies that the PACS exam is being transmitted to the viewing workstation. Then, the power switch is turned off or the power plug is pulled during transmission to simulate a hardware failure during the query and retrieval process. This failover simulation can be considered the worst-case scenario in PACS especially if the exam requested is a mission critical exam (eg, emergency surgery pre-operation PACS exam for review) and a hardware failure at the PACS controller occurs that impedes the crucial review by the physician. After the power to the module is switched off, the transmission is frozen for a certain amount of time. The images should continue to transfer to the viewing workstation once the Fault-Tolerant PACS controller has completed its CPU module failover. The final confirmation again was to open the PACS exam to display on the viewing workstation and verify the correct number of successfully transmitted images.

#### 4.2. Fault-Tolerant Server Performance

##### 4.2.1 Interactive Clinical PACS operations

Performance test measures the failover time of FT PACS server in an event of system component failures that occur during standard clinical PACS operations—archiving and distributing patient exams.

- **Test Scenario 1:** Ethernet Failure while archiving and distributing patient exams.
- **Test Scenario 2:** CPU module failure while archiving and distributing patient exams.
- **Test Scenario 2:** Disk failure while archiving and distributing patient exams.

Table 1 summarizes the recovery time for the scenario listed above. The PACS dataflow continues automatically after the system recovery. No data loss and no interruption of data flow have been observed. All Patient Exams were successfully transferred. Effect from the user's perspective, in front of display workstation, is a delay equal to the system failover time.

Common Faults	Ethernet	CPU module	Disks
Average Recovery Time	3-15 Seconds	20-40 Seconds	35-75 seconds

Table 1. Average system recovery time for common faults.

##### 4.2.2 Background Burn-In Test:

The automatic feedback distribution loop between the PACS controller, gateway, and viewing workstation was activated for a continuous period of three months. This is the burn-in period that simulates a PACS controller in a clinical setting. No system failure has been observed.

With the TMR Fault-Tolerant PACS server, applications execute concurrently on highly replicated hardware. In the event of a failure, work continues on the remaining and still fully functional hardware. The system and network performance are not affected except during the failover process that users will experience a delay equal to the system recover time. While the fault recovery may be effectively addressed by the FT design of hardware and system, the time required to recover from errors can vary from couple of seconds to 75 seconds depending on one or more of the following:

- 1) The nature of the failure
- 2) The elapsed time to discovery of the failure
- 3) The time required to resynchronize the functional hardware
- 4) The time required to reestablish network communications with switches
- 5) The time waiting for a SCSI timeout and then taking the alternative path to the external storage device.

#### 4.2.3 *Limit of DICOM Connection Timeout is about 2 minutes*

When hardware failure occurs in the middle of archiving and distributing patient exams, the gateway or display workstation keeps the DICOM connection alive and holds until the FT PACS server recovers. It is the DICOM retry mechanisms just like normal network retry process that hide the failure from PACS applications. We tested and found that when the network was manually disconnected for more than 2 minutes, the display workstation would be unable to re-establish the DICOM connection with the FT PACS server. The test result indicates that any system fault should be recovered before the client's application drops its DICOM connection. Otherwise, the clinical data flow will be interrupted and a restart of the application software to re-initiate the DICOM connection is needed.

### 5. SUMMARY

We have implemented a TMR-based FT PACS server integrated with external RAID and DLT storage devices. The TMR FT PACS server can automatically detect failures by comparing the activity of three synchronized modules. Each module performs exactly the same activities until one fails, in which case the system detects the deviation and identifies the faulty module by simple majority votes and removes it from service. The remaining two modules continue normal operation, with no adverse effect on PACS data flow and system performance. The FT PACS server has been evaluated by conducting a series of manually induced failover tests on its reliability, functionality and performance. It is concluded that the simple low-cost TMR FT server can be implemented and used as a reliable PACS server to achieve 24x7 continuous system availability. Meanwhile, our performance measurement provides a valuable benchmark for FT design and implementation in Hospital PAC systems.

### ACKNOWLEDGMENT

This work is partially supported by the US Army Medical Research and Materiel Command Contract No. DAMD17-99-P-3732, NIH National Library of Medicine Contract No. N01-LM-9-3538, and Reliant Health Care, Inc.

### REFERENCES

- 1 Huang HK. *PACS: Basic Principles and Applications*, Wiley & Sons, 1999.
- 2 H.K. Huang, F. Cao, B. J. Liu, J. Zhang, Z. Zhou, A. Tsai, G. Mogel, Fault-Tolerant PACS server design. *SPIE Medical Imaging*, Vol. 4323-14, February 2001.
- 3 H. K. Huang, B. J. Liu, F. Cao, M. Z. Zhou, J. Zhang, G. T. Mogel, J. Zhuang, X. Zhang, PACS Simulator: A Stand-alone Educational Tool. *SPIE Medical Imaging*, Vol. 4685-21, February 2002.

# Managed PACS Operation with An Automatic Monitoring Tool

Jianguo Zhang, Ruolin Han, Dongqing Wu, Xiaoyan Zhang, Jun Zhuang, Jie Feng\*, Mingpeng Wang\*, Guozhen Zhang\*, and Chuanfu Wang\*  
Laboratory for Medical Imaging Informatics, Shanghai Institute of Technical Physics, Shanghai,  
\*Huadong Hospital, Shanghai

## ABSTRACT

Huadong hospital in Shanghai with 800 beds provides health care services for inpatients and outpatients, as well as special senior and VIP patients. In order to move to digital imaging based radiology practice, and also provide better intra-hospital consultation services for senior and VIP patients, we started to implement PACS for hospital wide services from 1999, and also designed and developed an automatic monitoring system (AMS) to monitor and control PACS operation and dataflow to decrease the total cost of ownership for PACS operation. We installed the AMS on top of the Huadong Hospital PACS in the May of 2001. The installation was painless, did not interrupt the normal PACS operation, and took only one month. The PACS administrators with the AMS can now monitor and control the entire PACS operation in real time, and also track patient and image data flow automatically. These features make administrators take proper action even before user's complaint if any failure happened in any PACS component or process, they reduce the size of the management team, and decrease total cost of PACS ownership.

## 1. INTRODUCTION

There are many advantages of introducing picture archiving and communication system (PACS) to the conventional film-based operations in radiology and medicine [1]. For example, through the image display workstations, it is possible for radiologists or physicians to manipulate a digital image for value-added diagnosis, and through digital imaging plate technology or digital radiology (DR) technology, it is possible to improve the diagnostic value while at the same time reducing the radiation exposure to the patients. Also, in so far as PACS promotes more efficient operating environments, it can speed up health care delivery and reduce operation costs if they are properly installed or implemented in hospitals [2, 3]. However, the costs of owning, operating and maintaining PACS for hospital wide clinical services are usually very high, since no loss of image data, no interruption, high and continuous availability require the hospital to have fault-tolerant PACS with a well-trained PACS administration team and approved service contracts to maintain the PACS hardware and software components. In order to achieve the high and continuous availability in PACS operation, the PACS component status would be monitored seriously, and quick responds would apply to the component if any failure happened to any PACS key component either in hardware or software level. In order to protect the data loss and also for security issue, the PACS data flow, e.g., from acquisition to final display, would be tracked carefully. All these measures will increase the TCO (Total cost of ownership). This presentation described one approach to build networked monitoring subsystem on top of the PACS to assist the PACS management and to get the PACS component status and internal data flow more transparent to the administrators, and to make the PACS maintenance more easy to end users. The clinical evaluation of this monitoring subsystem was discussed and the results proved that AMS can decrease the TCO of a clinical PACS.

## 2. BACKGROUND

In China, more and more hospitals recognize that digital radiology department or digital hospital will be trend and try to introduce or develop PACS in their hospitals to improve the efficiency in health care services or to take advantages of digital imaging operations. The Huadong hospital with about eight hundred beds provides health care services for inpatients and outpatients, as well as special senior and VIP patients. The total outpatients and inpatients served daily are about 1,935 and 660 respectively. Also, there are about more than thirty medical consultation meetings held every month for senior and VIP patients. We started designing and planning PACS implementation in Huadong hospital from September of 1999. After two phase implementations [4], the PACS was operated daily in this hospital

and the digital images can be accessed by most radiologists through PACS display workstations, and there were more than two clinical services and applications using the PACS images in this hospital. The most challenges of running PACS in this hospital was to have a well-trained management team to maintain the entire PACS operation, PACS components status, and their dataflow control. But, this would increase the TCO of the PACS operation for this hospital, and also it was difficult to buildup this kind of team in short period of times. In order to decrease TCO of PACS operation and to achieve the high and continuous availability in PACS operation, we developed an automatic monitoring subsystem (AMS) on top of the PACS as tool to assist the PACS administrators to run and control the PACS operation.

### 3. PACS INFRASTRUCTURE AND MAJOR COMPONENTS

The PACS consists of a basic skeleton of hardware components (imaging device interfaces, storage devices, host computers, communication networks, display systems) integrated by standardized, flexible software subsystems for communication, database management, storage management, job scheduling or routing, error handling, and network monitoring. Figure 1 shows our PACS architecture designed for Huadong hospital. It consisted of modality image acquisition modules, central PACS server, display workstations, and application server or workstations. The image communication interfaces between these components are following DICOM standards and the communication roles of a component were mostly Service Class User (SCU), Service Class Provider (SCP) or both of Storage and Query/Retrieval Services. The acquisition modules were installed in modality sections, they functioned like mini-PACS inside the modality section [4], and like acquisition module in whole PACS architecture. The PACS server was UNIX based and installed the data center of the hospital. The display workstations and application server or workstations were installed in modality sections, clinical departments, or consultation centers.

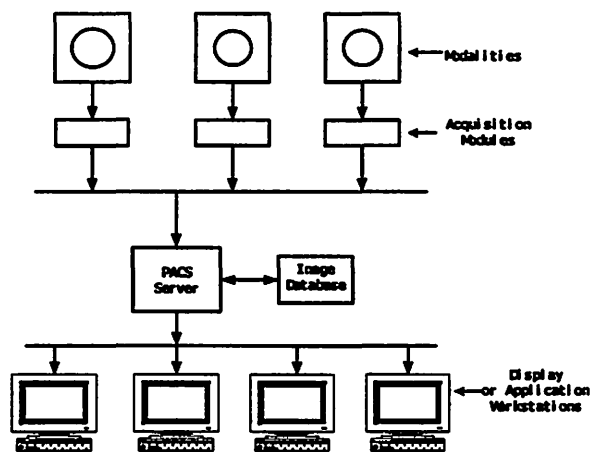


Figure 1. The PACS Architecture and Major Components in Huadong Hospital

Considering the radiology service models and administration situations (modality based), we designed the PACS network logically to be a branch of the whole hospital network infrastructure, and used VLAN (Virtual LAN) technology to separate the subnets. In order to have better communication performance, and better security protection, VLANs, which were grouped with ports and properly configured in the switches, were used to separate sub-networks among modality sections, clinical departments and VIP parts. For example, VLAN1 was for VIP users who can access the VIP patients' information, and VLAN2 is for general users who can only access common patients' information, et

al.. With this kind network design and implementation, we built our PACS network to be a more practical, manageable, and robust sub-system in the PACS. Figure 2 shows the PACS network configuration in Huadong Hospital.

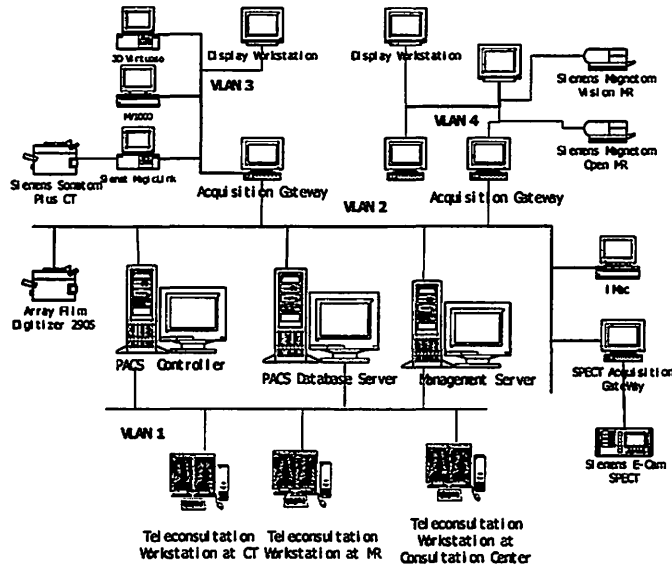


Figure 2 VLAN configuration in Huadong hospital PACS network

#### 4. PACS WORKFLOW AND MANAGEMENT

The incentives for this hospital to build PACS were: First, to improve radiology service efficiency and quality, for example, the radiologists in CT section can read images instantly with PACS workstations after images generated by CT modality, and create and send the preliminary reports to clinical physicians for patient management in time; Second, the medical experts or physicians need fast image accessing when consultation meetings opened; Third, more and more clinical services need to use digital images for their applications, for example, radiation therapy treatment planning, image fusion or registration between CT, MR and SPECT. So, the PACS operation and workflow were designed to meet the requirements both of radiology department work schedules and clinical services.

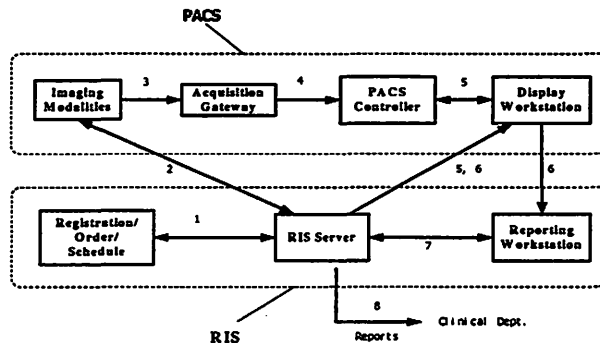


Figure 3. The diagram of radiological examination work/data flow with PACS and RIS in Radiology Department

We built the PACS integrated with our Web-based RIS (Radiological Information System) to provide daily service for radiology department. The Figure 3 shows the radiological examination work/data flow in Radiology Department with RIS-integrated PACS.

In order to achieve the high and continuous availability in PACS operation, the PACS component status would be monitored seriously, and quick responds would apply to the component if any failure happened to any PACS key component either in hardware or software level. In order to protect the data loss and also for security issue, the PACS data flow, e.g., from acquisition to final display, would be tracked carefully. So, the major maintenance and monitoring tasks for a PACS manger or administrator are:

- (1) Track all abnormal events happened in PACS components, such as PACS acquisition gateway, PACS server, and display workstations;
- (2) Monitor and control the PACS computer resource status and usages, e.g., storage spaces, user logon/off status, PACS process or service running status;
- (3) Continuously keep PACS dataflow without any interruption and guarantee the image secured used in PACS environment;
- (4) Monitor PACS image communication status and track patient/image dataflow;
- (5) Do troubleshooting on any problems or errors happened both in hardware and software components before user complaints.

Currently, the most PACS maintenance or monitoring tasks were done by well-trained PACS team in a hospital, or through contracted services. The cost of maintaining a large scale clinical PACS were usually very high, it was approximately 10%-15% (PACS installation) for one year. So, it is urgent to develop efficient tools to help the hospital IT (information technology) department to maintain the PACS operation. In following sections, We presented a new designed monitoring subsystem built on top of the PACS to assist the PACS management and to get the PACS component status and internal data flow more transparent to the administrators, and make the PACS maintenance more easy to end user.

## 5. PACS AUTOMATIC MONITOR SYSTEM FUNCTIONS AND ARCHITECTURE

We built the AMS to be three-tires networked system. It should be no overhead costs on PACS performance and operation, and provide following functions based on the requirements mentioned in above section:

- (1) Real-time capture all warning, error messages happened in PACS acquisition gateways, PACS server, and display workstations, and send them to central monitor server;
- (2) Periodically check PACS network connection and component running status;
- (3) Remote monitor PACS component computer resource status, e.g., storage spaces;
- (4) Remote control and operate PACS processes, and services running in PACS components;
- (5) Track patient/image dataflow in PACS components, and image usages;
- (6) Monitor remote display workstation logon/off status, guarantee images secured read and used;
- (7) Visually show the image dynamic flow status from one component to another in PACS network, and make PACS operation more transparent to PACS administrators or end users;
- (8) Route serious error or warning messages to an administrator through pager or fax to call emergency repairing or doing troubleshooting.

The AMS was consist of three parts [5]: Central monitor server running in a remote host independent of any PACS component, agent services running in any monitored PACS component, and a group of interfaces called by PACS processes. Figure 4 shows the AMS configuration integrated with the current PACS architecture. The monitor server was developed on Windows 2000 platform, and the software includes three parts: message communication services, database management process, and a display program. The agent services are daemon background processes running in Unix or NT platform, their major functions are to execute the management commands sent from the monitor server.

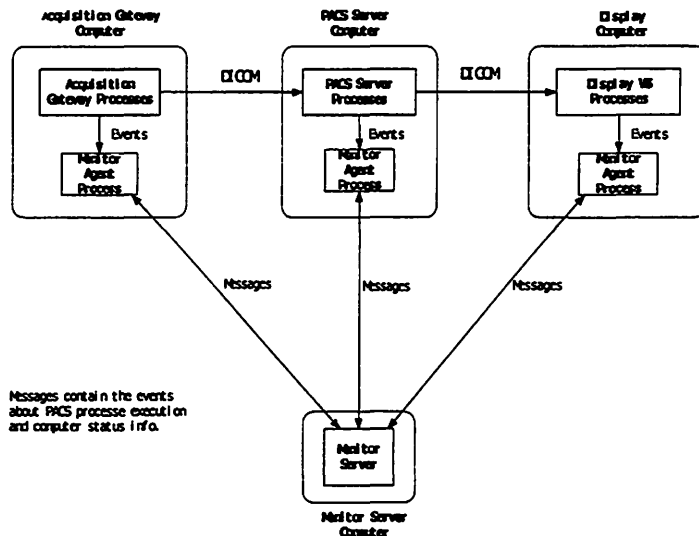


Figure 4. The diagram of the automatic monitor system integrated with PACS

## 6. AMS IMPLEMENTATION AND PRELIMINARY RESULTS

We started to implement AMS in Huadong Hospital PACS from the end of May, 2000, and completed the installation in the middle of the June. The agent services were installed in CT and MR acquisition gateway computers (Windows 2000), and the TeleCon display workstations [6], as well as, the PACS server (Sun Enterprise 450 with Sun Solaris 7 and Oracle 8i database). The monitor server software was installed in a Windows Advanced Server computer with the modem connection. The installation was painless, did not interrupt the normal PACS operation.

We laid a course of using AMS to manage and maintain PACS operation after AMS installation. First, we explained to the AMS users to understand the AMS major functions and architecture; Second, classified the remote messages sent from the PACS components to be three levels of normal, warning and error, and trained the users to read the messages or information displayed on the monitor server GUI program; Third, trained the users to take proper actions on a PACS component based on different messages or information. Now, the PACS management routing work of administrators with the AMS assistance becomes:

- 1) Read the AMS messages or information displayed on AMS server GUI;
- 2) Identify problem reasons or sources if they found the errors among the messages sent from a remote PACS component;
- 3) Fix the problems if they can, otherwise call for technical support;
- 4) Analyze the data information sent from agent services and give correct evaluation about PACS performance and resource usages;
- 5) Track patient/image dataflow (store-forward and query/retrieval), monitor the remote users logon/off status, guarantee images secured used;
- 6) Do statistics on radiological examinations with AMS statistical functions, e.g., count performed study numbers of every day on CT, MR, NM.

Following tables give the parts of summary reports of Huadong Hospital PACS operation by using the AMS.

Table I. Huadong Hospital PACS CT Store-Forward Communication Reports (From Dec. 24, 2001 to Jan. 24, 2002)

DATE	NUMBERS OF SERIES (CT DICOM GATEWAY to PACS-SERVER)
24, Dec., 2001	90
25, Dec.	60
26, Dec.	51
27, Dec.	15
28, Dec.	159
29, Dec.	5
30, Dec.	6
31, Dec.	69
1, Jan., 2002	6
2, Jan.	38
3, Jan.	74
4, Jan.	10
7, Jan.	51
8, Jan.	35
10, Jan.	92
11, Jan.	24
12, Jan.	32
14, Jan.	65
15, Jan.	87
16, Jan.	76
17, Jan.	70
18, Jan.	26
22, Jan.	28
Total(23 days)	1169
Average	50.83/day

Table II. Huadong Hospital PACS Query/Retrieval Reports for CT Exam.. (From Dec. 14 to 2001 to Jan. 23, 2002)

AE TITLES OF Q/R SCU	AE TITLES OF Q/R SCP	AE TITLES OF DICOM C-MOVE DESTINATIONS	SERIES NO. OF SUC. RETRIEVED	SERIES NO. OF FAILED RERIEVED	TOTAL NO. OF SERIES
HD1CT01PGWQR	IMAGE_SERVER	HD1CT01PGWST	14	3	17
HD1CT02PDPQR	IMAGE_SERVER	HD1CT02PDPST	139	2	141
HD1MR01PGWQR	IMAGE_SERVER	HD1MR01PGWST	282	22	304
SPECT_ESOFT	CT_SERVER	SPECT_ESOFT	5	7	12
QR250	IMAGE_SERVER	TELECON250	7	0	7
QR_RT	IMAGE_SERVER	BRAINLAB	18	0	18
Total□41days, from Dec. 14 to 2001 to Jan. 23, 2002□			465	34	499

Table III. Error Message Summary Reports (From Oct. 22 to Nov. 20 in Huadong Hospital)

Computer Name	Error Message Description	Error Numbers
PACS-SERVER	Failed On Patient Level Selection	72
	Failed To Send Series Out	74
	Failed To Opening Files	3
	Association Rejected From Peers	72
	AE Title Errors	53
	Rejected SOP classes	35
CT DICOM GATEWAY	Failed To Send Series Out	3
MR DICOM GATEWAY	Failed To Update Database	14
	Failed To Open Data Map Files	14
Total Error Messages		340

From the Table II and III, we see that AMS detected different kinds of errors from different PACS components at different levels. But, these errors were never interrupted the radiology workflow and PACS dataflow, since the AMS helped the PACS administrators efficiently doing troubleshooting before user's complain. Also, there was no much cost for the hospital operating and maintaining PACS both in the size of IT management team and resources.

## 7. CONCLUSIONS

We installed the AMS on top of the Huadong Hospital PACS. The installation was painless, did not interrupt the normal PACS operation, and took only half of month. The PACS administrators can now monitor the entire PACS operation and dataflow from the remote Monitor Server. The AMS can monitor and control the entire PACS operation in real time, and also track patient and image data flow automatically. These features make administrators take proper action even before user's complaint if any failure happened in any PACS component or process. It also reduced the size of the management team, and decrease total cost of PACS ownership.

## 8. ACKNOWLEDGEMENT

This work was supported in part by National Nature Science Foundation of China, and Chinese Academy of Sciences.

## 9. REFERENCES

- [1]. H. K. Huang, <<PACS Basic Principles and Applications>>, Press by Wiley-Liss, New York, 1999.
- [2]. H. K. Huang, K. Andriole, T. Bazzill, et al, "Design and implementation of a picture archiving and communications system: The second time", *J. Digital Imaging*, Vol.9, pp.47-59, 1996.
- [3]. H. K. Huang, A. Wong, L. Lou, et al., "Clinical experiences with a second-generation hospital-integrated picture archiving and communication system", *J. Digital Imaging*, Vol.9, pp.151-166, 1996.
- [4]. Jianguo Zhang, J. Zhuang, X. Zhang, et al, "Design and implementation of picture archiving and communication system in Huadong Hospital", *SPIE*, Vol. 4323, pp73-82, 2001.
- [5]. Jianguo Zhang, R. Han, D. Wu, et al, "Automatic Monitoring System for PACS Management and Operation", *SPIE*, Vol. 4685-49, 2002.
- [6]. Jianguo Zhang, J. Stahl, H. K. Huang, et al, "Real-time teleconsultation with high resolution and large volume medical images for collaborative healthcare", *IEEE Trans. Information Technology in Biomedicine*", Vol. 4, pp178-185, 2000.

# Automatic Monitoring System for PACS Management and Operation

Jianguo Zhang, Ruolin Han, Dongqing Wu, Xiaoyan Zhang,  
Jun Zhuang, and H. K. Huang\*

Laboratory for Medical Imaging Informatics, Shanghai Institute of Technical Physics, Shanghai  
\*Children Hospital Los Angeles, CA90027

## ABSTRACT

In order to achieve the high and continuous availability in PACS operation, the PACS component status would be monitored seriously, and quick responds would apply to the component if any failure happened to any PACS key component either in hardware or software level. In order to protect the data loss and also for security issue, the PACS data flow, e.g., from acquisition to final display, would be tracked carefully. All these measures will increase the total cost of ownership (TCO). We built an automatic monitoring system (AMS) on top of the PACS to assist the PACS management and to make the PACS component status and internal data flow more transparent to the administrators. The PACS AMS consists of two parts: monitoring agents running in each PACS component computer and a Monitor Server running in a remote computer. Monitoring agents are connected to all PACS processes running in each PACS component. The Monitor Server monitors each agent that allows the server to track the status of individual PACS process. The PACS managers can now monitor and control the entire PACS operation in real time, and also track patient and image data flow automatically.

**Keywords:** Monitoring, PACS, management.

## 1. INTRODUCTION

PACS is a large system integration consisting of many components. Many interrelated processes are running simultaneously in these components. Chances of any of these processes fail at a given period of time are high. When it happens, immediate attention and service is required for the PACS to resume its normal operation. Current PACS application software has only limited monitoring functions to alert the PACS manager should any of these processes fail. For this reason, a large management team is required to maintain a smooth PACS operation resulting in increasing the TCO.

Although there are some commercial network monitoring tool products, e.g. OpenView [1], Big Brother System [2], available to monitoring network status, but, most of them were built based on SNMP (small network management protocol) or their native protocol, and they were usually used to monitor or control the network node status or resources, but, it is difficult to use these kinds of products to help PACS administrators to manage PACS, for example, to monitor PACS image dataflow and related internal events, or to track study workflow, evaluate and analyze the PACS performance, help the PACS administrators to do troubleshoot if there was any failure either in hardware or software.

We have developed an automatic monitoring system (AMS) for PACS operation based on the concept of agent service and API (application program interface) model to alert the manager timely any process failure in the PACS operation. In this paper, we presented our architecture design and implementation of AMS built on top of our clinical PACS running in Huadong Hospital, and gave the preliminary results.

## 2. AMS DESIGN REQUIREMENTS

Although PACS is an integrated system, and consisted of different components and related devices, there are some basic and common requirements for AMS to monitor or manage these components or devices. The required features or functions for AMS on every component are:

- 1). Both normal and abnormal events collection, transmission and analysis, e.g., image receiving, sending, image file I/O operation, database update, or any failures on these operation;
- 2). PACS computer running status and resource usages, e.g., PACS processes, services, image storage spaces, and networking status;
- 3). PACS workstation security records, e.g., users logon/off date and time;
- 4). Patient/image dataflow tracking and workflow management;
- 5). PACS networking status and image communication performance;
- 6). PACS image data usage and analysis, e.g., image query/retrieval monitoring and tracking.

Since most of required features and functions are related to PACS architecture, software, operating system, dataflow, PACS operation modes, and DICOM, the AMS designing should consider how to build the monitoring system to meet these requirements. Also, the monitoring system should have no much more overheads on current PACS performance and costs. So, the criteria to design and to build the AMS are:

- 1). It should support cross-platform PACS, such as Unix and Microsoft NT (Windows 2000 or XP);
- 2). Its architecture should be open, and can be used for intranet PACS and inter-net PACS, the communication protocol from PACS components to AMS or from AMS to PACS should support TCP/IP;
- 3). The data or message structures or representations used in AMS should be consistent with the semantic descriptions of DICOM IOD (Information Object Definition), or other definitions used in DICOM.
- 4). Utmost to use standard management functions or utilities provided by operating system;
- 5). It should be easy to be integrated into current PACS architecture, and easy to be used and operated;
- 6). It should be cost-effective.

### **3. AMS ARCHITECTURE AND OPERATION MODES**

We had designed and developed a PACS monitoring and control subsystem for CR image acquisition and preprocessing with multi-level process structure [3]. That monitoring and control sub-system only was used for monitoring single node, not for networked distribution computation system such as entire PACS. So, we designed the AMS still with multi-level process structure, but, it would be distributed to most monitored PACS components, in other words, the AMS architecture was three-tiered structure with asynchronous communication with PACS components and processes. Figure 1 shows the AMS architecture integrated with PACS. It consisted of three kinds of modules: monitor server, agent services, and called APIs, or objects embedded in PACS processes

There are two kinds of operation modes in AMS: the Active mode and Passive mode. Figure 2 (a) and (b) show the communication relation between AMS modules in the two operation modes. In Active mode, the AMS sends commands to the Agent Services running in monitored PACS components, the Agents perform monitoring and management, or some special control functions, and send the results or reports back to the AMS server based on the command types. In this mode, the following PACS management and monitoring tasks are completed: 1) Collecting security records in PACS workstations; 2) Monitoring storage spaces or other resource status; 3) monitoring PACS process or service status; 4) Checking PACS networking connection status; 5) Monitoring patient/study workflow and image data usage. In Passive mode, the Agent Services trap the both normal and abnormal events sent from PACS processes, encode the events to proper messages with host and process information, and send them to AMS Server. The AMS Server classifies and analyzes the message information, inform the administrators to do the troubleshoot through modem or wireless connections if there are any serious errors happened in a PACS component. In this mode, the following monitoring functions are executed: 1) Tracking the PACS image dataflow; 2) Capturing the abnormal events

happened in a PACS component, and give proper troubleshoot solution or comments; 3) dynamically monitoring PACS image communication performance and status.

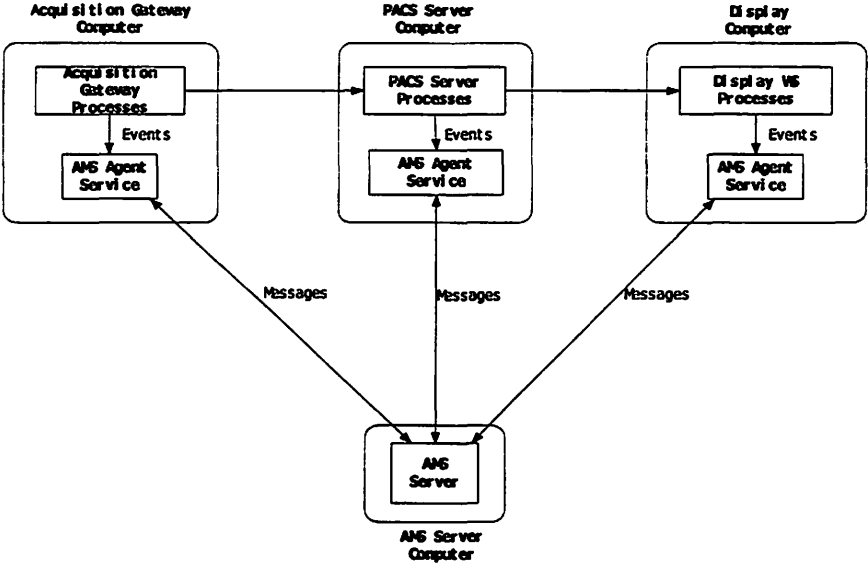
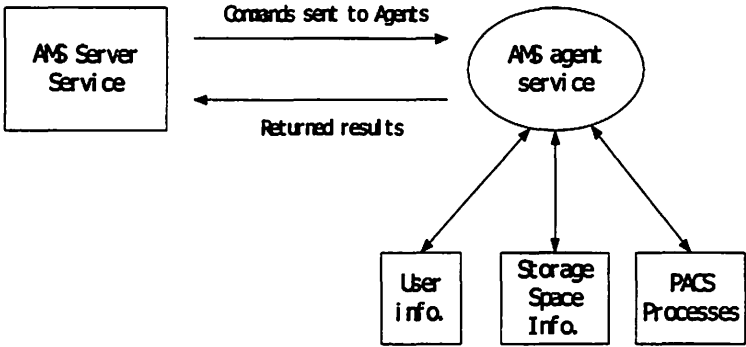
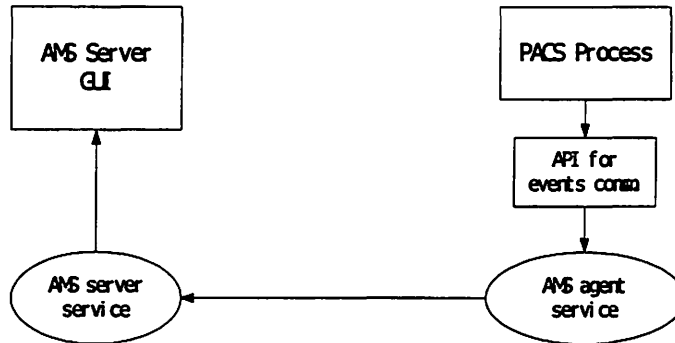


Figure 1. AMS architecture built on top of a PACS



(a). AMS internal communication in the Active operation mode.

In Active mode, the most functions or tasks are performed periodically. But, in passive mode, the monitoring tasks are executed real-time. The AMS mostly watches the PACS hardware and computer resource status in Active mode, and monitors and tracks the PACS software running status or PACS performance in the Passive mode.



(b). AMS internal communication in Passive operation mode with trapping events.

Figure 2. The communication relation between AMS modules.

## 8. AMS IMPLEMENTATION AND INSTALLATION

Since most PACS were built on Unix and Microsoft Windows NT/2000/XP platform, our AMS was also developed to support these two popular operating systems. The AMS Server was implemented on Windows NT/2000/XP platform, the Agent services and Called APIs were developed on both Unix (Sun Solaris) and Windows platforms. In order to decrease computation overheads on PACS computers, and do best to isolate AMS from the PACS, we widely used asynchronous communication technologies in AMS. The major functions and features AMS had are:

- (1) Real-time capture all warning, error messages happened in PACS acquisition gateways, PACS server, and display workstations, and send them to central monitor server;
- (2) Periodically check PACS components running status;
- (3) Remote monitor PACS component computer resource status, e.g., storage spaces, networking;
- (4) Remote control and operate PACS processes and services running in PACS components;
- (5) Track patient/image dataflow in PACS components, and analyze the image usages;
- (6) Monitor remote display workstation logon/off status, guarantee images secured read and used;
- (7) Visually show the image dynamic flow status from one component to another in PACS network, and make PACS operation more transparent to PACS administrators or end users;
- (8) Route serious error or warning messages to an administrator through pager or fax to call emergency repairing or do troubleshooting.

We started to implement AMS in Huadong Hospital PACS [4] from the end of the May, 2000, and completed the installation in the middle of the June. The agent services were installed in CT and MR acquisition gateway computers (Windows 2000), and TeleCon display workstations [5], as well as, the PACS server (Sun Enterprise 450 with Sun Solaris 7 and Oracle 8i database). The monitor server software was installed in a Windows Advanced Server computer with the modem connection. The installation was painless, did not interrupt the normal PACS operation. The AMS was also exhibited at InfoRAD, RSNA 2001 (Radiological Society of North America) [6].

We laid a course of using AMS to manage and maintain PACS operation. First, we explained to the AMS users to understand the AMS major functions and architecture; Second, classified the remote messages sent from the PACS components to be three levels of normal, warning and error, and trained the users to read the messages or information displayed on the monitor server display program; Third, trained the users to take proper actions on a PACS component based on different messages or information.

## 8. PRELIMINARY RESULTS

The major works of an administrator in monitoring and controlling PACS operation with AMS were to operate the AMS display program and read the messages or graphic information displayed on AMS. The routing works for an administrator using AMS to manage and maintain the PACS becomes:

- 1) Read the AMS messages or information displayed on AMS display program;
- 2) Identify problem reasons or sources if they found the errors among the messages sent from a remote PACS component;
- 3) Fix the problems if they can, otherwise call for technical support;
- 4) Analyze the data information sent from agent services and give correct evaluation about PACS performance and resource usages;
- 5) Track patient/image dataflow (store-forward and query/retrieval), monitor the remote users logon/off status, guarantee images secured used;
- 6) Do statistics on radiological examinations with AMS statistical functions, e.g., count performed study numbers of every day on CT, MR, NM.

The Figure 3 to Figure 8 are the GUI examples of AMS server display used by the PACS administrators. Figure 3 shows the status of the PACS network connection and image communication. The different colors on PACS component icons or network lines in Figure 3 mean the computer were in different status, the green means working, the red means the errors, the gray means idle. Figure 4 shows the message items sent from different PACS components, every item records the message type (normal, warning, or error), source, date/time, process, and the description about the message. Figure 5 shows the status of PACS computers distributed in the PACS network, e.g., storage spaces, processes, or services. The users can also remotely control the PACS processes from AMS server in the GUI of Figure 5. Figure 6 shows the part of PACS dataflow. It tracked the Patient/Study query/retrieval, and gave the performed status information. Figure 7 is about PACS workstation security records of users logon/off. From Figure 6 and 7, the administrators can track whom, in which workstation and in what times, queried and retrieved particular patient image studies.

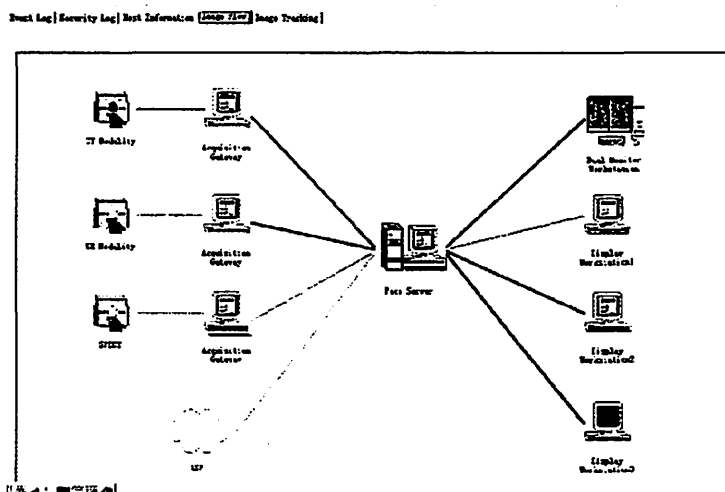


Figure 3. PACS network connection and image communication status monitored by AMS. The different colors on PACS component icons or network lines mean the computer were in different status, the green means working, the red means the errors, and the gray means idle.

Event Log | Security Log | Mail Information | Image Files | Image Tracking

Event	Event ID	Time	Date	User Name	Computer Name	Source	Description
Information	3002	15:17:43	2002-11-19	dev1	dev1	YachtCS-Web	
Information	3002	15:17:50	2002-11-19	dev1	dev1	YachtCS-Web	
Information	3004	09:54:00	20/11/2002	pacman	pacserver1.lan	image-server	Series 53 is read out successfully.
Information	3005	09:54:00	20/11/2002	pacman	pacserver1.lan	image-server	Series 54 is read out successfully.
Information	3004	09:54:00	20/11/2002	pacman	pacserver1.lan	image-server	Series 54 is read out successfully.
Error	0000	09:54:00	20/11/2002	pacman	pacserver1.lan	image-server	open file C:\AC999943_200211190010_20 failed
Information	3004	09:54:00	20/11/2002	pacman	pacserver1.lan	image-server	Series 55 is read out successfully.
Error	0000	09:54:00	20/11/2002	pacman	pacserver1.lan	image-server	open file C:\AC999943_200211190010_20 failed
Information	3004	09:54:00	20/11/2002	pacman	pacserver1.lan	image-server	Series 56 is read out successfully.
Information	3005	09:54:00	20/11/2002	pacman	pacserver1.lan	image-server	Series 56 is read out successfully.
Information	3004	09:54:00	20/11/2002	pacman	pacserver1.lan	image-server	Series 56 is read out successfully.
Information	3005	09:54:00	20/11/2002	pacman	pacserver1.lan	image-server	Series 56 is read out successfully.
Information	3004	09:54:00	20/11/2002	pacman	pacserver1.lan	image-server	Series 57 is read out successfully.
Information	3005	10:11:00	20/11/2002	pacman	pacserver1.lan	image-server	Series 57 is read out successfully.
Information	3004	10:11:00	20/11/2002	pacman	pacserver1.lan	image-server	Series 58 is read out successfully.
Information	3005	10:11:00	20/11/2002	pacman	pacserver1.lan	image-server	Series 58 is read out successfully.
Information	3004	10:11:00	20/11/2002	pacman	pacserver1.lan	image-server	Series 59 is read out successfully.
Information	3005	10:12:00	20/11/2002	pacman	pacserver1.lan	image-server	Series 59 is read out successfully.
Information	3004	10:12:00	20/11/2002	pacman	pacserver1.lan	image-server	Series 60 is read out successfully.
Information	3005	10:12:00	20/11/2002	pacman	pacserver1.lan	image-server	Series 60 is read out successfully.
Information	3004	10:12:00	20/11/2002	pacman	pacserver1.lan	image-server	Series 61 is read out successfully.
Information	3005	10:12:00	20/11/2002	pacman	pacserver1.lan	image-server	Series 61 is read out successfully.
Information	3004	10:12:00	20/11/2002	pacman	pacserver1.lan	image-server	Series 62 is read out successfully.
Information	3005	10:12:00	20/11/2002	pacman	pacserver1.lan	image-server	Series 62 is read out successfully.
Information	3004	10:15:00	20/11/2002	pacman	pacserver1.lan	image-server	Series 63 is read out successfully.
Information	3005	10:15:00	20/11/2002	pacman	pacserver1.lan	image-server	Series 63 is read out successfully.
Information	3004	15:30:00	20/11/2002	pacman	pacserver1.lan	image-server	Series 64 is read out successfully.
Information	3005	15:34:00	20/11/2002	pacman	pacserver1.lan	image-server	Series 64 is read out successfully.

Look... | Show... | Refresh | Update

Figure 4. The AMS displays the messages sent from different PACS components. Every record is with the message type (normal, warning, or error), source, date/time, process, and the description.

Event Log | Security Log | Mail Information | Image Files | Image Tracking

Event Name List:

Event Name	IP Address	Description
pacserver1	FE2:368:1:1F	San Zakaryia
dev03	FE2:368:1:25	Dr. Mag. J. Al-Sayid
pacserver2	FE2:368:1:15	Server in Lab
dev01	FE2:368:1:11	In Reception's
Gateway	FE2:368:0:12	Gateway to the Lab
dev02	FE2:368:1:23	Image s

Current Host: [Name] [File] [Name desc]

Process Name	Count
image-server.exe	193
all-antivirus.exe	79
bluetooth.exe	124

Services:

Service Name	Status
Any Client Service	Running
Center	Stopped
ImageServer	Running

Hard Disk Space:

Logical Drive	Free
C:\	300
D:\	214
E:\	64
F:\	98

Start Service | Stop Service

Figure 5. The AMS gives the status of PACS computers distributed in the PACS network, e.g., storage spaces, processes, or services.



real-time monitor and control the whole PACS components activities, and simplify and reduce the administration works, and make the PACS more easy to manage; (2) can get instant respond if any failure happened in any PACS component, and solve the problems prior end user aware about that, this would make the PACS more acceptable than those without early warning mechanism; (3) track patient/image data flow, and make the image accessing more manageable, this is other way to enhance PACS security. The AMS can be easily integrated into both on-site PACS and off site PACS (ASP mode PACS operation) to monitor and manage PACS operations. With these features mentioned above, the TCO in PACS operation, either with in house mode or ASP mode, would be decreased since it reduce the labor works and technical experience requirements for those who manage about PACS operations, and also reduce the risks of data loss and interruption, so that it would achieve the high and continuous availability.

## 7. ACKNOWLEDGEMENT

This work was supported in part by National Nature Science Foundation of China, and Chinese Academy of Sciences.

## 8. REFERENCES

- [1]. Hewlett-Packard, <http://www.openview.hp.com>.
- [2]. BB4 Technologies, <http://bb4.com>.
- [3]. Jianguo Zhang, H. K. Huang, "Multi-level adaptive process control of acquisition and post-processing of CR images in PACS environment", *Computerized Medical imaging and Graphics*, Vol. 22, 31-40, 1998
- [4]. Jianguo Zhang, J. Zhuang, X. Zhang, et al, "Design and implementation of picture archiving and communication system in Huadong Hospital", *SPIE*, Vol. 4323, pp73-82, 2001.
- [5]. Jianguo Zhang, J. Stahl, H. K. Huang, et al, "Real-time teleconsultation with high resolution and large volume medical images for collaborative healthcare", *IEEE Trans. Information Technology in Biomedicine*", Vol. 4, pp178-185, 2000.
- [6]. Jianguo Zhang, R. Han, D. Wu, et al, "Automatic monitoring system for PACS operation", *Radiology*, Vol. 294(P), pp737, 2001,

# **Integrating a DICOM Acquisition and Distribution Gateway for Micro-CT Imaging in a PACS Environment**

Jun Zhuang, Dongqing Wu, Wei Xie, Jianguo Zhang  
Shanghai Institute of Technical Physics, Chinese Academy of Sciences, Shanghai

Rex Moats, Marvin D. Nelson, Fei Cao, Michael Zhou, H.K. Huang  
The Childrens Hospital Los Angeles/University of Southern California

## ***Purpose:***

Micro Computerized Tomography (MicroCT) systems were developed mostly for small animal body imaging research. It can be used to scan animal bodies to obtain anatomic structure images *in vivo* without scarifying the animal, so that researchers can continue studying the induced disease or gene manipulation over the life cycle of the animal.

The volume of a series of CT images generated by MicroCT is usually very large and its sizes varies from 32 MB (256 x 256 x 2 x 256) to 2 GB (1024 x 1024 x 2 x 1024) These images often need to be transferred from one site to another for different research purposes and management. Since raw MicroCT images were non-DICOM compliance, it is difficult to take advantage of the matured PACS technologies to transfer, archive, manage or display these images. Here, we present a newly developed DICOM acquisition gateway to interface the MicroCT imaging system with a PACS Research Server to achieve automatically MicroCT images acquisition and data management.

## ***Methods:***

The software package was developed based on the MicroCT system, named MicroCAT developed by ImTek, Inc (P. O. Box 10346 Knoxville, TN, 37939). It uses a 1024 x 1024 element CCD array coupled with a high-resolution phosphor screen as the X-ray detector. The imaging area can be changed from 50mm x 50mm to 70mm x 70mm. After scanning the object, the MicroCT system usually outputs reconstructed volume images from size 256 x 256 x 2 x 256 to 1024 x 1024 x 2 x 1024, according to the pre-setting of the reconstruction algorithm. The output data files included raw image data files with "att" format and log files, which record scanning parameters and reconstruction information.

The image acquisition gateway was designed to have four modules with a Graphic User Interface for manually input some DICOM header information pertinent to the animal experiment. The first module has the capability to capture reconstructed raw MicroCT images with their log files. Second module is DICOM encoding process. It creates DICOM objects, fills the DICOM header structure with information both from log files and manual settings, and converts raw image data to DICOM format. Third module is for local image management. It consists of an image

database and a management tool. The last module is a communication process working as DICOM Storage SCU (Service Class User) to send encoded DICOM images to remote PACS computers or DICOM conformance viewers for display or image management.

***Results:***

In last three months, we successfully acquired and processed 18 series Micro-CT images with the acquisition gateway. After image processing, they can be automatically sent to any PACS display workstation to be viewed and manipulated, or a PACS DICOM archiving server for querying and retrieving later on by workstations. The package is in the process of being integrated to the MicroCT scanner as a complete imaging system.

***New or Breakthrough:***

Introducing the state-of-art PACS technologies to biomedical imaging, and deploying PACS application research tools in new research area.

***Conclusions:***

The MicroCT imaging acquisition gateway was designed and developed based on DICOM standard and MicroCT imaging data flow requirements. It can automatically acquire raw MicroCT images, encode them to DICOM format, and send the images to remote DICOM compliance sites. Using the developed acquisition gateway can integrate MicroCT imaging system into a PACS infrastructure, and enable potential users to obtain benefits from matured PACS technologies. The same package can be integrated to other manufacturers' MicroCT, MicroPET or MicroMRI imaging modality.

***Keywords:***

MicroCT, Imaging Acquisition Gateway, DICOM, PACS

# Teleconferencing with Dynamic Medical Images

Johannes N. Stahl, Jianguo Zhang, Christian Zellner, Eugene V. Pomerantsev, Tony M. Chou, and H. K. Huang, *Senior Member, IEEE*

**Abstract**—Dynamic images, a sequence of static images displayed in rapid succession and perceived as a continuous motion by the human eye, are widely used in medicine. One of the primary objectives of telemedicine is the transmission of such images to a distant location to manage clinical problems remotely. A broad variety of methods is available to acquire, store, transmit, and display these images. However, the context of the clinical problem determines which of these methods can be deployed in a telemedicine solution. This paper discusses the advantages and disadvantages of the different technologies and presents an example of a teleconferencing system for interventional cardiology.

This system acquires cardiac angiography and intravascular ultrasound images and transmits them over an existing Internet connection to a distant location. It is specifically optimized for clinical conferencing, where time is limited for each case presentation during the conference, compared to the relatively long time available for the conference preparation. The system takes advantage of this characteristic by transmitting the images well in advance of the clinical conference and displaying them synchronously in both locations during the conference. This allows for the preservation of the original image quality.

**Index Terms**—Cardiac angiography, interventional cardiology, teleconferencing, tele-imaging, telemedicine.

## I. INTRODUCTION

ONE important aspect of telemedicine is the exchange and remote presentation of medical multimedia documents. Images are among the most important and commonly used types of medical documents [1]. In an ideal world, these images would be available immediately, in original quality, and in the place they are needed. Although the technology exists to reach this goal, it remains very expensive. Under most circumstances, the designer of a telemedicine solution will have to resort to more common, less expensive technologies. This forces a compromise between the image quality, the time required for transmission, the number of destinations, and the cost to build and maintain the system.

Manuscript received May 2, 1999; revised September 10, 1999. This work was supported in part by the National Library of Medicine under Contract N01-LM-6-3547.

J. N. Stahl and J. Zhang are with the Laboratory for Radiological Informatics, Department of Radiology, University of California, San Francisco, San Francisco, CA 94143-0628 USA.

C. Zellner and T. M. Chou are with the Cardiology Division, Department of Medicine, University of California, San Francisco, CA 94143 USA.

E. V. Pomerantsev is with UCSF-Stanford Health Care, Stanford, CA 94305 USA.

H. K. Huang was with the Laboratory for Radiological Informatics, Department of Radiology, University of California, San Francisco, CA 94143-0628 USA. He is now with the Department of Radiology, Children's Hospital of Los Angeles/University of Southern California, Los Angeles, CA 90027 USA.

Publisher Item Identifier S 1089-7771(00)03955-8.

There exists a wide array of available multimedia and communication technologies to acquire, to transmit, and to present medical images. One of the most crucial tasks in designing a telemedicine system is to analyze the problem and select the appropriate tools to solve it. The appendices give an overview of types of dynamic medical images and possible telemedicine applications. Also explained are commonly used technologies for their compression, transmission, and display.

For the purpose of this paper, it is reasonable to distinguish between static and dynamic images. Dynamic images are composed of a sequence of static images which, when displayed in rapid succession, are perceived as continuous motion by the human eye. Because dynamic images consist of a sequence of static images, they share many of the properties of static images. However, we want to discuss them separately for two reasons. First, the amount of data and the processing time required to use dynamic images in telemedicine are significantly higher. Second, they require display and storage strategies, which are distinct from those used for static images.

In this paper, we will present an example of a teleconferencing system for interventional cardiology that demonstrates how dynamic images can be used in a clinical setting.

Our goal for this project was to establish collaborative conferencing facilities between the departments for interventional cardiology at UCSF Medical Center in San Francisco, California and Stanford University Medical Center in Stanford, California. It was the intention of the cardiologists to have joint interactive conferences covering recent interventional procedures. The modalities to be used were cardiac catheterization angiography (CA) and intravascular ultrasound (IVUS).

The desired functionality were the following.

- Studies from either hospital should be sent to the other.
- During the conference, there should be a joint interactive review of the cases and a real-time discussion about the procedures.
- Both sides should be able to present their cases and learn from the other side's comments.
- The same system should also be used for the review of studies during local in-house conferences.

## II. MATERIALS AND METHODS

The dynamic images originate from two different sources: Digital Imaging and Communications in Medicine (DICOM) [2] files from digital cardiac angiography equipment (Camtronics Medical Systems, Hartland, WI and GE Medical Systems, Waukesha, WI) and analog tapes in S-VHS format from the IVUS imaging system (Boston Scientific, Natick, MA, and Endosonics, Rancho Cordova, CA). The DICOM images are imported through a DICOM gateway that connects

TABLE I  
 PROPERTIES OF THE TWO IMAGING MODALITIES USED IN THE CARDIOLOGY TELECONFERENCING SYSTEM

	CA images	IVUS images
Format	DICOM	MPEG-1
Resolution	512x512	350x240 (sub-sampled 4:1 from 700x480 NTSC signal)
Frame Rate	30 f/s	29.97 f/s
Compression	JPEG lossless, ratio 3:1	MPEG lossy with inter-frame compression, ratio 16:1 (64:1 including subsampling)
Data rate	20 Mbit/s	1.2 Mbit/s
Typical duration	8 seconds	1 minute
Typical files size	20 Mbytes	10 Mbytes
Number of sequences per patient	~15	2
Total	300 Mbytes	20 Mbytes

CA: cardiac angiography; IVUS: intravascular ultrasound.

the proprietary fiber-optic network of the Camtronics system with the main campus network. The analog IVUS tapes are digitized into MPEG-1 format using a Broadway 2.5 MPEG capture board (Data Translation, Marlboro, MA).

Table I shows the basic properties of both modalities and the approximate amount of data produced. The two hospitals have a permanent data connection via two T1 lines, with a combined bandwidth of 3 Mbit/s. This bandwidth, however, has to be shared with all other users of the campus network.

The system was implemented on the Windows NT operating system platform, and the programming language was Microsoft Visual C++. The basic architecture of the system was based on an earlier teleconsultation system for static radiological images [3]. The modifications necessary to add support for dynamic images were relatively minor.

### III. IMPLEMENTATION

#### A. Problem Analysis

The analysis of the problem showed that conferences were to be held on a weekly basis for local conferencing (UCSF only) and on a monthly basis for teleconferencing (UCSF/Stanford). During early experiments, we learned the following.

- All the cases to be presented during the conferences would be known at least 24 h in advance.
- During the conference, the images within a case would be reviewed within a very short time, so the display had to be very fast.

As a result, much of our development focus was on conference preparation. Every task that could be done ahead of the conference should be done during the preparation phase, leaving only the necessary minimum for the conference itself. We found that the following tasks can be performed ahead of the conference:

- import of DICOM files from the modality;

- capture of IVUS video tapes to MPEG files;
- reconciliation of patient demographic data in the system's database;
- transmission of the images to the remote workstation (off-line);
- adjustment of the display parameters (e.g., brightness/contrast).

During the conference, the only task should be to select a patient from a list and to switch between individual image sequences by pressing a button. Sequence playback should start immediately without latency on both workstations and stay synchronized at both sites.

Most of the images can be reviewed with these simple activities. However, in problematic or doubtful cases, the physicians can immediately switch to an interactive review with more elaborate image manipulation functions:

- remote dual cursor for the demonstration of image features;
- playback controllable by both sides;
- window/level and zoom controls;
- static image display with ROI measurements;
- slow-motion, forward/reverse, and fast random positioning.

#### B. System Architecture

The system consists of four main modules (see Fig. 1):

- 1) a DICOM storage manager that receives images from the acquisition modalities and forward them to the remote workstation;
- 2) a database that keeps track of the images and the store-and-forward process;
- 3) a display subsystem for the visualization of static and dynamic images;
- 4) a remote control system that allows real-time interactive discussions.

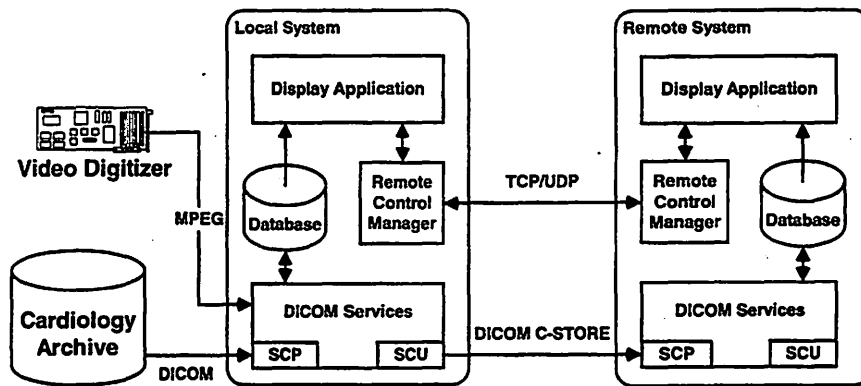


Fig. 1. Major software components of the teleconferencing system and data flow paths between the local and the remote side. SCP: service class provider; SCU: service class user. MPEG data is encapsulated in DICOM for the C-STORE operation.

1) *Image Transmission:* We use the DICOM protocol for the purpose of off-line transmission of the data. The DICOM service is realized as a Windows NT system service that communicates with the other modules through the Distributed Component Object Model (DCOM) protocol. The DICOM service implements a C-STORE service class provider (SCP) and service class user (SCU). The SCP can receive images from both the modalities and the other workstation. The SCU module sends images to the second workstation.

The DICOM sequences received from the CA system are compliant with the DICOM standard and can be transmitted directly with DICOM. For the MPEG-encoded ultrasound video, there exists no appropriate DICOM standard, so we had to use a private service-object-pair (SOP) class for the transmission. This class encapsulates the MPEG-encoded images in a DICOM object.

During the conference preparation, the system transmits the data using a compressed DICOM transfer syntax. However, since both the DICOM and MPEG files are already stored in a compressed form, there is no need for additional compression/decompression cycles during the image transmission. Instead, our system transmits the already compressed data without further alteration.

The system uses Secure Socket Layer (SSL) encryption technology [4] for the data transmission to ensure patient privacy and data integrity.

2) *Database:* The system database stores patient demographic data, study and series information, and image parameters in a form analogous to the DICOM real-world object model. It also controls the conference schedule and keeps track of images to be transmitted between the workstations. Both the DICOM system service and the conferencing application use the database to store persistent settings. The database is implemented using the Microsoft Jet database engine and the Open Desktop Database Connectivity (ODBC) interface.

3) *Image Display:* The display module uses the DirectShow technology (Microsoft Corporation, Redmont, WA) for dynamic image display. DirectShow is an extensible multimedia architecture that gives the application very detailed control over the media presentation [5]. It allowed us to combine static

image display with dynamic image display in a single window [6].

The DirectShow system uses a "filter" paradigm for the representation of multimedia streams. DirectShow filters are pieces of software that perform an operation on the media stream. Several filters can be connected to build a "filter graph," which as a whole can present the data dynamically to the user. Media samples originate from a "source" filter and are passed through several "transform" filters, before they reach the "renderer filter" that performs the actual display.

The DirectShow system has built-in filters for the display of MPEG-encoded sequences. To display DICOM-encoded multiframe images with DirectShow, we created two custom-built filters (Fig. 2):

- A DICOM parser filter that can parse the contents of a DICOM-compliant file and identifies the individual image frames (called media samples in the DirectShow terminology) contained in the file. This filter can read the image frames both randomly and sequentially and pass them down the DirectShow filter graph. These image frames are still compressed.
- A decompressor filter that can decode the DICOM-compatible image compression, usually lossless JPEG for CA files. This filter uses a very fast commercial package for the decompression (Pegasus Software, Tampa, FL), so that the decompression can be performed in real time.

The advantage of this architecture is that additional filters inserted after the decompression filter can be used for both MPEG and DICOM images. Such additional filters that we created for the teleconferencing system were:

- a contrast filter that performs lookup-table (LUT) operations on the images to allow brightness/contrast adjustments;
- an edge-enhancing filter to increase the sharpness of the images; this filter was necessary because the cardiologists were used to viewing the images with moderate edge enhancement (refer to Fig. 3);
- a remote cursor filter that embeds a remote pointer into the images for the interactive discussions and that provides

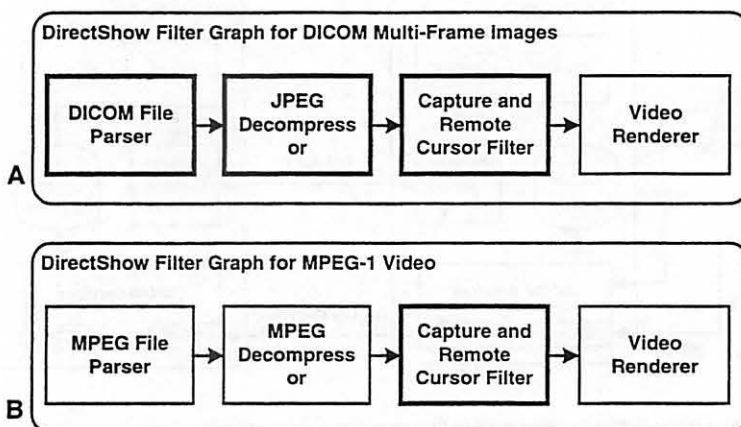


Fig. 2. Arrangement of DirectShow filters in a filter graph for the display of dynamic images: (A) Filter graph architecture for DICOM multi-frame images; (B) Filter graph for standard MPEG files. The filters with bold frames have been developed by us specifically for the conferencing application. The filters with thin frames are part of the standard DirectShow distribution. Additional image processing filters are not shown for clarity.

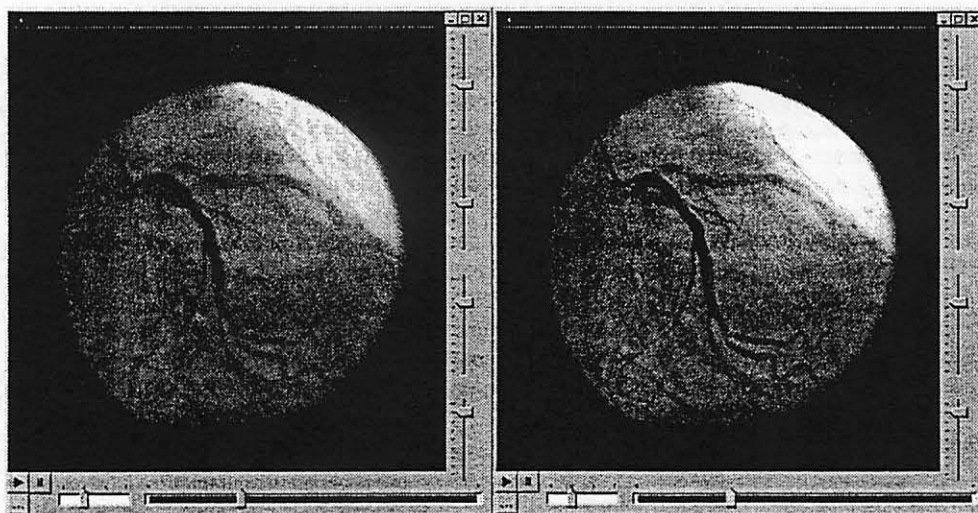


Fig. 3. Display of a dynamic CA series without edge enhancement (left) and with edge enhancement (right). The details of smaller vessel branches are more clearly visible with edge enhancement. The filter uses an unsharp mask with a  $7 \times 7$  pixel approximated Gaussian filter.

still image capture functions (still image capture is necessary for image evaluation functions, such as ROI measurements);

(Other functions, such as zooming and panning, were provided by the default DirectShow renderer filter, so we did not need to implement them ourselves.) An important aspect of these filters was speed. The DICOM images are encoded in  $512 \times 512$  pixels, 8 bit/pixel at a frame rate of 30 frames/s. We needed to perform the image processing functions in real time. To accomplish this, we implemented the image processing functions in assembler code that takes advantage of the MMX extension of the Pentium II processor (Intel Corporation, Santa Clara, CA). This extension has Single Instruction Multiple Data (SIMD) commands that process up to 8 pixels with a single instruction. Using these technologies, we were able to read the DICOM images from a disk and decode, process, and display them at a sustained frame rate of 23 frames/s on a 400-MHz Pentium II CPU.

Since this was still short of 30 frames/s, we combined the streaming display mode with a memory cache to further increase the performance. Cardiology multiframe images are usually displayed in a loop that is repeated multiple times. To avoid delays when a sequence is started, we use the streaming mode as default. This means that images are read from the disk "on the fly" in real time and displayed immediately during the first pass. However, the decoded images are not discarded but are kept in a memory cache. During subsequent passes, images can be displayed from the cache, resulting in significantly better performance. The required frame rate of 30 frames/s could be reached and even exceeded during the second and subsequent passes. The difference between the first pass with 23 frames/s and the second pass with 30 frames/s can only be noticed under careful observation.

4) *Remote Control*: One of the most important aspects of our system is the ability to allow real-time remote interaction 90

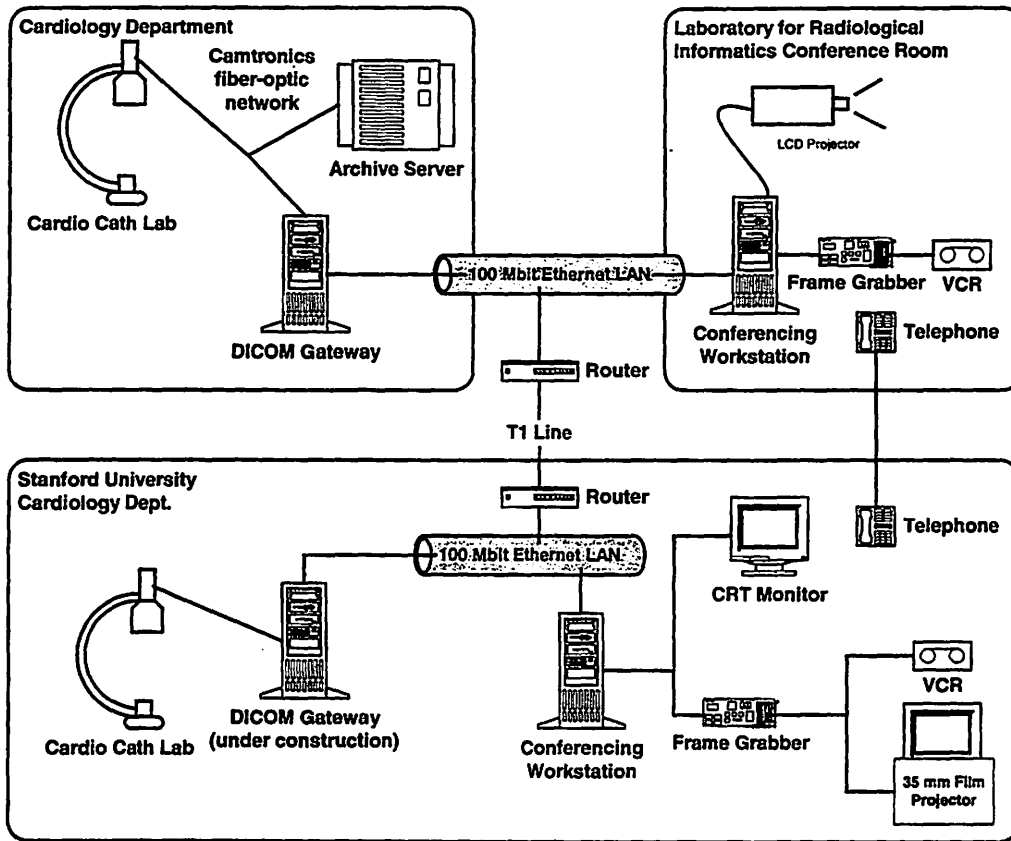


Fig. 4. Network diagram of the conference facilities at UCSF/Stanford Health Care.

during the conferences. This feature allows the physicians in San Francisco and Stanford to review the dynamic images synchronously in real time, although the image files are transmitted offline in advance. The necessary functions are implemented in the remote control manager module, the core of which we already developed for an earlier project [3].

During the conference, the remote control manager establishes a real-time connection to its peer at the remote workstation. Both systems exchange TCP/IP messages that keep the state of both workstations in synch. The manager uses a combination of the TCP stream protocol and the UDP datagram protocol for the message exchange, because we experienced a significant latency between the systems when using TCP alone. We identified the Nagle algorithm, an internal buffering scheme used by TCP/IP implementations [7], to be the reason for these latencies.

We implemented two methods to guarantee synchronization of the dynamic image display [6]. First, we had to compensate for timing differences between the workstations. We found that a synchronization difference of more than  $\pm 300$  ms can be noticed by the users, so it was our goal to maintain synchronization within these limits.

The DirectShow system is controlled by internal software reference timers. These timers prioritize real-time behavior, so that, in the event that one CPU is not fast enough to process the images in time, the system will start to skip frames in order to keep

up with real time. For this reason, differing CPU clock speeds will not cause the systems to desynchronize. However, small errors in the software timers can cumulate over time. To compensate for this, the remote control manager exchanges synchronization messages in 3-s intervals. If a difference in the stream positions is detected, the faster system slows by 5% until synchronization is restored.

Second, we had to take into account network-imposed latencies that occur at the network layer of a TCP/IP-based WAN and will affect even UDP datagrams. On the global Internet, these latencies can be 500 ms and higher. The remote control manager estimates the latency by measuring the round-trip time (RTT) for data packets and dividing it by 2. This latency is added to all timestamp messages received from the remote workstation.

#### IV. RESULTS

We evaluated the teleconferencing system both technically and clinically. During the development phase, we set up the audiovisual conference system at the Laboratory for Radiological Informatics (LRI) conference room (see Fig. 4).

The system consists of a PC (Pentium II CPU, 400 MHz, 128 MB RAM) and an LCD projector (Proxima Corporation, San Diego, CA). The system has a 100-Mbit/s fast Ethernet connection to the UCSF campus network, which has links to

TABLE II

RESULTS OF THE CLINICAL CONFERENCES PERFORMED SO FAR. ALL FIGURES ARE AVERAGED OVER ALL CONFERENCES. THE DATA TRANSMISSION TIME REFERS TO THE TRANSMISSION BETWEEN THE CAMTRONICS ARCHIVE SYSTEM AND THE TELECONFERENCE SYSTEM FOR THE LOCAL CONFERENCES AND TO THE TRANSMISSION BETWEEN UCSF AND STANFORD FOR THE TELECONFERENCES

	Local conferences (UCSF only)	Tele-conferences (UCSF and Stanford)
Number of conferences performed	12	6
Number of patients per conference	~8	~4
Total amount of data per conference	~2 GB	~800 MB
Time for data transmission	45 min. (LAN)	90 min. (T1 line)
Conference preparation	2-3 hours	3-4 hours
Conference duration	90 min.	45 min.

both the DICOM gateway of the cardiac catheterization laboratory and the T1 line to the Stanford campus. The Stanford site has a similar setup in the cardiology conference room, using a 21-in CRT monitor instead of an LCD projector. A speaker telephone is used for voice communication.

1) *Conference Preparation:* As expected, considerable time was needed to prepare the conferences. Images were retrieved from the modality into the computer's hard disk at least 12 h before the conference. This task took about 45 min using the campus LAN. The digitization of the IVUS sequences lasted between 1 and 2 h. Due to the lower bandwidth on the WAN connection, data transmission to Stanford usually required about 90 min, although fewer cases were sent for the teleconferences. Initially, a DICOM gateway was not available at the Stanford campus, so the angiography images there were also digitized to MPEG format from 35-mm celluloid film.

The total time spent for conference preparation was usually 2-4 h for 4-10 cases, which includes the time needed to digitize the analog IVUS tapes. Compared to conventional (nondigital) conferencing, this is not unusual effort. We intentionally left enough time to compensate for possible transmission problems, although both the LAN and the WAN connections proved to be very reliable.

2) *Conference:* We found that there is a very tight schedule during the clinical conferences. The time available to review the images of a single patient is typically less than 5 min, during which 15-20 angiographic and ultrasound series are displayed. To avoid delays in the image display, we had to use the "streaming" display mode (refer to Appendix E) for the angiographic sequences, although this mode requires very fast hardware and software to maintain an appropriate frame rate.

The ultrasound series were less problematic, since they were subsampled 4:1 during digitization, which reduces the data rate. The fast rate at which the cardiologists browse through the sequences also requires a very easy and effective user interface for the software. The most important user interface feature was the ability to switch to the next or previous series by pressing a single key.

The performance of the software was satisfactory overall. There were no significant disruptions due to technical failures. The image quality of the cardiac angiography was identical to

the original, because only lossless compression was used. The quality of the ultrasound images was slightly less compared to those on VHS tape, but still rated adequate for conferencing purposes. The LCD projector has a lower contrast resolution than a CRT monitor, but this shortcoming was offset by the larger viewing angle of the projected images. The conferences were usually attended by 6-10 physicians. The overall results are summarized in Table II.

## V. DISCUSSION

The teleconferencing system we designed has been successfully tested for use in cardiology conferencing. The fact that the conferences were always scheduled well in advance enabled us to use the images in their original quality without compression-induced artifacts. Our remote control and synchronization technology allowed us to transmit the images in advance but to display them in real time during the conferences.

This approach is well optimized for conferencing, where there is time for preparation but little time during the conference. However, the same approach may be less advantageous for other applications. For instance, the time required to transmit the images in original quality over a WAN (T1 line) is about 20-30 min for a single patient (about 200 Mbytes). This time is acceptable for conferencing purposes, but too long for remote monitoring during a procedure.

A possible solution to this problem might be a hybrid system that can use both real-time transmission and offline transmission. For instance, a remote monitoring system for cardiology could transmit the fluoroscopy images of the catheter manipulations in real time with reduced quality, while the angiographic sequences could be transmitted with a small delay, but in original quality. Such a system could provide timely and accurate information for the remote monitoring of cardiological interventions. The availability of the Next Generation Internet (NGI) with a higher bandwidth in the near future may alleviate these developments.

We are currently developing a hybrid system. The DirectShow technology that we use in our teleconferencing system is capable of displaying real-time streaming video and also supports a wide selection of video capture devices, making it an ideal tool to integrate both types of dynamic images into a single application.

TABLE III  
CHARACTERISTICS OF DIFFERENT TYPES OF DYNAMIC IMAGES

	"Video" - type dynamic images	"Multi-Frame" dynamic images
Analog/digital	Typically analog	Always digital
Format	Usually standard video format (NTSC, PAL, S-VHS), standard resolution and frame rate	Non-standard resolution and frame rate, File format either DICOM or proprietary
Length	Typically > 1 minute, sometimes continuous or live	Recorded in short sequences, typically < 1 minute
Application in Medicine	Ultrasound, Endoscopy, Fluoroscopy, Intraoperative	Angiography, Cardiac angiography, Ultrasound
Image quality	Intermediate	High

Deployment of this technology in clinical practice, however, is more difficult than conferencing alone. The obstacle is that, for a system to be used during clinical procedures, it needs to be tightly integrated with the imaging modality itself in order to facilitate the data preparation step. This level of integration requires close collaboration with the manufacturer of the modality.

## VI. CONCLUSIONS

It is our opinion that the success of a telemedicine application depends on its close adaptation to the clinical setting. It therefore cannot rely on a single technology. Given the broad range of imaging modalities, clinical requirements and local conditions, the designer of a telemedicine application needs to select those technologies that accomplish the clinical goal and not vice versa.

The clinical significance of telemedicine in cardiology has been shown; however, it was also found that compromises in the image quality might negatively affect the patient's outcome [8]. While future high-bandwidth networks such as the NGI may provide high-speed, high-quality image transmission, the currently limited bandwidth on WAN connections enforces a time-versus-quality tradeoff.

In this situation, it seems reasonable to combine real-time, low-quality video-conferencing technologies with low-speed, high-quality store-and-forward technologies as presented in this paper. This is especially important as one of the challenges of telemedicine is to provide high-quality medical services in remote or rural areas, where true high-speed networks will not be available very soon.

### APPENDIX A TYPES OF DYNAMIC IMAGES

Dynamic images are used in many different ways in medicine. Although there are overlaps, we can distinguish two major types of dynamic images: video and multiframe images. Differentiating between these two is not always easy. Table III shows the major characteristics of both types. The separation between these two types is important, since they require different strategies for storage, transmission, and display in telemedicine applications.

**Video-type** dynamic images originate from imaging modalities that produce standard analog video signals. These modalities include, for instance, most ultrasound scanners, most flu-

oroscopy systems, or endoscopic equipment. These images are traditionally stored on S-VHS tapes. Commercial video-conference systems can transmit this type of images very easily for telemedicine purposes.

**Multiframe-type** dynamic images originate in digital form from specialized medical equipment, such as angiography systems or certain advanced ultrasound scanners. Frame rate, resolution, and bit depth can differ from standard video signals. In many cases, the digital files are compatible to the DICOM standard, but are incompatible with regular analog video processing systems. Because of the large amounts of digital data, these images are typically created in short individual sequences rather than in a continuous fashion.

### APPENDIX B TELEMEDICINE APPLICATIONS WITH DYNAMIC IMAGES

**Remote monitoring** is an application in which dynamic images (e.g., fluoroscopy images during a radiological interventional procedure) are transmitted in real time or near real time to another location, where a physician monitors the procedure. The remote physician can give advice regarding the diagnostic and therapeutic strategies. This type of application can be optimized for specific equipment and modalities, since it will usually only be used between closely related institutions.

**Emergency consultation** is performed during or immediately after a procedure between a satellite site or imaging center and a more specialized hospital. Images of suspicious findings are sent to the specialized hospital for review. The experts can then determine, for instance, whether or not a patient needs to be transferred to the specialized center for treatment. Due to the wide range of possible satellite sites, this application usually relies on standard communication equipment, such as videoconference systems. The communication is asymmetric, since images are sent only in one direction and no interactive discussion is required.

**Expert consultation** is different from remote monitoring in that it does take place after the actual procedure rather than during the procedure. The physician who performed the examination discusses the findings recorded in the images with an expert at a distant location. The consultation may address images from other modalities and has an interactive discussion

component. Images can be transmitted either live on an *ad hoc* basis or in advance of the consultation.

**Clinical conferencing** differs from expert consultation in that it often has an interdisciplinary scope involving different modalities from various sources, it has a more elaborate schedule, and possibly more than two parties participate. It is insofar more complex than expert consultation. The common property is that, for clinical conferencing, images can be transmitted well in advance.

#### APPENDIX C TRANSMISSION METHODS

When dynamic images are to be used in telemedicine applications, it is necessary that the images be transmitted between two geographically distant sites. Depending on the type of images, the desired quality, the communication infrastructure, and the application, there are several options to implement the transmission. We can distinguish two major strategies for the transmission of dynamic images.

**Real-time transmission** requires that images be displayed at the receiver's site at almost the same time as they are generated at the local site. To achieve this goal, the data rate of the images must stay within the bandwidth of the communication line. This implies that, if the data rate of the original images exceeds the communication bandwidth, compression has to be used in order to maintain the real-time capability. Assuming that the data rate produced by a given imaging modality is fixed, the amount of compression and subsequently the quality of the image at the receiver's site is determined by the available communication bandwidth.

**Offline transmission** can be used if a delay between the generation of the images and the display is acceptable. Images are transmitted to the remote site in a store-and-forward fashion and can be reviewed simultaneously in after the transmission is completed. This mode of operation introduces an additional degree of freedom for the designer of the application. Because the transmission delay can be adjusted, the compression ratio and thus the quality of the images can be chosen to meet the requirements of the application.

#### APPENDIX D COMPRESSION METHODS

Because of the huge amounts of data that need to be transmitted for teleconferencing with dynamic images, image compression is often necessary. The amount of compression required is determined by three factors: 1) available communication bandwidth; 2) acceptable transmission delay; and 3) required image quality. The weight of the individual factors depends on the type of telemedicine application, and usually a compromise has to be reached. Taking into account these constraints, several compression methods can be chosen.

**Lossless compression** compresses the images into a data stream that can be expanded back into images that are mathematically identical to the original. The most commonly used algorithms for lossless compression are the Huffman encoding method [9], the Lempel-Ziv algorithm [10], [11], and the lossless JPEG algorithm [12], [13]. The quality of the images is not altered by these methods, but the maximum compression ratio is only about 3:1.

**Lossy compression** produces images that are visually very similar, but not mathematically identical to the original. This yields a better compression ratio, about 5:1 to 20:1. However, the alterations to the images may result in loss of image details or creation of artifacts. The extent to which these changes in the images can be tolerated for medical purposes is still being investigated. The most commonly used lossy compression methods are the JPEG method [12] and the wavelet transform method [14]. The JPEG method is well studied and standardized, but recent papers suggest that the wavelet method may produce better results [15].

**Subsampling** is a rather crude compression method that reduces the image data by simply reducing the image resolution and/or the frame rate of an image sequence. The quality reduction caused by subsampling is worse compared to the lossy compression methods. However, it is a very fast method that is often used in real-time applications to reduce the amount of data for subsequent compression methods. Data reduction by subsampling amounts to a compression of typically 4:1 to 16:1.

**Interframe compression** uses the third dimension of dynamic images, which is time. The correlation between two adjacent images is usually high. The difference between them contains less information and can be compressed to a higher degree. Advanced methods, such as MPEG, can even compensate for movements such as camera sweeps [16]. The drawback of interframe compression is that random access to individual images out of a sequence can be difficult and slow. Some medical applications require random access to individual images.

#### APPENDIX E DISPLAY METHODS

The display of dynamic images on a computer monitor is challenging for both hardware and software. The screen display needs to be updated at the frame rate of the sequence, typically 30 frames/s. To maintain a constant flow of data under these circumstances requires a careful system design that avoids bottlenecks. Medical applications can use two strategies to achieve this goal.

**The memory cache strategy** loads all the images into the main memory of the computer before playback is started. This strategy guarantees high performance even on slow computers. However, this strategy can only be used for short sequences that fit entirely into the memory. Another drawback of this method is that the display cannot begin until all images are loaded, which can cause a considerable delay.

**With streaming playback**, images are displayed as they are received and are discarded as soon as they are replaced by subsequent images. While this technique can play sequences of very long or even unlimited length, it also requires very high processing power or dedicated video processing hardware in order to maintain the frame rate. Another drawback of streaming playback is that random access to individual images can become slow.

#### REFERENCES

- [1] S. T. C. Wong and H. K. Huang, "Networked multimedia for medical imaging," *IEEE Multimedia*, vol. 4, pp. 24-35, 1997.
- [2] *Digital Imaging and Communications in Medicine (DICOM): Version 3.0.*, 1993, ACR/NEMA.

- [3] J. Zhang, J. N. Stahl, K. S. Song, and H. K. Huang. "Real-time tele-consultation with high resolution and large volume medical imaging." in *PACS Design and Evaluation: Engineering and Clinical Issues*, S. C. Horii and G. J. Blaine, Eds. SPIE, 1998, vol. 3339, pp. 185-190.
- [4] The SSL Protocol Version 3.0, A. O. Freier, P. Karlton, and P. C. Kocher. (1996). [Online]. Available: <http://home.netscape.com/eng/ssl3/draft302.txt>
- [5] A. Chatterjee and A. Maltz. "Microsoft directshow: A new media architecture." *SMPTE J.*, vol. 106, pp. 865-871, 1997.
- [6] J. N. Stahl, J. Zhang, X. Zhou, A. Lou, E. V. Pomerantsev, C. Zellner, and H. K. Huang. "Tele-consultation for diagnostic video using internet technology." in *Proc. IEEE Multimedia Technology & Applications Conf.*, 1998, pp. 210-213.
- [7] J. Nagle. "Congestion control in IP/TCP internetworks." in *RFC 896*, 1984.
- [8] J. Tobis, V. Aharonian, P. Mansukhani, S. Kasaoka, R. Jhandyala, R. Son, R. Browning, L. Youngblood, and M. Thompson. "Video networking of cardiac catheterization laboratories." *Amer. Heart J.*, vol. 137, pp. 241-249, 1999.
- [9] D. A. Huffman. "A method for the construction of minimum-redundancy codes." *Proc. IRE*, vol. 40, pp. 1098-1101, 1952.
- [10] A. Lempel and J. Ziv. "Compression of two-dimensional data." *IEEE Trans. Inform. Theory*, vol. IT-32, pp. 2-8, 1986.
- [11] J. Ziv and A. Lempel. "A universal algorithm for sequential data compression." *IEEE Trans. Inform. Theory*, vol. IT-23, pp. 337-343, 1977.
- [12] G. K. Wallace. "The JPEG still picture compression standard." *Commun. ACM*, vol. 34, pp. 30-40, 1991.
- [13] Y. W. Nijim, S. D. Stearns, and W. B. Mikhael. "Differentiation applied to lossless compression of medical images." *IEEE Trans. Med. Imaging*, vol. 15, pp. 555-559, 1996.
- [14] B. J. Erickson, A. Manduca, P. Palisson, K. R. Persons, F. Earnest, 4th, V. Savcenko, and N. J. Hangiandreou. "Wavelet compression of medical images." *Radiology*, vol. 206, pp. 599-607, 1998.
- [15] J. Ricke, P. Maass, E. L. Heanninen, T. Liebig, H. Amthauer, C. Stroszczyński, W. Schauer, T. Boskamp, and M. Wolf. "Wavelet versus JPEG (Joint Photographic Expert Group) and fractal compression. Impact on the detection of low-contrast details in computed radiographs." *Investigative Radiology*, vol. 33, pp. 456-463, 1998.
- [16] J. L. Mitchell, W. B. Pennebaker, C. E. Fogg, and D. J. LeGall. *MPEG Video Compression Standard*. New York, NY: Chapman & Hall, 1997.



**Christian Zellner** received the M.D. degree from the Ludwig-Maximilians University, Munich, Germany, in 1995.

He received postgraduate training as a house officer in Internal Medicine at the North Staffordshire General Hospital, Stoke-on-Trent, U.K., from 1995 to 1996. Since 1996, he has worked as a Post-Doctoral Fellow in the Cardiology Division at the University of California, San Francisco. His major research interests are cardiovascular imaging and intracoronary 2-D and 3-D ultrasound.



**Eugene V. Pomerantsev** received the M.D. degree from Moscow Medical Academy, Moscow, Russia, in 1977 and the Ph.D. degree for his studies in quantitative coronary angiography and ventriculography in 1991.

He was a resident in cardiology from 1984 to 1989 at the Moscow Medical Academy and an invasive cardiologist from 1985 to 1992 with the Cardiology Research Center in Moscow. He was a senior research fellow with the San Francisco Heart Institute, Daly City, CA. He worked as an administrator of cardiovascular database at Stanford, CA, from 1994 to 1999. Presently, he is a Director of Information Systems of the Knight Center for Interventional Cardiovascular Therapy, Massachusetts General Hospital, Boston. His major research interests include quantitative coronary angiography and ultrasound, digital imaging in cardiology, and database development.



**Tony M. Chou** is Assistant Professor of Medicine, Director of the Adult Cardiac Cath Labs and Interventional Cardiology Service. His research interests include coronary reactivity, especially in response to hormonal influences, applications of intravascular ultrasound, new device technologies, and angiogenesis.



**H. K. Huang (SM'88)** is Professor and Director of Informatics, Department of Radiology, University of Southern California, Los Angeles, and Adjunct Professor, Department of Radiology, University of Iowa, Iowa City. He pioneered the picture archiving and communication system (PACS) research program and developed the PACS at the University of California at Los Angeles in 1991 and the hospital-integrated PACS at the University of California at San Francisco in 1995. His current research interest is in digital mammography,

tele-imaging, image informatics infrastructure, and next-generation Internet. He has co-authored and authored seven books and published over 200 articles. His recent book is *PACS: Basic Principles and Applications* (New York: Wiley, 1999). During the past 15 years, he has received over 15 million dollars in PACS, medical image informatics, and image processing related research grants and contracts.

Dr. Huang was inducted into the Royal College of Radiologists, U.K., as an Honorary Fellow for his contribution to PACS research and development in 1992, the American Institute of Medical and Biological Engineering as a Founding Fellow for his contribution to medical imaging in 1993, and the EuroPACS Society as an Honorary Member for his contribution to PACS in 1996.



**Johannes N. Stahl** received the M.D. degree from the University of Saarland, Homburg, Germany, in 1992.

Besides his medical studies, he worked as a software developer at the Fraunhofer-Institute of Biomedical Engineering in St. Ingbert, Germany. He was a resident in neurology and radiology at the University of Saarland from 1993 to 1997. Thanks to a scholarship from the Deutsche Forschungsgemeinschaft, he is currently a research fellow in the Laboratory for Radiological Informatics,

Department of Radiology, University of California at San Francisco. His major research interests include PACS design and development and networked multimedia technologies in radiology.



**Jianguo Zhang** received the B.S. and M.S. degrees from Shangdong University, China, in 1984 and 1987 and the Ph.D. degree in optics from the Chinese Academy of Science in 1991.

From 1994 to 1998, he was a research fellow in the Laboratory for Radiological Informatics, Department of Radiology, University of California at San Francisco. Currently, he is a Professor at Shanghai Institute of Technical Physics, Chinese Academy of Science. His major interests include CR image processing, medical image display, PACS,

medical imaging informatics, networked multimedia system for medical imaging applications, and optics.

# Real-Time Teleconsultation with High-Resolution and Large-Volume Medical Images for Collaborative Healthcare

Jianguo Zhang, Johannes N. Stahl, H. K. Huang, *Senior Member, IEEE*, Xiaoqiang Zhou, S. L. Lou, and Koun S. Song

**Abstract**—Real-time consultation between referring physicians or radiologists with an expert is critical for timely and adequate management of problem cases. During consultation, both sides need to: 1) synchronously manipulate high-resolution digital radiographic images or large volume MR/CT images; 2) perform interpretation interactively; and 3) converse with audio. We present a specifically designed teleconsultation system in a digital imaging and communication in medicine picture archiving and communication systems clinical environment. The system uses bidirectional remote control technology to meet critical teleconsultation application requirements with high-resolution and large-volume medical images operated in a limited-bandwidth network setting. We give the system design and implementation methods, and also describe the teleconsultation procedure and protocol used in this system. Finally, laboratory and clinical evaluation results are discussed.

**Index Terms**—Digital imaging and communication in medicine (DICOM), display workstation, picture archiving and communication systems (PACS), telemedicine, teleradiology.

## I. INTRODUCTION

The managed care trend in healthcare delivery systems expedites the formation of teleradiology expert centers. In the expert center model of teleradiology [1], the medical images are sent from the examination sites to a remote site where an expert radiologist will make the diagnosis. The report is then transmitted to the examination site where a primary physician can prescribe the treatment immediately.

There are two teleradiology models [1]: simple and complex teleradiology. In the simple model, an image is sent from a scanner, e.g., CT, or a film digitizer, to the expert center or home using low-quality teleradiology equipment and slow-speed communication technology. In this situation, a desktop personal computer with simple display software and a telephone modem connection may be sufficient to perform the teleradiology operation.

The complex teleradiology model occurs when many images including prior studies are required for comparison. In addition, both sites may need to interactively and synchronously manip-

ulate and interpret the same large volume high-resolution computed radiography (CR) image set (16 MB/example) or magnetic resonance (MR), computed tomography (CT), and ultrasound (US) sequential images (8–20 MB/example) in real time. This communication will only address the complex teleradiology model, which we prefer to call teleconsultation.

In this paper, we present a specifically designed teleconsultation system with real-time bidirectional remote control technology to meet critical teleconsultation application requirements with high-resolution and large-volume medical images in a limited bandwidth network environment. This design is integrated in a clinical digital imaging and communication in medicine (DICOM) picture archiving and communication systems (PACS) environment.

## II. BACKGROUND AND REQUIREMENTS

The University of California at San Francisco (UCSF) comprises two medical centers. The distance between the main campus (UCSF Medical Center) and Mt. Zion Hospital (MZH) is 2 km. There are about 1.0 Gbytes of MR/CT neuroimages transmitted daily through an asynchronous transfer mode (ATM OC3) network (with a T1 line as the backup) from MZH to UCSF Medical Center for review. These images are first sent from MZH scanners to the clinical PACS server at UCSF and then routed to several display workstations [2], [3] for experts to make a diagnosis. Usually, referring physicians or radiologists view MR/CT images at MZH and, when necessary, would request the expert to “overread” from a PACS workstations at UCSF. They would discuss the case via telephone. With this type of consultation, both parties cannot study the same image set dynamically by paging through them synchronously and collaboratively with cine, zoom, window/level, and graphic overlay operations.

For this kind of teleconsultation, neither conventional Computer-Supported Cooperative Work (CSCW) software nor PACS workstations [2], [3] would be sufficient for two reasons [4].

- 1) Off-the-shelf CSCW solutions, e.g., whiteboard applications, lack the functionality required for the processing of radiological images and do not provide PACS connectivity via the DICOM standard [5].
- 2) PACS workstations do not have the necessary capability for interactive teleconsultation that requires real-time dual-cursor telecommunication technology [6], [7].

Therefore, it is necessary to integrate the remote control communication component with the medical image processing

Manuscript received January 4, 1999; revised September 3, 1999. This work was supported in part by the National Library of Medicine under Contract N01-LM-6-3547.

J. Zhang is with the Shanghai Institute of Technical Physics, Shanghai, China. J. N. Stahl, X. Zhou, and S. L. Lou are with the Laboratory for Radiological Informatics, University of California, San Francisco, CA 94143-0628 USA.

H. K. Huang is with the Department of Radiology, Childrens Hospital of Los Angeles/University of Southern California, Los Angeles, CA 90027 USA.

K. S. Song is with the ASAN Medical Center, Seoul, South Korea.

Publisher Item Identifier S 1089-7771(00)02129-4.

component. This can be done in several ways, each of which has its distinct advantages and disadvantages:

- 1) Conventional application-sharing software (e.g., Intel ProShare or Microsoft NetMeeting) could be used in conjunction with PACS software. This can be realized very quickly, but will result in a very poor performance, since the application-sharing software cannot make any assumption about the purpose of the software.
- 2) A CSCW toolkit can be used to add the communication functionality to existing medical imaging software. This may also lead to performance drawbacks, since the communication model and the imaging software architecture are only partially compatible and the integration remains more or less superficial.
- 3) A medical imaging software can be created from the ground up with the communication facilities built in. This method is the most complex, but it can also result in the best performance, since the communication protocol and the software architecture can be optimized for each other.

We chose the last method to implement our system, since high-resolution and large-volume medical images require optimal performance. The required functionality for the system is as follows:

- 1) provide real-time teleconsultation services for high-resolution and large volume medical images (MR/CT, CR, US, mammography);
- 2) synchronously manipulate images on both local and remote sites including remote cursor, window/level, zoom, cine mode, overlay, and measurement;
- 3) interface to PACS through the DICOM standard [5];
- 4) can be used in intranet (LAN) and internet (WAN) environment with TCP/IP protocol;
- 5) can be operated in scalable network connections including ATM, Ethernet, and modem;
- 6) have similar graphic user interface and image manipulation functions as the standard PACS workstation to minimize user's retraining; and
- 7) be cost-effective.

In the following, we describe our teleconsultation system designed to satisfy the aforementioned conditions.

### III. IMAGE DISPLAY PROCEDURE

Real-time teleconsultation relies on the synchronization of the local (referring site) and the remote (expert site) workstation. For this reason, we first review the sequential operations involved in displaying and manipulating images in this section. In a clinical PACS environment [8], images are first acquired by the image modality acquisition computer, sent to the PACS server through a DICOM gateway, then delivered to different workstations according to some routing schedules. Fig. 1 shows the data flow of images generated from modalities to PACS workstations in clinical environments [3]. After images arrive at the workstation, they are first stored in a local database, accessed by the user through the graphic user interface, and displayed on the monitors.

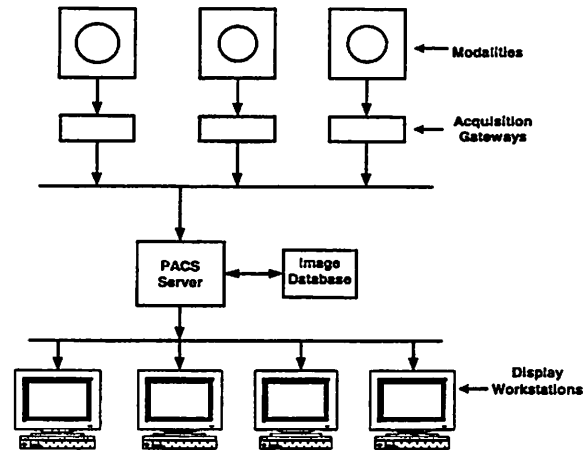


Fig. 1. Image data flow from modalities to display workstations in a PACS network environment.

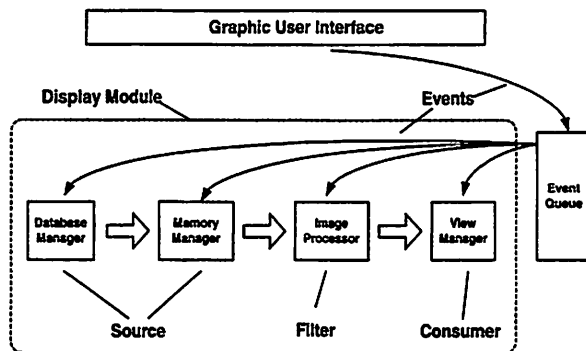


Fig. 2. Image data flow in the display pipeline driven by events in a display program.

The major functionality of a workstation is to display and manipulate images with a graphic user interface (GUI) combined with image management and image processing functions, e.g., window/level, zoom, pan, rotation, cine, etc. [9].

In an event-driven window environment, the user's manipulations of the GUI windows or displayed images by using the input devices (mouse or keyboard) are translated into events. The procedure to display images can be described as a flow of image data through an image processing pipeline, which is controlled by these events, as shown in Fig. 2.

The major idea of designing a teleconsultation system is to provide a mechanism to control image data flow not only in the local workstation, but also in a networked remote workstation. This control should be identical for both the local and remote sites, and both sites should synchronize their operations in real time.

### IV. TELECONSULTATION SYSTEM DESIGN

#### A. Communication Analysis of Medical Image Teleconsultation

Teleconsultation involves a referring site and an expert site. Between the two sites, three kinds of communications are required:

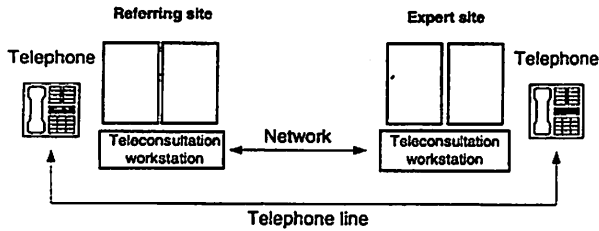


Fig. 3. Diagram of the teleconsultation system.

- 1) Image transmission from the referring physician or general radiologist site to the expert site.
- 2) Synchronization of their manipulations on displayed images in both sites.
- 3) Voice conversation between the referring physician and the expert.

Among these three types of communications, image transmission involves the largest amount of data, but it can usually be performed before the consultation session unless it is an emergency case. Image preloading can be done with various kinds of network, e.g., high-speed ATM network, T1 line, Internet, or telephone, depending on the requirements for the turn-around time. According to our analysis of the image display procedure, events must be exchanged in real time between the two sites to synchronize the manipulation operations on the images. Since the events are usually very short messages, even conventional telephone lines (DS-0 line with 28 kbits/sec bandwidth) can be used to transmit this kind of message in real time. Voice communication can be carried out through a second telephone line.

#### B. Hardware Configuration of the Teleconsultation System

Based on the communication analysis and the expert model of teleradiology [1], we designed a real-time teleconsultation system that consists of two sites: the expert site and the general physician or radiologist site. The hardware configuration of the teleconsultation system at each site includes:

- 1) one workstation that is linked with the other with an Ethernet, ATM, or modem connection;
- 2) high-resolution display boards which can be configured to support single or dual monitors;
- 3) high-resolution grayscale monitor (dual monitors as option);
- 4) telephones for audio communication.

Fig. 3 shows the schematic of our teleconsultation system.

#### C. Software Architecture

We designed the teleconsultation system, which can synchronize the user operation and has the ability to exchange messages in real time between the local and remote sites. The consultation workstation has a message routing, an interpretation function module, an authoring function, and standard display and manipulation functions similar to a PACS workstation. Based on the teleconsultation requirements mentioned in Section II, and the analysis on the image display procedure in Section III, we designed the teleconsultation software architecture with following modules:

- 1) an image display GUI for display and teleconsultation;
- 2) a database manager for medical image display and teleconsultation authoring;
- 3) a memory manager for image data memory management;
- 4) an image processor for processing image;
- 5) an image viewer for image rendering and display;
- 6) an event interpreter for local and remote message dispatching;
- 7) a remote control manager for routing messages between local and remote sites.
- 8) an event/message queue used to transfer the events and remote messages from GUI and remote manager to display module;
- 9) a queue used to transfer the encoded messages from Event Interpreter to remote manager;
- 10) a teleconsultation database used to store the information of selected patients, studies, series, images, as well as expert names, hospitals, and hosts;
- 11) DICOM communication services for DICOM image receiving and sending between the teleconsultation system, scanners, and PACS server.

Fig. 4 shows the schematic of the software architecture. The function modules (1), (2), (3), (4), and (5) are designed similar to those of normal PACS workstations as described in Section III.

Modules (6) and (7) are specifically designed for bidirectional remote control for teleconsultation. Module (6), the event interpreter, collects the events coming from the display module and encodes them for transmission and puts them into a queue (module 9), which transfers the messages to module (7). Module (7), the remote control manager, picks up the encoded messages and sends them to the remote site, and receives the remote messages and posts them to the display module for remote control of the display behavior.

Module (10) is a teleconsultation database for image display and consultation, and module (11) is for the DICOM communication services for transferring DICOM images between teleconsultation workstations and PACS or imaging modalities. In the following, we describe the bidirectional remote control technology used in our teleconsultation system and explain how these modules work together to enable the consultation functionality.

#### D. Bidirectional Remote Control Technology in a Teleconsultation Workstation

1) *Event Handling*: Since most window (X window or Windows NT) display programs are driven by events (or messages), the consultation system should exchange the event (or message) information between both sites to synchronize the operation. However, the events generated by the GUI are relatively low-level system-dependent events. In order to allow communication between systems with different hardware configurations, for instance, different screen resolutions, the system-level events have to be translated into application-level events prior to transmission.

All events generated by the GUI are processed by the event interpreter (module (6) in Fig. 4), which are interpreted within

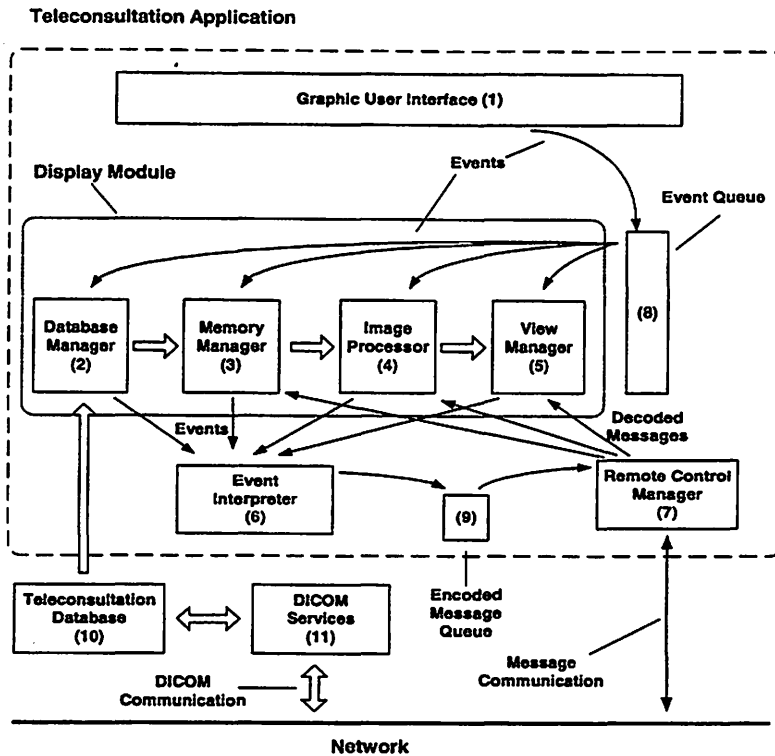


Fig. 4. Software architecture and data flow in a teleconsultation workstation.

the context of the current application state. The module translates them into atomic, self-contained application-level events that trigger specific application-state transitions. The application-level events are routed into two paths: one copy of the event is used to alter the state of the local application, while another copy is passed on to the remote control manager module, which encodes the event into a message and transmits it over the network to the remote site.

Messages that the remote control manager receives from the remote site are dispatched to the display module in cooperation with the event interpreter, which uses it to trigger application state transitions in the same way as the local events. Although the remote control manager uses separate threads for asynchronous network communication, the events received from the remote site will be routed synchronously through the main message queue. This mechanism assures that state transitions can only be executed in the main application thread, effectively avoiding application-state corruption and inconsistencies.

2) *Message Routing*: Effective communication requires very fast and immediate update of remote cursor and image manipulations to create the illusion of "presence" of the remote partner. Early experiments with TCP/IP-based communication exhibited a noticeable latency and sluggishness in the movements of the remote cursor. This observation was also made with off-the-shelf whiteboard applications, e.g., Microsoft Net-Meeting. Experiments with different socket parameter settings revealed that the reason for this behavior is the Nagle algorithm used by TCP/IP socket implementations to reduce network

traffic by grouping small messages into larger network packets [10]. Disabling the Nagle algorithm (the Windows socket implementation allows this by setting the TCP\_NODELAY socket option) improves the quality of the remote cursor movements at the price of significantly increased network traffic.

We developed a network communication model that minimizes both the latency of remote manipulations and network traffic. For this model, we categorize events into key events which affect the final application state and so-called advisory events that represent transitory states and are only used to improve the smoothness and immediacy of remote manipulations. For example, a user changes the brightness of an image by pressing the left mouse button and dragging. Every movement of the mouse during this operation results in an immediate change of the image brightness. Using this visual feedback, the user keeps dragging until the desired brightness level is reached, at which point he releases the mouse button and sets the final value. For the application state, only this last value represents a key event, while all the intermediate settings serve the purpose of visual feedback and are therefore advisory.

In our model, key messages are sent through a TCP stream-oriented channel that provides guaranteed delivery and a consistent application state. The advisory messages are sent through a UDP datagram channel that provides immediate low-latency communication with low overhead. However, since UDP datagrams are subject to packet loss and message reordering, we provided special measures to eliminate possible side effects.

Since the messages are advisory by definition and not necessary to maintain the proper application state, the loss of an advisory message can be safely ignored. To provide a safeguard against message reordering, we use two sequence counters, which are attached to each message. The first counter is increased for each key message and sets the frame for subsequent advisory messages. Any advisory message is marked with the frame counter of the last key message sent. Additionally, each advisory message is marked with a secondary counter that indicates the sequence in which they were sent within the frame. The secondary counter is reset to zero for each frame.

On the receiving side, the key messages always arrive in the proper order since they are sent through the TCP stream channel. Out-of-order advisory messages can be detected by two means. First, if an advisory message carries a frame counter that is different from that of the last key message received, it is considered out-of-frame. Secondly, if the secondary counter of an advisory message is lower than the highest secondary counter received so far within the frame, it is considered out-of-order. In both cases, the message will be ignored, since its content has already been invalidated by a subsequent message. Again, ignoring out-of-order advisory messages is safe since they are not necessary to maintain the proper application state.

3) *Coordinate Transformation*: One problem that we addressed in our design is the interoperability between different screen configurations. For example, the referring physician might only have a single monitor with a medium resolution, whereas the expert might use a dual monitor system with a high resolution. In this situation, interoperability between the systems is difficult, even if both systems run the same operating system and applications. We reviewed some commercial teleradiology applications, for instance, RadWorks,<sup>1</sup> which uses Microsoft NetMeeting on top of conventional PACS workstation software, and the CHILI system [4] that uses its own communication protocol. Both systems require exactly the same screen resolution in both workstations in order to operate properly.

We wanted our system to be interoperable between different screen resolutions for the following reason: the nature of teleconsultation is usually asymmetric, between a number of general radiologists or physicians and an expert radiologist in an expert center. It can be expected that the general radiologist performs teleconsultation only infrequently, whereas the expert performs it regularly. Since the monitors are a major cost factor in medical imaging workstations, it is quite reasonable for the general radiologist to have less expensive hardware with lower resolution than the expert. It was, therefore, our design goal to enable proper communication between two systems with different screen resolutions, but to keep the results of image manipulation, such as mouse moving positions, consistent on both local and remote systems.

To achieve this goal, we used two measures.

- 1) Our system uses continuous zoom for all display operations. Most of the medical image display software we use in our hospital restricts zoom operations to integer factors, i.e., 1×, 2×, 3×, etc., for performance reasons.

Combined with the fact that the matrix sizes of medical images usually are powers of 2, e.g., 512, 1024, or 2048, this leads to a fixed screen resolution and layout. Using arbitrary zoom factors allows us to use a flexible screen layout and to adjust the application to any screen resolution.

- 2) When arbitrary zoom factors are used to adjust to different screen configuration, it can no longer be assumed that two communicating workstations use the same zoom factor for the images. The communication module uses only image-relative coordinates for the message exchange instead of screen-relative coordinates. This allows systems with different screen resolution (and therefore varying zoom factors) to communicate.

## V. TELECONSULTATION PROCEDURE AND PROTOCOL

With the teleconsultation system described in Section IV, a teleconsultation session proceeds as follows. When cases require consultation, a general physician or radiologist first reviews the images from the imaging modality or the PACS workstations and pushes them to the local teleconsultation workstation using the DICOM protocol. At the teleconsultation workstation, the referring physician then performs data authoring supplied by the teleconsultation system and sends the images to the teleconsultation workstation located at the expert site. This can be done through either the LAN if it is within the same building or campus or through the WAN if it is far away. Later, either the general physician or an expert can call the other site to start the consultation session.

The teleconsultation protocol has three steps: data formatting, data authoring, and data presentation.

*Data formatting*: The first step is to convert all input images for teleconsultation to the DICOM standard if they are not already DICOM. This is done at the acquisition gateway or at the PACS server as shown in Fig. 1.

*Data authoring*: The authoring procedure is to prepare the image data for teleconsultation. This step is necessary because both teleradiology workstations need to operate on the same set of image data in order to guarantee synchronicity. The data authoring procedure lets the user define a set of images, which is then synchronized between the workstations by exchanging messages (or application level events) through the network. The authoring module is an integrated component in the software package (inside the Database Manager module) "TeleConApp." Fig. 5 shows the data authoring procedure. There are three steps in data authoring.

- 1) The general physician or radiologist uses the TeleConApp program to create an object called the virtual envelope which includes information of the selected patients, studies, and series; as well as the host name of the expert site, the name of the consultant from the teleconsultation local database. Note that the virtual envelope does not yet contain any images. The virtual envelope is sent to the expert site through a network with DICOM communication services.
- 2) After the expert site receives the session envelope, both sides exchange the images using the DICOM C-STORE

<sup>1</sup>[Online]. Available: <http://www.appicare.com>

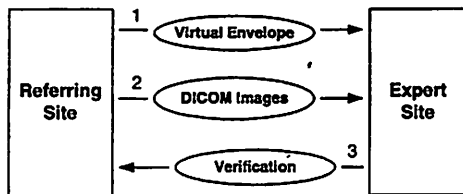


Fig. 5. Data authoring procedure for teleconsultation.

protocol until they have identical copies of the images referenced in the envelope.

- 3) After the image transmission is completed, the referring site issues a DICOM C-FIND operation to verify successful transmission of the images. Once the session envelope has been marked as verified, a real-time consultation session can be initiated.

*Data presentation:* Before the data presentation, both the expert and the general physician site have the virtual envelope and image data. After initiating the consultation session, the data presentation is beginning. During data presentation, either site can operate the TeleConApp program to display and manipulate images and related information, and conversation between the two is carried on through telephone. TeleConApp synchronizes the operations of image display and manipulation at both sites.

## VI. TELECONSULTATION SYSTEM IMPLEMENTATION AND RESULTS

### A. System Implementation

We implemented the teleconsultation system on the Microsoft Windows NT platform. We developed the software using the DOME (DOME image system, inc., Waltham, MA 02154, USA) DIMPL image-processing library for image processing. We used a DOME Md2/PCI display board to support dual monitor configuration for high resolution and large volume medical image display. Also, the two workstations in the system can be configured to different display resolutions or one workstation with single monitor and the other with dual monitors.

### B. Laboratory Evaluation

The teleconsultation system was first tested in the Laboratory for Radiological Informatics (LRI), UCSF, with the Ethernet and modem connections for message communication. Twenty patients with more than 2000 different modality images including GE MR/CT, Siemens CT, Fuji, and Agfa CR were randomly selected and pushed from the UCSF PACS server to one teleconsultation workstation through the local PACS network with the DICOM communication standard. Then the image data were authored in the workstation and staged into consultation sessions in both sites.

We performed the teleconsultation operations through our LAN with Ethernet and modem connections, respectively. During consultation, both sites manipulated images, performed ROI measurements, and talked via telephones. We measured the data transmission rate for the image transfer portion of the system and the latency of the remote control component. The

TABLE I  
TRANSMISSION SPEED IN THE LABORATORY  
ENVIRONMENT USING 100 BASE T ETHERNET LAN CONNECTIONS

Image Characteristics		Transfer Speed	
Modality	Size (Kbytes)	Speed (Kbytes)	SD
MR	128	1245	404
CT	512	2962	1058
CR	8192	2971	554

MR: magnetic resonance; CT: computed tomography.

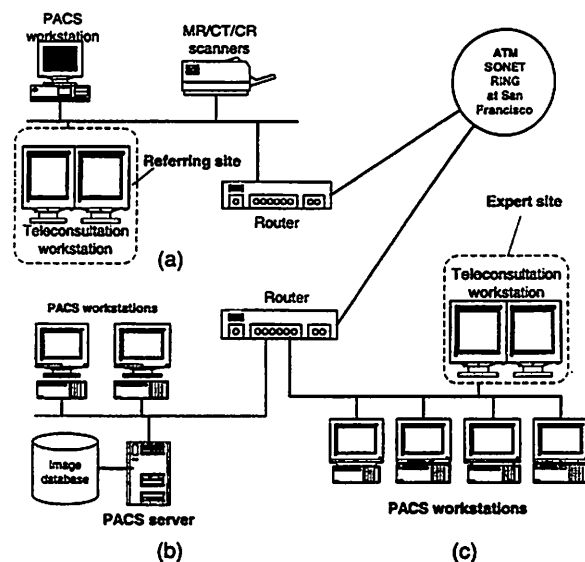


Fig. 6. WAN network connection of the teleconsultation system for MZH/UCSF teleconsultation services. (a) Referring site located at the MZH Neuroradiology Section reading room. (b) UCSF clinical PACS located at LRI. (c) Expert site located at the Neuroradiology Section reading room of the UCSF Medical Center.

latency was compared with the latency of a standard CSCW application (Microsoft NetMeeting) used in conjunction with our system.

The results of the data transmission tests in a laboratory environment are shown in Table I. It should be noted that the numbers reflect the effective application-level throughput, which includes the time required for disk I/O, consistency checking, and database updating and is, therefore, lower than the raw bandwidth of the network.

In the latency comparison, we found that NetMeeting updates the cursor position only twice a second, resulting in a very coarse cursor movement on the receiving side and an average latency of 250 ms. In contrast, our teleconsultation system using the UDP channel exhibited a delay of less than 10 ms, which was not perceivable. In addition, the cursor movement was very smooth, subjectively identical to the original on the sending machine. We experimentally modified our system to use TCP for the transmission of the cursor movements. This manipulation alone led to jumpy cursor movements and delays up to 200 ms, very similar to NetMeeting.

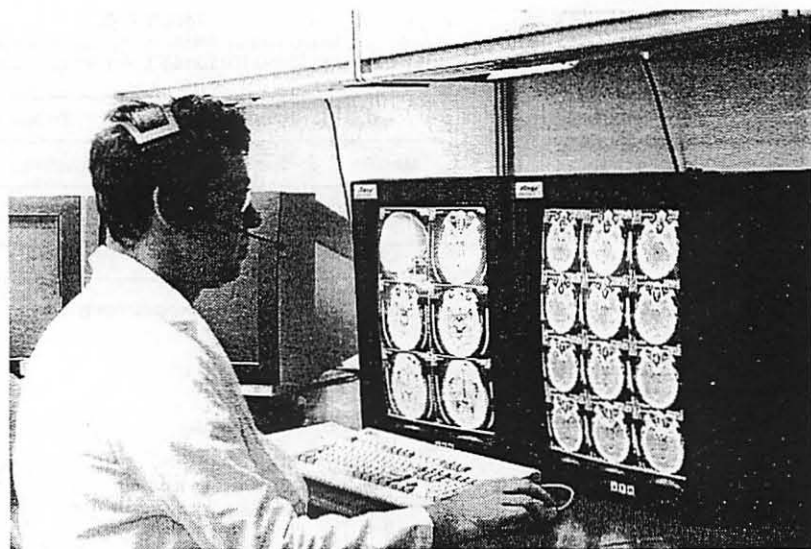


Fig. 7. Photos of the actual teleconsultation installation at: (a) UCSF and (b) Mt. Zion.

TABLE II  
TRANSMISSION SPEED IN THE CLINICAL SETTING USING ATM OC-12 LAN AND WAN CONNECTIONS

Image Characteristics		Transfer from PACS to Teleconsultation System (Long Hospital, UCSF)		Transfer from Long Hospital, UCSF, to Mt. Zion Hospital	
Modality	Size (Kbytes)	Transfer Speed (Kbytes/s)	SD	Transfer Speed (Kbytes/s)	SD
MR	128	598	268	318	16
CT	512	1432	290	889	211
CR	8192	712	21	1196	140

The system was exhibited at InfoRAD, RSNA 97 (Radiological Society of North America), Chicago, IL [11].

### C. Preliminary Clinical Experience

We installed the system in the Neuroradiology Section of the UCSF Medical Center and MZH through WAN network connections, as shown in Fig. 6. The WAN connection between two sites is an ATM OC-12 Sonet ring, and audio communication is through a regular telephone line. We use a PACS workstation (IMPAX, Agfa) at MZH to preview cases and pushed images from that workstation to the teleconsultation workstation (referring site) using the authoring protocol. Later, images were transmitted to the other teleconsultation workstation (expert site) at UCSF. Fig. 7(a) and (b) show the pictures of teleconsultation workstations located in MZH and UCSF Neuroradiology Section reading rooms, respectively.

In the first clinical test phase, the radiology residents on duty in MZH send the accumulated neuroradiological cases of the day to the UCSF main campus for a collaborative readout with a senior neuroradiologist. Such a reading session typically covers four to six patients, most of whom received one magnetic resonance (MR: typically 200 images; 25 Mbytes) or computed tomography (CT: typically 40 images, typically 20 Mbytes) study. A typical MR study consists of about 200 images of 128 kbytes each; a CT study has about 40 images of 512 kbytes each. The

amount of data for each study is mostly between 20 and 30 Mbytes. Our preliminary results cover 12 of these sessions.

Half an hour before the scheduled teleconsultation, the resident at MZH transferred the new images as well as prior studies from the PACS archive to the teleconsultation workstation. This process lasted typically between 5 and 10 min, depending on the number of images. Since the residents already knew the images, the authoring phase was usually very short, only 1 or 2 min. Transmission of the data to the UCSF main campus again lasted about 5 min. Table II shows the observed transmission speed between the PACS and the teleconsultation system and between the teleconsultation system for different modalities. The numbers indicate that the performance of DICOM image communication in a clinical setting depends on a large number of factors, including the size of the images, the underlying physical network, and the overall network usage. Usually, the resulting speed is only a small fraction of the bandwidth possible in a controlled laboratory environment.

Overall, the preparation time for a reading session was about 15 to 20 min. However, since most of this process does not need human intervention, it can be done in a batch mode. At the scheduled time, the resident called the senior neuroradiologist on the phone (we used headsets for convenience) and initiated the teleconsultation. Due to the prior authoring process, all patients, studies, and images were preloaded at the beginning of the reading session, so that the navigation between the different

patients is very fast and convenient. We observed that in most cases the senior neuroradiologist took control of the image display and browsed through the images while the resident at MZH presented the clinical details of the discussed case. The senior radiologist demonstrated specific findings to the resident using the dual cursor ability.

We found that the collaborative readout sessions lasted between 15 and 20 min, which, according to the physicians, is about the same amount of time they need for a conventional reading session with this number of patients. However, they saved a large amount of time because they did not need to travel between the two hospital locations when there are serious or difficult cases that need a referring physician or a general radiologist working together with a senior radiologist to perform interpretation.

## VII. CONCLUSIONS

We have developed a cost-effective teleconsultation system in a clinical DICOM PACS environment for collaborative healthcare application. This system provides data authoring and synchronizes image display and manipulation on both the general physician/radiologist and the expert site during consultation through remote cursors. This system allows real-time collaborative consultation of serious or difficult cases with high-resolution and large-volume medical images in a limited bandwidth network environment.

The system relies both on standardized technologies, such as DICOM and TCP/IP network protocols, and on innovative techniques such as advanced message routing concept for remote control functionality. The combination of these technologies leads to the following benefits.

- 1) The system can be used in any DICOM-compliant PACS network or stand alone in conjunction with DICOM-compatible modalities
- 2) The system supports a scalable range of network connections, ranging from ATM over the Internet to modem connections
- 3) The system performs a high level of real-time feedback, enabling the user to effectively perform interactive teleconsultation.

We are in the process of accumulating long-term data about the system performance for various teleconsultation applications including daily readout, second opinion, and emergency reading. Automatic logging procedures are being implemented to track these events.

## REFERENCES

- [1] H. K. Huang, "Teleradiology technologies and some service models." *Computerized Medical Imaging and Graphics*, vol. 20, pp. 59-68, 1996.
- [2] H. K. Huang, K. Andriole, T. Bazzill, S. L. Lou, A. W. Wong, and R. L. Arenson, "Design and implementation of a picture archiving and communication system: The second time." *J. Digital Imaging*, vol. 9, pp. 47-59, 1996.
- [3] H. K. Huang, A. W. Wong, A. S. Lou, T. M. Bazzill, K. Andriole, J. Zhang, J. Wang, and J. K. Lee, "Clinical experience with a second-generation hospital-integrated picture archiving and communication system." *J. Digital Imaging*, vol. 9, pp. 151-66, 1996.
- [4] U. Engelmann, A. Schroter, U. Baur, O. Werner, M. Schwab, H. Muller, and H. Meinzer, "A three-generation model for teleradiology." *IEEE Trans. Inform. Technol. Biomed.*, vol. 2, pp. 20-25, 1998.
- [5] *Digital Imaging and Communications in Medicine (DICOM): Version 3.0.*, 1993. ACR/NEMA.
- [6] T. Wendler, K. J. Monnich, and J. Schmidt, "Chapter 6: Digital image workstation," in *Picture Archiving and Communication System in Medicine*, H. K. Huang, O. Ratib, and A. R. Bakker, Eds. New York, NY: Springer, 1991.
- [7] S. L. Lou, H. K. Huang, and R. L. Arenson, "Workstation design. Image manipulation, image set handling, and display issues." *Radiol. Clin. North Amer.*, vol. 34, pp. 525-544, 1996.
- [8] H. K. Huang, "Toward the digital radiology department [editorial]." *Eur. J. Radiol.*, vol. 22, p. 165, 1996.
- [9] H. K. Huang, S. L. Lou, and W. P. Dillon, "Neuroradiology workstation reading in an inter-hospital environment: A nineteen month study." *Computerized Medical Imaging and Graphics*, vol. 21, pp. 309-17, 1997.
- [10] J. Nagle, "RFC 896." Congestion Control in IP/TCP Internetworks, 1984.
- [11] J. Zhang, K. S. Song, H. K. Huang, W. A. W. and J. Stahl, "Tele-consultation for thoracic imaging." *Radiology*, vol. 205, p. 743, 1997.

Jianguo Zhang, for a photograph and biography, see this issue, p. 96.

Johannes N. Stahl, for a photograph and biography, see this issue, p. 96.

H. K. Huang (SM'88), for a photograph and biography, see this issue, p. 96.

Xiaoqiang Zhou, photograph and biography not available at the time of publication.

S. L. Lou, photograph and biography not available at the time of publication.

Koun S. Song, photograph and biography not available at the time of publication.

# Some connectivity and security issues of NGI in medical imaging applications

Yu Fan <sup>a</sup>, Kyung Hwang <sup>b</sup>, Michael Gill <sup>c</sup> and H.K. Huang <sup>a,\*</sup>

<sup>a</sup> *Laboratory for Radiological Informatics, University of California at San Francisco, 530 Parnassus Ave., Rm CL-158, San Francisco, CA 94143-0628, USA*

<sup>b</sup> *Enterprise Network Services, University of California at San Francisco, 250 Executive Park Blvd., Suite 2000, San Francisco, CA 94134, USA*

<sup>c</sup> *Lister Hill National Center for Biomedical Communications, National Library of Medicine, 8600 Rockville Pike, Bethesda, MD 20894, USA*

**Abstract.** The next generation internet (NGI) or Internet2 is an initiative for the integration of higher speed backbone communication networks as a means to replace the current inadequate Internet for many applications including medical imaging. This paper first reviews the current status of the Internet2 and reasons why telemedicine and teleradiology require its service. A case study is given using the private ATM OC-3 network at the Laboratory for Radiological Informatics, UCSF as an example for connecting a local site to the Internet2. Network security and data integrity are discussed in both the global and the local network level. Some preliminary results on Internet2 performance in the regional and the national level, as well as comparing with other WAN technologies are given.

**Keywords:** Internet, Internet2, Next Generation Internet (NGI), medical imaging, telemedicine, teleradiology, data security



**Yu Fan** is currently a postdoctoral research fellow at the Laboratory for Radiological Informatics (LRI), Department of Radiology, University of California at San Francisco (UCSF). Dr. Fan received his degrees in Biomedical Engineering from Tsinghua University (Beijing, P.R. China) in 1993(B.A.), 1994 (M.S.) and 1997 (Ph.D.). He was a postdoctoral scholar in the Department of Biomedical Engineering and Human Factors at Wright State University, Dayton, Ohio from 1997 to 1998. Since 1998 he has been working in the LRI. Dr. Fan's research interests are medical informatics, telemedicine, and ultrasound imaging. His current research is telemammography.

**Kyung Hwang** is Senior Network Engineer at the Enterprise Network Services, UCSF since 1997. He received his B.S. at Sam Houston State University, Tx in Computer Science. He was in active military service: served as a communication officer in Europe from 1988–1992; taught computer science for European Division of City College Chicago and Central Texas College in Germany from 1992–1993; and wide area network manager from 1993–1997. His research interest is in high speed wide area network.

---

\* Present address: Department of Radiology, Childrens Hospital of Los Angeles/University of Southern California, Mailstop #81, 4650 Sunset Boulevard, Los Angeles, CA 90027, USA, Tel./Fax: +1 818 889 9411; E-mail: hkhuang@aol.com.



**Michael J. Gill** is an electronics engineer with the Communications Engineering Branch of the Lister Hill National Center for Biomedical Communications, a research and development division of the National Library of Medicine. His activities include the design, development, testing, evaluation and documentation of communications systems. He conducts experimental parts of Branch research programs including those involving the Next Generation Internet (NGI) and the Internet2. He represents the National Institutes of Health on the Joint Engineering Team (JET). The JET is a multi-agency group coordinating technical issues relating to implementing the NGI. His research interests include image transmission, Asynchronous Transfer Mode, satellite communications, communications systems and computer communications systems and performance measurement. He is a Senior Member of the IEEE. Prior to joining NLM, he worked for MCI Communications in Washington, DC, in the area of private line analog and digital telecommunications circuit design. He received the B.S. degree in electrical engineering from the University of Maryland College Park Maryland.



**H.K. Huang**, Professor and Director of Informatics, Childrens Hospital Los Angeles/University of Southern California since January 1, 2000. Before that he was Professor and Director of Laboratory for Radiological Informatics, Department of Radiology, University of California at San Francisco, USA; and faculty of the UCSF/UC Berkeley Bioengineering Program. He was the Kan Tong Po Visiting Professor at the Hong Kong Polytechnic University from December 1999 to February 2000. He is also an Adjunct Professor, Department of Radiology, University of Iowa. Dr. Huang pioneered in picture archiving and communication system (PACS) research program, and developed the PACS at UCLA in 1991, and the hospital-integrated PACS at UCSF in 1995. Dr. Huang's current research interest is in digital mammography, tele-imaging, image informatics infrastructure, and next generation Internet. He has co-authored and authored seven books and published over 200 articles. His recent book is 'PACS: Basic Principles and Applications' in 1999 by John Wiley and Sons. Since joining the University of California, Dr. Huang has received over 15 million dollars in PACS, medical image informatics, and image processing related research grants and contracts. He has trained over 20 Ph.D. students and 40 Post doctoral Fellows. Dr. Huang was inducted into the Royal College of Radiologists, England as an Honorary Fellow, for his contribution in PACS research and development in November, 1992; the American Institute of Medical and Biological Engineering as a Founding Fellow, for his contribution in medical imaging in March 1993; and the EuroPACS Society as an Honorary Member for his contribution in PACS in October, 1996.

## 1. Introduction

During the past several years, Internet has encountered unexpected demands by various applications including medical imaging. The characteristics of medical imaging, especially in radiology, are different from other types of data in two aspects: its file size is very large (e.g., a mammography examination with four images is about 160 Mbytes) [1], and some image examinations require near real-time transmission for practical use [2,3]. Standard Internet, therefore has not been able to fulfill the transmission bandwidth requirement in daily clinical applications. Due to health care reform, telemedicine and teleradiology gradually form an integral part in the US health care delivery system. The problem of high-speed transmission of large volume medical images has become very critical [4]. During the past several years, the NGI initiative [5] utilizing various high-speed network backbones including the CalREN-2 (California Research and Education Network), the vBNS (very high performance Backbone Network Service), and the Abilene to form the Internet2 infrastructure provides an opportunity for tackling this problem [6-8]. This paper considers some connectivity and security issues of NGI in medical imaging applications. In connectivity, at the global level, we review the relationship between CalREN-2, vBNS and Abilene, and at the local level the components required for the end user to connect to the Internet2. In security, we consider the hardware and software firewalls [9] and image data encryption [10].

## 2. Background

### 2.1. NGI initiative

The NGI initiative was announced by the US federal government On October 10, 1996 based on multi-agency federal research and development programs with several major goals, among them are:

- Develop advanced networking technologies.

- Develop revolutionary applications that require advanced networking.
- Demonstrate these capabilities on testbeds that are 100 to 1000 times faster than today's Internet.

In the health care area, telemedicine and emergency medical response team support, are some of the potential application areas for the NGI [5,11].

## 2.2. *Internet-2, vBNS, Abilene, and CalREN-2*

Internet2 is an academic collaborative effort to develop advanced high speed Internet technology, and to develop applications vital to research and education missions of higher education, such as telemedicine, digital libraries, and virtual laboratories that are not possible with the technology underlying today's Internet. Today over 150 US universities, working together with partners in industry and government, are leading the Internet2 project.

In 1995, MCI/Worldcom (Washington, DC) formed a partnership with the National Science Foundation (NSF) to create the vBNS. MCI/Worldcom has also provided NSF designated organizations with the necessary connection to the vBNS.

In 1999, the Abilene, under the development by UCAID in partnership with Qwest Communications (Denver, CO), Nortel (Northern Telecom, Brampton, Ontario, Canada) and Cisco Systems (San Jose, CA), is planned to be a high-performance network dedicated to support of the Internet2 project.

GigaPoPs (gigabit Points of Presence) are regional network aggregation points being formed by Internet2 universities to connect to a variety of high performance, and other types of networks. GigaPoPs provide scalable high-speed connection points. A joint proposal entitled 'CalREN-2 (the California Research and Education Network)' submitted by GigaPoPs in California was funded by the National Science Foundation in 1997. The goal of CalREN-2 is for the members to connect to the Internet2 for their respective applications. This proposal defined a focused strategy to begin building the CalREN-2 network as the advanced communications services for all institutions of higher education in California.

The university-led Internet2 effort and the federally-led NGI initiative are complementary and are already working together in many areas. The Internet2 program is in partnership with the NSF merit-based High Performance Connections Program. Over 90 Internet2 universities have received competitively awarded grants to support connections to advanced backbone networks such as UCAID's Abilene and NSF's vBNS. Over 28 NGI research projects were funded by the National Library of Medicine during the past two years to explore the health care related applications.

## 2.3. *Telemedicine and teleradiology*

Telemedicine can be simply defined as the delivery of health care using telecommunications and computer technologies. Teleradiology is a subset of telemedicine dealing mainly with images and related data. There are two models in telemedicine and teleradiology; the referring physician or health care provider can either consult with individual specialists at various places through a network, or request opinions from a consolidated expert center where different types of consultation services are provided [3].

In the expert teleradiology center consultation process, three scenarios are possible: telediagnosis, teleconsultation, and telemanagement [3,12]. For telediagnosis, the patient's examination results and imaging studies are done at the referring physician's remote site and data and images are transmitted to the expert center for diagnosis. The urgency of this service is nominal and turn around can take between four hours to a day. For teleconsultation, the patient may be still waiting at the examination site, while the referring doctor requests a second opinion or diagnosis from the expert center within half an hour. For telemanagement, the patient may still be on the gantry or in the examination room at the remote site, and the expert is supposed to provide immediate management care to the patient in situ. Despite these three different scenarios in teleradiology, the requirement of low cost, high speed NGI is obvious because of the large image file size in medical images.

### 3. Connection to the Internet2 – a case study

#### 3.1. Global environment

Currently, the Internet2 backbone is composed of several backbone networks described above which can use both ATM (asynchronous transfer mode) and PoS (packet over Sonet) technologies dependent on the locality of the backbone network. For this reason, when transmitting data through the Internet2 backbone, the data may go through several cell-to-packet and packet-to-cell conversions. From the end user's point of view, once the data passes through the local network gateway, there is no more local control over how the data will be transmitted through the backbone. For this reason, the total network performance will depend on the routing of the data through the Internet2 backbone as well as the routing of the data within the sending and the receiving sites. Also, data security will have two levels, one at the transmitting and receiving sites, and the other due to the Internet2 built-in security system. The details of the global Internet2 architecture is beyond the scope of this paper. In the following we will restrict the description to the method of connection from the local site to the Internet2 backbone.

#### 3.2. Local environment

In this section we describe the method of connecting to the Internet2 backbone from a local site. We use the environment at the Laboratory for Radiological Informatics (LRI), University of California, San Francisco (UCSF) as a case study [13], and link this local environment to the Internet2. Our three tested sites which also link to Internet2 are: Stanford University (Stanford, CA); Lister Hill National Center for Biomedical Communications, National Library of Medicine (NLM, Bethesda, MD); and Cornell University (Ithaca, NY). The campus network architecture for Stanford and NLM is known while Cornell's is not.

##### 3.2.1. UCSF existing network environment

###### Campus network

The University of California, San Francisco consists of two major campuses, Parnassus campus (UCSF) and Mount Zion Hospital (MZH), and two administrative offices in the San Francisco Bay Area. It is also affiliated with the San Francisco VA Medical Center (SFVAMC), and the San Francisco General Hospital (SFGH).

Figure 1 shows current UCSF DMZ (DeMilitarized Zone) network architecture. The main component is the fast Ethernet core routers which connect all the campus offices and Laboratories together. LRI is connected to the core through router lri158-r1. For the current UCSF Internet connection which is through UC SMDS (Switched Multimegabit Data Service), there are two paths (as of July 1999):

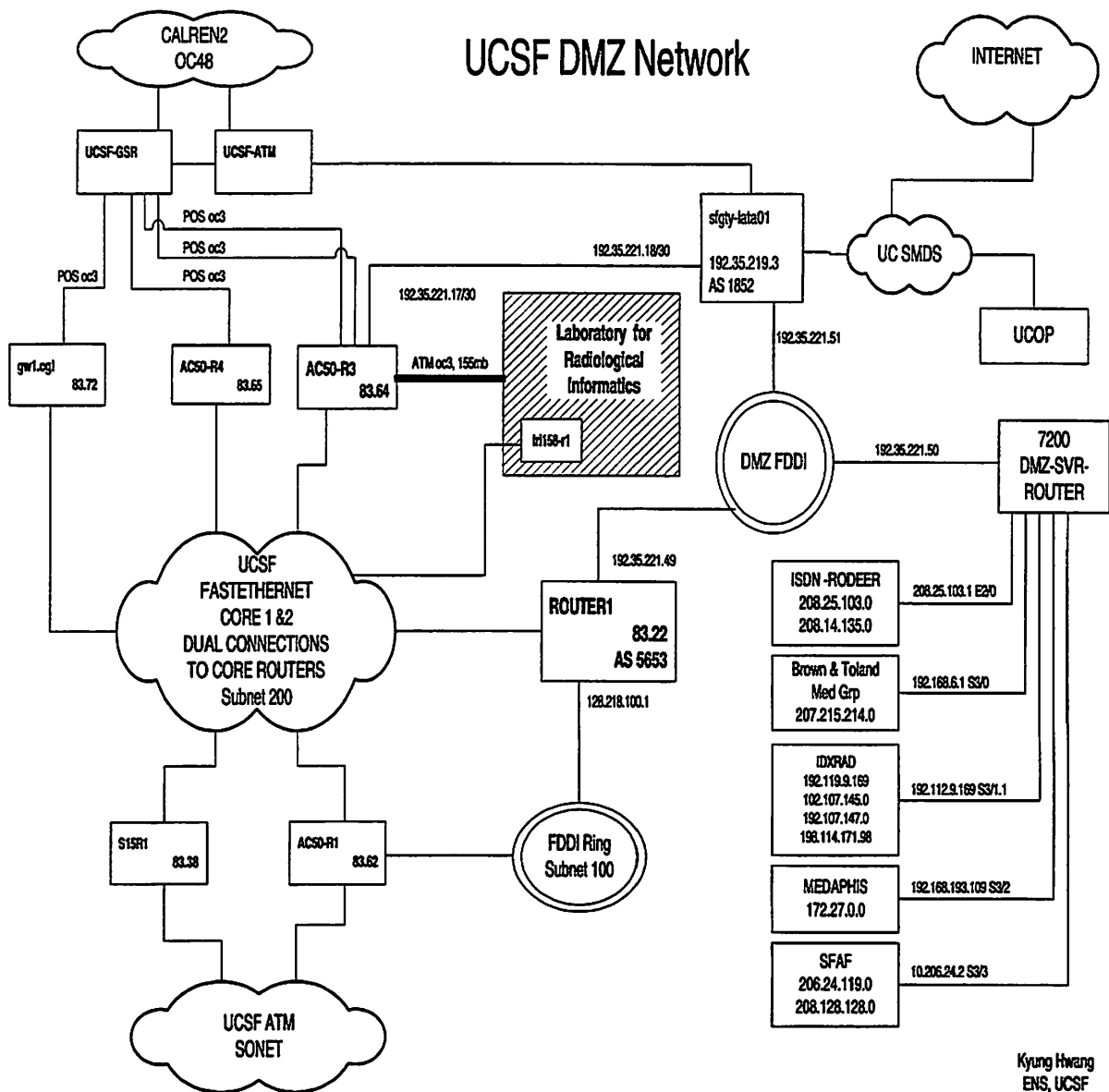
ROUTER1 -> DMZ FDDI -> sfgty-lata01, and  
AC50-R3 -> sfgty-lata01.

The UCSF Internet-2 connection (through CalREN-2) was established by the campus ENS (Enterprise Network Service) using three separate routers at:

AC50-R3  
AC50-R4, and  
gw1.cgl,

connecting to the UCSF CalREN-2 GSR (Gigabit Switch Router) drop. These three connections are available for end user to access the Internet2. In the Preliminary Results Section, we will present some data obtained through using these three connections.

There are two types of CalREN-2 drop in UCSF. One is PoS (OC-12) connecting to a Gigabit Switch Router (GSR) and the other is two connections to ATM (OC-12) switch. One of the UCSF core routers (AC50-R3) is connected to the GSR by dual OC-3 PoS (Packet over Sonet) connections. And for redundancy there is another OC-3 PoS connection between the GSR and another core router (AC50-R4).



Kyung Hwang  
 ENS, UCSF  
 22 Mar 1999

Fig. 1. UCSF campus network architecture.

Both routers are connected to the LRI switch (Cisco 2900) which is labeled as ATM/IP Converter in Fig. 3 (left). This switch has both Fast Ethernet and ATM interfaces. It is used as the gateway between the IP network and ATM network.

**Dedicated Internet2 connection for medical imaging applications**

In order to investigate the possible improvement of Internet2 performance at the local level, we are working on two direct connections from LRI to the UCSF-GSR and UCSF-ATM by bypassing other campus traffic and routing in the Campus network cloud for dedicated medical image applications. The first connection links LRI directly to ACR50-R3 (bold line, Fig. 1). The second is to connect LRI directly to the UCSF CalREN-2 ATM drop which is



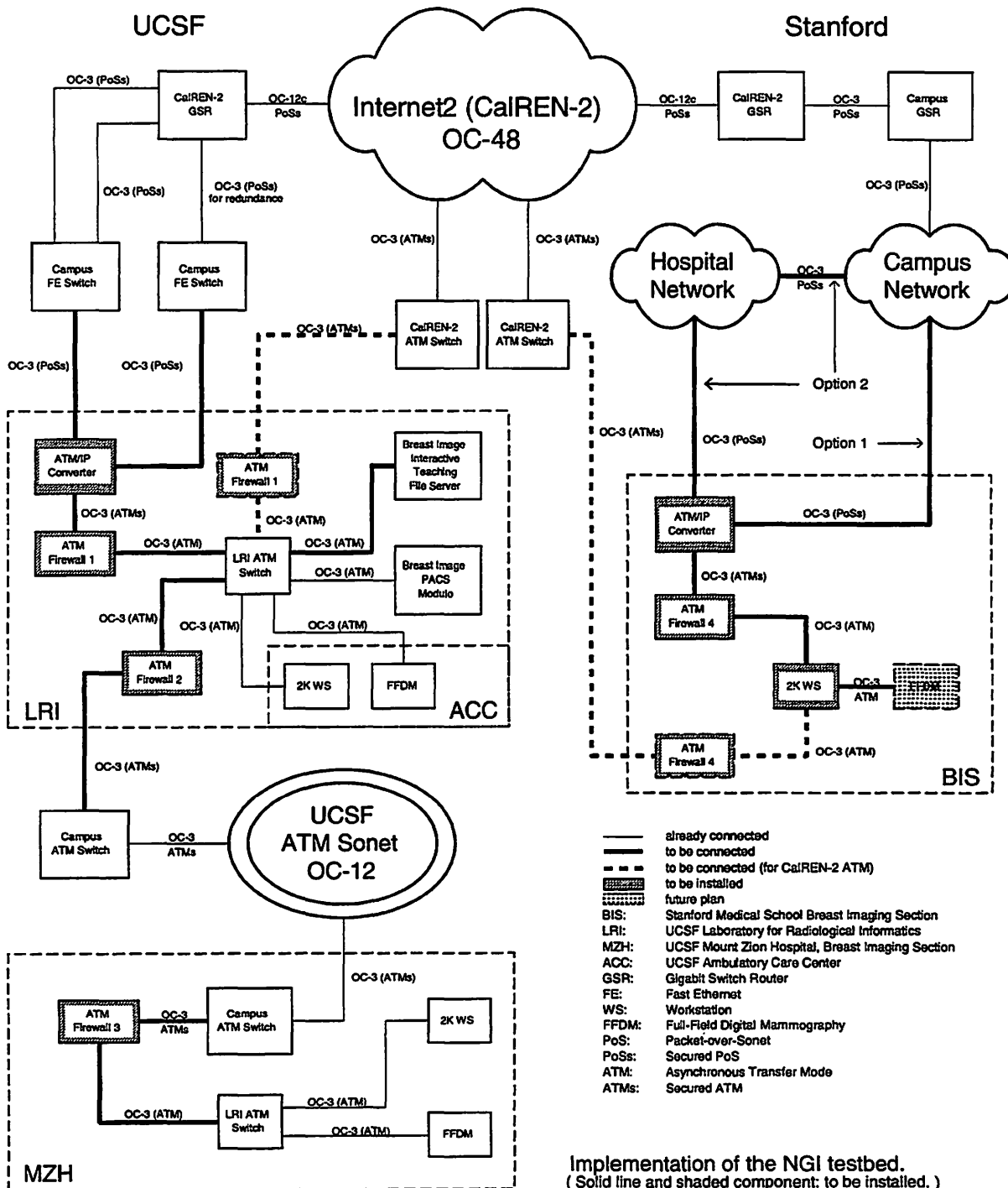


Fig. 3. Implementation plan of the NGI testbed between UCSF and Stanford.

this paper, we focus our attention at the local level, that is, the responsibility of the end user. We use the telemammography application at UCSF as an example. In this application, the question raised often is how authentic is the digital mammogram after it is transmitted through an open network. Generally, trust in digital data is characterized in terms of privacy, authenticity, and integrity of the data. Privacy refers to denial of access to information by unauthorized individual. Authenticity refers to validating the source of a message. Integrity refers to the assurance that the data was not modified accidentally or deliberately in transit. Thus, privacy is the responsibility of the Internet2, the campus network authority, and the end user's private network manager, and in that order; authenticity and integrity are the responsibility of the end user.

In a telemammography application, the end user is responsible for maintaining its private network and its network and data security. First consider the network security, since the network used is ATM, an ATM hardware firewall will be needed [9]. A software firewall will be insufficient due to the fact that software encryption and decryption will delay the transmission speed for telemanagement application. The encryption delay in current ATM OC-3 cell-based hardware firewall is on the order of 32  $\mu$ s, well acceptable for telemanagement applications [16]. The ATM hardware firewall is placed between the local ATM switch and the cell-packet converter as shown in Fig. 3. Once the data is encrypted via the ATM firewall, data is secured up to the point specified by the hardware.

The end user is also responsible for guaranteeing the integrity of the image data. This level of security is mostly done based on the concept of digital signature of the image using some existing cryptography algorithms while the image is being generated. The digital signature based on certain characteristics of the medical image and related patient data will provide additional protection and assurance of data authenticity and integrity that are not available in the ATM firewall. In general the digital signature concept consists of four steps:

- (1) Image pre-processing: To segment objects of interest from background and extract patient information from the DICOM (Digital Imaging and Communication in Medicine) image header.
- (2) Image digest: To compute an image digest (or digital signature) of the segmented image based on its characteristics using the MD5 digest or other algorithm [10].
- (3) Data encryption: To produce a digital envelope containing the encrypted image digest and corresponding patient information from the image header.
- (4) Data embedding: To embed the digital envelope into the image. This is done by replacing the least significant bit of a random pixel of the image by one bit of the digital envelope bit stream and repeating for all bits in the bit stream.

For an example of the digital signature approach in telemammography applications, see Reference [10]. The combination of the ATM hardware firewall and software digital signature during the image generation will meet the basic requirements for image security.

## 5. Preliminary results

### 5.1. NGI performance

Some preliminary experiments were performed at LRI to validate the connection and performance of the local ATM network between LRI and MZH, CalREN-2 from LRI to Stanford University, and Internet2 from LRI to Cornell University. The performance is shown in Table 1. Table 2 delineates the data path between LRI and Stanford, and between LRI and Cornell.

To avoid the disk I/O influences of using regular FTP software, a different test was made by using a commercial software package, Pegasus, developed by Ganymede (Morrisville, NC) to simulate TCP/IP applications. Two test sites were set up; one at LRI (West coast) and one at NLM (East coast). The simulating TCP application was FTP Get, the data were 4 digital mammograms each with 40 Mb, the schedule was every 15 min from Thursday to Tuesday. Figure 4 shows the results from 8/19/99 to 8/24/99. Table 3 delineates the data path between LRI and NLM. The Internet2 paths use CalREN-2 and vBNS (per Tables 1–3) for the national connection, and only CalREN-2 for the regional.

Table 1  
Comparison of performance between private ATM OC-3, CalREN-2, and Internet2

UCSF Sonet Ring * between LRI and MZH, OC-3	CalREN-2 ** between LRI and Stanford University (ftp.cs.stanford.edu)	Internet-2 ** between LRI and Cornell University (ftp.cs.cornell.edu)
94.05 Mbps	00:54 am, 5/28/99: > 16.01 Mbps 09:45 am, 5/28/99: > 15.45 Mbps 02:55 pm, 5/28/99: > 15.67 Mbps 06:13 pm, 5/27/99: > 15.74 Mbps 09:25 pm, 5/27/99: > 15.85 Mbps	00:55 am, 5/28/99: > 572.83 Kbps 09:44 am, 5/28/99: > 574.78 Kbps 03:03 am, 5/28/99: > 572.92 Kbps 06:10 pm, 5/27/99: > 574.32 Kbps 09:20 pm, 5/27/99: > 575.85 Kbps

\*Test tools: Sun Sparc Ultra-2, Solaris 2.5.1, UNIX ftp software.

\*\* Test tools: Pentium-2/300, WS\_FTP95 (32 bit). The performance was influenced by the remote server (environment unknown) and the number of users at that time.

Table 2  
Data path between LRI and Stanford, and between LRI and Cornell

LRI–Stanford	
1	router.lri.ucsf.edu (128.218.60.1)
2	ac50-r3.ucsf.edu (128.218.200.7)
3	192.35.221.6 (192.35.221.6)
4	STAN-UCSF.POS.calren2.net (198.32.249.1)
5	i2-gateway.Stanford.EDU (171.64.1.214)
6	Core3-gateway.Stanford.EDU (171.64.1.222)
7	Gates-gateway.Stanford.EDU (171.64.3.41)
8	ftp.cs.Stanford.EDU (171.64.67.150)
LRI–Cornell	
1	router.lri.ucsf.edu (128.218.60.1)
2	ac50-r3.ucsf.edu (128.218.200.7)
3	192.35.221.2 (192.35.221.2)
4	vBNS-UCSF.Calren2.net (198.32.251.5)
5	cs-atm0-0-22.nor.vbns.net (204.147.131.233)
6	CORNELLNET2-ATM4-0-0-1.CIT.CORNELL.EDU (128.84.0.249)
7	HOL2-8540-VL8.CIT.CORNELL.EDU (132.236.222.142)
8	CERBERUS-EXT.CS.CORNELL.EDU (128.84.154.7)
9	FTP.CS.CORNELL.EDU (128.84.154.132)

## 5.2. Telemammography in different network environments

We also compared the performance of available wide area network technologies for transmitting digital mammograms. A typical mammography examination at UCSF consists of four images, 46 Mbytes/image, or 184 Mbytes/exam [1,14]. Table 4 shows the time estimated to transfer 184 Mb images under various network environments.

## 6. Discussion

Internet2 consists of many existing high-speed network backbones including vBNS, CalREN-2, and Abilene. These backbones use cell-based ATM and packet-based PoS technologies. In order for the end user to connect to and take advantage of the Internet2, a major overhaul of the local network architecture is necessary. Compatible

Throughput Analysis Summary

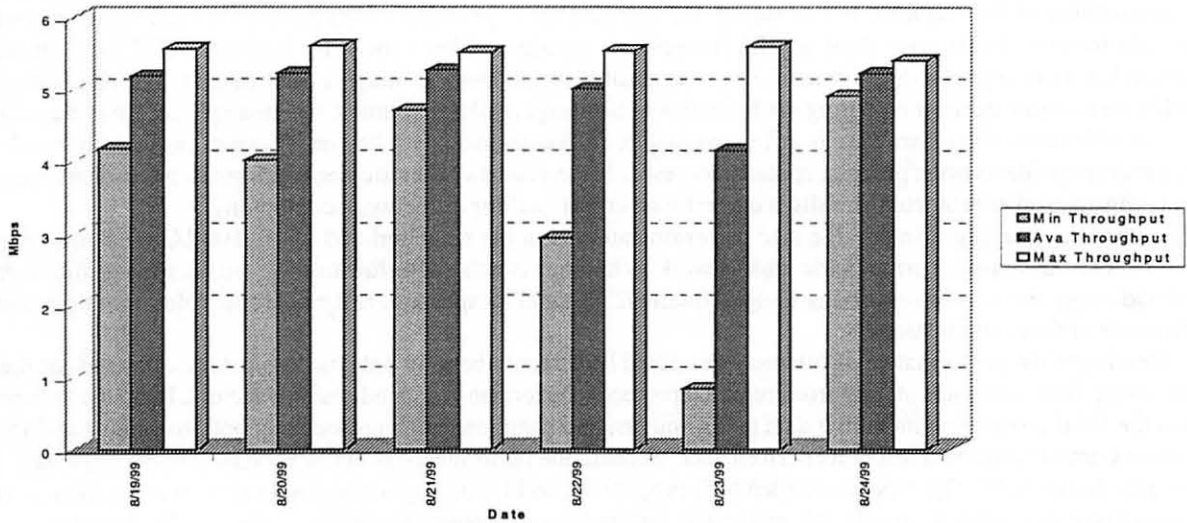


Fig. 4. NGI performance between LRI and NLM.

Table 3  
Data path between LRI and NLM

1	router.lri.ucsf.edu (128.218.60.1)
2	ac50-r3.ucsf.edu (128.218.200.7)
3	192.35.221.6 (192.35.221.6)
4	vBNS-UCSF.Calren2.net (198.32.251.5)
5	jn1-at1-0-22.wae.vbns.net (204.147.132.209)
6	130.14.2.1 (130.14.2.1)
7	julessun.nlm.nih.gov (130.14.35.64)

Table 4  
Time estimated to transmit a 184 Mbytes mammography examination under various network environment

Local ATM (Measured 90 Mbps) LRI-MZH	Internet (Estimated 200 kbps)	T1 (Estimated 1.5 Mbps)	NGI (nation wide estimated based on 5 Mbps, Fig. 4)	NGI (regional based on > 15 Mbps, Table 1)
16.4 s	2.04 h	15.8 min	4.9 min	< 1.64 min

performance network routers and packet-cell converters should be used in the new architecture. We provide a case study using the ATM OC-3 private network at the Laboratory for Radiological Informatics (LRI), UCSF as an example for connecting a local site to the Internet2.

In this connection, there are two possible paths. The first one goes through the CalREN-2 ATM switch directly from LRI, and no cell-packet conversion is necessary. The conversion, should it be needed, will be taken care of by the Internet2 after the data reaches the global network. The second path is to convert the ATM cells to packets by an ATM/packet converter in the private network at LRI before it goes out to the campus network. The first path bypassing the UCSF campus network infrastructure should provide a better performance. However, not every end user would have an ATM private network, and not every high-speed backbone has an ATM drop allowing for the direct connection. We are in the process of connecting, and testing the performance of these possible paths.

Internet2 will provide necessary data security at the global level. But the data security at the local level is the responsibility of the end user. In this regard, the end user has to provide its own private network security as well as data integrity. In the case study at LRI, the network security is taken care of by hardware ATM OC-3 firewall which has an encryption delay time of 32  $\mu$ s, acceptable for all medical imaging applications. The data integrity relies on software encryption during the formation of the image, still a very time consuming process. For the packet protocol firewall, since hardware is not yet available, current technology relies on software. In order to speed up the encryption/decryption process, special processors in the main switches are needed. Research and development in hardware packet protocol firewalls is currently an urgent goal for the network community.

In medical imaging, average file size per examination is in the neighborhood of 10–100 Mbytes, and getting bigger. For this reason, current wide area network technology is either too slow or too costly for telemedicine and teleradiology applications involving images. Internet2, fast and inexpensive, is the potential solution for the rising demands of these applications.

Results on the performance of Internet2 described here should be used only as preliminary estimates, as these data were collected without a rigorous research protocol. Performance depends on two factors. First, the Internet2 and the local connection including data paths, routers, and communication protocols in both the global and local network architecture will affect its performance. Second, the performance is application dependent, especially in the health care field. The recently funded NGI projects on health care applications should shed some light in this respect (see Acknowledgement). We expect the performance of Internet2 to improve substantially during the next several years compared with the results shown here.

## Acknowledgement

This work is partially supported by contracts N01-LM-6-3547 and N01-LM-9-3538 from the National Library of Medicine, and DAMD17-99-P-3732 from the US Army Medical Research and Materiel Command. We thank SL Lou and WK Wong for discussion on the Campus network connection at the Stanford site shown in Fig. 3.

## References

- [1] H.K. Huang and S.L. Lou, Telemammography: a technical overview, *RSNA Categorical Course*, 1999, pp. 273–281.
- [2] H.K. Huang, Telemedicine and teleradiology technologies and applications. *Min. Invas. Therapy* 5/6 (1997), 387–392.
- [3] H.K. Huang, Teleradiology technologies and some service models. *Comp. Med. Imaging & Graphics* 20 (1996), 59–68.
- [4] H.K. Huang, R.L. Arenson, W.P. Dillon, A.S.L. Lou, T. Bazzill and A.W.K. Wong, Asynchronous Transfer Model (ATM) Technology for Radiologic Communication. *Am. J. Roentgenology* 164 (1995), 1533–1536.
- [5] [Http://www.ngi.gov](http://www.ngi.gov).
- [6] [Http://www.internet2.edu](http://www.internet2.edu).
- [7] [Http://www.ngi.gov](http://www.ngi.gov).
- [8] [Http://www.calren2.net](http://www.calren2.net).
- [9] Celotek Corporation, Encrypting ATM Firewall, <http://www.celotek.com>.
- [10] X.Q. Zhou, S.L. Lou and H.K. Huang, Authenticity and integrity of digital mammographic images, *Proc SPIE, Medical Imaging*, Vol. 3662-16, 1999.
- [11] NGI Implementation Plan, <http://www.ccic.gov/ngi/implementation>.
- [12] J. Zhang, J.N. Stahl, H.K. Huang, X. Zhou, S.L. Lou and K.S. Song, Real-time teleconsultation with high resolution and large volume medical images for collaborative health care. *IEEE Trans. Inform. Tech. Biomed.* (1999) (accepted).
- [13] H.K. Huang, *PACS: Basic Principles and Applications*, John Wiley's & Sons, NY, 1999, p. 521.
- [14] S.L. Lou, E.A. Sickles, H.K. Huang, D. Hoogstrate, F. Cao, J. Wang and M. Jahangiri, Full-field direct digital telemammography: technical components, study protocols and preliminary results, *IEEE Trans. Inform. Tech. Biomed.* 1(4) (1997), 270–278.
- [15] H.K. Huang, A.W.K. Wong and X. Zhu, Performance of Asynchronous Transfer Mode (ATM) local area and wide area networks for medical image transmission in clinical environment, *J. Comp. Med. Imag. & Graphics* 21(3) (1997), 165–173.
- [16] Celotek Corporation, Cellcase product line, <http://www.celotek.com>.



# Current Status and Future Advances of Digital Radiography and PACS

## Key Components of System Integration in Modern Healthcare

In a modern integrated healthcare environment (IHE), digital technology plays a vital role in the success of its operation. The hospital information system (HIS), picture archive and communication systems (PACS), and electronic medical or patient record (EMR or EPR) systems are some of the information systems forming an integral part of the entire healthcare enterprise. HIS handles patient records, billing, patient workflow, and other administrative functions. PACS manages the imaging-related examinations, diagnoses, and reports. EMR or EPR facilitates the process of individual patient records. These information systems complement each other, forming the cornerstone of the modern integrated healthcare delivery system [1].

This article describes the current status and future advances of two components in this large-scale digital healthcare delivery system: digital radiography (DR) and PACS, as well as their relationship with other healthcare information systems, HIS, and EPR. In DR, we review computed radiography and describe the current advances in DR technology. The measurements of spatial resolution, image contrast, and signal-to-noise ratio

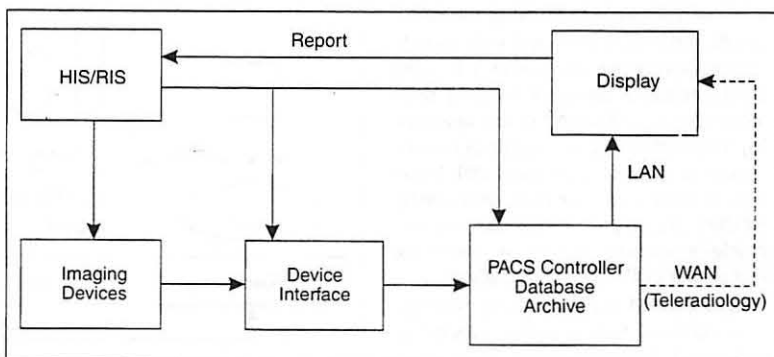
(SNR) of DR are given. In PACS, we emphasize DR and PACS integration and its utilization in several applications, including outpatient clinics, emergency rooms, imaging centers, and teleradiology. The importance of medical imaging informatics in the future practice of medicine based on integrated PACS is also outlined.

### PACS, Teleradiology, and Radiography PACS and Teleradiology

PACS was introduced in the mid 1980s and became mature in late 1990s. It manages radiological examinations, collects digital images from computed tomography (CT), magnetic resonance imaging (MRI), ultrasound (US), nuclear medicine (NM), computed radiography (CR), DR, and film scanners; archives them strategically; and selectively distributes them to proper locations for review.

PACS is a system integration of many classes of imaging computer systems connected by various networks (see Fig. 1). These computer systems include radiological imaging devices, device interfaces, PACS controllers with database and archive, PACS controllers with database and ar-

Xinhua Cao<sup>1</sup>, H.K. Huang<sup>1,2</sup>  
<sup>1</sup>Laboratory for Radiological Informatics,  
 Department of Radiology  
 University of California, San Francisco  
<sup>2</sup>Children's Hospital Los Angeles/  
 University of Southern California



1. A general block diagram of PACS.

chive servers, and display workstations. These components and networks are controlled by the PACS software. In addition, the PACS is interfaced with other healthcare information systems including the HIS, the radiology information system (RIS), and the EMR or EPR. If wide-area network (WAN) communication technology is augmented to PACS, that portion in PACS is called teleradiology [2].

Currently, over 100 large-scale and many medium- and small-scale PACS and teleradiology systems are being used in the world [3, 4]. PACS and teleradiology, although each has its own system architecture and plays a different role in the healthcare delivery system, each use many common technologies, in particular CR and DR.

### Projection Radiography

In radiology examination, about 70% is projection radiography [2]. Traditionally, there are two ways to acquire an image from projection radiography after the X-ray exposure. One method uses a screen/film combination as a detector, and the image is formed on the film. Or, in the case of fluorography (a relatively very small portion of projection radiography examinations), an image intensifier tube is used to record the image, which is then converted to video signals for display on a cathode ray tube (CRT). Therefore, in order for PACS and teleradiology to function, the film or the video image must first be converted to a digital image. For fluorography, the process is simply to convert the video signal through a video digitizer that is quick and inexpensive. On the other hand, digitizing films is a labor-intensive and often time-consuming process. For these reasons, new imaging acquisition methods have to be developed to replace the conventional screen/film detector.

Two approaches are possible. The first is to use existing equipment in the radiographic procedure room and only modify the image-receptor component. CR using photostimulable phosphor imaging plate technology is an example of this approach [5]. This method requires minimal modifications in the procedure room and, therefore, is more easily adopted immediately for daily clinical practice. CR has been successfully implemented as an integrated component of PACS and teleradiology.

The second approach is to redesign conventional radiographic procedure equipment, including the image receptor and/or the geometry of the X-ray beams.

## Digital radiography can improve the image quality and operation efficiency and at the same time reduce the cost of projection radiography examination.

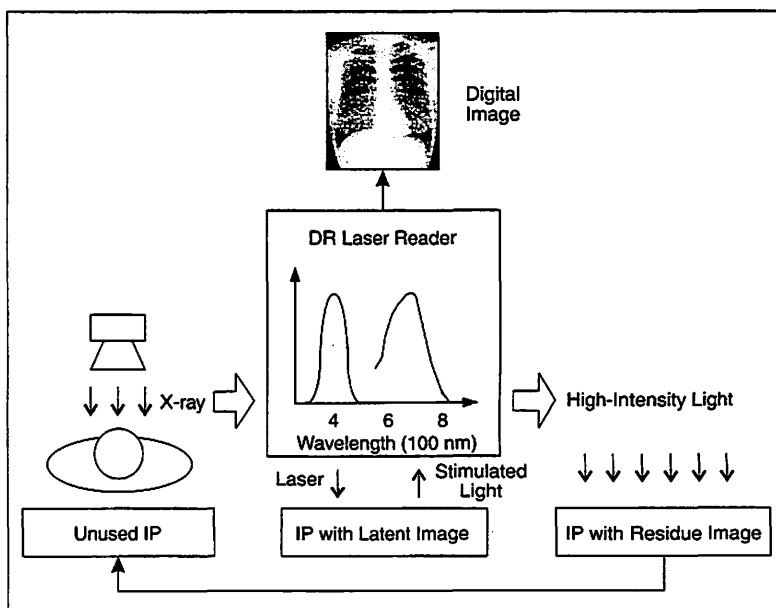
This method is, therefore, more expensive to adopt, but it offers the advantages of lower X-ray scatter, better X-ray quantum absorption, and conversion that would otherwise not be available in the screen/film detector.

### Computed Radiography

The CR system as a replacement of the screen/film detector was introduced in the mid 1980s and became very popular in the

mid to late 1990s. Most PACS and teleradiology applications in the intensive care units (ICUs) and emergency room (ER) use CR. CR technology uses a photostimulable phosphor imaging plate (IP) ranging from 200 mm × 250 mm to 350 mm × 430 mm in size, similar to the screen/film detector. Most CR systems use portable IP, except for some dedicated chest units. The systems are portable in the sense that the IP is inside a cassette just like the screen/film detector. Before the X-ray exposure, the technician carries the cassette with the IP inside to the radiography unit. After exposure, the cassette is fed to the CR reader, which first extracts the IP from the cassette, then uses a laser to release the latent image from the plate. The released latent image in the form of light energy is converted to electrical signals, then to a digital image. After the reading, the residue latent image in the IP has to be erased by a high-intensity light before it can be reused again. This procedure thus involves multiple steps: insert the IP in the cassette, expose the IP, read the IP, form the digital image, erase the IP, and put the IP back into the cassette (see Fig. 2).

The dedicated chest CR detector unit does not use a cassette. Instead, multiple IPs are inside a light-tight environment, and plates are cycled within the housing of the unit after each exposure. The dedicated chest unit is permanently aligned with the X-ray assembly. In order to form a digital image, the CR reader has to release the la-



2. The formation of the CR image.

**An advantage of DR is that it can potentially minimize the number of steps before the image becomes available for display and diagnosis.**

tent image from either the portable or dedicated IP by using a laser beam.

Through the past years, CR has gradually replaced many conventional screen/film projection radiography procedures, and it has been successfully integrated in PACS operations. The advantages of CR are that it requires only a minimal change in the radiographic room as well as that its image quality is acceptable for most examinations. However, the technology itself has certain inherent limitations. First, it requires two separate steps to form a digital image: a laser to release the light energy in the latent image from the IP, and a photomultiplier to convert the light to an electrical signal. Second, although the IP is a good image detector, its SNR and spatial resolution are still not ideal for some specialized radiographic procedures. Third, the IP re-

quires a high-intensity light to erase the residue of the latent image before it can be reused, adding an extra step in the imaging-acquisition operation. Also, many IPs are needed during the CR installation, and just as many screens are required in the screen/film detector system. IP has a limited number of exposure uses; is breakable, especially in the portable unit; and is expensive to replace. Manufacturers are working diligently on its improvement.

**Digital Radiography**

During the past five years, research laboratories and manufacturers have devoted tremendous energy and resources to investigating new DR systems other than CR. The main reasons are that DR can improve the image quality and operation efficiency and at the same time reduce the cost of projection radiography examination, while CR technology has inherent weaknesses in fulfilling such requirements. In order to compete with conventional screen/film and CR, a good DR system should:

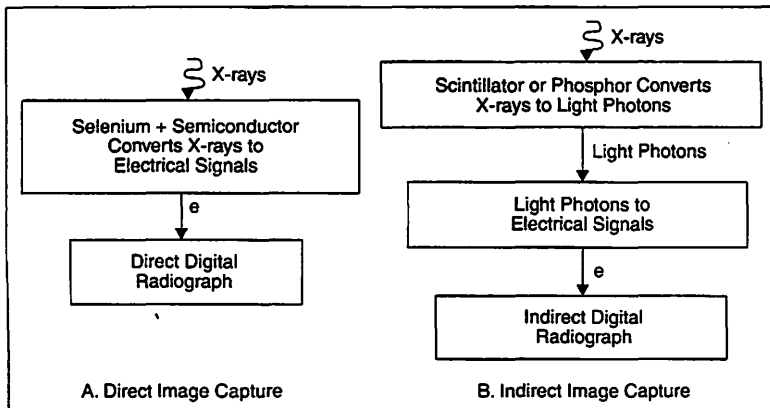
- have a high detective quantum efficiency (DQE) detector with 2-3 or higher line pair/mm spatial resolution;
- produce digital images of high quality;
- comply with industrial standards;
- have an open architecture for connectivity
- deliver low dosages to patients;
- be easy to operate;
- yield the digital image in seconds after X-ray exposure;
- be compact in size; and
- offer competitive cost savings.

Three prevailing scanning modes in digital are areal, line (or slot), and flying-spot. CR and digital fluorography, discussed above, belong to the areal mode. Some digital mammography sys-

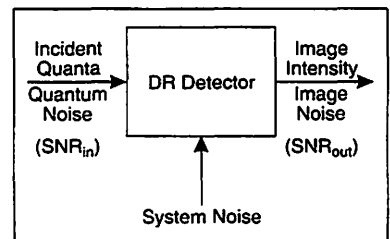
tems use a slot-scanning mode. The flying-spot mode requires a very long scanning time because data acquisition is pixel-by-pixel, resulting in a very short life of the X-ray tube. For this reason the flying-spot has not been very popular in recent DR design [2].

Depending on the method of X-ray photon conversion, DR can be categorized into direct and indirect image capture methods. In indirect image capture, attenuated X-ray photons are first converted to light photons by the phosphor or the scintillator, from which the light photons are converted to electrical signals. The signals are digitized and reformatted to form the DR image. The direct image-capture method generates a digital image without going through the light photon conversion process. Figure 3 shows the difference between the direct and the indirect digital capture methods. The advantage of the direct image-capture method is that it eliminates the intermediate step of light photon conversion. The disadvantages are that the engineering involved in direct digital capture is more elaborate, and that it is inherently difficult to use the detector for dynamic image acquisition due to the necessity of recharging the detector after each read out [6].

Current technology trends in areal detection mode use flat-panel sensors, which can be one large panel or several smaller panels put together. The indirect capture method uses either amorphous silicon phosphor or scintillator panels. The direct capture method uses an amorphous selenium panel. It appears that the direct capture method has the advantage over the indirect capture method in that it eliminates an intermediate step of light photon conversion. However, because of the engineering difficulty, it may be several years before commercial products based on the direct capture will become available for daily clinical use. The areal scan method has the advantage of being fast in image capture, but it also has two disadvantages;



3. Direct versus indirect digital radiography image capture.



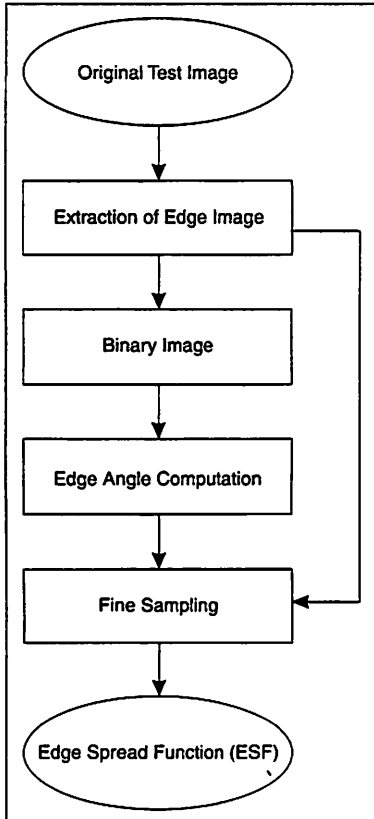
4. Detective quantum efficiency of a DR system.

one being the high X-ray scatter described above. The second is that the manufacturing of flat panels for radiographic applications is limited to only a few companies, which creates a supply shortage.

### Image-Quality Assessment Of Digital Radiography

#### Performance Parameters

The image quality of DR can be evaluated by three parameters: spatial resolution, image contrast, and the noise property. The assessment methods can be divided into two basic approaches: subjective and objective. Subjective assessment is based on statistical evaluation of observer performance; for example, receiver operating characteristic (ROC) analysis has been used extensively in conventional film-screen imaging systems [2]. However, using ROC for evaluating digital imaging quality is more complicated because various image processing methods (such as image enhancement) and display modalities (display parameters) will influence observer performance.



5. Image preprocessing to determine the ESF.

Subjective assessment also requires a large number of carefully selected cases, as well as a large number of observers, in order for the study to be meaningful. In recent years, much work based on objective assessment of conventional radiography has been revitalized for digital radiography [7-14]. New methods of measuring detective quantum efficiency (DQE), modulation transfer function (MTF), noise power spectrum (NPS), and noise equivalent quanta (NEQ) as fundamental performance parameters of digital imaging systems have been developed.

The DQE can be interpreted as the overall efficiency of the system, and MTF, NPS, and NEQ can be interpreted as the spatial resolution, noise, and SNR of the system, respectively. The DQE can be defined as:

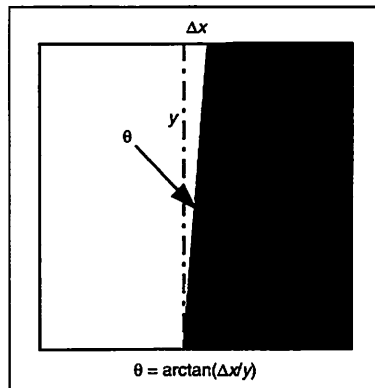
$$DQE(q, \nu) = \frac{SNR_{out}^2}{SNR_{in}^2} \quad (1)$$

where  $q$  is the incident X-ray dose and  $\nu$  is the one-dimensional (1-D) spatial frequency;  $SNR_{out}$  and  $SNR_{in}$  are signal-to-noise ratios of the output (image) and input (incident X-ray quanta) of the digital imaging system, respectively (see Fig. 4). For an ideal imaging system (no system noise and  $MTF = 1$ ),  $SNR_{out}^2 = SNR_{in}^2$ , and  $DQE = 1$ .

The square of the SNR of incident X-ray quanta  $SNR_{in}^2$  can be provided by the X-ray tube manufacturer or measured by using:

$$SNR_{in}^2 = \frac{(\int \Phi(E) E dE)^2}{\int \Phi(E) E^2 dE} \quad (2)$$

where  $\Phi(E)$  is the spectral distribution of the output X-rays, which can be deter-



6. The computed edge angle.

## The integration of DR into PACS will elevate the efficiency of the imaging component in the healthcare system.

mined from the given kVp value, filtration, and tube characteristics [15].

For monochromatic radiation, Eq. (2) becomes:

$$SNR_{in}^2 = \Phi_0 \quad (3)$$

which means that the SNR of the incident X-rays is simply equivalent to the quanta number per unit area  $\Phi_0$ . This result can also be proved by quantum statistics under the assumption of a Poisson distribution [16].

The square of the SNR of system output is often expressed by the number of quanta as NEQ:

$$NEQ = SNR_{out}^2 = \frac{I^2(q, \nu)}{NPS(q, \nu)} \quad (4)$$

where  $I^2(q, \nu)$  and  $NPS(q, \nu)$  are the signal power spectrum and the noise power spectrum of the output image, respectively. Both are functions of incident X-ray dose  $q$  and 1-D spatial frequency  $\nu$ .

The  $I^2(q, \nu)$  can be written as:

$$I^2(q, \nu) = [I_0(q) MTF(\nu)]^2 = I_0^2(q) MTF^2(\nu) \quad (5)$$

where  $I_0(q)$  is the DC (zero spatial frequency) component of signal intensity, and MTF is the 1-D modulation transfer function of the imaging system. Therefore, Eq. (4) can be rewritten as:

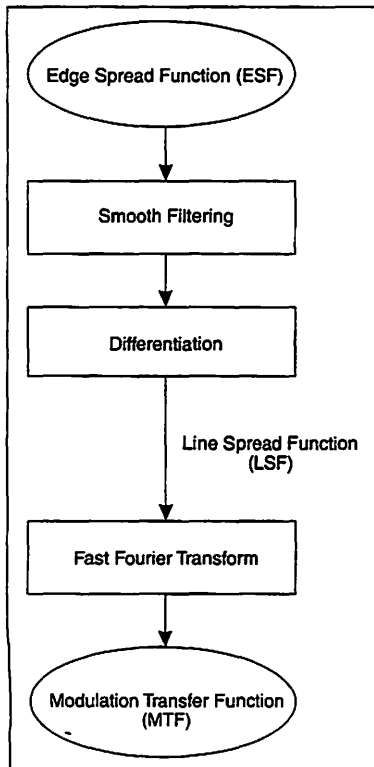
$$NEQ(q, \nu) = \frac{I_0^2(q) MTF^2(\nu)}{NPS(q, \nu)} \quad (6)$$

The functions on the right-hand side of the equation can be obtained as follows. A uniform plastic rectangular block (or filtration) is exposed with various X-ray tube (kVp) settings, and the filtered X-rays after the block (filtration) are mea-

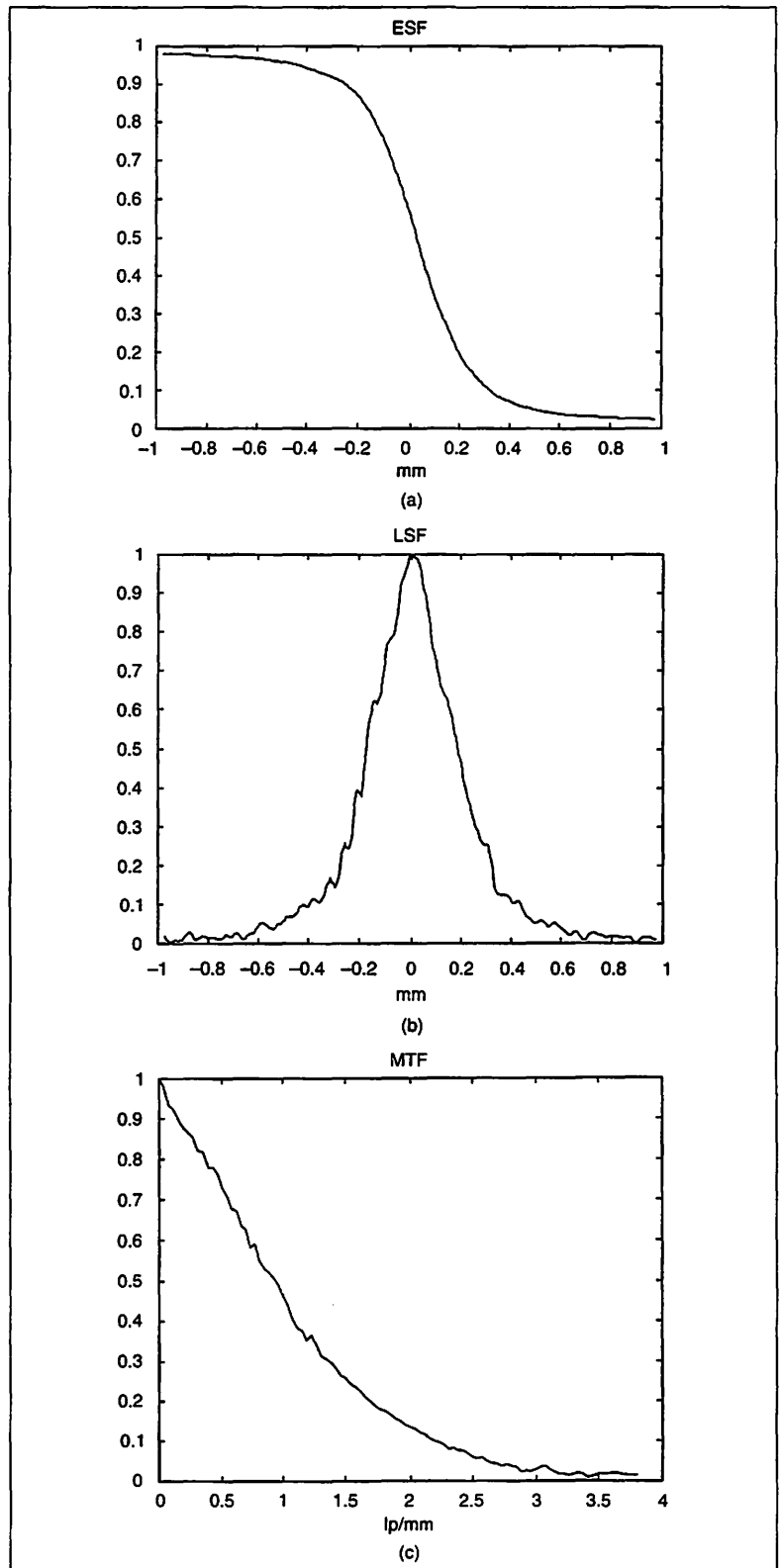
sured as the input dose ( $q$ ), with the detector reading as the image. The result is many uniform images as a function of " $q$ ." The signal intensity  $I_0(q)$  can be measured by computing the average of the same large area in these images as a function of  $q$ . Each large area can also be used to compute the NPS( $q, \nu$ ), as described below.

The MTF of a digital imaging system can be measured either by evaluating the response of the system to a periodic bar pattern, or by computing the line spread function (LSF) of the system using a narrow slit phantom. The bar pattern or the slit is placed in a certain direction with respect to the global coordinate system of the output image. The MTF( $\nu$ ) is determined by taking the 1-D Fourier transform of the LSF with respect to that direction. Another, similar, method for determining the MTF is to measure the edge spread function (ESF) of the system by imaging an X-ray opaque object with a sharp edge. Then, the ESF is differentiated perpendicular to the edge to generate the LSF, and the MTF can be similarly obtained by using the Fourier transform [2].

For a given  $q$ , the noise power spectrum NPS( $q, \nu$ ) can be obtained by using



7. ESF data processing.



8. Results after ESF data processing: (a) ESF, (b) LSF, and (c) MTF.

the large area in the corresponding image as follows. First, consider a line of pixels in the same direction as the bar pattern used in measuring the MTF in the large area. The average and the variance of pixels on this line are computed. The 1-D Fourier transform (FT) of the line variance is then obtained. Repeat the same procedure for all lines in the large area. The average of the sum-of-squares of the Fourier spectrum of all variances, spanning the entire large image area, line by line, is the NPS( $q,v$ ). Notice that the spatial frequency "v" has the same direction in the MTF( $v$ ) as in the NPS( $q,v$ ).

### An Example

As an example, in the following the measurement procedure and results of MTF from the ESF of a digital radiography system are described.

### Image Acquisition

The digital imaging system used in this measurement was the Swissray AddOn, DR Multi-System (Hochdorf, Switzerland), which allows direct cassette-less acquisition of digital radiography with an Add-On-Bucky CCD detector [17]. The system installed at the San Francisco Veterans Administration Medical Center (SFVAMC) supports the DICOM 3.0 format [18] and makes it available for direct connection with the PACS. All test images were securely transmitted to the Laboratory for Radiological Informatics, University of California at San Francisco (LRI-UCSF), via a public network, using a virtual private networking (VPN) technique.

A 0.5 mm-thick 300 × 150 mm copper sheet with air as the background was used for acquiring an edge image. The sheet

was positioned on the AddOn detector at a slight angle to the pixel array. The slight angle is necessary to increase the number of data points along the edge for more accurate computation. A digital image of the copper sheet was taken under the exposure condition of 85 kVp, 6.4 mAs, with a 2.6 mm Al filtration and a 10:1 grid.

### Edge Image Processing

After the test image was acquired at SFVAMC and transmitted to a workstation at LRI-UCSF, the image was processed as shown in Fig. 5 to determine the ESF of this DR imaging system.

For computing the 1-D MTF of the imaging system, a 500 × 500 subimage containing the edge was extracted from the original 2 K × 2.5 K DR image. In order to calculate the exact angle of the edge relative to the image array, a binary image (black-white) was obtained by thresholding the extracted subimage. The angle of the edge can be calculated directly from the binary image by trigonometry, as illustrated in Fig. 6, or determined using the Hough transform [19].

Since each ESF, a line profile across the edge of the edge image, has a tiny shift relative to the edge, a fine-sampling ESF can be obtained by reprojecting each ESF and combining adjacent ones, as described by Fujita [20] and Samei [21].

### ESF Data Processing

Data processing, as shown in Fig. 7, includes smooth filtering, differentiation, and the fast Fourier transform (FFT).

After reprojection, the fine-sampling ESF needs to be smoothed by filtering before being converted to the LSF. Adaptive filtering or polynomial-fit filtering was used so that the sharp part at the center of

ESF can be preserved. Then, the smoothed ESF was numerically differentiated to obtain the LSF; i.e:

$$LSF(k) = \frac{ESF(k+1) - ESF(k-1)}{2}, \quad (7)$$

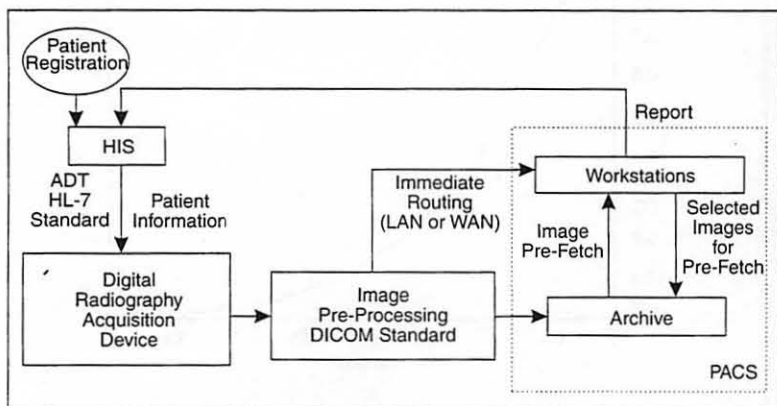
Finally, the MTF of the imaging system was obtained by taking the FFT of the LSF. Figure 8 shows the results of the ESF, LSF, and MTF.

## System Integration of Digital Radiography with PACS

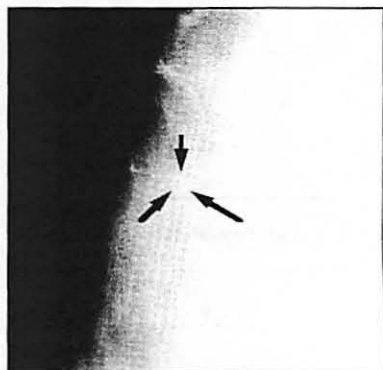
One major advantage of DR is that it can potentially minimize the number of steps before the image becomes available for display and diagnosis. In order to fully use this capability of DR, it should be integrated with the PACS and/or teleradiology. The main criterion of an effective integration is to have the DR image available for display as soon as it is captured. Figure 9 shows a method of integration.

As shown in Fig. 9, while the DR image is being generated, the HIS transmits ADT (admission, discharge, and transfer) information in the HL-7 standard format to the PACS archive. From there, the system triggers the prefetch function to retrieve relevant images from the patient historical examinations and appends them to the patient folder in the archive. The folder is forwarded to the workstation after the current examination. With a local-area network (LAN), PACS is used for forwarding; with a WAN, teleradiology is used.

After the DR image is available from the imaging system, certain image preprocessing is performed to enhance visual quality. For example, in digital mammography, preprocessing functions



9. Implementation of digital radiography with PACS.



10. A digital mammogram and an automatic enhanced image delineating fatty tissue and a lesion near the skin. (Courtesy of Dr. SL Lou.)

include segmentation of the breast from the background and determination of pixel value ranges of various breast tissues for automatic window and level adjustment. Figure 10 shows a digital mammogram and an automatic enhanced image delineating fatty tissue and a lesion near the skin. Segmentation of the breast allows image size reduction, resulting in rapid display of the image. Segmentation also provides certain parameters for centralizing and formatting the image on the screen for better visualization [22].

In digital chest radiography, removal of image background due to X-ray collimation as well as generation of an automatic look-up table for various parts of the anatomical structure are critical [23]. The collimation background appears as white on a softcopy display, which reduces the reader's visual perception threshold. Figure 11 shows a chest image before and after automatic background removal. The automatic look-up table generation allows for rapid reading, which is essential for operation efficiency.

In order for the DR to follow industry standards for system integration, it is necessary to use the digital imaging and communication in medicine (DICOM) standard.

After preprocessing, the image is immediately routed to workstations pertinent to the clinical application, from which the image is appended to the patient folder, which has already been forwarded

by the archive. The current DR image and historical images can be displayed simultaneously at the workstations for comparison. The image should also be sent to the PACS for long-term archive.

Another critical component in the DR system integration is the display workstation, which should be able to display images with the highest quality possible. The image display time should be within several seconds, and there should be pre- and instantaneous window and level adjustments. Most currently available CRT monitors with 2000 lines of resolution are adequate for DR display. The newly introduced flat-panel display is very attractive because of its high brightness, light weight, small size, and easy-to-tilt angle to accommodate the viewing environment. Figure 12 shows a side-by-side comparison of an active matrix LCD display versus a conventional CRT display of a DR image. The same DR image simultaneously is routed with the same look-up table to the LCD and CRT displays.

### Applications of DR in a Clinical Environment

As shown in Fig. 13, the DR detector can be configured as a general complete radiography system, such as a C-arm with table or a dedicated chest unit, or as an add-on detector to an existing radiography unit. The space requirement for DR is equivalent to a corresponding conventional radiography room. The add-on DR detector requires the replacement of the

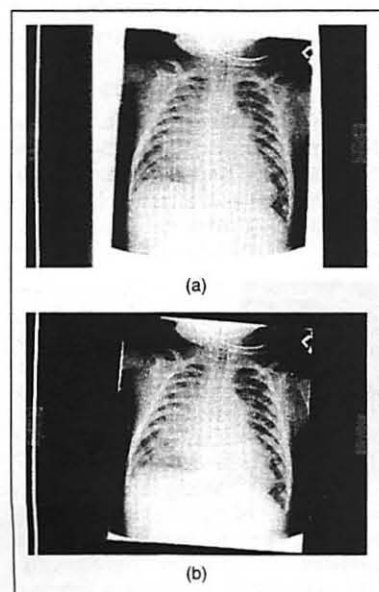
Bucky system in an existing radiography system. Regardless of configuration, the major applications of DR are in the conventional radiography room, the outpatient clinic, the imaging center, the emergency room, and in teleradiology, as described in the following sections.

### Outpatient Clinic

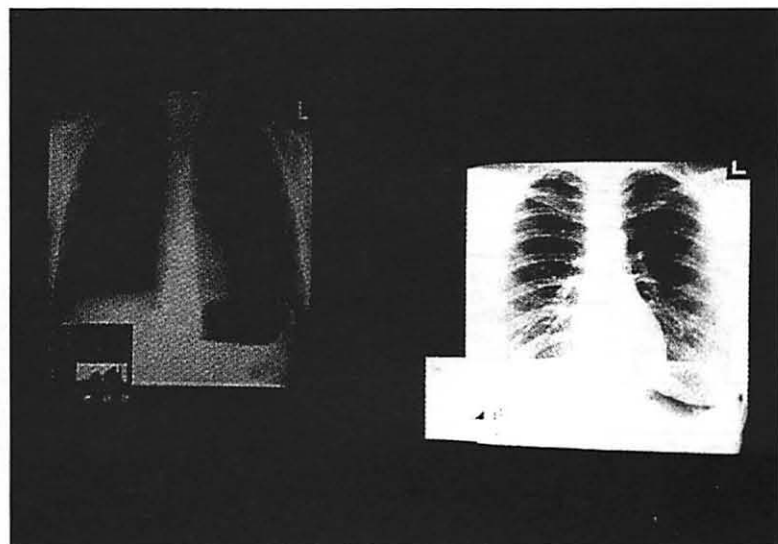
Figure 14 shows a schematic of patient workflow in a filmless outpatient clinic. Patients first register, change garments, queue up for the examination, walk to the DR unit, get imaged, change back to street clothes, and walk to the assigned physician room where the images are already available for viewing. In the background, while the patient registers, the HIS sends patient information to the PACS outpatient server. The server retrieves relevant historical images, waits until the DR images are ready, appends new images to the patient image folder, and forwards it to the assigned physician room where images are displayed automatically when the patient arrives. This patient workflow is most efficient and cost-effective. The operation is totally automatic, filmless, and paperless. All human intervention is eliminated, except during the X-ray procedure.

### Imaging Center and Teleradiology

Even when HIS-PACS is not available (for example, in a small imaging center), this outpatient workflow is still valid with three modifications:



11. A chest image (a) before and (b) after an automatic background removal. (Courtesy of Dr. J. Zhang.)



12. Side-by-side comparison of a DR image displayed on a workstation with a CRT (left) and an active matrix LCD (right). The image on the LCD is much brighter, revealing anatomies otherwise not easily visible on the CRT.

- 1) Change the HIS to a patient registration system that is generally available in most imaging centers.
- 2) Change the PACS outpatient server to a DR server connected to the patient registration system.
- 3) Make the DR server capable of distributing images, including to remote expert centers, using teleradiology systems (see Fig. 14).

The DR manufacturer should provide these components for system integration, or a system specialist can work with the DR manufacturer to provide the system integration.

### Emergency Room

In the emergency room, a CR/DR tandem or a dedicated C-arm DR is required because certain patients may not be able to stand up for an upright-position examination. However, the patient workflow shown in Fig. 14 should still be valid.

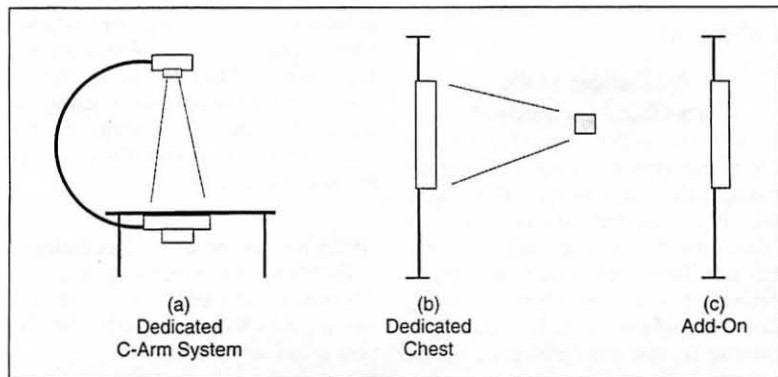
### Future Advances DR, PACS, and IHE

The trend in healthcare is toward system integration in which the concepts of the EPR/EMR or IHE will prevail. PACS and teleradiology are an integral part of EMR and IHE, and both require DR and CR for successful operation. For this reason, the introduction of DR and CR into everyday clinical care is crucial. The integration of CR into PACS has been successful in several clinical applications. The integration of DR into PACS will elevate the efficiency of the imaging component in the healthcare system. In order to implement DR into a totally integrated healthcare enterprise, we must consider carefully the total system integration concept. The DR system has to be DICOM compliant for connection to PACS, with system connectivity capable of receiving industry-standard patient information

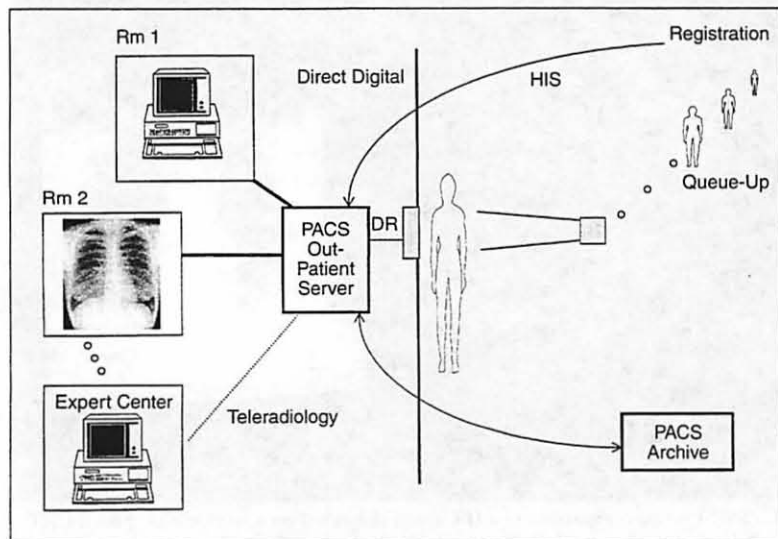
such as in HL-7 format, and connected to high-quality display workstations for accurate and speedy review. DR provides a means for eliminating film, and its integration into PACS and teleradiology allows for a cost-effective, streamlined integrated healthcare-delivery system.

### Medical Image Informatics

PACS originated as an image management system for improving the efficiency of radiology practice. It has evolved into a hospital-integrated PACS dealing with information media in many forms, including voice, text, medical records, images, and video recordings. To integrate these various types of information requires the technology of multimedia: hardware platforms, information systems and databases, communication protocols, display technology, and system interfacing and integration. As more PAC systems are implemented, the contents of their databases will grow. The richness of information within PACS provides an opportunity for a completely new approach in medical research and practice via the discipline of medical informatics, in particular medical image informatics [24]. Many longitudinal and horizontal clinical and research studies requiring large-scale multimedia data can be designed and implemented from the availability of PACS-related data. Results from these studies will change the traditional method used in the practice of medicine, from local healing to a global healthcare delivery system.



13. Three configurations of DR.



14. Filmless outpatient clinic with DR and PACS.

### Acknowledgments

This work is partially supported by the National Library of Medicine N01-LM-6-3547 and the US Army Medical Research and Materiel Command DAMD17-96-C-6111.



Xinhua Cao received his Ph.D. from the Xi'an Jiaotong University, Xi'an, P.R. China, where he became an assistant professor. Dr. Cao joined LRI, UCSF working with Dr. Huang on image quality measurement of digital radiography systems. Dr. Cao's research interests are in hardware and system development of digital radiography, dual-energy imaging, digital image processing, digital image quality evaluation, telemammography, and PACS applications.

H.K. Huang pioneered in picture archiving and communication system (PACS) research. He developed the PACS at UCLA in 1991 and the hospital-integrated PACS at UCSF in 1995. Dr. Huang's current research interest is in digital mammography, teleimaging, image informatics infrastructure design, and next-generation Internet. He has coauthored and authored seven books and published over 200 articles. His most recent book is *PACS: Basic Principles and Applications* (1999, Wiley). During the past 15 years, Dr. Huang has received over \$15 million in PACS-, medical image informatics-, and image processing-related research grants and contracts. He has mentored 15 Ph.D. students and trained over 30 postdoctoral fellows during the past 15 years.

Dr. Huang was inducted into the Royal College of Radiologists, England, as an Honorary Fellow, for his contribution in PACS research and development in November 1992; the American Institute of Medical and Biological Engineering as a Founding Fellow, for his contribution in medical imaging in March 1993; and the EuroPACS Society as an Honorary Member for his contribution in PACS in October 1996.

**Address for Correspondence:** H.K. Huang, Professor and Director of Informatics, Department of Radiology, Childrens Hospital of Los Angeles/University of Southern California, Mailstop #81, 4650 Sunset Boulevard, Los Angeles, CA 90027. Tel. and Fax: +1 823 671 1588. E-mail: hkuang@aol.com.

## References

1. HIMSS and RSNA, *Integrating the healthcare Enterprise: IHE Year 1 Demonstration Concept - HL7 Message Implementation*. Rev. 1.0, May 26, 1999.
2. Huang HK: *PACS: Basic Principles and Applications*. New York: Wiley, 1999, p. 521.
3. Bauman, RA, Gell, G, et al.: Large picture archiving and communication systems of the world - Part 1. *J Digital Imaging* 9(3): 99-103, 1996.
4. Bauman, RA, Gell, G, et al.: Large picture archiving and communication systems of the world -Part 2. *J Digital Imaging* 9(4): 172-177, 1996.
5. Takano TL (Ed): *Computed Radiography*. Berlin: Springer-Verlag, 1987.
6. Rowlands JA: Digital x-ray systems based on amorphous selenium. *AJR* 167: 409-411, 1996.
7. Dobbins JT III, Ergun DL, Rutz L, Hinshow DA, Blume H, and Clark DC: DQE(f) of four generations of computed radiography acquisition devices. *Med Phys* 22(10): 1581-1593, 1995.
8. Stierstorfer K and Spanh M: Self-normalizing method to measure the detective quantum efficiency of a wide range of x-ray detectors. *Med Phys* 26(7): 1312-1319, 1999.
9. Kamm KF, Steiner R, and Tikorn K: Assessment of objective image quality in digital radiography: Non-invasive determination of the detective quantum efficiency. *SPIE Medical Imaging* 2708: 194-205, 1996.
10. Zhao W and Rowlands JA: Digital radiography using active matrix readout of amorphous selenium: Theoretical analysis of detective quantum efficiency. *Med Phys* 24(12): 1819-1833, 1997.
11. Siewerdsen JH, Antonuk LE, El-Mohri T, Yorkston J, and Huang W: Signal, noise power spectrum, and detective quantum efficiency of indirect-detection flat-panel imagers for digital radiology. *Med Phys* 25(5): 614-628, 1998.
12. Bradford CD and Pepler WW: Performance characteristics of Kodak computered radiography system. *Med Phys* 26(1): 27-36, 1999.
13. Launders JH, Kengyelics SM, and Ciwen AR: A comprehensive physical image quality evaluation of a selenium based digital x-ray imaging system for throx radiography. *Med Phys* 25(6): 986-997, 1998.
14. Dobbins JT III: Effect of undersampling on the proper interpretation of modulation transfer function, noise power spectra, and noise equivalent quanta of digital imaging systems. *Med Phys* 22(2): 171-181, 1995.
15. Hillen W, Schiebel U, and Zaengel T: Imaging performance of a digital storage phosphor system. *Med Phys* 14(5): 774-751, 1987.
16. Barrett HH and Swindell W: *Radiological Imaging: The Theory of Image formation, Detection, and Processing*. New York: Academic, 1981.
17. *Swissray AddOn Multi-System with Swiss Vision User Manual*. Swissray International Inc., 1997.
18. *Digital Imaging and Communications in Medicine (DICOM)*. National Electrical Manufacturers' Association. Rosslyn, VA: NEMA, 1996; PS 3.1-1996-3. 13-1996.
19. Gonzalez RC and Woods RE: *Digital Imaging Processing*. Reading, MA: Addison-Wesley, 1992.
20. Fujita H, Tsai DY, Itoh T, Doi K, Morishita et al.: A simple method for determining the modulation transfer function in digital radiography. *IEEE Trans Med Imag* 11(1): 34-39, 1992.
21. Samei E and Flynn MJ: A method for measuring the presampled MTF of digital radiographic systems using an edge test device. *Med Phys* 25(1): 102-113, 1998.
22. Lou SL, Sickles EA, Huang HK, et al.: Full field direct digital tele mammography: Technical components, study protocols, and preliminary results. *IEEE Trans Inform Technol Biomed* 1(4): 270-278, 1997.
23. Zhang J and Huang HK: Automatic background recognition and removal (ABRR) of computed radiography images. *IEEE Trans Med Imag* 16(6): 762-771, 1997.
24. Huang HK, Wong STC, and Pietka E: Medical image information infrastructure design and applications. *Med Informatics* 22(4): 279-289.



---

# A New Approach to Teleconferencing with Intravascular US and Cardiac Angiography in a Low-Bandwidth Environment<sup>1</sup>

---

*Johannes N. Stahl, MD • Jianguo Zhang, PhD • Chris Zellner, MD  
Eugene V. Pomerantsev, MD, PhD • Tony N. Chou, MD • H. K. Huang,  
DSc*

A common problem in radiology teleconferencing is the difficulty of transmitting a large volume of data over communication channels with a relatively low bandwidth. Although videoconferencing systems are easily implemented, they generally require lossy image compression, which can lead to significantly altered findings. A teleconsultation and teleconferencing system was developed that uses a store-and-forward approach with high-quality dynamic medical images obtained with intravascular ultrasonography and cardiac angiography. The system allows use of high-resolution dynamic images while preserving their original quality and can be adapted to different clinical applications with varying requirements. The system involves a standard preparation procedure to transmit images from one location to another prior to a conference; once the conference starts, however, the system becomes fully automatic and synchronizes the display and manipulation of images in both locations without further image data transmission. In general radiologic applications, the system is superior to videoconferencing systems in that it does not require specialized hardware and dedicated high-bandwidth communication links. Further investigation with large-scale studies will be required to determine whether these benefits can lead to more widespread acceptance of such a system in routine clinical practice and whether teleconferencing itself can enhance the effectiveness of clinical procedures.

---

Abbreviations: DICOM = Digital Imaging and Communications in Medicine, LAN = local area network, LCD = liquid crystal display, MPEG = Moving Picture Expert Group, PC = personal computer, VHS = Video Home System

Index terms: Computers • Computers, diagnostic aid • Computers, multimedia • Digital imaging and communications in medicine (DICOM) Radiology and radiologists, design of radiological facilities • Teleradiology

RadioGraphics 2000; 20:1495-1503

<sup>1</sup>From the Laboratory for Radiological Informatics, Department of Radiology (J.N.S., J.Z., H.K.H.), and the Cardiology Division, Department of Medicine (C.Z., T.N.C.), University of California, San Francisco; and the Department of Cardiology, Stanford University Medical Center, Stanford, Calif (E.V.P.). Recipient of a Cum Laude award for an infoRAD exhibit at the 1998 RSNA scientific assembly. Received August 17, 1999; revision requested September 20 and received January 10, 2000; accepted January 21. Supported in part by the National Library of Medicine and the Deutsche Forschungsgemeinschaft. Address correspondence to J.N.S., Radiologische Klinik, Abt Radiodiagnostik, Universitätsklinikum, Geb 49, 66421 Homburg/Saar, Germany (e-mail: [jnstahl@yahoo.com](mailto:jnstahl@yahoo.com)).

---

## Introduction

The American College of Radiology broadly defines the term *teleradiology* as "the transmission of radiological images from one location to another for the purpose of interpretation and/or consultation" (1). In this article, we use the term *teleconsultation* to describe a process during which two or more physicians hold a consultation regarding doubtful or problematic cases over a certain distance by means of telecommunication. Teleconsultation consists of two components: the exchange of multimedia documents (eg, images, video, text) and the interactive verbal and graphical discussion of the related findings and their consequences. In addition, we use the term *teleconferencing* to describe a consultation in which both parties present cases as peers, in contrast to the asymmetric physician-consultant relationship usually seen in consultation. The system described in this article was originally designed for teleconsultation but has been extended to include teleconferencing.

We use the term *dynamic images* to describe a sequence of images displayed in rapid succession so that the human eye perceives continuous motion. The most commonly used dynamic imaging modalities in radiology are ultrasonography (US) and angiography. We prefer the term *dynamic images* to the term *video* because the latter is very closely associated with the analog video format used in television and videocassette recording equipment. Dynamic angiographic images, for example, are not necessarily compatible with this format.

Conferences and consultations are a natural part of clinical practice. For consultations requiring the presentation of materials to a specialist in a more or less distant location, it has been traditional to use regular mail or couriers or to travel to the conference in person. Teleconferencing and teleconsultation might help reduce the time and cost associated with these procedures. However, although teleconferencing and teleradiology systems have been available for a number of years, they are still not as widely accepted by general radiologists for high-quality dynamic imaging as was anticipated at their inception.

A common problem in radiology teleconferencing is that a large amount of data must be transmitted, but the available communication channels have a relatively low bandwidth. At

present, increasing the bandwidth (eg, using an asynchronous transfer mode network) is often not an option due to high costs and limited availability of high-bandwidth connections. Two basic strategies exist to avoid this bottleneck. If the images need to be transmitted in or near real time, image compression—possibly resulting in a loss in quality—must be applied. If a time interval between image transmission and display is acceptable (eg, if the conference is scheduled to take place after the examination), the images can be transmitted in advance (eg, overnight) without compression. This procedure is often referred to as store-and-forward teleradiology.

For static radiologic images, store-and-forward teleradiology is a well-established method. For dynamic images, most solutions published to date have used real-time transmission by means of videoconferencing systems, which digitize analog video signals and send them digitally over the network. These systems are easy to set up and use; however, they invariably require lossy image compression, unless costly high-bandwidth networks such as asynchronous transfer mode are used. This compression can result in significant alteration of the findings (2). Concerns about compromised image quality might be one of the reasons why teleconferencing with dynamic images is not yet widely accepted for clinical procedures.

In this article, we present a prototypical system for store-and-forward teleconferencing with dynamic medical images. We outline implementation details, present preliminary clinical experience, and discuss the advantages and disadvantages of such a system.

## Background and Objectives

The authors' institutions operate two major academic medical centers 30 miles apart. Cardiologists in both centers use intravascular US, a relatively new imaging technique for the planning and assessment of coronary intervention (3). As part of a cooperative effort, educational conferences involving participants from both centers are held on an irregular basis. During these conferences, both sides present recent interventional cases studied with intravascular US and cardiac angiography and discuss possible strategies, interpretations, and outcomes.

Thus far, these conferences have been held using conventional methods. Cardiologists travel the 30 miles between the centers by car and

---

transport the materials on Video Home System (VHS) tapes and 35-mm celluloid film. Our goal was to develop a high-quality teleconferencing system that would not only reduce travel time and facilitate the conferencing process but also allow a level of quality and interactivity similar to that possible with conventional methods. Initially, the installation of a videoconferencing system was discussed. However, it became evident during these discussions that the image quality requested by the cardiologists could not be achieved with the available network bandwidth (two T1 lines [1.5 Mbits/sec each]).

As we looked for alternative solutions, it became obvious that a store-and-forward solution would be ideal because the schedule of planned conferences allowed sufficient time between image acquisition and the conference. Because we could not locate a system for store-and-forward teleconferencing with dynamic images, we decided to design our own system based on an existing teleconsultation system for static radiologic images (4).

## Materials and Methods

### Images

We used images obtained with two modalities: cardiac angiography and intravascular US. The intravascular US studies were always recorded on S-VHS videotape in National Television System Committee format. The cardiac angiography studies were recorded digitally in the Digital Imaging and Communications in Medicine (DICOM) format (5) (512 × 512 pixels, 8-bit gray scale, lossless compression). DICOM-compatible cardiac angiography studies were stored on recordable compact disks or could be retrieved electronically through a local area network (LAN).

For materials to be used in a digital conferencing system, they must be available in digital format. Although the DICOM cardiac angiography studies were already recorded digitally, we had to convert the analogous intravascular US sequences. The video signal was digitized and compressed into Moving Picture Expert Group (MPEG)-1 format (352 × 240 pixels, 24-bit color, lossy compression) (6) using a personal computer (PC) with a video digitizer board (Data Translation, Marlboro, Mass).

### Hardware and Network Architecture

The conferencing system consists of two PCs with Intel Pentium II 400-MHz processors, 128 Mbytes of RAM, and 10 Gbytes of disk storage (Dell, Round Rock, Tex). The system at one location is equipped with a liquid crystal display (LCD) projector (1,024 × 768 pixels) (Proxima, San Diego, Calif), whereas the system at the other location includes a regular 21-inch cathode ray tube monitor for viewing. Both systems are equipped with Matrox Millennium II graphic adapters (Matrox Graphics, Toronto, Ontario, Canada) that provide real-time video scaling functions. For fast, lossless decompression of DICOM images, we used a commercial high-performance decompression library (Pegasus Imaging, Tampa, Fla).

The conferencing systems are installed in the conference rooms of the two cardiology departments. The systems are connected to the LAN (100 Mbits/sec) of their institutions, which are linked by two T1 lines (1.5 Mbits/sec each). The LAN also provides a connection to the DICOM catheterization laboratories and to the PC used for image digitization. For voice communication, we simply use a standard conference telephone equipped with a speaker. Digital voice-over-Internet solutions that we tested as possible alternatives were difficult to configure and provided inferior sound quality.

### Software Architecture

A large number of technologies and software products are available for displaying dynamic images. With regard to medical images, these products may be regarded as either general-purpose or specialized. General-purpose video software can display a large variety of digital video formats (eg, MPEG, AVI [Microsoft, Redmond, Wash], QuickTime [Apple Computer, Cupertino, Calif]) (6). In contrast, specialized medical viewers with enhanced functionality are available for DICOM images. Architectural differences between the two groups make it difficult to integrate them in a single application.

For our project, however, it was desirable to use a single display architecture that could be used for both general-purpose video and DICOM multiframe images. Because the DICOM format is relatively simple compared with advanced digital video formats, we decided to start with a general-purpose video tool kit and then add DICOM support, rather than vice versa.

Because our system was designed for the Windows NT platform (Microsoft), we used the Microsoft DirectShow technology. DirectShow is a general-purpose multimedia tool kit that uses a filter graph model to build various kinds of multimedia applications (7). We found DirectShow to be ideally suited for our purpose because (a) it utilizes PC hardware resources very well and provides high-quality images, (b) it supports a large number of common video formats and can easily be extended for specialized medical formats (eg, DICOM), and (c) it provides a high level of control over the playback process (eg, frame-accurate positioning, slow motion, zooming/panning).

We added the dynamic image capability to the teleconsultation system described earlier. This system provides basic teleradiology services such as store-and-forward file transmission and a remote control component with real-time dual cursor functionality that are compatible with the dynamic image component. The system uses the DICOM protocol for image transmission. We implemented a private service-object-pair class that allows transmission of the MPEG video files, which are not DICOM-compatible.

The dynamic image component provides the user interface for the DirectShow pipeline (Fig 1). The pipeline is dynamically assembled from the available filters, depending on the type of media to be presented (Fig 2). This is transparent to the application, so that for the dynamic image component there is no difference between DICOM angiography and MPEG US. DICOM sequence files are handled within the DirectShow pipeline with a custom filter that we developed.

During the conference, the dynamic image component communicates with its counterpart at the remote site so that both can display the same image sequence in synchronicity. Start/pause commands, display parameters, playback speed, and sequence position are transmitted over the network and used to generate the same output on

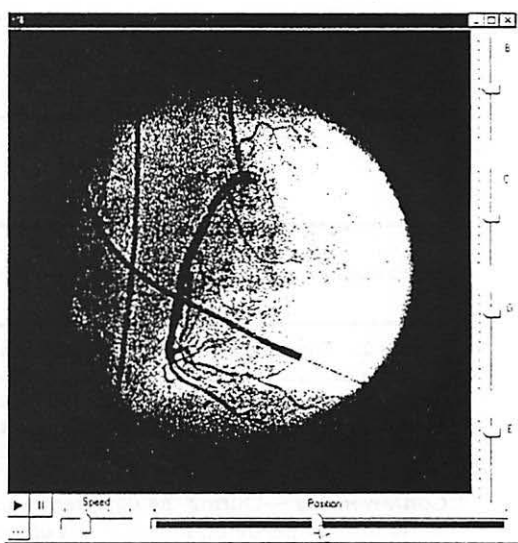


**Figure 1.** User interface for the DirectShow pipeline. The controls include play/pause (buttons in lower left-hand corner), playback speed, sequence position, brightness (B), contrast (C), gamma correction (D), and edge enhancement (E).

both computers. This works in both directions, so that either side can assume control at any time.

The software package can be set up and configured on any PC within minutes if sufficient hardware resources are available.

### Teleconferencing Procedure

The teleconferencing procedure consists of three phases: data preparation, data transmission, and conferencing.

**Data Preparation.**—DICOM sequences are transmitted over the LAN to the teleconferencing workstation, and analog videotapes are digitized. Because digitization of analog materials relies on time-consuming manual operation, DICOM-compatible modalities are to be preferred because they greatly simplify and automate the process.

**Data Transmission.**—Prior to the conference, the necessary documents are exchanged between the two locations over the wide area network. This process may take a considerable amount of time depending on the available network bandwidth; however, it is fully automated in unattended mode and may, for example, be performed overnight. The selection of materials and the start of transmission are achieved in a matter of minutes. At the end of the data transmission phase, the workstations in both locations possess identical copies of the images from the two hospitals

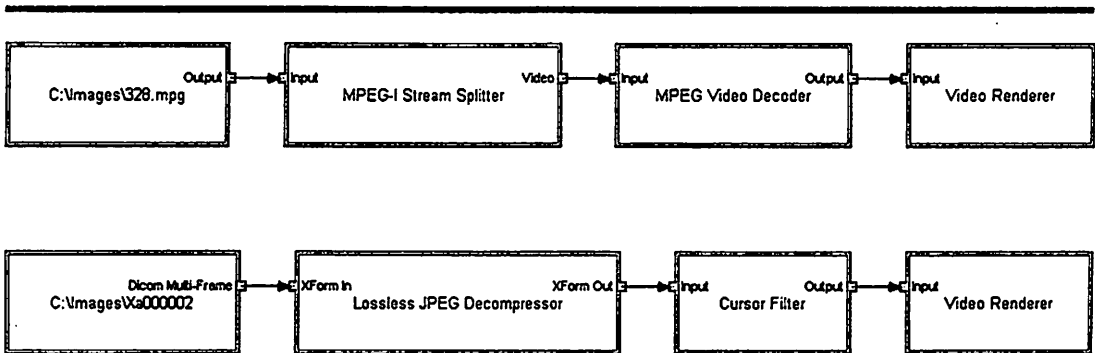


Figure 2. DirectShow pipelines. The filter graph for MPEG-encoded video sequences (top) consists of an MPEG splitter, a decoder filter, and a video renderer (Microsoft). The filter graph for the DICOM angiography files (bottom) includes the DICOM multiframe filter and the JPEG decompressor filter provided by the authors as well as another custom filter (cursor filter), which embeds the remote pointer into the video data.

**Conferencing.**—During the conference, the workstations operate on identical sets of locally stored image data so that only the control information has to be exchanged. Thus, the bandwidth requirements during the conference are very low. Even a dial-up modem (33.6 Kbits/sec) would be sufficient to maintain real-time communication.

It is assumed that during a conference session, the time available for image presentation is very limited. Therefore, it is necessary to spend some time in preparation to ensure that all images and image sequences are immediately available at the time of the conference. This is very similar to preparation for traditional clinical conferences, during which all needed materials are to be collected. The preparation time required with our system is comparable to that required for a conventional conference.

## Results

### Laboratory Results

We performed a number of laboratory tests to objectively assess image quality and system performance. For the DICOM images, we subjectively compared the image quality produced with the teleconferencing system with that produced with the commercial DICOM viewing software running on the same computer. As expected, there was no noticeable difference in image quality because the DICOM images are lossless compressed. However, there was quality degradation between the DICOM images and the origi-

nal images because the modality scans the images at  $1,024 \times 1,024$  resolution and subsamples to  $512 \times 512$  resolution for export to DICOM. This is a limitation of the DICOM interchange format rather than the teleconferencing system.

The MPEG video sequences were compared side by side with the original S-VHS tapes played on a professional videocassette recorder. There was noticeable quality degradation caused by reduction of resolution from about  $800 \times 420$  to  $352 \times 240$  and compression-induced artifacts. However, because the spatial resolution of the intravascular US technique itself is rather poor, the cardiologists found that the visibility of anatomic details and pathologic findings such as calcification and soft plaque was still adequate for conferencing purposes. We did not verify these results with a formal quality evaluation because they are consistent with the results from other studies that compared MPEG-1 with S-VHS for echocardiography and found major discrepancies in only 2.7% of cases (8).

The frame rate for the MPEG-1 video was 29.97 frames/sec, which was identical to that for the original sequence. For the DICOM images, we could match the 30-frames/sec frame rate of the original sequence only when the optional image edge-enhancement algorithm was deactivated. With active edge-enhancement, the maximum frame rate was 22 frames/sec, which could

---

be compensated for either by playing the sequence at two-thirds speed or by skipping every third frame. We expect that the new generation of 550-MHz processors has sufficient processing power to perform edge-enhancement at full frame rate.

However, the synchronization mechanism is independent of central processing unit clock speed and frame rate because absolute positions (expressed in milliseconds from start of sequence) are used for positioning and synchronization. In the laboratory test, the difference in synchronization between the two systems connected through a LAN was less than 300 msec, even if the systems had different clock speeds (266 MHz vs 400 MHz). For wide area connections, the difference in synchronization could not be measured exactly due to lack of an absolute reference time source. However, subjective tests did not reveal a noticeable difference. The new global positioning system absolute reference time system (Advanced Network & Services, Armonk, NY) being installed in our laboratory will allow more precise measurements.

## Clinical Results

**Local Conferences.**—We documented 12 clinical conferences in “local mode” at one institution to subjectively assess image quality and performance under clinical conditions. In the local conferences, we found that overall the system fulfills the requirements of clinical conferencing: high image quality, ease of use, and fast operation. Some modifications, such as the addition of gamma correction and edge-enhancement filters, were necessary to improve the quality of the images displayed with the LCD projector. Direct comparisons between the LCD projector and a high-quality cathode ray tube monitor revealed that the latter provided superior contrast and gray-scale resolution. However, the LCD projector provided a larger viewing angle of the projected image for a relatively large audience of eight to 12 physicians.

Regarding ease of use, the main criterion was whether there were significant delays during the conference that could be attributed to the operation of the conferencing system. Initial handling and reliability problems could be resolved with

improvements in the software. With the updated software, efficiency was superior to that of conventional equipment (videocassette recorder and 35-mm film projector) because the need to change film rolls and tape cassettes was eliminated.

Regarding performance, we found that one of the requirements during conferencing was the ability to display the angiographic series in a DICOM cardiac angiography study (typically 10–15 series) in very rapid succession. With our system, one can switch to the next series in a study by pressing a single button, with playback starting immediately. This mode of operation obviates prefetching of the series from the computer's hard disk into main memory, which would increase the possible frame rate but would also increase the time until playback could be started. For this reason, we found that high-speed image processing algorithms and high-performance PCs are necessary for efficient clinical conferencing.

We also found that up to 2 hours is required to prepare for a conference, depending on the number of analog studies that require digitization. The automatic transmission of DICOM digital angiograms over the LAN took about 1 hour for six to eight patients (about 15 angiographic sequences [300 Mbytes of image data] per patient) but could be performed without user intervention. Including the digitized intravascular US studies, the amount of data per patient was typically 400 Mbytes. The total amount of data required for a single conference averaged 3 Gbytes. Up to 4 hours was required to transmit the materials over the dual T1 connection between the two hospitals, also without user intervention. This is more time than what would be expected with a 3-Mbits/sec connection, because the lines are shared with other campus users. Overall, we found it reasonable to plan a teleconference at least 24 hours in advance, whereas a local conference could be set up in less than 3 hours. The Table shows a comparison of the time requirements for classical conferencing versus teleconferencing.

**Teleconferences.**—We performed eight teleconferences between the two medical centers. The most important finding was that communication was possible and effective, not only in a technical sense but also in terms of human interaction. At

**Time Requirements for Classical Conferencing versus Teleconferencing**

Phase	Classical Conference		Teleconference		Future Teleconference (anticipated)	
	Time Required	Task	Time Required	Task	Time Required	Task
Data preparation	1 h	Collect films, copy videotapes	2 h	Collect and digitize films and videotapes	10 min	Retrieve DICOM sequences from archive
Data transmission	1 h	Drive car to conference	4 h	Transmit images over network (unattended)	15 min*	Transmit images over high-speed network
Conference	1 h	Discuss cases	1 h	Discuss cases	1 h	Discuss cases
Cleanup	1 h	Return by car	1 min	Delete files	1 min	Delete files

\*Assumes availability of the proposed Next-Generation Internet.

both centers, the system was operated primarily by a cardiologist who was trained to use the system. The other team members presented pertinent clinical information over the speaker-equipped telephone and used the remote mouse cursor to point out interesting findings or create image annotations.

Our evaluation criteria for the teleconference were (a) whether all of the six to eight scheduled cases could be discussed within the time allotted for the conference, and (b) whether significant communication problems (eg, misunderstandings, need to repeat sentences, need to replay images) occurred. Surprisingly, the system evaluated positively for both criteria, even for the first teleconference. A possible explanation is that, according to our observations, the physicians focused their attention mostly on the images, even when talking to each other during the traditional conferences. Therefore, they could adapt relatively easily to the fact that their communication partners were only virtually present in the teleconferences.

The cardiologists could easily subjectively reconstruct the descriptions and provide meaningful input regarding the presented cases. The conversations and discussions about the cases were very natural.

### Discussion

The combination of off-line transmission of dynamic images and real-time synchronized playback offers a number of advantages over videoconferencing with real-time video transmission.

First and most important, the store-and-forward technology allows use of high-resolution dynamic images with their original quality preserved, whereas videoconferencing systems allow use of only low-quality compressed images due to bandwidth limitations. In many clinical applications similar to cardiology conferencing, low image quality is not acceptable, and teleconferencing would not be possible with a videoconferencing system.

Second, the DirectShow technology allows our system to use many different digital video formats, with images varying from original quality (DICOM) to low quality (highly compressed) (MPEG, AVI [Microsoft]). Thus, with this system it is possible to balance image quality, transmission time delay, and bandwidth requirements for optimal cost-effectiveness. Figure 3 shows the relationship between these three parameters. No conferencing system can be optimal in more than two parameters. A fast, high-quality system will

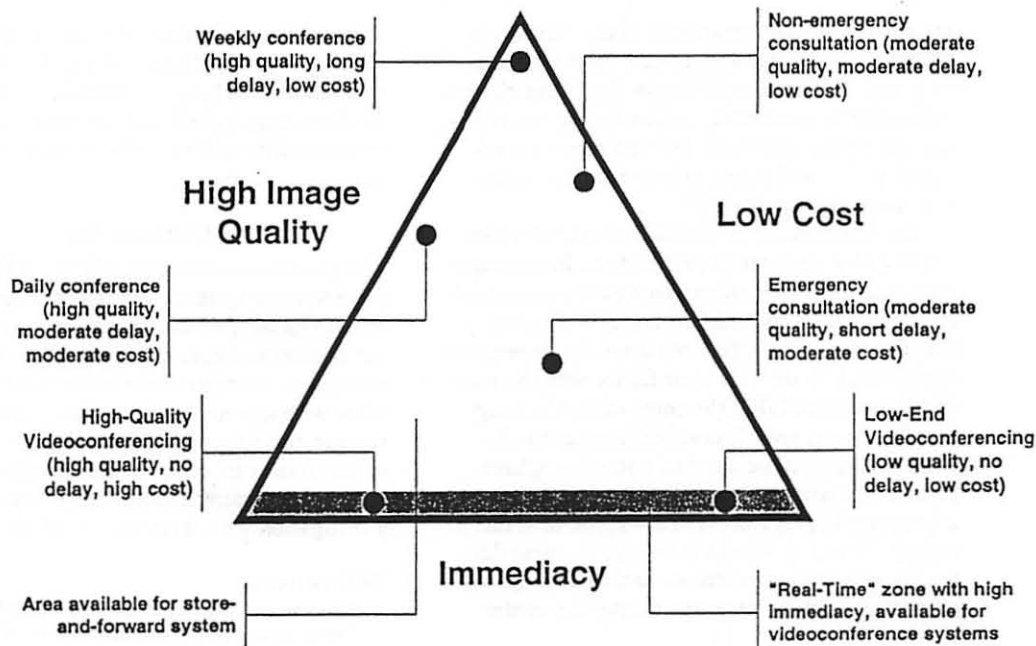


Figure 3. Relationship between image quality, immediacy, and cost-effectiveness. A location close to the edge of the triangle represents a high value for the corresponding parameter. With real-time videoconferencing, the transmission delay is near zero by definition and immediacy is high (gray area). Thus, improving image quality means higher costs owing to increased bandwidth requirements. By allowing a variable delay, a store-and-forward system can use the entire range of combinations (white area) to find the best compromise between the three factors depending on clinical requirements.

be costly, whereas a low-cost system will be either slow or low-quality. Because a real-time videoconference is fast by definition, any improvement in quality will result in higher costs owing to increased bandwidth. With store-and-forward technology, transmission delay becomes the third variable in the equation. For example, increasing the delay between acquisition and conferencing can improve image quality without affecting the cost of the system. The system can therefore be adapted to different clinical applications with varying requirements (Fig 3).

Third, a dynamic sequence is usually very short but will be reviewed several times during a conference. Our system will transmit the image data only once but can play the data back many times. In contrast, a videoconferencing system does not store the video once it is displayed; it must retransmit the entire sequence for each replay, effectively wasting bandwidth.

Fourth, our consultation system allows parties at both sites to control the playback process (eg, pause, replay, zoom, look-up table adjustment). This allows true interactive discussion of the findings. A videoconferencing system allows only one-way communication, with one site passively receiving the images transmitted by the other.

There are, of course, possible drawbacks to the system. Certain clinical applications can be implemented only with real-time transmission of dynamic images. For example, remote monitoring of examinations in progress or assistance during interventional procedures requires immediate feedback from the remote party. In this particular clinical application, the dynamic images can be transmitted directly to our system with DICOM, thus bypassing the data preparation phase for immediate consultation. Depending on the bandwidth, the delay required for this transmission can be as short as a few seconds; unlike with a videoconferencing system, however, it cannot approach zero. Whether this is acceptable depends

entirely on the circumstances of the clinical application. From our experience, most consultation and conferencing will take place after the examination is completed, in which case the delay created by the store-and-forward process is acceptable and will result in better image quality and increased interactivity.

Another possible problem involves the effort required for conference preparation. In our experience, most of this effort involved digitization of the analog intravascular US tapes. We expect that the amount of effort required can be reduced significantly in the very near future with the transition to digital, DICOM-compatible US imagers. Of course, any clinical conference that involves several physicians and patients requires some preparation effort (eg, collecting and sorting materials), regardless of the mode of conferencing. The goal should always be to streamline the presentation of materials so that time spent in preparation can be regained during the conference.

Our system can support a number of practical conferencing applications. For example, in cardiology it is common practice for patients with coronary artery disease to undergo cardiac catheterization in community hospitals or imaging centers. Some of these patients may be eligible for cardiac surgery, which can be performed in specialized heart surgery centers. Because this is usually elective surgery, consultations between cardiologists and cardiac surgeons are routinely held to determine therapeutic strategy (ie, conservative, interventional, surgical). Traditionally, this is done either by traveling to a conference or by mailing the images. In this setting, teleconferencing could be used to save travel time or increase interactivity while preserving diagnostic image quality.

In radiology, similar consultations are being held between general radiologists and their counterparts at specialized interventional centers (eg, for embolizations). Typically, these consultations are less frequent than those related to cardiology due to the lower prevalence of the diseases in question. In this setting, our teleconferencing system has an additional advantage over videoconferencing systems in that it does not require specialized hardware and dedicated high-bandwidth communication links.

In both applications, the topics of discussion are elective procedures that need to be performed in a specialized hospital. Store-and-forward teleconferencing is ideal in these situations because image quality and ease of use are more important than immediacy.

## Conclusions

Compared with commercially available videoconferencing systems, the teleconferencing system we developed can significantly improve image quality and ease of use for certain clinical applications. Whether these benefits can lead to more widespread acceptance of such a system in routine clinical practice and whether teleconferencing itself can enhance the effectiveness of clinical procedures must be the subject of further investigation with large-scale studies.

## References

1. American College of Radiology. ACR Standard for Teleradiology: ACR Standards, Res 35, 1998. Retrieved May 12, 1999 from the World Wide Web: [http://www.acr.org/departments/stand\\_accrd/standards/pdf\\_standards/diag/telerad.pdf](http://www.acr.org/departments/stand_accrd/standards/pdf_standards/diag/telerad.pdf)
2. Tobis J, Aharonian V, Mansukhani P. Video networking of cardiac catheterization laboratories. *Am Heart J* 1999; 137:241-249.
3. Gorge G, Ge J, Erbel R. Role of intravascular ultrasound in the evaluation of mechanisms of coronary interventions and restenosis. *Am J Cardiol* 1998; 81:91G-95G.
4. Zhang J, Stahl JN, Song KS, Huang HK. Real-time teleconsultation with high resolution and large volume medical imaging. In: Horii SC, Blaine GJ, eds. *Medical imaging*. San Diego, Calif: SPIE, 1998; 185-190.
5. ACR/NEMA. *Digital Imaging and Communications in Medicine (DICOM): version 3.0*. Washington, DC: ACR/NEMA Standards Publication, 1993.
6. Boudier T, Shotton DM. Video on the Internet: an introduction to the digital encoding, compression, and transmission of moving image data. *J Struct Biol* 1999; 125:133-155.
7. Chatterjee A, Maltz A. Microsoft DirectShow: a new media architecture. *J Soc Motion Pict Televis Eng* 1997; 106:865-871.
8. Soble JS, Yurow G, Brar R. Comparison of MPEG digital video with super VHS tape for diagnostic echocardiographic readings. *J Am Soc Echocardiogr* 1998; 11:819-825.

# Digital hand atlas and web-based bone age assessment: system design and implementation

F. Cao<sup>a,\*</sup>, H.K. Huang<sup>a</sup>, E. Pietka<sup>b</sup>, V. Gilsanz<sup>c</sup>

<sup>a</sup>Department of Radiology, University of California, San Francisco, CA 94143-0628, USA

<sup>b</sup>Department of Nuclear Medicine, Medical University of Silesia, PL-40 752 Katowice, Poland

<sup>c</sup>Department of Radiology, Children's Hospital Los Angeles, Los Angeles, CA, USA

Received 1 November 1999; accepted 14 February 2000

---

## Abstract

Bone age assessment is a procedure frequently performed in pediatric patients to evaluate their growth disorder. A simple method commonly used in bone age assessment is atlas matching by a radiological examination of a left-hand radiograph against a small reference set of Greulich–Pyle atlas patterns of normal standards. The method however can lead to significant deviation in age assessment, due to a variety of observers with different levels of training. The Greulich–Pyle atlas developed in the 1950s based on middle upper class white populations, is also not fully applicable for children of today, especially regarding the standard development in other racial groups.

In this paper, we present our system design and initial implementation of a digital hand atlas and computer-aided diagnostic (CAD) system for Web-based bone age assessment. The CAD system is built on top of existing picture archiving and communication system (PACS), as well as recent advances in Internet technology. It consists of a hand atlas database, a CAD module and a Java-based Web user interface. The digital atlas is based on a large new set of clinically normal hand images of diverse ethnic groups. A relational image database system is used to organize hand images, their extracted quantitative features and patient data. The digital atlas removes the disadvantages of the currently out-of-date Greulich–Pyle atlas and allows the bone age assessment to be computerized. The Java-based Web user interface allows users to interact with the hand image database from browsers. Users can use a Web browser to push a clinical hand image to the CAD server for a bone age assessment. Quantitative features on the examined image, which reflect the skeletal maturity, are then extracted and compared with patterns from the atlas database to assess the bone age. The digital atlas method based on open system Internet technology provides an alternative to supplement or replace the traditional one for a quantitative, accurate and cost-effective assessment of bone age. © 2000 Published by Elsevier Science Ltd.

**Keywords:** Digital hand atlas; Web; Pediatric radiology; Skeletal age assessment; Computers

---

## 1. Introduction

Bone age or skeletal age assessment is a procedure performed in pediatric patients to evaluate their growth disorder, determine their growth potential, and monitor the therapy effects of growth. The growth potential of an individual depends largely on the progression of ossification within the epiphysis. Bone age is a measurement of the epiphyseal center development. It is an important procedure in the diagnosis and management of endocrine disorders, diagnostic evaluation of metabolic and growth abnormalities, deceleration of maturation in a variety of syndromes, malformations, and bone dysplasias.

A simple method frequently used in bone age assessment is atlas matching by a radiological examination of a left

hand and wrist radiograph against a reference set of atlas patterns of normal standards. Although the hand and wrist does not contribute to the height of an individual, the radiograph of this part of the body has been proven valuable and is commonly used in assessment of bone age. The reference set of patterns currently used extensively is Greulich and Pyle [1] atlas that includes one hand image pattern per year of age. The pattern in the atlas, which appears to resemble the clinical image, is selected. Since each pattern in the atlas represents a certain year of age for a normal child, the selection assigns the patient's bone age. The difference between the assessed bone age and the chronological age indicates abnormalities in patient's skeletal development.

The hand atlas matching method is universally used due to the advantages of simplicity, minimal radiation exposure and the availability of multiple ossification centers for evaluation of maturity. The method, however, is mostly qualitative and not accurate. It is liable to deviations by

---

\* Corresponding author. Tel.: +1-323-671-3848; fax: +1-323-671-1588.

E-mail address: fcao@pacbell.net (F. Cao).

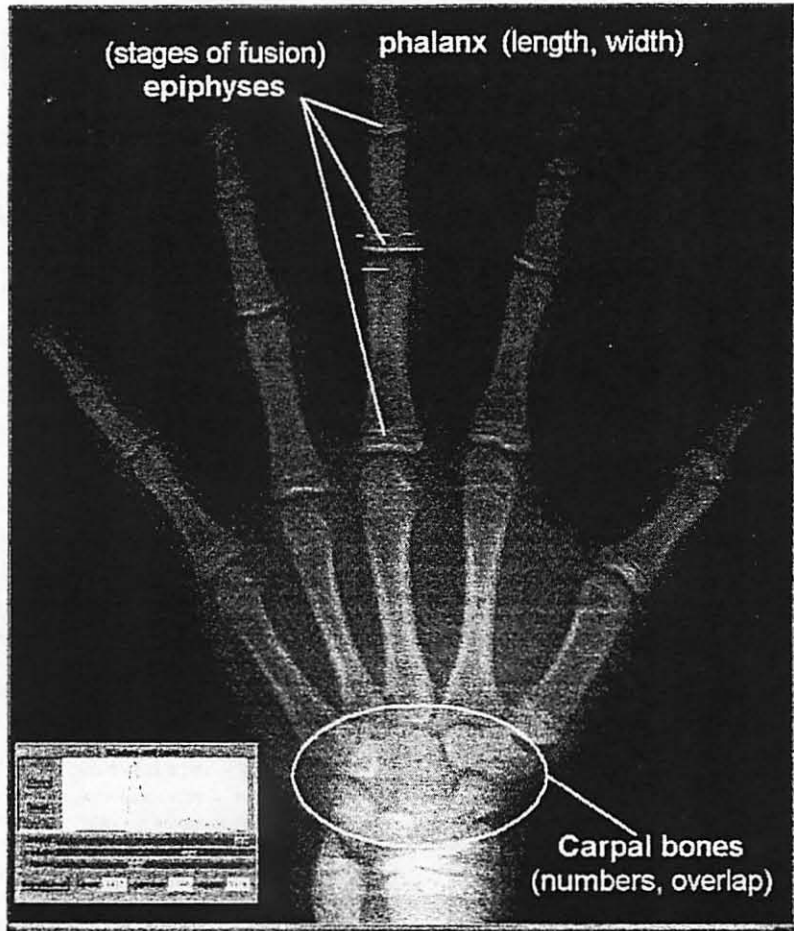


Fig. 1. Region of interests and parameters used in bony feature extraction and bone age assessment. This is a screen shot from the image display window. The small window in the lower-left corner shows a histogram and provides a user with a manual window-level-gamma adjustment.

subjective nature of various observers. Furthermore, the atlas itself, which was developed by Greulich and Pyle [1] in 1950s based on middle class white populations, is not fully applicable for today's children especially regarding the standard development in other racial groups [2–4].

Many efforts have been made to increase the accuracy of the bone age assessment and to overcome the ethnic and racial differences in skeletal maturation. The Tanner and Whitehouse [5] (TW2) method is based on assigning an individual score to several bones in the hand and wrist, and then obtaining the bone age by the total score. Schmid and Moll [6] developed standards for the German population, Eklof and Ringertz [7] devised a method for evaluation of maturation based on the bone length and width of the Scandinavian people, and Sugiura [8] has published standards for both sexes for Japanese children.

The computer-aided methods have also been under development to quantify radiological findings that may support the bone age assessment [9,10]. The Tanner–Whitehouse (TW2) scoring method has been computerized by perform-

ing the Fourier transform on radiographs digitized by a video camera [11]. The method is quite tedious and time consuming to perform. Pietka and Huang [12] started seven years ago a computer-assisted analysis in bone age assessment and have since then conducted a series of studies on bony feature extraction by image processing [13–16]. They first identify the regions of interest (ROI) that are the most significant in bone age assessment, i.e. the phalanx, epiphyses and carpal bone areas as marked in Fig. 1, and then apply variety of image processing techniques to extract the quantitative features associated with these ROIs. These computer-extracted parameters are associated with race, age, sex and Tanner maturity index [17], providing a valuable means of quantitative measurements that form the basis for computer-assisted bone age assessment.

The greatest impact of a more accurate, objective, and reproducible technique for assessing skeletal maturity would be in refining the treatment for certain endocrine and musculoskeletal diseases. The evaluation of the response to growth hormone, for example, is particularly

imprecise. A computerized analysis of a patient being studied on multiple occasions during therapy could simultaneously provide a determination of bone age and a detailed report of the changes from one study to another. In patients evaluated for surgery to correct scoliosis or leg-length discrepancy, inaccuracies in bone age determination can lead to mistakes in the timing of the surgery. Scoliosis does not usually progress after the patient is skeletally mature; a misdiagnosed bone age determination can lead to unnecessary surgery if the bone age is underestimated, or premature intervention if the bone age is overestimated. In the case of leg-length discrepancies, incorrect timing of corrective surgery can result in insufficient or excessive therapy, both of which can result in deformity and disability.

We have been in a process of constructing a digital hand atlas since 1997. The digital hand atlas built on a hospital-integrated picture archiving and communication system (PACS) can overcome the shortcomings of the traditional atlas. Building a current and clinically useful atlas is a tedious process. Large set of images along with all relevant patient data have to be accumulated over the years, constantly maintained and replenished with new materials. It is possible to do that only when the atlas is built under the PACS environment [18,19] and integrated with the hand image acquisition machines such as CR (computer radiograph), in which digital images and relevant patient data can be easily selected and incorporated into the atlas. The digital atlas manifests itself in an image database, consisting of a large set of 1120 high-resolution reference images with computer-extracted bone objects and quantitative features. It would grow over time, allowing a continuous accrual of normal standards and improving the assessment accuracy of bone age.

To make the digital atlas widely available to and easily accessible by clients, a thin-client distributing environment such as the Web is a preferred development and deployment platform that might otherwise be limited to only a few local workstations. The Web technologies have progressed from a static simple Web page to dynamic one including whose content is built on the fly when a user requests it. Major database vendors have also implemented the Web technology into their database products for interactive database query through Web. In other words, rather than loading the huge atlas database (about 10 Gbytes in size) and its software package on every client's machine, people will use common Web browsers to interact with the atlas. The Web browser will take care of most of the user-interface concerns and allow us instead to focus on the computer-assisted diagnosis (CAD) model of encoding work flow and linking of appropriate task-specific modules/tools on the server side. With the maturity of PACS technology and recent advances in open system Internet technology, we will be able to develop a large and sharable hand atlas as a clinical reference and use the Web as a delivering platform. Clients will use widely available Web browsers to browse the digital atlas, view the hand images and push

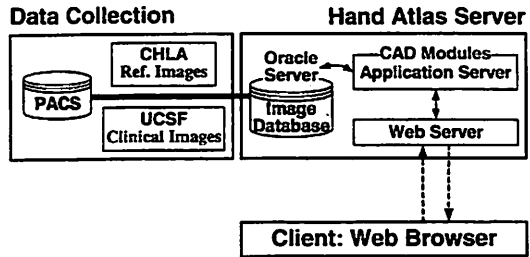


Fig. 2. System architecture (PACS, Picture Archive and Communication System; CHLA, Children's Hospital, Los Angeles; UCSF, University of California at San Francisco; CAD, Computer-aided Diagnosis).

clinical images to the web server for automatic bone age assessment.

In this paper, we present the system design and integration, a Web-based client-server model for computer-aided bone age assessment and our initial implementation of the digital atlas database.

## 2. System architecture for the digital hand atlas

Fig. 2 shows the system architecture and the building blocks for a digital hand atlas in a Web-based environment [20]. It includes the collection of hand images and their relevant patient data, the hand atlas database and server, and the Web interface. This architecture can also be described in the framework of CAD in a PACS environment [18,19]. PACS has evolved into a hospital-integrated information system with a voluminous amount of image and associated data in its database. Integrating of the CAD in a PACS environment can facilitate the usefulness of CAD in medical practice and take advantage of the already available resources in PACS, such as image storage, retrieval mechanism and communication network.

The digital atlas server is to extend clinical-oriented PACS for CAD purposes. The extension takes the form of the server hosted on a machine separated from PACS. It is important to build a separate server for handling the CAD modules so as not to impact the performance of PACS in its fulfillment of high-priority tasks of supporting day-to-day radiological services. The acquisition workstation and the database server are Digital Imaging and Communications in Medicine (DICOM) compliant. Both have been implemented [21] on the Sun SPARC Ultra-II platform. The hand image acquisition has been standardized as shown in Fig. 3. All hand images along with their relevant patient information are retrieved through the acquisition computer, automatically transferred to and stored in the RAID disks, and then inserted into our newly established atlas image database.

The digital atlas server, currently hosted on the Sun SPARC Ultra-II platform, uses a thin-client 3-tier architecture— atlas database, CAD application and Web servers. It allows open

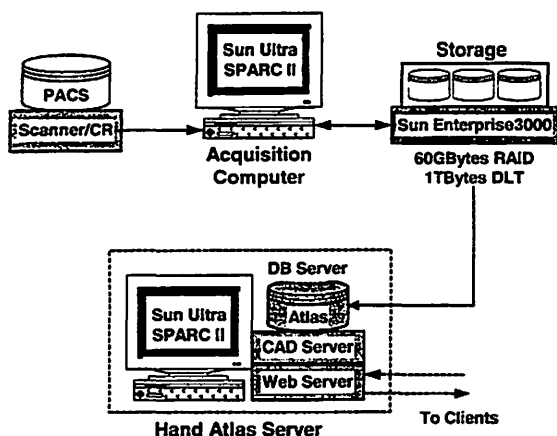


Fig. 3. System configuration of the atlas server and image acquisition workstations. The workstations use the Sun SPARC Ultra-II platform (Sun Microsystems, Mountain View, California) with one 200 MHz CPU and 128 Mbytes of memory, one 24 bits Creator video display board and 1280 × 1024 console monitor. The acquisition computer is used to acquire a hand and wrist image from PACS, computed radiography (CR) system or laser film scanner at UCSF and CHLA. A Fuji FCR-9000 (CR) systems is used for the full resolution CR images (2 × 2.5K × 10 bits), A 2 × 2.5K film scanner provided by Abe Sekkei Inc. (Tokyo, Japan) is used for film digitization with a 100 μm spot size and sampling distance, and 12 bits resolution. The digital hand images are stored permanently in a 60 Gbytes redundant array of inexpensive disks (RAID) and 1 Tbytes DLT (digital linear tape) library controlled by a Sun Ultra Enterprise 3000 server machine. The hand images and their relevant medical information are then sent to the atlas server machine and organized into an image database for a client's access via Web.

access from Web by clients running in Unix, PC or Macintosh. The digital hand atlas is an image database managed by Oracle relational database server. The Application Server acts as a platform for reusable logic, taking responsibility for application code that might otherwise reside at the client or the database server. It contains the image processing and CAD bone age assessment modules, bringing together the Web with the digital atlas database. It also provides other middleware functionality such as quality service (scalable, reliable, secure, and manageable), tight database integration, easy migration of legacy applications and reliable transactions for network clients.

### 3. Data collection

The first step in generating the atlas is to select left hand and wrist images either computed radiography (CR) or digitized film images, from healthy normal children. The normal reference images are categorized according to the ethnic origin and sex since these two factors have the most effect on bone growth. Based on our previous estimation [15], for pre-pubertal children 5 images for each group would be needed to detect a difference between manual and computer-assisted measurements of the distal, middle,

and proximal bones. Whereas, for children during puberty, 10 images at each group would be needed to detect a difference between manual and computer measurements. Consequently, 140 reference images are needed for each race-sex group from normal newborn to 18 years of age. Total of 1120 reference images (140 × 8 groups) is going to be collected from boys and girls of European, African, Hispanic, and Asian descent. As an example, Fig. 4 shows the database query result summarizing the currently collected reference images for the African American female group.

The information obtained from this data set would overcome the scarcity of studies assessing the differences between skeletal and chronological age in nonwhite children in this country, and will cover the entire range from birth to skeletal maturity. This is the only study, to our knowledge, that analyses the differences between skeletal and chronological age for children, of various ethnic backgrounds of the 1990s from birth to skeletal maturity.

As of today, over 500 normal hand images from newborn to 18 years have been selected at Children Hospital of Los Angeles (CHLA) by Dr Gilsanz. The reference hand images have been and will continue to be selected at CHLA by Dr Gilsanz. He and his colleagues recruit, interview, and examine the local children to obtain the left hand and wrist images, which are considered to be clinically normal and standard. All relevant patient information, including the chronological age, date of birth, date of examination, race, sex, height, weight, trunk height and Tanner maturity index have also been collected. The films (if not CR) are forwarded to and digitized at UCSF with a film scanner (Abe Sekkei Inc., Japan) to 100 μm sampling distance and 12 bits resolution. Both CR and digitized images are first assured of the quality and then transferred to the atlas server for computer-assisted bony feature extraction. The images along with their pertinent patient information and extracted bony objects will then be indexed into an image atlas database.

Meanwhile, the daily clinical bone age assessment cases, which use the traditional Greulich and Pyle method, are collected locally at UCSF. About 400 left-hand images along with relevant information from selected patients who came to the UCSF for clinical bone age assessment have been retrieved from the UCSF PACS/RIS systems. The bone age assessment cases at UCSF continue at a rate of 25 cases per month. This clinical data set will be used for checking and refinement of the digital hand atlas, comparing the conventional method with the digital atlas CAD method.

### 4. Atlas database development

The digital hand atlas is a medical image database currently managed by Oracle 8i data server (<http://www.oracle.com/database/oracle8i> Oracle Corporation, Redwood Shores, CA). Oracle 8i is the Oracle's newly released database specifically designed to manage the new medium

Hand Atlas Summary Report - Microsoft Internet Explorer

Address: http://boneage.h.ucsf.edu/Atlas/Report.html

Race:  Sex:  Run Report

Atlas Summary Reports

Click on the Group ID links to show the detailed patient info.

Race	Sex	Group ID	Age Grp	Age Avg (yr)	Tanner Avg	Height Avg (cm)	Weight Avg (kg)	Img Req	Img Num	Img Bad
BLK	F	<a href="#">BLKF00</a>	00	47	1.00	64.13	6.18	5	3	0
		<a href="#">BLKF01</a>	01	1.50	1.00	78.32	10.30	5	5	0
		<a href="#">BLKF02</a>	02	2.41	1.00	84.06	11.30	5	5	0
		<a href="#">BLKF03</a>	03	3.68	1.00	99.92	14.40	5	5	0
		<a href="#">BLKF04</a>	04	4.56	1.00	106.94	17.50	5	5	0
		<a href="#">BLKF05</a>	05	5.61	1.00	113.90	19.76	5	5	0
		<a href="#">BLKF06</a>	06	6.47	1.00	118.50	22.30	5	5	0
		<a href="#">BLKF07</a>	07	7.57	1.00	124.44	26.98	5	5	0
		<a href="#">BLKF08</a>	08	8.62	1.00	131.26	28.56	5	5	0
		<a href="#">BLKF09</a>	09	9.21	1.00	139.98	35.38	5	5	0
		<a href="#">BLKF10</a>	10	10.35	1.50	144.58	37.76	10	10	0
		<a href="#">BLKF11</a>	11	11.56	3.00	150.95	42.86	10	10	0
		<a href="#">BLKF12</a>	12	12.52	3.10	156.25	49.82	10	10	0
		<a href="#">BLKF13</a>	13	13.40	4.10	159.11	50.28	10	10	0
		<a href="#">BLKF14</a>	14	14.54	4.30	161.15	54.58	10	10	0
		<a href="#">BLKF15</a>	15	15.39	4.60	164.26	57.05	10	11	0
		<a href="#">BLKF16</a>	16	16.41	4.90	164.77	58.63	10	10	0
		<a href="#">BLKF17</a>	17	17.45	5.00	165.03	63.96	10	10	0
		<a href="#">BLKF18</a>	18	18.53	5.00	159.79	60.31	10	10	0
		sum						140	139	0
M		<a href="#">BLKM00</a>	00	69	1.00	69.66	8.70	5	4	0
		<a href="#">BLKM01</a>	01	1.48	1.00	81.65	12.13	5	4	0
		<a href="#">BLKM02</a>	02	2.55	1.00	88.76	13.70	5	5	0
		<a href="#">BLKM03</a>	03	3.32	1.00	98.92	15.50	5	5	0
		<a href="#">BLKM04</a>	04	4.74	1.00	107.60	18.63	5	6	0
		<a href="#">BLKM05</a>	05	5.81	1.00	120.62	23.00	5	5	0

Fig. 4. Screen shots from a Web browser, showing the query results from the Web-enabled hand image database. The columns show the group ID, race, sex, age group, average age and Tanner maturity index in the group, number of images required for each group in the atlas, and number of images currently available. The last row shows the total numbers of hand images required and currently collected.

of the Internet in addition to supporting traditional relational data. We have further extended and customized the Oracle 8i data server to manage medical image data, including high-resolution hand images, their bone objects and their relational dependencies. The data server will also support assessment of skeletal maturity in clinical diagnosis and research. One of the greatest barriers to medical information systems is the integration of all patient data—including images—into an intelligent image database [22]. New tools are required not only to store clinical information together with high-resolution images, but also to provide radiological findings describing the stage of skeletal development and use them together with clinical data for

the final assessment of the developmental stage of the patient.

Building a current and clinically useful hand atlas for various ethnic groups is a tedious process. Large standard set of normal hand images along with all relevant patient data have to be accumulated over the years, constantly maintained and replenished with new materials. It becomes possible and also cost-effective when the atlas is built under a PACS environment from which new images and relevant patient data can be easily selected and incorporated into the digital atlas to increase the statistical power of the CAD. In this case, when a pediatric patient comes in for hand X-ray examination and is determined as normal, then the image

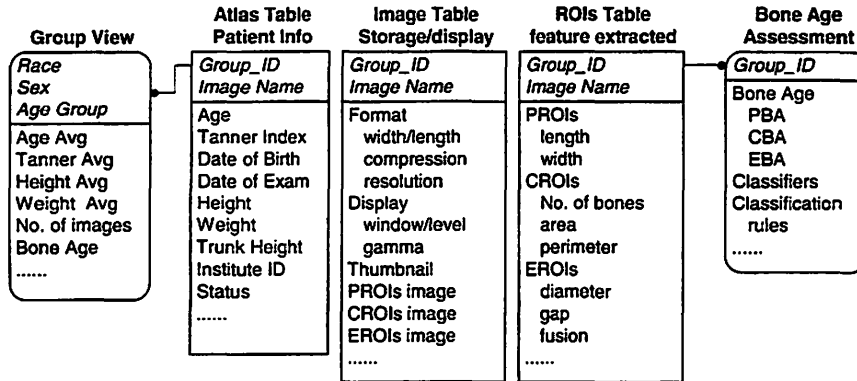


Fig. 5. Digital atlas database structure and object relationship. As marked in Fig. 1, PROI stands for phalangeal region of interest, CROI for carpal bones region of interest and EROI for epiphyseal region of interest. In the table of bone age assessment, PBA is phalangeal bone age derived from the extracted quantitative features in PROIs. CBA is carpal bone age based on CROIs and EBA is epiphyseal bone age based on EROIs.

and related data can be query/retrieved through the PACS database and downloaded to the digital hand atlas database.

The atlas database will provide an information infrastructure for clients to access, correlate, query, and organize all the patient hand and wrist radiographs. It is based not only on traditional medical records but also on hand image contents, such as bone objects extracted from phalangeal (PROI), carpal bone (CROI), and epiphyseal (EROI) regions of interest. It can access and manipulate regions of interest in images defined in object data model as a relation database system does for arbitrary portions of data defined in records and tables. Making the case for medical image databases must also require addressing it as a long-term system, not a one-shot event. Thus, the atlas database development and management will provide:

- Integration of image data and radiological finding with the traditional texture-based database.
- Structural objects of image segments representing the regions of interest in a hand image.
- Relationships among medical records and verity of bone objects.
- Feasible way of classification, to map the bone objects to bone age.
- Modular implementation, to allow a modified (extended) structure of data record to be built on and to complement what already exists so that the database developed is a dynamic process. Additional normal hand images can be appended to increase the sample size and new discriminatory features can be introduced to improve the statistical power of the database.
- Portability of the methodology and software across various computing platforms from a large-scale PACS to a minimum configuration with a digitizer and a workstation allows the outcome of the project to be implemented in other clinical settings.

Fig. 5 shows the currently implemented database tables representing hand data structures following the above atlas

design guidelines. The atlas table contains all relevant textual data of a patient hand image. It is indexed by a group ID and an image file name. A group ID such as BLKF12 uniquely determines the race (BLK), sex (F) and year of age (12)-three key elements in classifying a patient's bone age. The image name in the table points to a high-resolution hand image stored offline outside of database.

### 5. Bone age CAD server

As the Web has evolved from its origins as a simple delivery mechanism—suitable for small files and applications—to a platform for complex applications and dynamic database publishing, Web servers and Web technology have not, in general, kept pace. A Web-based medical application such as our digital atlas and bone age assessment demands new robust, scalable architectures and a new class of servers, acting as a middleware to support a large image size, complicated image process, distributed and heterogeneous application environment. The middleware application server acts as a platform for reusable logic, taking responsibility for application code that might otherwise reside at the client or the database server. In the case that the digital hand atlas is used for Web-based bone age assessment, the application server contains the image processing and CAD bone age assessment modules. The application server brings together the Web technology with the digital atlas database. It also provides other middleware functionality such as quality service (scalable, reliable, secure, and manageable), tight database integration, easy migration of legacy applications and reliable transactions for network clients.

We currently use Oracle Application Server 4.0 (Oracle Corporation, Redwood Shores, CA) as an integration platform to host our server-side software/tools packages. These packages have been developed in variety of programming languages and image libraries for image acquisition, processing, managing and display. The CAD model will encode

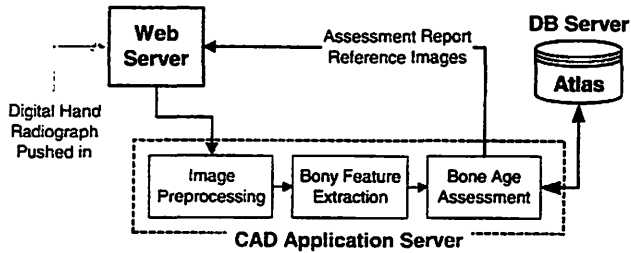


Fig. 6. Data flow for the Web-based bone age assessment.

workflow and link task-specific tools on the server side, specifically for the following:

**Image acquisition:** Image acquisition software is built into the CAD atlas server. Hand images can be transmitted from an independent CR or film digitizer to the atlas for bone age assessment. DICOM client software as well as its Web interface will also be integrated into the CAD server. The users can retrieve from the digital atlas the hand images and corresponding child data as a reference through the Web. Meanwhile, a user can send in a request to retrieve a patient hand image from a remote DICOM compliant PACS for online bone age assessment on the CAD server.

**Image processing:** The CAD server provides many image-processing services that are computationally intensive operations, thus reducing the hardware and software requirements on the client's machine. The services include image format conversion from and to the standard DICOM format, image background removal to eliminate the useless area in the radiograph, and image feature extraction and classification for bone age assessment. The services also include image manipulation functions, such as image compression, scaling, and pre-defined window-level-gamma adjustment so that the best image display quality will be achieved on a remote client's monitor without manual intervention. The image processing packages have been developed on the Sun Solaris platform with image libraries Matlab (MathWorks, Inc., Natick, MA.), XIL (X Image Library, Sun Microsystems, Mountain View, Calif.), variety of commonly available free image libraries, as well as several in-house programs specially for bone age assessment [15].

**Web-based bone age assessment:** Fig. 6 shows a work-up sequence for a Web-based bone age assessment and illustrates the role that the CAD server plays between the Web server and the digital atlas database. A patient hand image to be examined will be pushed in through the Web server. The image is passed on to the CAD server for preprocessing and feature extraction. The radiological findings associated with the extracted bony features are then compared with corresponding values from the hand atlas database and therefore to determine the patient's bone age. An assessment report along with relevant

hand images is then sent back to the client's browser through the Web server.

**Data security:** Bone age assessment across open network raises an important security issue of privacy, authenticity and integrity for sensitive medical image data. To ensure security, we will implement three levels of measures in the digital atlas system. The first level is provided by the Oracle application server, which supports the following:

- Secure Sockets Layer (SSL) Version 3, which addresses this problem by scrambling data sent from the server to browsers in such a way that only the browsers can unscramble the information when they receive it. Any intermediate computers involved in routing the information see only gibberish that they cannot decipher. SSL is an emerging standard for secure data transmission over the Internet.
- Basic and digest authentication schemes, which prompt the user to enter a user name and password before processing the user's request.
- IP-based and domain-based restriction schemes, which allow access to files only if the client is from a list of IP addresses or domain names.

The second level is to use a firewall to secure the hand atlas server. The firewall will be placed in front of the Web server. In this case, the firewall provides access for browser to Web server communication, and allows secure HTTP and SSL protocols to pass through.

The third level is to embed encrypted digital signatures onto a digital hand image. These digital signatures are based on certain characteristics of the hand image and patient-related information. The embedded information can be extracted and decrypted by the receiving site to verify the authenticity of the sender as well as the integrity of the image and patient information, which are not available in the previous two levels of securities. We will develop a digital signature scheme based on the techniques we implemented for digital mammography [23].

## 6. Java-based Web user interface

Java is a platform-independent programming language. We will develop a Java-based user interface for browsing the digital atlas and for online bone age assessment. The

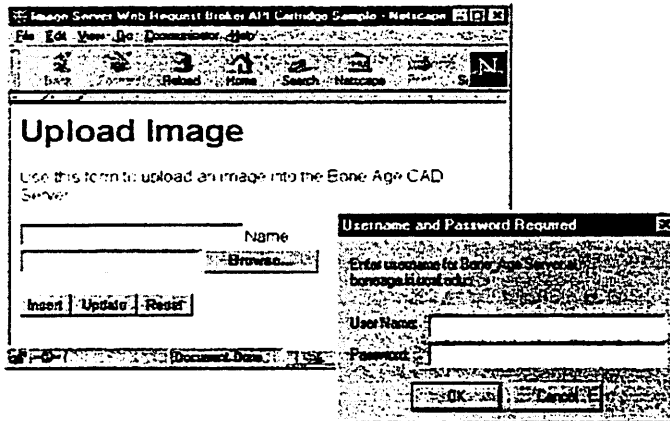


Fig. 7. An example of form shown in a user's browser window for uploading a patient's image to the Bone-age CAD server.

interface written in Java, known as a Java applet, can be automatically downloaded to and executed from user's web browsers without requirement of additional software installation on client sides. It facilitates the use of Web browsers to navigate the digital hand atlas and manipulate images interactively using any common computer systems. Meanwhile, the interface written in Java language can also serve as a standalone application, which can be distributed along with the atlas and installed on clients' machines in case there is no dedicated network connection to the atlas server.

The Web-based paradigm is essentially a request/response model. The Web browser takes care of most of user-interface concerns, rendering the Web pages dynamically formed on the fly by procedures in the digital atlas server. The server procedure first generates an Hypertext Markup Language (HTML) login form as shown in Fig. 7. The user's login typically will result in a Web-to-database procedure that determines the user's privilege and role. The server then sends back to the user an HTML main page containing hot links, on each of which the user can click on to perform a specific task.

When the user clicks on a link requesting an on-line bone age assessment, the Web server sends back a form, similar to the one in Fig. 7, for uploading clinical hand images. The user can upload the images from a local hard disk to the server simply by dropping the image files from their window file manager to the uploading window or from another remote server by specifying a Uniform Resource Locator (URL) address for the CAD server to fetch. Upon receiving the hand images and patient data from either the DICOM compliant PACS or a stand-alone image acquisition device, the server will call a procedure, illustrated in Fig. 6, to do feature extraction from the uploaded hand image and interact with the digital atlas database for bone age assessment. The assessment report will be formatted in HTML and sent back to the user. The report contains assessment results, thumbnails for accessing full-size hand images and links to manage records in the user's private database.

A user can also interactively query and browse the digital hand atlas database via web. Fig. 8 shows an example of Java applet for accessing reference hand images and their relevant information. An atlas query form at the top shows the image groups based on race, sex, age and other essential group information. The query form provides an easy way for a user to select an interesting group from the atlas. The records under the queried group are listed with their relevant patient information—age, date of birth, date of examination, height, weight, trunk height and Tanner maturity index. At the bottom are the thumbnails that can be selected and clicked on to display a full-size hand image. The selected image will then be displayed on a separated image display window similar to one in Fig. 1.

Fig. 1 is a screen shot of the left hand and wrist image. A platform-independent image viewer based on Java technology will be developed to handle full-size image display. The image is first displayed at a reduced resolution to fit the window since the full resolution hand images (2×2.5K) from older children groups are too big to display on the regular computer monitor. This permits images of various age classes to be displayed for an easy preview. The reduced image can be expanded to full resolution one with a vertical and a horizontal scroll bar to control the viewing window. The image tools will include window-level adjustment, gamma correction, scroll, scaling and zoom, and image comparison.

A demonstration of Web-based atlas browsing and bone age assessment has been set up at <http://boneage.lri.ucef.edu>.

## 7. Distribution and Web deployment of the digital hand atlas

The digital hand atlas will be available to other hospitals, as a reference standard for assessment of bone age. The atlas server will be in our laboratory (Laboratory for Radiological

Hand Atlas Query Java Applet - Microsoft Internet Explorer

File Edit View Favorites Tools Help

Address http://boneage.lri.ucsf.edu/HandAtlas/BAQuery.html

File Options

Race: BLK Sex: M AgeGroup: 12 Query

Row#	Group_ID	Image Name	Age	Tanner	DOB	DOE	Height(cm)	Weight(kg)	Trunk(cm)
1	BLKM12	3156.img	12.05	3		94.07.29	161.50	48.60	78.70
2	BLKM12	3157.img	12.12	1	1982.12.06	95.01.20	142.50	31.90	71.12
3	BLKM12	3159.img	12.35	1	1982.08.16	94.12.23	143.20	32.70	68.58
4	BLKM12	3763.img	12.41	1	1985.06.28	97.11.26	146.40	50.90	72.39
5	BLKM12	3160.img	12.42	1	1982.03.30	94.09.01	154	39.70	76
6	BLKM12	3161.img	12.61	2.50	1983.08.31	96.11.11	162	50.70	80.65
7	BLKM12	3162.img	12.61	2	1984.03.10	96.10.17	149	35.10	69.85
8	BLKM12	3163.img	12.61	3	1984.03.10	96.10.17	153	39.30	69.85
9	BLKM12	3164.img	12.82	2	1982.09.15	95.07.13	148.20	40.10	73.66
10	BLKM12	3165.img	12.91	3		96.06.26	159.90	48	79.36

Action:Goto record Row: 5 of 10 State:Existing Log

#1-3156 #2-3157 #3-3159 #4-3763 #5-3160

#6-3161 #7-3162 #8-3163 #9-3164 #10-3165

Applet started Internet

Fig. 8. A Java applet used for dynamically querying the hand atlas from client's Web browser. Atlas records can be queried by race, sex and age group listed at the top. The queried records are shown in the table below with all relevant patient information. At the bottom are the thumbnails that can be clicked on to display full-size hand images.

Informatics) at UCSF. The clients at the other sites can use a commonly available Web browser on any computer platform to access our digital atlas server for bone age assessment. There is no need for any additional software installation or management on clients' sides. The atlas and all its relevant software packages reside on the server. Real-time atlas image browsing and bone age assessment needs a dedicated network connect at speed faster than 10 Mbits/s so that a full-size hand image (average 6 Mbytes in size, 3 Mbytes lossless compressed) can be displayed in less than 8 s. Meanwhile, the image processing and bone age assessment on the server side takes about additional 3–5 s. We formulate the follow-

ing procedures for bone age assessment via Web, based on the network speeds.

- Real-time atlas browsing and bone age assessment (network speed >10 Mbits/s): Potential Sites
  - (1) PACS workstations and radiology reading rooms at UCSF via LAN. All current PACS workstations at UCSF are able to communicate with our servers over either asynchronous transfer mode (ATM) OC-3 at the speed of 155 Mbits/s [24] or fast Ethernet at 100 Mbits/s.
  - (2) UCSF, MZH, SFVA and SFGH in the San Francisco Bay Area. The four sites shown in Fig. 9 are

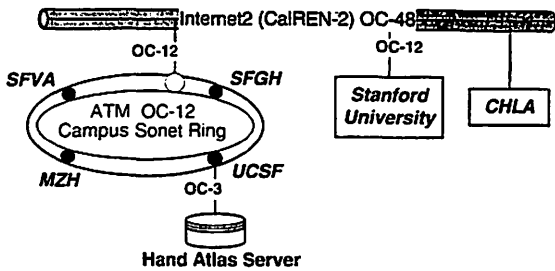


Fig. 9. Fast wide area network (WAN), currently connecting UCSF and potential Web sites for real-time atlas browsing and bone age assessment. The primary local area network (LAN) for the digital atlas server located at UCSF, is the 155 Mbits/s OC3 ATM with Fast Ethernet (100 Mbits/s) as a backup. The OC3 ATM port connects to UCSF ATM OC-12 Sonet Ring, which links in the San Francisco Bay Area the four hospitals: UCSF, MZH, SFVA and SFGH. The CalREN2 OC-48 backbone provides a statewide Internet2 connections to Stanford University Hospital of the UCSF/Stanford Health Care Enterprise.

currently capable to communicate over ATM OC-3 at the speed of 155 Mbits/s [25].

(3) *UCSF, CHLA and Stanford University Hospital over CalREN Internet2*. The connection shown in Fig. 9, to be fully functional in the first quarter of next year, will allow us to test the Web-based bone age assessment over the California statewide fast WAN.

- Offline bone age assessment (network speed >1 Mbits/s). For a T-1 line about 1.5 Mbits/s and public Internet at a speed greater than 1 Mbits/s, the clinical hand images can be uploaded to the server offline in a batch job and the bone age assessment reports will be viewed later.

In addition, the user interface written in platform-independent Java language can also be packaged with the atlas database and distributed to the other sites, acting as either another server or standalone application. However, the maintenance of the off-site server will be the responsibility of the site.

A comprehensive user-log mechanism to record user activities will be developed on the atlas server. This system documents progress and performance by user's bone age processes. The user log database managed by the atlas server at UCSF will provide performance evaluation feedback for users and will also be used to evaluate the effectiveness of the bone age assessment algorithms.

## 8. Summary

This paper presents the system architecture for a digital hand atlas with a large reference set of normal hand images and the methods to implement a Web-based computer-assisted diagnostic system for bone age assessment. The architecture is built on top of existing clinical information system and current Internet technologies. It illustrates the potential of these cutting-edge technologies in medical

informatics, and provides a new, cost-effective and convenient way of assessing bone age.

This is an ongoing project. Currently we are refining the algorithms for bone feature extraction, fully integrating system components and building Java-based Web interface. By the end of this study, there will be a medically accepted standard hand atlas able to be used as a reference. The digital atlas will be constantly updated and replenished with new materials, removing the disadvantages of the currently used one, incomplete and out-of-date. A computer-assisted image analysis will permit the diagnosis to be standardized and become more objective and reproducible. A Java-based Web interface provides a platform independent, cost-effective, and widespread means to assess the bone age.

## Acknowledgements

This research is partially supported by a NIH Grant no. R01-LM06270.

## References

- [1] Greulich WW, Pyle SI. Radiographic atlas of skeletal development of hand wrist. Stanford, CA: Stanford University Press, 1959.
- [2] Garn SM. The applicability of North American growth standards in developing countries. *Can Med Assoc J* 1965;93:914-9.
- [3] Roche AF et al. National Center for Health Statistics: skeletal maturity of youths 12-17 years: racial, geographic area and socioeconomic differentials, United States. In: Roche AF, Roberts J, Hamill PVV, editors. *Vital and health statistics. Series 11-no. 167*. DHEW Pub. no. (HRA) 79-1654. Health Resources Administration. Washington: US Government Printing Office, October 1978.
- [4] Loder RT, Estle DT, Morrison K, Eggleston D, Fish DN, Greenfield ML, Guire KE. Applicability of the Greulich and Pyle skeletal age standards to black and white children of today. *Am J Dis Child* 1993;147:1329-33.
- [5] Tanner JM, Whitehouse RH. *Assessment of skeletal maturity and prediction of adult height (TW2) method*. London: Academic Press, 1975.
- [6] Schmid F, Moll H. *Atlas Der Nonmalen und pathologischen hand-skeletenwicklung*. Berlin: Springer, 1960.
- [7] Eklöf O, Rigertz H. A method for assessment of skeletal maturity. *Ann Radiol* 1967;10:330-6.
- [8] Sugiura Y, Nakazawa O. *Roentgen diagnosis of skeletal development*. Tokyo, Japan: Chugai-Igaku Company, 1972.
- [9] Michael DJ, Nelson AC. HANDX: a model-based system for automatic segmentation of bones from digital radiographs. *IEEE Trans Med Imaging* 1989;8:64-69.
- [10] Levitt TS, Hedgcock MW. Model-based analysis of hand radiographs. *Proc SPIE* 1989;1093:563-70.
- [11] Tanner JM, Gibbons RD. A computerized image system for estimating Tanner-Whitehouse 2 bone age. *Horm Res* 1994;42:282-7.
- [12] Pietka E, McNitt-Gray MF, Huang HK. Computer-assisted phalangeal analysis of hand radiographs. *IEEE Trans Med Imaging* 1991;10:616-20.
- [13] Pietka E, Kaabi L, Kuo ML, Huang HK. Feature extraction in carpal bone analysis. *IEEE Trans Med Imaging* 1993;12:44-49.
- [14] Pietka E, Huang HK. Epiphyseal fusion assessment based on wavelets decomposition analysis. *Comput Med Imaging Graphics* 1995;19:465-72.

- [15] Pietka E, Huang HK. Image processing techniques in bone age assessment. In: Leondes CT, editor. *Medical imaging techniques and applications*. New York: Gordon and Breach Science, 1997. pp. 221–72 (chap. 5).
- [16] Pietka E. Image standardization in PACS. In: Bankman IN, editor. *Medical image processing*. New York: Academic Press, 2000 (in press).
- [17] Tanner JM. Physical growth and development. In: Forfar JO, Arnell CC, editors. *Textbook of pediatrics*. Edinburgh: Churchill Livingstone, 1978. pp. 249–303.
- [18] Huang HK. *Picture archiving and communication: principles and applications*. New York: Wiley, 1999 (p. 521).
- [19] Huang HK, Cao F, Pietka E. CAD in PACS environment. *First International Workshop on Computer-Aided Diagnosis*, Chicago, September 1998, p. 20–23.
- [20] Cao F, Huang HK, Pietka E, Gilsanz V. Digital hand atlas and computer-aided bone age assessment via Web. *SPIE Medical Imaging* 1999;3662-59.
- [21] Cao F, Huang HK, Pietka E, Gilsanz V, Ominsky S. Diagnostic workstation for digital hand atlas in bone age assessment. *Proc SPIE Med Imaging* 1998;3335:608–14.
- [22] Wong STC, Huang HK. A hospital integrated framework for multimodality image database management. *IEEE Trans System, Man, Cybernetics* 1996;26(4):455–69.
- [23] Zhou XQ, Huang HK, Pietka E, Gilsanz V. Authenticity and integrity of digital mammographic images. *SPIE Med Imaging* 1999;3662-16.
- [24] Huang HK, Arenson RL, Dillon WP, Lou ASL, Bazzill T, Wong AWK. Asynchronous transfer mode (ATM) technology for radiologic communication. *Am J Roentgenol* 1995;164:1533–6.
- [25] Lou SL, Sickles EA, Huang HK, Hoogstrate D, Cao F, Wang J, Jahangiri M. Full field direct digital telemammography: technical components, study protocols, and preliminary results. *IEEE Trans Inform Tech Biomed* 1997;1(4):270–8.

**Fei Cao, PhD** is currently an Assistant Professor in the Department of Radiology, Children's Hospital of Los Angeles/University of Southern California. His research activities have been in design and implementation of high-resolution image display workstation, clinical computer applications and medical multimedia, image database, high-speed medical image transmission, and Web applications.

**H.K. Huang, DSc** is currently a Professor and Director of Informatics, Department of Radiology, Children's Hospital of Los Angeles/University of Southern California. He implemented a PACS at the University of California-Los Angeles in 1991 and a second-generation PACS at the University of California-San Francisco in 1994. His current research interests include infrastructure design for medical informatics, image processing and communication, telemedicine.

**Eva Pietka, PhD** is currently a Professor in the Department of Nuclear Medicine, Medical University of Silesia, Poland. Her main research interests include medical image processing, communication and database.

**Vincente Gilsanz, MD** is a Professor of Pediatric Radiology, Children's Hospital of Los Angeles. He has a long-term interests and expertise in quantitative digital radiography.

# Fault Tolerant Picture Archiving and Communication System and Teleradiology Design

H. K. Huang, DSc

Fei Cao, PhD

Jianguo Zhang, PhD

Brent J. Liu, PhD

M.L. Tsai, BS

A picture archiving and communication system (PACS), a large computer network and system integration for medical images and database, is a mission critical system for around-the-clock daily clinical operation. The operational reliability of any PACS is vital. This chapter will review the concepts of fault tolerance (FT), high availability (HA), and continuous availability (CA) as means to categorize the degree of reliability of mission critical systems. Possible causes of PACS failure will be discussed. Two main criteria in a PACS operation are that there be no loss of image data and no interruption of data flow. The chapter presents these criteria in detail and also delineates ways to satisfy them using current PACS technology. A case study, based on clinical experience with various failures in PACS controller archive servers that have caused clinical operation downtime, is discussed along with methods of remedy. The chapter concludes with the current concept of FT PACS design.

## INTRODUCTION

HA and CA are the two commonly used terms categorizing the degree of reliability in operating a large computer network system. A continuum of HA solutions ranges from a 99% system availability rate (88 hours downtime/year, using the simple "hot spare" technology) to 99.99% availability (1 hour downtime/year, with clustered server-based solutions using hardware and fail-over software). FT systems are CA solutions, with the highest (99.999%) availability rate and minimum downtime of 5 minutes/year. PACS is a mission critical operation, continu-

ing 24 hours a day and 7 days a week, and it requires continuous availability. In PACS, three operational criteria are vital to the system's success: no loss of data, continuous availability of the system, and acceptable system performance. This chapter considers the first and second issues.

PACS is a system integration of medical images and patient databases (1). The integration involves many components, including imaging modalities, computers, display workstations, communication devices, network switches, and computer servers housing healthcare databases. In this chapter, we loosely distinguish between PACS and teleradiology by their network connection. When the network connection used in PACS involves only a local area network (LAN) or intranet, we refer to PACS. If both intranet and Internet (wide area network [WAN]) are involved, then we refer to teleradiology. Figure 8.1 shows a generic PACS architecture, and Figure 8.2 shows the logical connection of some basic components in PACS and teleradiology. PACS and teleradiology are mission-critical systems running around the clock with no tolerance for failure. For convenience, we will not distinguish between PACS and teleradiology in the discussion of fault tolerant design.

## CAUSES OF SYSTEM FAILURE

Integrated computer and network system failure can be caused by human error, natural disaster, software, or component hardware. Table 8.1 shows a current survey on the causes of system downtime (2).

Although no formal data on the causes of PACS downtime has been reported, based on field experi-

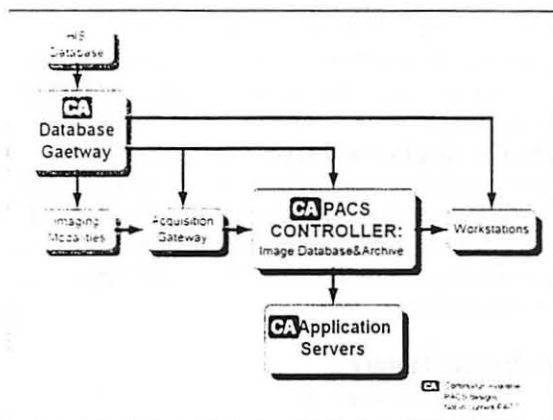


**Figure 8.1** Generic picture archiving and communication system (PACS) components and data flow. CA = continuous available components replacing single-point-of-failure components: database gateway, PACS controller, and application servers.

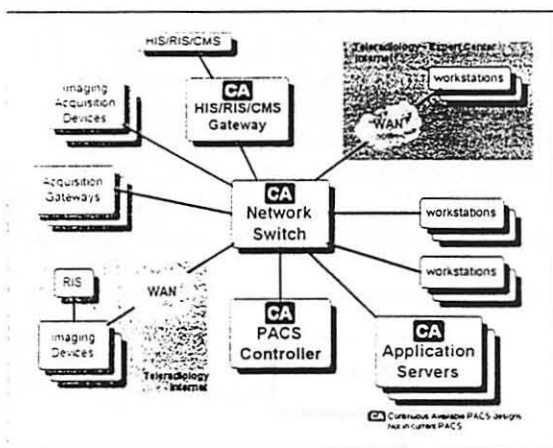


**Figure 8.2** Physical connection of picture archiving and communication system (PACS) and teleradiology. Numerals = data flow; CA = continuous available components replacing single-point-of-failure components: network switch, PACS controller, and application servers.

ence, we can assume that PACS follows the same trend of downtime causes as a general computer and network system in Table 8.1. Among these causes, natural disaster is not predictable and, hence, cannot be avoided. However, the effects of natural disaster can be minimized for PACS downtime by choosing proper locations for installation, taking proper natural disaster precautions, and using off-site backup. Properly chosen locations and special precautions can minimize system shutdown as a result of natural disaster, and off-site backup can prevent loss of data.

The reliability of current software and the refinement of system design have greatly improved efforts to minimize human error in PACS. Redundancy in software architectural design allows the system to be recovered gracefully after a software failure. Minimizing human intervention during the PACS operation in the system design can lower the rate of human error. However, hardware failure, either in the computer, disk, communication processor, or network, is unpredictable and, hence, difficult to avoid.

We will not discuss natural disaster and human error in this chapter. We also assume that the entire PACS software is fully debugged and is immune to failure. In fault tolerant PACS design, we will address only the issue of what would happen if some hardware components fail and how to take care of such a failure so that the PACS operation will not be compromised.

If a hardware component involved is the single point of failure (SPOF), for example, the PACS controller that is the main server of the PACS, the failure can render the entire system inoperable until the problem is diagnosed and resolved. Other critical hardware components that cannot tolerate failure are cluster servers, application servers, Web servers, network switches, imaging acquisition gateways, and database gateways. A failure of one of these components may cripple that branch of operation, which in turn may interrupt the complete system operation. Component failures also frequently result in the loss of data. Both interruption of operation and loss of data are unacceptable in a totally digital clinical environment. On the other hand, a failure of a display workstation is not so critical, because there are duplicate workstations. The failure may cause inconvenience to the user, but it does not cripple the system. Smith et al. (3) described the painful experience of a major PACS server failure and a method to reverse back to film-based operation.

Often a software remedy is integrated in various PACS components to minimize the impact to system operation as a result of hardware component failure. The software remedy to hardware failure is elaborate in design, difficult to implement, and make data and state recovery difficult. In the following sections, we first categorize some of these failures and methods for their remedy provided by current PACS technology. A case study of PACS controller archive server downtime and its remedy is given based on clinical experience. We conclude with the current concept of a FT PACS design.

**TABLE 8.1**  
**Causes of Computer and Network System Downtime (2)**

Computer hardware .....	24%
Hard disk drive .....	26%
Communication processor .....	11%
Data communication network .....	10%
Software .....	22%
Human error .....	6%
Others .....	1%
Total .....	100%

## NO LOSS OF IMAGE DATA

### Redundant Storage at Component Levels

To ensure that no image data is lost, a PACS always retains two copies of an image on separate storage devices until the image has been archived successfully to a long-term storage device (for example, an optical disk or tape library). Figure 8.3 shows the various storage subsystems in PACS. This backup scheme is achieved via the PACS intercomponent communication system, which can be broken down as follows:

- At the imaging device.** Images are not deleted from the imaging device's local storage until technicians have verified the successful archiving of individual images to another storage device via the PACS connections. In the event of failure of the acquisition gateway process or of the archive process, images can be resent from the imaging device to PACS.
- At the acquisition gateway computer.** Images acquired in the acquisition gateway computer remain on its local magnetic disks until the archive subsystem has acknowledged to the acquisition gateway computer that a successful archive has been completed. These images are then deleted from the magnetic disks residing in the acquisition computer, so that storage space from these disks can be reclaimed.
- At the PACS Controller.** Images arriving in the archive server from various acquisition gateways are not deleted until they have been successfully archived to the permanent storage (Fig. 8.3B). On the other hand, all archived images are stacked in the archive server's cache magnetic disks or RAID

(Fig. 3A) and will be deleted based on their aging criteria (for example, number of days ago an examination was performed or discharge or transfer of a patient).

- At the display workstation.** Images stored in the designated display workstation will remain there until the patient is discharged or transferred. Images in the PACS archive can be retrieved from any display workstations via PACS intercomponent communication.

### The Archive Library

The archive (optical disk, digital linear tape [DLT]) library consists of multiple input/output drives and controllers housed inside the jukebox, which allow concurrent archival and retrieval operations on all of its drives. A redundant power supply is essential for uninterrupted operation. To build a FT in the PACS server, a back-up archive system can be used. Two copies of identical images can be saved through two different paths in the PACS network to two archive libraries. Ideally, the two libraries should be in two different buildings in case of natural disaster. To reduce the cost of redundant archiving, the primary unit can be an optical disk or DLT library, and the back-up unit is a DLT. Figure 8.4 shows a low-cost backup archive design for no loss of image data.

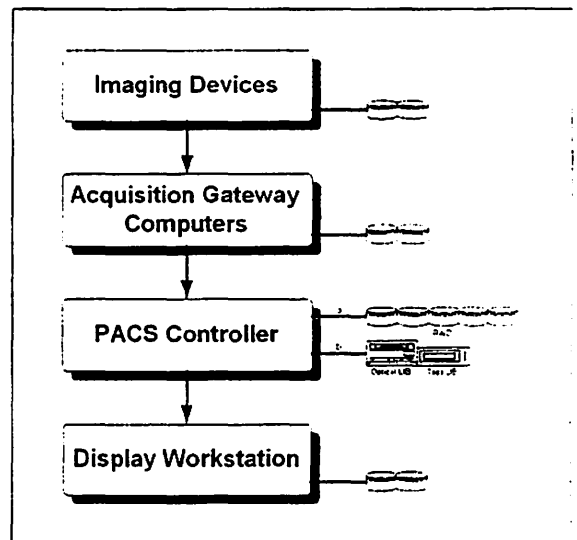


**Figure 8.3** Various storage subsystems in the picture archiving and communication system to ensure no loss of image data. Until an individual image has been archived in the permanent storage (for example, CD-ROM, WORM, digital linear tape), two copies are retained on separate storage devices.

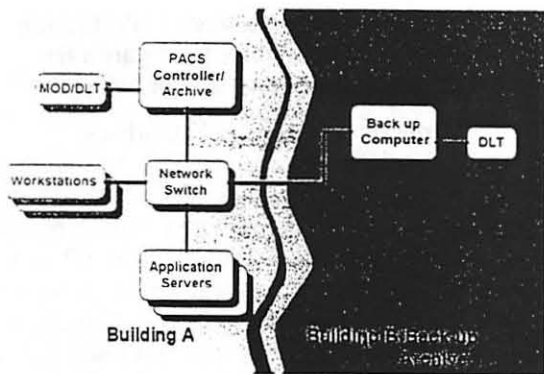


**Figure 8.4** A low-cost, back-up tandem design for no loss of image data.

### The Database System

The database system comprises redundant database servers, running identical reliable commercial database systems, with structured query language (SQL) utilities. A mirrored database (that is, two identical databases) can be used to duplicate the data directory during every PACS transaction involving the server. The back-up database can reside in a different computer or in a different partition of the same disk of the same computer. The first configuration provides a better FT. The mirroring feature of the database system provides the entire PACS database with uninterrupted data transactions that guarantee no loss of data in the event of system failure or a disk crash. Although the second method, using a different partition of the same disk, is not FT for a whole disk crash, it guarantees the continuous availability of PACS database during the disk partition failure. The benefits of the second configuration are low cost, easy implementation, and management of the mirroring database.

### NO INTERRUPTION OF PICTURE ARCHIVING AND COMMUNICATION DATA FLOW

#### Picture Archiving and Communication Data Flow

PACS is a networked and component-integrated system. Figure 8.1 shows a generic architecture. The functions of major components and networking facilities are:

- Imaging modalities: generate medical images.
- Acquisition gateways: acquire images, process images, and send images to PACS controller. The

PACS controller has three components: the controller, database server, and archive units.

- Controller: receive images from acquisition gateways, intelligently route images to display workstations, access PACS database to update/query image related records, access archive units to store or retrieve images, and provide query/retrieve services for display workstations.
- PACS database server: perform PACS image-related information management.
- PACS archive units: store images for short- and long-term archive.
- Display workstations: display PACS images for diagnosis.
- PACS networking facilities: connect PACS components.

An image in a PACS component is usually processed by a sequential processing chain with a first-in-first-out (FIFO) model, as shown in Figure 8.5.

For example, in a Digital Imaging Communication in Medicine (DICOM)-compliant computed radiography (CR) acquisition gateway computer, "Process 1" in Figure 8.5 is the storage SCP (service class provider) process receiving DICOM CR images from the CR reader and "Process i+1" is the storage SCU (service class user) process sending the image to the PACS controller. The other processes (2,...i) perform image-processing tasks necessary for downstream image archive and display in the PACS controller and display workstations. The queues, "Queue 1" to "Queue i," are structured files (if they are located in disk drives) or tables (if they are in database), used for transferring image-processing tasks between the processes. In the following, we will use the collective term "image processing" to represent these processes.

### Possible Failure Situations in Picture Archiving and Communication System Data Flow

The hardware of any component shown in Fig. 8.5 can fail, and the failure will interrupt the PACS data flow through that component. If the component is the SPOF, such as a PACS controller, a network switch or an application server, it may render the entire system inoperable.

By the same token, any key hardware device in a component computer can fail, as shown in Figure 8.6, which in turn, can crash the component computer and stop any image processing procedures in that computer. The result is the interruption of data flow or even loss of images.

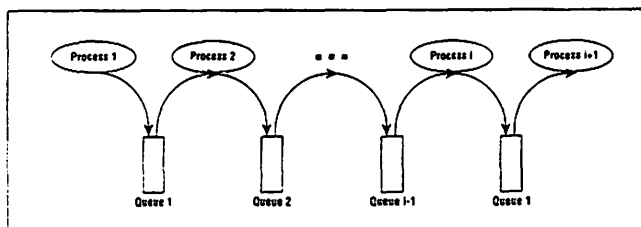


**Figure 8.5** The first-in-first-out (FIFO) image processing model in a picture archiving and communication system component.

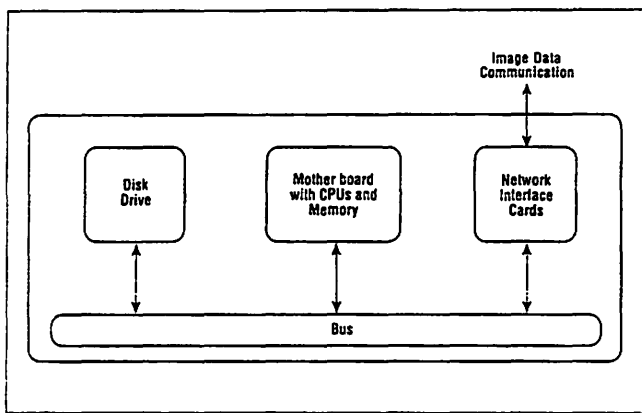


**Figure 8.6** Key devices in a component computer.

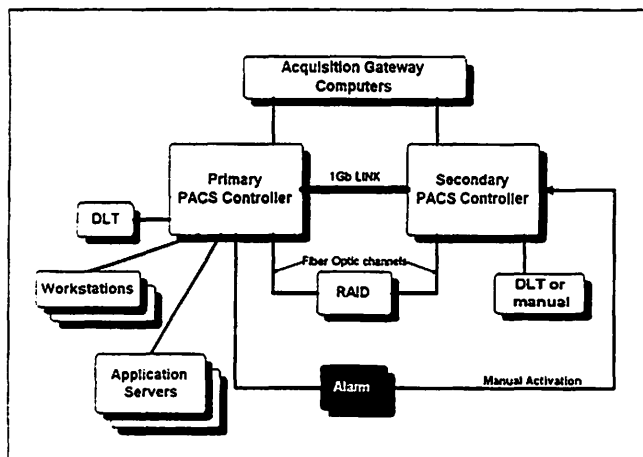


**Figure 8.7** Design of a tandem picture archiving and communication system controller with manual activation of the secondary controller.

## Methods and Drawbacks in Protecting Data Flow Continuity from Hardware Component Failures and Drawbacks

### Hardware Solutions and Drawbacks

Two solutions are offered. The first is hardware redundancy, in which a backup computer or a tandem system is used to replace an online failed computer. Figure 8.7 shows the design of a manually activated tandem PACS controller. The second solution is to use a cluster server as the main PACS server. The PACS controller is composed of multiple servers controlled by a cluster manager.

Hardware solutions have two drawbacks. First, they are expensive, because of the hardware redundancy and the software involved in designing the fail over. Second, it is tedious and labor intensive to recover the current state after a component failure. In the case of hardware redundancy, if the primary component fails, the secondary will take over. After the primary is fixed and on-line again, it will take tremendous efforts to shift the operation from the secondary back to the primary. In the case of cluster server, if one clustered server fails, the recovery process and the return to the original operational state are also very tedious.

### Software Solutions and Drawbacks

Two solutions are offered. The first is to design the image data flow in such a way that any image in a transit state has at least two softcopies in two different components, respectively. The second is to utilize the principle that the chance of simultaneous failure of two hardware devices is much less than that of either one of them. This principle can be used to minimize the loss of image data during an image processing procedure resulting from device failure in a component. A snake road design in the image processing software can be used to partition the FIFO model (described in Fig. 8.5). In this design, data will pass through different hardware devices, for example, between the motherboard (CPU) module (or the network card module if the process is for communication) and the hard disk drive alternatively, as shown in Figure 8.8.

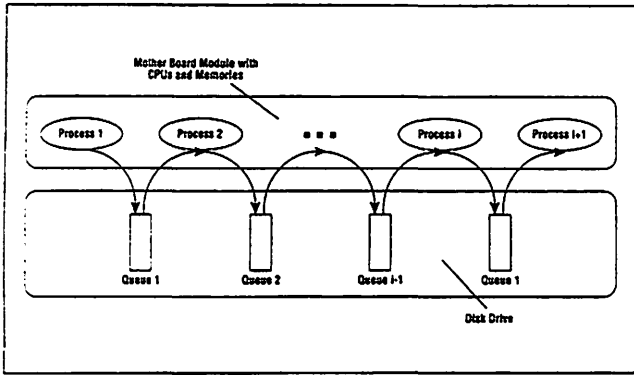


**Figure 8.8** The snake road design to minimize loss of data as a result of hardware failure during an image processing procedure.

The drawback of the first software solution is that it makes the whole PACS software architecture complicated and also increases the costs of storage, administration, and software maintenance. The drawback of the second software solution is that it will slow down the execution of the image processing procedure as a result of too many disk I/O operations for reading and writing of a large image data file. The software architecture is also very weak, because any failure in a software process will break down the image processing procedure chain in the snake road. As a result, it decreases the whole PACS performance and may even produce the image stacking effect in some processing steps, which can eventually overflow the capacity of the local disks, leading to the loss of image data.

### Current Picture Archiving and Communication System Technology in Addressing Fault Tolerance

Current PACS technology utilizes a mix of software and hardware approaches in addressing PACS FT. Multiple copies of an image are always in existence at one time in various components until the image is archived in long-term storage. A second copy of the archived image is stored off line but not necessarily in a library system, because of the expense involved.

To ensure that there is no interruption of PACS data flow, larger PAC systems use distributed server architecture, and almost all systems have a mirrored database design. Most PAC systems incorporate specific software design to avoid the interruption of data flow as a result of hardware component failure. However, hardware failure occurs most often in the hard disk drive. In this case, the data flow in the branch of

the PACS operation related to the disk drive will be interrupted. If the disk is a component in the PACS controller, the data flow in the complete system will be interrupted, and only local functions in image acquisition and workstations can remain in operation. No effective method has yet been devised to circumvent this hardware failure.

### CLINICAL EXPERIENCES WITH ARCHIVE SERVER DOWNTIME: A CASE STUDY

The Saint John's Health Center (St. John's), Santa Monica, CA, is used here as a case study to describe possible component failures in a PACS archive server causing operation downtime. Methods of remedy are discussed. Current PACS FT technology is also described.

#### Background

St. John's is a 224-bed community hospital that performs approximately 120,000 radiology exam procedures each year. Of those exams, approximately 90% are digitally acquired and stored in a PACS archive server. The archive server is also responsible for prefetching and distribution of any current and previous exams. It also provides patient location information for automatic image distribution to specific review workstations located on the hospital's clinical floors. Like all traditional LAN PACS, the archive server is the command center for St. John's PACS.

The hardware configuration for the archive server consists of a SUN Ultra2 workstation, two mirrored hard disks, a RAID (redundant arrays of independent disks) 4 server, and an optical disk jukebox with two drives and a single robotic arm. The SUN Ultra2 workstation has one 4.1-Gb hard disk that contains the system software and the application software for the archive server. Attached to the workstation is a separate unit that contains two 4.1-Gb mirrored hard disks. This mirrored hard disk device contains mirrored data of the patient and image directories of all the exams stored in the RAID and magnetic optical disk jukebox. A third copy of the databases is stored on a separate optical disk offline, and the backup is performed on a daily basis. The RAID 4 system is connected to the Ultra 2 workstation via the small computer system interface (SCSI) port and is a 90-Gb array of hard disks. This RAID system holds about 2 weeks worth of current exams for fast retrieval. In addition, these exams are archived long-

term in the MOD jukebox. The MOD jukebox contains a single robotic arm that retrieves the platters and inserts them into one of two drives for exam retrievals. The jukebox has the capacity to contain 255 platters for a total of 3.0 Tb of data, compressed at a ratio of 2.5:1. The SPOFs for the archive server are the single-system hard disk and one CPU motherboard of the SUN Ultra2 workstation. However, the database, which is a crucial part of the server, is mirrored on two hard disks with a third offline daily backup.

### **PACS Server Downtime Experience**

During a period of 1.5 years of 24-hour, 7-days-per-week operation, the archive server has encountered a total of approximately 4 days of downtime, spread across three separate downtime incidents. The first two incidents were the result of system hard disk failures (Fig. 8.5). The third downtime was the result of a CPU motherboard failure (Fig. 8.6). A description of downtime procedures and events and ensuing uptime procedures will be presented to give a snapshot of how archive server downtime affects the clinical workplace.

#### **Hard Disk Failure**

The first two archive server downtimes involved the failure of the server system hard disk. Because the system software and the application software reside on this hard disk, the archive server was considered completely down. The initial diagnosis was made during the early evening hours. A new hard disk was ordered by service staff, and the service representative arrived early the next morning to begin bringing the server back up. This was accomplished by replacing the hard disk with a new one and then installing the system software. Once the system software had been installed and properly configured, the next step was to install the server application software. The application setup is complex, especially during the second downtime, because the application software had just undergone a new software upgrade and only two service personnel within the organization had a complete understanding of the installation procedures for the new upgrade. In both cases, the server was brought up by the end of the day, for a total of 1.5 days of downtime for each incident.

#### **Motherboard Failure**

The third archive server downtime involved the CPU motherboard. The nonvolatile random access memory (NVRAM) on the motherboard failed and

needed replacement. The failure occurred once again during the early evening, and the initial diagnosis was made. A new CPU motherboard was ordered, and the service representative arrived early the next morning. The hardware was replaced, and tests were made to insure that all hardware components within the archive server workstation were fully functioning. Because the hard disk was not corrupted or damaged, the server was brought up around noontime, for a downtime of approximately 1 day.

### **Effects of Downtime**

#### **At the Management Level**

During the archive server downtime, normal operations and routines that were performed automatically had to be adjusted and readjusted once the server was brought back up. These adjustments had a major impact on the clinical workflow. Under normal conditions, all new exams were automatically routed to the review workstations on the hospital floors, based on the location of the patient. Information on the location of the patient is obtained from the archive server, which, in turn, obtains it from the radiology information system (RIS) interface. Prefetched exams were distributed to the corresponding workstations, along with the current exams for comparison. In addition, radiologists and referring physicians may query and retrieve on demand for any previous exams not located on the local workstation. Once the archive server experiences downtime, the workflow changes radically. Communication between all staff personnel is crucial to relay the current downtime status and implement downtime procedures. The technologists must manually distribute the exams to the specific reading workstation along with the corresponding review workstation on the floors. Therefore, what normally takes one mouse click action to begin autorouting becomes a series of manual operations to send to multiple separate workstations. For the clerical staff, hardcopy reprints for offsite clinics are not possible, because most exams requested for hardcopy reprint do not reside on the local workstations and cannot be obtained with a query and retrieve command. For the radiologists, any new exams acquired during the downtime will not be available as prefetched exams at the local reading workstation for comparisons. In addition, neither radiologists nor referring physicians can query and retrieve any exams from the archive any exams.

#### **At the Local Workstation Level**

Exam data management procedures on the local

workstations are implemented as well during the downtime of the archive server. At the onset of downtime, some workstations will have exams that were in the process of being sent to the archive. These sending jobs need to be cleared from the queue before they start to affect the performance of the workstations. In addition, any automatic archiving rules must be turned off on the local workstations so that no additional exams will be sent to the archive when it is down.

### **Downtime Lasting More Than 24 Hours**

To prepare for possible downtime longer than 24 hours, some exams may need to be deleted from the local workstation after they have been read and archived, to make room for incoming new exams. This process can only be performed manually and thus can be very time consuming, depending on the total number of workstations that receive new exams. Once the archive server is up and running again, the uptime procedures for the reading workstations must be implemented. All automatic archiving rules need to be activated. Any new exams that have not been archived must be archived manually. Finally, query and retrieve tests must be performed on the workstation to insure that the PACS is fully operational once again. These final uptime procedures for the workstations consume about 2 hours of time in addition to the server downtime to bring the system to full operational status.

### **Impact of the Downtime to Clinical Operation**

In these three downtime experiences, St. John's has not lost any image data. In addition, the mirrored database disk system has sustained no damage. In fact, with all the downtime procedures implemented, the end-users only experience the inconvenience of not having the query-and-retrieve functionality and the availability of previous exams for comparison studies.

## **CONCEPT OF CONTINUOUS AVAILABLE PICTURE ARCHIVING AND COMMUNICATION DESIGN**

The case study of St. John's is an example of the current FT PACS design in clinical practice. The concept of CA PACS design is to minimize manual intervention and changes in management and workstation daily operation routines, because these recovery procedures are tedious and labor intensive in clinical operation, not to mention the steps required to bring back the PACS engineering operation. There-

fore, an ideal FT design avoids the existence of SPOF in the system. The PACS controller and each application server are potential SPOFs of the system. The question is how to avoid these SPOFs in the system so that PACS will be continuously available in case any SPOF occurs. If we use hardware solutions, the PACS as a whole will be very expensive and difficult to maintain. If we use software solutions, the software development effort will be extensive, and the system performance will suffer, as witnessed in the case study.

The current concept in CA PACS design is to remove any SPOF in the complete system by a new CA component with four characteristics. First, this CA component has an up time of 99.999% (downtime: 5 minutes per year) to satisfy the CA requirement. Second, should this CA component fail as a result of failure in any of its hardware devices, its recovery should be automatic without human intervention, and that recovery time should be within seconds. Third, this CA component is a one-to-one replacement of the existing PACS component requiring no modification of the existing system. And fourth, the replacement is easy to install and affordable. Figures 8.1 and 8.2 are versions of the CA PACS design, which is identical to a generic PACS architecture except that all possible SPOFs (PACS controller, application servers, database gateway computer, and network switch) are replaced by the CA components. Progress is being made along this line of research and development (4).

## **ACKNOWLEDGMENT**

This work is partially supported by the U.S. Army Medical Research and Materiel Command Contract No. DAMD17-99-P-372, NIH National Library of Medicine Contract No. N01-LM-9-3538, and Reliant Care, Inc.

## **REFERENCES**

1. Huang HK. *PACS: Basic Principles and Applications*. New York, NY: Wiley & Sons; 1999:521.
2. Resilience Corporation. *Resilience Corporation Technical Report, 2000*. Available at: IMEX Research.com
3. Smith, DV, Smith S, Bender GN, et al. Evaluation of the medical diagnostic image support system based on 2 years of clinical experience. *J Digit Imaging*. 1995;8:75-87.
4. Huang HK, Cao F, Zhang J. Fault-tolerant design and implementation of the PACS controller. Presented at: Radiological Society of North American, 2000 RSNA InfoRAD Exhibit, 9609. Chicago, IL, November 2000.

# Network Latency and Operator Performance in Teleradiology Applications

Johannes N. Stahl, Wyatt Tellis, and H.K. Huang

Teleradiology applications often use an interactive conferencing mode with remote control mouse pointers. When a telephone is used for voice communication, latencies of the data network can create a temporal discrepancy between the position of the mouse pointer and the verbal communication. To assess the effects of this dissociation, we examined the performance of 5 test persons carrying out simple teleradiology tasks under varying simulated network conditions. When the network latency exceeded 400 milliseconds, the performance of the test persons dropped, and an increasing number of errors were made. This effect was the same for constant latencies, which can occur on the network path, and for variable delays caused by the Nagle algorithm, an internal buffering scheme used by the TCP/IP protocol. Because the Nagle algorithm used in typical TCP/IP implementations causes a latency of about 300 milliseconds even before a data packet is sent, any additional latency in the network of 100 milliseconds or more will result in a decreased operator performance in teleradiology applications. These conditions frequently occur on the public Internet or on overseas connections. For optimal performance, the authors recommend bypassing the Nagle algorithm in teleradiology applications.

Copyright © 2000 by W.B. Saunders Company

**KEY WORDS:** teleradiology, computer supported cooperative work, internet, network latency, Nagle algorithm.

**T**ELERADIOLOGY applications often include an interactive conferencing mode that enables 2 or more physicians to discuss a problematic or doubtful case by means of remote control mouse pointers. These pointers are used to point to the findings on the images that are being discussed over a voice communication channel such as a telephone. Although this method enhances the quality and reliability of the teleradiology procedure, it also is a complex task that requires accurate audiovisual coordination.

Increasingly, public interconnected networks, such as the Internet, are being used for teleradiology. One of the pitfalls in using the Internet and the underlying network protocol TCP/IP is the network latency. Network latency is the time a data packet takes to travel from the origin to the destination. On the Internet, a data packet passes through many intermediate nodes, each of which delays the packet through internal processing and routing

mechanisms. Wood et al<sup>1</sup> reported network round-trip-times (which are approximately twice the latency) between 18 and 424 milliseconds, depending on the type of connection.

In addition to the latencies that occur on the network itself, the TCP/IP protocol uses an internal optimization scheme called the Nagle algorithm,<sup>2</sup> which can delay the delivery of small data packets by up to 350 milliseconds even before they are sent to the network. The purpose of this algorithm is to improve the efficiency of the communication over many intermediate nodes by collecting small data packets into a single larger packet. The downside of this method is that small data packets are not sent immediately when they are generated, but later when the large packet is complete. Because the data packets used to transmit the position of the remote cursor between 2 teleradiology systems are very small (only a few bytes), teleradiology applications can be affected by the Nagle algorithm. This results in jerky movements of the remote cursor, because the cursor position messages do not arrive continuously, but intermittently, as the large network packets are transmitted.

Combined, the network latency and the Nagle algorithm can lead to an audiovisual dissociation with the effect that there is a temporal discrepancy between the position of the remote mouse cursor and the verbal description received over the voice channel, usually a telephone. The purpose of this report is to determine the possible effects of this dissociation on the performance of the user in a teleradiology context.

## MATERIALS AND METHODS

To measure the operator performance, we needed to design test tasks that resemble the operation of a teleradiology system

---

*From the Laboratory for Radiological Informatics, University of California, San Francisco, CA.*

*This work was partially supported by the National Library of Medicine Contract No. N01-LM-6-3547 and by a scholarship from the Deutsche Forschungsgemeinschaft (Sti 517/1-1).*

*Address reprint requests to Johannes N. Stahl, MD, Radiologische Klinik, Abt. Radiodiagnostik, Universitätsklinik, 66421 Homburg/Saar, Germany.*

*Copyright © 2000 by W.B. Saunders Company*

*0897-1889/00/1303-0006\$10.00/0*

*doi:10.1053/jdim.2000.8058*

and can be measured quantitatively. We also needed a teleradiology system that can systematically simulate different network latencies.

We modified a teleradiology system developed at our institution,<sup>3</sup> which uses the User Datagram Protocol (UDP) for the transmission of the remote cursor position. This protocol has a latency of less than 10 milliseconds on a local area network (LAN). We added a programmable delay loop to the program that can simulate various network conditions by delaying outgoing data packets by an adjustable time.

We designed a synthetic test image that consists of white numbers 1 to 50 randomly distributed on a black background (Fig 1). We developed 2 test tasks that were performed by test persons using a pair of teleradiology systems in separate rooms and talking to each other over a telephone.

A. The first test person randomly points to a number on the image and waits for the second person to correctly communicate the number through the telephone. After the number has been identified by the second person, the first person points to another

randomly selected number. This procedure is repeated for 40 numbers out of the 50 numbers on the test image. The time required to correctly identify all 40 numbers is measured with a chronometer.

B. The first test person moves the cursor across the numbers. In approximately 5-second intervals, without halting the movement, the first person instructs the second person over the telephone to identify the number under the cursor at that instant. Both test persons quietly write down the number and continue until 10 numbers are recorded. The number sequences noted by the 2 test persons are compared, and the number of errors is counted.

Both tasks simulate 2 radiologists identifying and describing structures on an image by combined visual and audible communication. The first task (task A) was designed to avoid mistakes by having the test persons cross check the numbers over the telephone and to measure the effects of the latency on the time required to perform the task. The second task (task B) measures

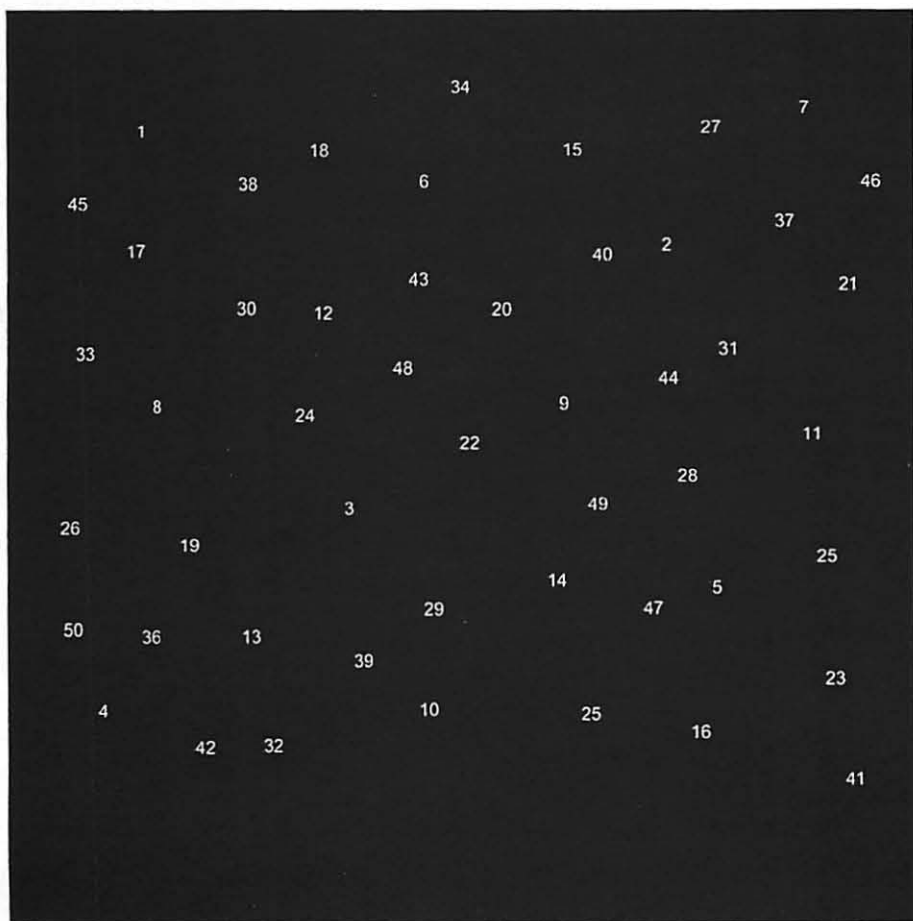


Fig 1. Test image with randomly distributed numbers.

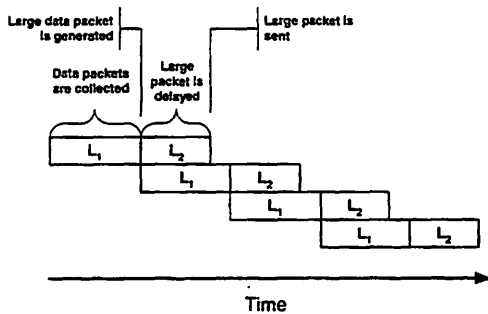


Fig 2. Timing diagram of the simulated composite latency. During the first  $L_1$  period data packets are collected. When the timer  $L_1$  elapses, a large packet is generated and delayed by the time  $L_2$ . The timer  $L_1$  is reset and newly generated data packets are collected. When the timer  $L_2$  elapses, the large data packet is sent. The delay loops  $L_1$  and  $L_2$  overlap each other.

the number of communication errors introduced by the latencies when no cross checking or audible feedback is performed.

Both tasks were performed by 5 test persons (nonradiologists, 22 to 30 years old) and repeated for 2 sequences of simulated latencies. The first sequence used a simple, constant latency simulating the latency of the physical network. We used the latencies 0, 250, 500, 750, and 1,000 milliseconds.

In the second sequence, we used a composite latency consisting of a variable portion  $L_1$  simulating the Nagle algorithm, and a constant portion  $L_2$  simulating the network latency. The variable portion  $L_1$  will collect data packets into 1 large packet for the programmed time. Once the timer  $L_1$  has elapsed, the large data packet is delayed by the time  $L_2$  and then sent over the network. The 2 delay loops operate overlapped, so that while the timer  $L_2$  delays the large packet, the timer  $L_1$  is restarted, and newly generated small packets are collected. Please refer to Fig 2 for timing details. For the second sequence, we used combined latencies of 200, 250, 300, 400 and 500 milliseconds. We omitted the long latencies of 750 and 1,000 milliseconds, because the first sequence already showed that these latencies affect the performance intolerably. Instead, we used different combinations of  $L_1$  and  $L_2$  to simulate the combined latencies of 400 and 500 milliseconds.

## RESULTS

Our first finding was that the results are very reproducible, although interindividual differences exist. Table 1 shows the results for task A with different constant latencies. When the latency was set to 0 the test persons needed, on average, 64 seconds to complete task A. Our expectation was that this time would increase by 10 seconds for each additional 250 milliseconds of latency (250 ms/number  $\times$  40 numbers/task = 10 s/task). This prediction is shown as the dotted line in Fig 3. The figure shows that with 250 milliseconds latency the test persons performed the task actually faster than predicted, whereas latencies of 400 milliseconds

Table 1. Average Times Required to Complete Task A With Simulated Constant Latency

Latency (ms)	0	250	500	750	1000
Linear prediction (s)	63.8	73.8	83.8	93.8	103.8
Time required (s)	63.8	71.2	87	101	116.2
Standard deviation (s)	3.35	4.87	7.35	10.20	7.89

NOTE.  $n = 5$ .

and above result in a worse-than-predicted performance. This difference is statistically significant (the times required to complete task A, normalized to the predicted value, differ for the latencies 250 milliseconds and 500 milliseconds with  $P = .019$  in paired  $t$  test).

With the composite delay, the results were almost identical (Table 2 and Fig 4). An interesting observation was that there is no significant difference between the different combinations of  $L_1$  and  $L_2$  and an equivalent constant latency of ( $L_1 + L_2$ ). This indicates that although the variable latency  $L_1$  delays the packets on average only by  $L_1 \times 0.5$ , the effect on the performance in task A is the same as that of a constant delay of  $L_1$ .

The tests with task B showed a sharp increase in the number of errors for latencies above 400 milliseconds (Fig 5). In these tests, there was no significant difference in the number of errors between the sum of  $L_1$  and  $L_2$  and an equivalent constant delay, except for the 750-millisecond delay (Table 3).

## DISCUSSION

Our results show that when performing complex audiovisual communication tasks dissociation between the visual and the audible input caused by network latencies results in possible communica-

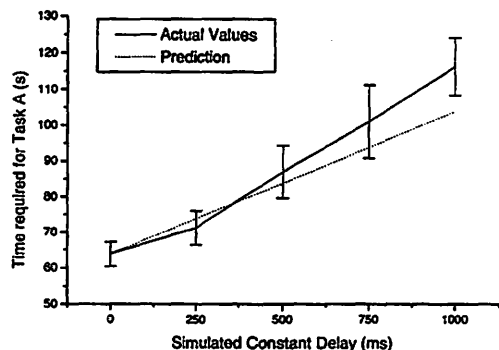


Fig 3. Results for task A with simulated constant delay (solid line). The predicted values are shown as a dotted line.

**Table 2. Average Times Required to Complete Task A With Simulated Composite Latency**

	250	400	500	200	300	400	500
Total latency (ms)	250	400	500	200	300	400	500
Variable latency ( $L_1$ , ms)	249	250	249	100	200	300	400
Constant latency ( $L_2$ , ms)	1	150	251	100	100	100	100
Linear prediction (s)	73.8	79.8	83.8	71.8	75.8	79.8	83.8
Time required (s)	72.4	79.2	88.6	68.8	74.4	82.4	89.6
Standard deviation (s)	5.32	6.18	5.68	4.38	4.62	4.34	6.66

NOTE. N = 5.

tion errors and slower performance of the human operators. Latencies below 300 milliseconds are barely noticeable by the test persons, which is reflected in the better-than-predicted performance for the 250-millisecond latency. A possible explanation for this phenomenon is that 300 milliseconds are close to the reaction time for voice commands.

When the latency exceeds 400 milliseconds, the performance becomes increasingly worse than what could be predicted by simply adding the cumulated latency to the original performance. This coincides with a subjective loss of confidence expressed by the test persons.

This also is true for variable latencies that are caused by the Nagle algorithm. Our results suggest that regarding the operator performance, the effects of the Nagle algorithm are identical to a constant latency of the same magnitude as the maximum latency of the Nagle algorithm (usually 300 milliseconds). We proved this finding by performing an additional test series for task A with the TCP protocol instead of the UDP protocol, without additional simulated latency. The average time

required for task A under these conditions was  $77.2 \pm 5.36$  seconds, which is slightly longer than with a 300-millisecond constant delay (compare Table 2).

This is important insofar that when TCP is used as the communication protocol for teleradiology applications, the Nagle algorithm will impose a minimum effective latency of 300 milliseconds, which adds to any unavoidable latency caused by the physical network. Under these conditions, the remaining headroom to keep the total latency under 400 milliseconds becomes very narrow.

It could be debated whether the test tasks that we used are an adequate simulation of real-world teleradiology and whether the effects of the network latency on the performance will be the same under real-world conditions. Our results show that the test persons could compensate for very long latencies by increasing their concentration and by slowing the verbal communication. Although these mechanisms can maintain the communication, they also may lead to increased fatigue and a loss of confidence.

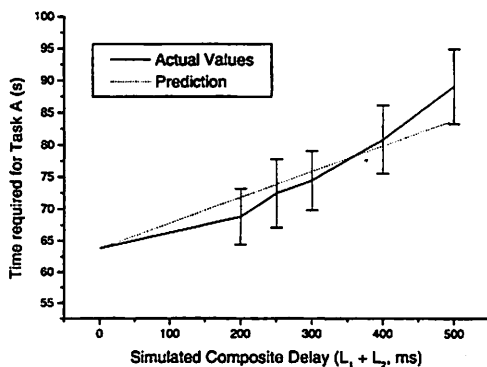


**Fig 4. Results for task A with simulated composite latency (solid line). The predicted values are shown as a dotted line. Please note the different scale of the x-axis compared with Fig 3. The values for the different combinations of  $L_1$  and  $L_2$  are combined in this graph, because they do not differ significantly.**

## CONCLUSION

Interconnected public networks such as the Internet can be a useful tool for teleradiology applica-

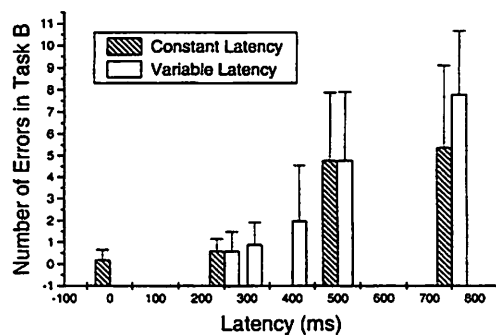


**Fig 5. Number of errors (incorrect numbers out of 10 total numbers) encountered during task B, depending on the network latency.**

**Table 3. Average Number of Errors (Incorrect Numbers out of 10) Encountered During Task B for Constant Latencies (left,  $L_1 = 0$ ) and Composite Latencies (right,  $L_1 > 0$ )**

Total latency (ms)	0	250	500	750	250	300	400	500	750
Variable latency ( $L_1$ , ms)	N/A	N/A	N/A	N/A	200	250	250	250	250
Constant latency ( $L_2$ , ms)	0	250	500	750	50	50	150	250	500
Average no. of errors	0.2	0.6	4.8	5.4	0.6	0.9	2	4.8	7.8
Standard deviation	0.45	0.89	3.11	3.71	0.55	1.02	2.55	3.09	2.86

NOTE. N = 5.

tions in many regards. However, the designers of such applications should be aware of the potential pitfalls. We could show that network latencies above 400 milliseconds could significantly degrade the performance of teleradiology users in simulated tasks. Because the Nagle algorithm used by TCP/IP implementations already imposes a latency of about 300 milliseconds, the recommended 400 milliseconds can be exceeded under certain network conditions.

Although future implementations of the Internet such as the Next-Generation Internet (NGI) certainly will provide faster performance and minimized latency, it is nevertheless our conclusion that for optimum performance, the Nagle algorithm should be bypassed in teleradiology applications, if possible. This can be done by either disabling the algorithm, which some socket implementations

allow, or by using the UDP protocol instead of TCP for the remote cursor. The latter approach, although more efficient, requires additional strategies to compensate for possible packet loss or packet reordering that can occur with UDP communication.

#### REFERENCES

1. Wood FB, Cid VH, Siegel ER: Evaluating internet end-to-end performance: Overview of test methodology and results. *J Am Med Inform Assoc* 5:528-545, 1998
2. Nagle J: Congestion control in IP/TCP internetworks. Internet Engineering Task Force (IETF) RFC 896, <http://www.ietf.org/rfc/rfc0896.txt>, 1984
3. Zhang J, Stahl JN, Song KS, et al: Real-time teleconsultation with high resolution and large volume medical imaging, in Horii SC, Blaine GJ (eds): *Medical Imaging*. San Diego, CA, SPIE, 1998(3339), pp 185-190

# Three-Dimensional Image Compression with Wavelet Transforms

Jun Wang  
Collabria

H. K. Huang  
Children's Hospital of  
Los Angeles/University  
of Southern California

1	Background . . . . .	851
2	Wavelet Theory . . . . .	851
	2.1 Basic Wavelet Theory and Multiresolution Analysis • 2.2 One-, Two-, and Three-Dimensional Wavelet Transform	
3	Three-Dimensional Image Compression with Wavelet Transform . . . . .	853
	3.1 Block Diagrams • 3.2 Mathematical Formulation of the Three-Dimensional Wavelet Transform • 3.3 Wavelet Filter Selection • 3.4 Quantization • 3.5 Entropy Coding	
4	Wavelet Filter Selection for a 3D Image Data Set . . . . .	855
	4.1 3D CT and MR Volume Data Sets • 4.2 Wavelet Filters for 2D Slice • 4.3 Wavelet Filters for the Interslice Direction • 4.4 Comparison of 2D Wavelets, 3D Wavelets, and JPEG	
	References . . . . .	861

## 1 Background

Image compression can be performed in the original spatial domain or in a transform domain. In the latter case, the image is first transformed, and a subsequent compression operation is applied in the transform domain. An example is the conventional cosine transform method used in the standard JPEG (Joint Photographic Experts Group) algorithm. The use of the wavelet transform for image compression has drawn significant attention since the publication of the works by Daubechies [1] and Mallat [2]. The primary advantage of the wavelet transform compared with the cosine transform is that the wavelet transform is localized in both the spatial and frequency domains; therefore, the transformation of a given signal will contain both spatial and frequency information of that signal. On the other hand, the cosine transform basis extends infinitely, with the result that the spatial information is spread out over the whole frequency domain. Because of this property, wavelet image compression has shown promising results on medical images. Although compression techniques are mainly applied to two-dimensional (2D) images, the increasing availability of three-dimensional (3D) CT and MR volume data sets raises the need for 3D compression techniques [3,4]. This chapter presents compression with 3D wavelet transforms and discusses the selection of wavelet filters. The

compression outcomes of 3D data sets with JPEG and 2D wavelet transform are also compared to the compression obtained with the 3D wavelet transform approach.

## 2 Wavelet Theory

### 2.1 Basic Wavelet Theory and Multiresolution Analysis

Image transformation relies on using a set of basis functions on which the image is projected to form the transformed image. In the cosine transform, the basis functions are a series of cosine functions and the resulting domain is the frequency domain. In the case of the wavelet transform, the basis functions are derived from a mother wavelet function by dilation and translation. In the one-dimensional (1D) wavelet transform the basis functions are obtained using the mother wavelet function  $\psi(x)$  such that

$$\psi_{a,b}(x) = \frac{1}{\sqrt{a}} \psi\left(\frac{x-b}{a}\right), \quad (1)$$

where  $a$  and  $b$  are the dilation and translation factors,

respectively. The continuous wavelet transform of a function  $f(x)$  is expressed as

$$F_w(a, b) = \frac{1}{\sqrt{a}} \int_{-\infty}^{\infty} f(x) \psi^* \left( \frac{x-b}{a} \right) dx, \quad (2)$$

where  $*$  is the complex conjugate operator.

The basis functions given in Eq. (1) are redundant when  $a$  and  $b$  are continuous. It is possible, however, to discretize  $a$  and  $b$  so as to form an orthonormal basis. One way of discretizing  $a$  and  $b$  is to let  $a = 2^p$  and  $b = 2^p q$ , so that Eq. (1) becomes

$$\psi_{p,q}(x) = 2^{-p/2} \psi^*(2^{-p}x - q), \quad (3)$$

where  $p$  and  $q$  are integers. The wavelet transform in Eq. (2) then becomes

$$F_w(p, q) = 2^{-p/2} \int_{-\infty}^{\infty} f(x) \psi^*(2^{-p}x - q) dx \quad (4)$$

Since  $p$  and  $q$  are integers, Eq. (4) is called a wavelet series. This representation indicates that the wavelet transform contains both spatial and frequency information.

The wavelet transform also relies on the concept of multi-resolution analysis, which decomposes a signal into a series of smooth signals and their associated detailed signals at different resolution levels. The smooth signal at level “ $m$ ” can be reconstructed from the “ $m+1$ ” level smooth signal and the associated “ $m+1$ ” detailed signals.

## 2.2 One-, Two-, and Three-Dimensional Wavelet Transform

We use the 1D case to discuss the concept of multiresolution analysis. Consider the discrete signal  $f_m$  at level  $m$ , which can be decomposed into the  $m+1$  level by convolving it with the  $h$  (low pass) filter to form a smooth signal  $f_{m+1}$  and  $g$  (high pass) filter to form a detailed signal  $f'_{m+1}$ , respectively, as shown in Fig. 1. This can be represented with the following equations using the pyramidal algorithm suggested by Mallat [2]:

$$\begin{aligned} f_{m+1}(n) &= \sum_k h(2n-k) f_m(k) \\ f'_{m+1}(n) &= \sum_k g(2n-k) f_m(k). \end{aligned} \quad (5)$$

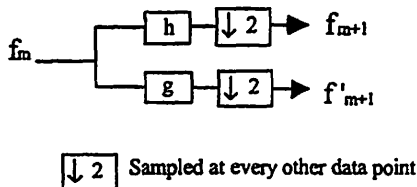


FIGURE 1 Decomposition of a signal  $f_m$  into a smooth  $f_{m+1}$  and a detailed signal  $f'_{m+1}$ .

Here,  $f_{m+1}$  is the smooth signal and  $f'_{m+1}$  is the detailed signal at the resolution level  $m+1$ . The total number of discrete points in  $f_m$  is equal to that of the sum of  $f_{m+1}$  and  $f'_{m+1}$ . For this reason, both  $f_{m+1}$  and  $f'_{m+1}$  have to be sampled at every other data point after the operation described in Eq. (5). The same process can be further applied to  $f_{m+1}$ , creating the detailed and smooth signal at the next resolution level, until the desired level is reached.

Figure 2 depicts the components resulting from three levels of decompositions of the signal  $f_0$ . The horizontal axis indicates the total number of discrete points of the original signal, and the vertical axis is the level,  $m$ , of the decomposition. At the resolution level  $m=3$ , the signal is composed of the detailed signals of the resolution levels  $f'_1$ ,  $f'_2$ , and  $f'_3$  plus one smooth signal  $f_3$ . Signals at each level can be compressed by quantization and encoding methods to achieve the required compression ratio. Accumulation of these compressed signals at all levels can be used to reconstruct the original signal  $f_0$ .

In the case of the 2D transform, the first level will result in four components, the  $x$ -direction and the  $y$ -direction (see Fig. 4, left and middle). Figure 3 shows a two-level wavelet decomposition of a head MR image.

Three-dimensional wavelet transforms can be computed by extension of the 1D and 2D pyramidal algorithm, since the multidimensional wavelet transform can be formulated to be separable. One level of the decomposition process from  $f_m$  to  $f_{m+1}$  is shown in Fig. 4. First, each line in the  $x$ -direction of the 3D image data set is convolved with filters  $h$  and  $g$ , followed by subsampling every other voxel in the  $x$ -direction to form the smooth and detailed data lines. The resulting voxels are convolved with  $h$  and  $g$  in the  $y$ -direction, followed with subsampling in the  $y$ -direction. Finally, the same procedure is applied to the  $z$ -direction. The resulting signal has eight components. Since  $h$  is a low-pass filter, only one component,  $f_{m+1}$ , contains all low frequency information. The rest of the seven components convolve at least once with the high-pass filter  $g$ , and therefore contain the detailed signals  $f'_{m+1}$  in different directions.

The same process can be repeated for the low-frequency signal  $f_{m+1}$ , to form the next level of wavelet transform, and so forth, until the desired level is reached.

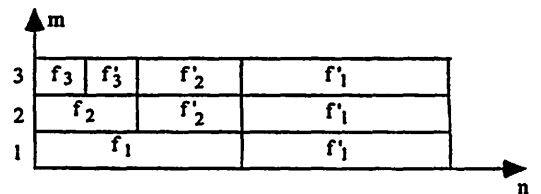


FIGURE 2 A three-level wavelet decomposition of a signal.

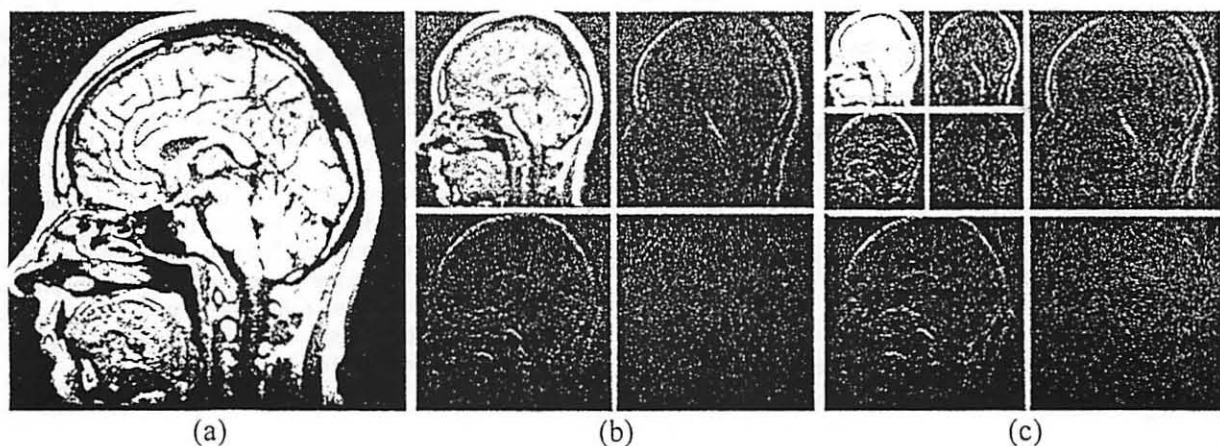


FIGURE 3 Wavelet decomposition of a MR image. (a) Original; (b) one-level decomposition; (c) two-level decomposition. In each level, the left upper corner shows the smooth image; the other three quadrants are the detailed images.

### 3 Three-Dimensional Image Compression with Wavelet Transform

#### 3.1 Block Diagrams

The wavelet transform is a very effective method for compressing a 3D medical image data set yielding a high compression ratio image with good quality. Figure 5 shows the block diagrams of 3D wavelet transform compression and decompression. In the compression process, a 3D wavelet transform is first applied to the 3D image data set, resulting in a 3D multiresolution representation of the image. Then the wavelet coefficients are quantized using scalar quantization. Finally, run-length and

Huffman coding are used to impose entropy coding on the quantized data. These steps are described in Section 4.

The decompression process is the inverse of the compression process. The compressed data are first entropy decoded, a dequantization procedure is applied to the decoded data, and the inverse 3D wavelet transform is used, resulting in the reconstructed 3D image data.

#### 3.2 Mathematical Formulation of the Three-Dimensional Wavelet Transform

The 3D wavelet transform is based on a scaling function  $\phi$  and seven wavelet functions  $\Psi$ . All eight functions are separable,

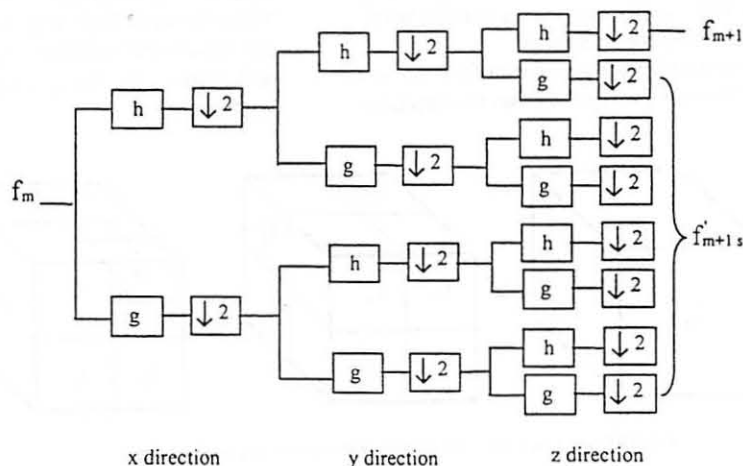


FIGURE 4 Three-dimensional wavelet decomposition.

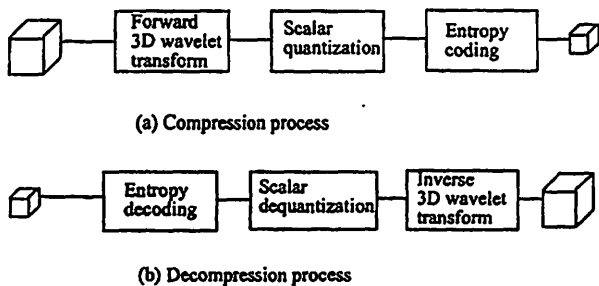


FIGURE 5 Block diagrams of image compression and decompression using the 3D wavelet transform.

that is, they can be expressed by the product of three 1D functions, one for each dimension. The scaling function has the form

$$\Phi = \phi(x)\phi(y)\phi(z), \quad (6)$$

where  $\phi(x)$ ,  $\phi(y)$ , and  $\phi(z)$  contain the low-pass filter  $h$  in the  $x$ ,  $y$ , and  $z$  directions, respectively (see Eq. (5)).

The seven wavelet functions have the form

$$\begin{aligned} \Psi^1(x, y, z) &= \phi(x)\phi(y)\psi(z), \\ \Psi^2(x, y, z) &= \phi(x)\psi(y)\phi(z), \\ \Psi^3(x, y, z) &= \psi(x)\phi(y)\phi(z), \\ \Psi^4(x, y, z) &= \phi(x)\psi(y)\psi(z), \\ \Psi^5(x, y, z) &= \psi(x)\phi(y)\psi(z), \\ \Psi^6(x, y, z) &= \psi(x)\psi(y)\phi(z), \\ \Psi^7(x, y, z) &= \psi(x)\psi(y)\psi(z), \end{aligned} \quad (7)$$

where  $\psi(x)$ ,  $\psi(y)$ , and  $\psi(z)$  contain the high-pass filter  $g$  in the  $x$ ,  $y$ , and  $z$  directions, respectively. During each level of the transform, the scaling function and the seven wavelet functions are applied, respectively, to the smooth (or the original) image at that level, forming a total of eight images, one smooth and seven detailed images. The wavelet coefficients are the voxel values of the eight images after the transform.

Figure 6 shows two levels of 3D wavelet transform on an image volume data set. The first level decomposes the data into

eight components:  $f_1$  is the low (smooth) resolution portion of the image data, and the remaining blocks are high (detailed) resolution components. As Fig. 6 indicates,  $f_1$  can be further decomposed into eight smaller volumes labeled  $f_2$  and  $f_2'$ s. The detailed images  $f_1'$  on level 1 contain higher frequency components than those  $f_2'$  of level 2.

With properly chosen wavelet functions, the low-resolution component in the  $m$  level is  $1/(2^3)^m$  of the original image size after the transformation, but contains about 90% of the total energy in the  $m$  level. It is clear that the high-resolution components are spread into different decomposition levels. For these reasons, the wavelet transform components provide an efficient representation of the original image for compression purposes. Different levels of representation can be encoded differently to achieve a desired compression ratio.

### 3.3 Wavelet Filter Selection

The selection of wavelet filters is a crucial step that dictates the performance of image compression. A good filter bank should be reasonably fast, should provide a transform where most of the energy is packed in a small number of coefficients, and should not introduce distortions. The following characteristics address these points.

- (1) *Compact support*: Compact support wavelets and scaling functions have values inside a finite range and are zero outside the range, therefore they can be implemented with finite impulse response (FIR) filters. Since filtering with FIR filters is generally much faster than filtering with infinite impulse response (IIR) filters, compact support wavelets provide fast processing.
- (2) *Smoothness*: The smoothness of a wavelet is commensurate with the highest order at which its moment vanishes such that  $\int x^m \psi(x) dx = 0$  for  $m = 0, 1, \dots, N - 1$ . Wavelets with high degree of smoothness minimize distortions and will likely lead to better representation with most of the energy packed in a smaller number of coefficients.

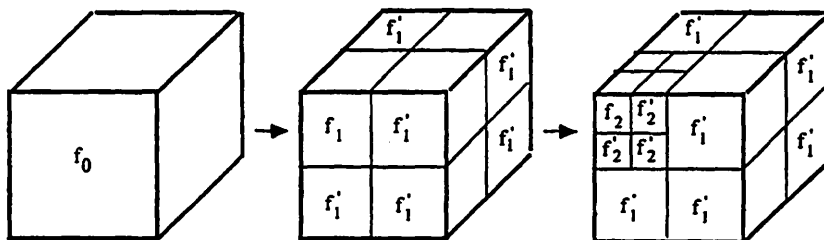


FIGURE 6 A two-level 3D wavelet transform on an image volume data set.

- (3) *Symmetry*: Symmetry is a desirable characteristic of a filter because it provides a linear phase in the frequency response of the filter. Filters with linear phase will produce less distortion.
- (4) *Filter length*: A short filter allows fast computation of the wavelet transform, but smoothness is obtained with long filters. Image compression is based on a trade-off between the filter length and compression performance. In general, the following types of wavelet filters perform well for 3D MR and CT images
- (a) Daubechies orthogonal wavelet from D4–D20 [1]
  - (b) Coiflet filters [5]
  - (c) Biorthogonal wavelet filters [6–8].

### 3.4 Quantization

The second step of compression is quantization. The purpose of quantization is to map a large number of input values into a smaller set of output values by reducing the precision of the data. This is the step in which information may be lost. Wavelet transformed data are floating-point values and consist of two types: low-resolution image components, which contain most of the energy, and high-resolution image components, which contain the information from sharp edges.

Since the low-resolution components contain most of the energy, it is important to maintain the integrity of this component of the data. To minimize data loss in this portion, each floating-point value can be mapped to its nearest integer neighbor (NINT). In the high-resolution components of the wavelet coefficients, there are many coefficients of small magnitude that correspond to the flat areas in the original image. These coefficients contain very little energy, and we can eliminate them without creating significant distortions in the reconstructed image. A threshold number  $T_m$  is chosen, such that any coefficient smaller than  $T_m$  will be set to zero. Above the threshold  $T_m$ , a range of floating-point values will be mapped into a single integer. An example of quantization for high-frequency coefficients is

$$a_q(i, j, k) = NINT \left[ \frac{a(i, j, k) - T_m}{Q_m} \right], \quad a(i, j, k) > T_m$$

$$a_q(i, j, k) = 0; \quad -T_m \leq a(i, j, k) \leq T_m$$

$$a_q(i, j, k) = NINT \left[ \frac{a(i, j, k) + T_m}{Q_m} \right], \quad a(i, j, k) < -T_m, \quad (8)$$

where  $a(i, j, k)$  is the wavelet coefficient in three dimensions,  $a_q(i, j, k)$  is the quantized wavelet coefficient,  $m$  is the number of the level in the wavelet transform, and  $Q_m = Q2^{m-1}$ , with  $Q$  being a selected constant. The threshold  $T_m$  can be set as a constant for all levels or it can be a function of  $m$ . After

quantization each coefficient will take an integer value within a finite range.

### 3.5 Entropy Coding

In the third step, the quantized coefficients are subjected to run-length coding followed by Huffman coding. Run-length coding examines consecutive quantized coefficients and determines sequences made of coefficients that have the same value. Each sequence is represented by the common value and the number of coefficients in the run, resulting in considerably more compact information compared to the entire sequence of coefficients [9]. In the quantization process, thresholding of the high-frequency components results typically in a large number of zeroes, and run-length coding can be expected to reduce the size of data significantly. After run-length coding, the data can be further compressed if each value of the data stream is represented with a new code that minimizes the total number of bits in the data. When values are considered one at a time, Huffman coding is the optimal technique for this process [9]. It assigns to each value a new code with a varying number of bits, such that values that appear frequently in the data are coded with a small number of bits, whereas those that appear infrequently can be coded with larger number of bits. Typically, a significant level of data reduction can be obtained with Huffman coding.

## 4 Wavelet Filter Selection for a 3D Image Data Set

### 4.1 3D CT and MR Volume Data Sets

The performance of a filter set also depends on image characteristics. The smoothness, sharpness, and noise of an image affect the compression performance of a filter set [10]. For a three-dimensional image set, the image characteristics may differ within 2D slices and in the interslice direction. A uniform 3D wavelet may not provide the best performance because the correlation of pixels within a slice is different from that between slices. Typically, the distance of adjacent pixels within a slice varies from 0.3 to 1.2 mm, whereas the distance between slices can be much higher. Each slice has a certain thickness and two adjacent slices are separated by a gap. We define the slice distance to be the sum of the slice gap and slice thickness. Typically, the slice distance varies from 1 to 10 mm for CT images and from 1.5 to 8 mm for MR images. Hence, the optimal wavelet filter set within slices (in the  $x$  and  $y$  directions) may not be the same as the optimal wavelet filter set in the slice ( $z$ ) direction.

Image characteristics such as resolution, noise, and sharpness are determined by anatomy and image modality. Tables 1

TABLE 1 Selected CT image sets for evaluating wavelet filters

Anatomy	Pixel size (mm)	Pixel size (mm)
Abdomen	0.66	0.83
Brain	0.39	0.43
Chest	0.66	0.94
Spine	0.29	0.43

and 2 show CT and MR image sets, respectively, selected to test the performance of wavelet filters on images with different modality, anatomy, technique of acquisition, and pixel size.

The smoothness of an image  $f(x, y)$  can be quantified using the autocorrelation function defined as

$$c(m, n) = \sum_x \sum_y f^*(x, y) \cdot f(x + m, y + n), \quad (9)$$

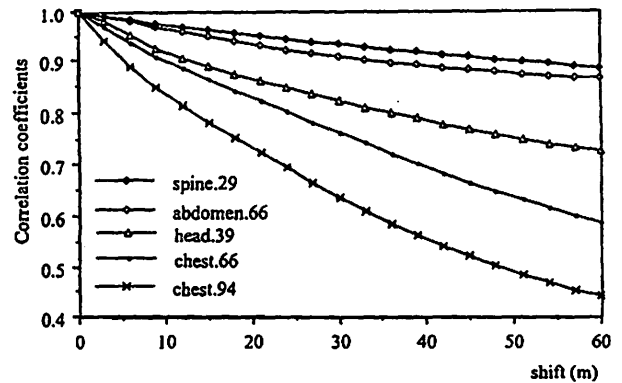
where  $*$  stands for the complex conjugate, and  $m$  and  $n$  are integers that define the spacing (lag) between pixels in the  $x$  and  $y$  directions, respectively. The correlation coefficients are defined as

$$cc(m, n) = \frac{c(m, n)}{c(0, 0)}. \quad (10)$$

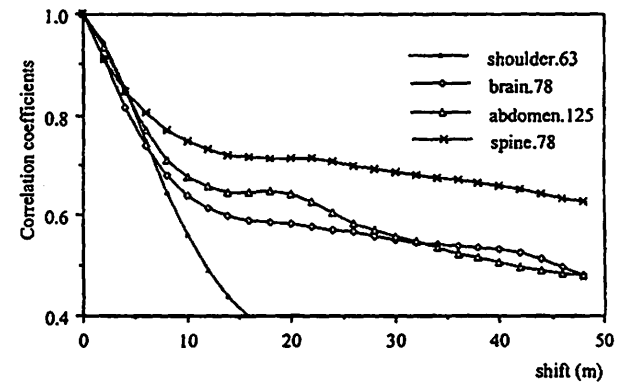
Figure 7 shows the correlation coefficients as a function of  $m$  when  $n = 0$ , i.e.,  $cc(m, 0)$ , for the sample images stated in Tables 1 and 2. A larger correlation indicates that adjacent pixels are more likely to have similar values. Images with higher correlation coefficients generally have lower high-frequency components, have fewer sharp edges, and appear smoother.

For CT images (Fig. 7a) the correlation coefficients of the spine and abdomen images are much larger than those of the head and chest images. Therefore, spine and abdomen images are comparatively smoother and have lower high-frequency components. In general, an image with a smaller pixel size has higher correlation coefficients than the one with a larger pixel size for the same anatomy. For example, the chest image with 0.66-mm pixel size (chest.66) has higher correlation coefficients than the chest image with 0.94-mm pixel size (chest.94) in Fig. 7a.

For most MR images (Fig. 7b), the correlation coefficients are very close in value when the shift,  $m$ , is small. In general, for the same pixel shift, CT images have larger correlation



(a)



(b)

FIGURE 7 Correlation coefficients of sample images: (a) CT, (b) MR.

coefficients than MR images because CT images are often smoother than MR images.

## 4.2 Wavelet Filters for 2D Slice

Five wavelet filters that provide a good trade-off between compression quality, compression ratio, and computational efficiency are given in Table 3. The first column in Table 3 indicates the type of the filter bank and the number of the

TABLE 2 Selected MR image sets for evaluating wavelet filters

Anatomy	Pixel size (mm) T1 weighted	Pixel size (mm) T1 weighted	Pixel size (mm) T2 weighted
Abdomen	0.84	1.25	***
Brain axial	0.78	1.17	***
Brain coronal	0.78	1.17	***
Knee	0.55	***	0.55
Shoulder	0.55	***	0.63
Spine	0.70	1.10	0.78

**TABLE 3** Five best wavelet filters for CT and MR image compression<sup>a</sup>

Filter banks	Filter coefficients
9/7	$h_0$ 0.026749, -0.016864, -0.078223, 0.266864, 0.602949, 0.266864, -0.078223, -0.016864, 0.026749 $g_0$ 0.045636, -0.028772, -0.295636, 0.557543, -0.295636, -0.028772, 0.045636
13/11	$h_0$ -0.00599119, 0.00265816, 0.03343325, -0.02367046, -0.04870418, 0.27101229, 0.54252426, 0.27101229, -0.04870418, -0.02367046, 0.03343325, 0.00265816, -0.00599119 $g_0$ 0.01002830, 0.00444934, -0.07688893, -0.04890542, 0.31686063, 0.58891216, 0.31686063, -0.04890542, -0.07688893, 0.00444934, 0.01002830
17/11	$h_0$ 0.00134975, -0.00135360, -0.01201420, 0.00843901, 0.03516647, -0.05463331, -0.06650990, 0.29754791, 0.58401575, 0.29754791, -0.06650990, -0.05463331, 0.03516647, 0.00843901, -0.01201420, -0.00135360, 0.00134975 $g_0$ 0.01020092, 0.01023007, -0.05566486, -0.02854447, 0.29546394, 0.53662880, 0.29546394, -0.02854447, -0.05566486, 0.01023007, 0.01020092
Daubechies20	0.026670057901, 0.188176800078, 0.527201188932, 0.688459039454, 0.281172343661, -0.249846424327, -0.195946274377, 0.127369340336, 0.093057364604, -0.071394147166, -0.029457536822, 0.033212674059, 0.003606553567, -0.010733175483, 0.001395351747, 0.001992405295, -0.000685856695, -0.000116466855, 0.000093588670, -0.000013264203
Coiflet 6	-0.00169185102, -0.00348787622, 0.01919116068, 0.02167109464, -0.09850721332, -0.05699742448, 0.45678712217, 0.78931940900, 0.38055713085, -0.07043874879, -0.056514193868, 0.03640996261, 0.00876013071, -0.01119475927, -0.001921335414, 0.00204138098, 0.00044583040, -0.00021625728, 0.0004458303975, -0.00021625728

<sup>a</sup>The first three are biorthogonal and the last two are orthogonal.

coefficients. The first three filter banks are biorthogonal, and the last two are orthogonal. The second column in Table 3 presents the filter coefficients. For the biorthogonal filter banks, both low-pass  $h_0$  and high-pass  $g_0$  filters are listed. For the orthogonal filter banks, only the low-pass coefficients are given since the high-pass filter can be easily obtained from the low-pass filter using the orthogonality property as follows:

$$\begin{aligned}
 g(j) &= (-1)^j h(1-j) \\
 \sum_j h(j) &= \sqrt{2} \\
 \sum_j g(j) &= 0.
 \end{aligned}
 \tag{12}$$

The performance of the wavelet filters listed in Table 3 was evaluated using the sample images described in Tables 1 and 2. The quality of the compression is often measured with the root-mean-square error (RMSE) between the original image  $f(x, y, z)$  and the image  $f_c(x, y, z)$  reconstructed after compression such that

$$\text{RMSE} = \left\{ \frac{\sum_{x,y,z} [f(x, y, z) - f_c(x, y, z)]^2}{N} \right\}^{1/2}, \tag{11}$$

where  $N$  is the total number of pixels in the image.

The comparative study indicated that compression was similar with all five filters, but the three biorthogonal filter banks slightly outperformed the orthogonal filter banks.

### 4.3 Wavelet Filters for the Interslice Direction

#### Sample Images for Evaluation of Wavelet Filters

Since the pixel sizes in the  $x$  and  $y$  directions are very different from the slice distances, the best filter bank used in the slice direction may be different from that of the  $x$  and  $y$  directions. The best filters for the interslice direction were determined using 12 different 3D image data sets from various anatomical and imaging modalities as described in Table 4. The first column in the table is the name for each image set where the first two letters represent the image modality and the next two letters represent the anatomy. The last letter, a or c, in the MR sets stands for axial or coronal, respectively. As indicated in the fourth column, the slice distance varies from 1 to 7 mm.

#### Evaluation of Wavelet Filter Banks

With a fixed filter bank in the  $x$  and  $y$  directions, for example, the 9/7, the performance of different wavelet filters can be evaluated by applying them to the  $z$ -direction of the 3D image sets described in Table 4. The three best filters for the  $z$  direction were the 9/7, Daubechies4 (D4) [1], and Haar [11]. Figure 8 shows an example of the compression results for two different CT knee image sets at 1-mm and 5-mm slice distances. The two image sets were from the same patient, but two different studies. The compression ratios obtained by applying the 9/7 wavelet to the image set with a 1-mm slice distance were better than those of the D4 and Haar (Fig. 8a). In contrast, the Haar wavelet seems to perform better for image sets with 5-mm slice distances (Fig. 8b). This figure also indicates that for the same RMSE, thinner slice distances yield a higher compression ratio.

TABLE 4 MR and CT image sets with various slice thicknesses for evaluation of wavelet filters in the z-direction

Image	Modality	Anatomy	Slice distance (mm)	Pixel distance (mm)	# of slices
CTBR1	CT	Brain	1	0.41	51
CTBR3	CT	Brain	3	0.43	31
CTBR5	CT	Brain	5	0.41	24
CTKE1	CT	Knee	1	0.43	151
CTKE5	CT	Knee	5	0.43	31
CTSP3	CT	Spine	3	0.39	69
CTCH7	CT	Chest	7	0.74	43
MRBR1.5-a	MR	Brain-axial	1.5	1.02	124
MRBR3-a	MR	Brain-axial	3	1.17	47
MRBR6-a	MR	Brain-axial	6	0.78	26
MRBR4-c	MR	Brain-coronal	4	1.17	45
MRBR6-c	MR	Brain-coronal	6	0.78	28

#### 4.4 Comparison of 2D Wavelets, 3D Wavelets, and JPEG

This section presents some compression results using two 3D image data sets. The first is a 3D MR brain data set obtained with a GE 5x Sigma Scanner with 26 images and a slice distance of 6 mm. Each image is 256 × 256 × 12 bits. The second set is a 3D CT spine from a GE CT scanner with 69 images and a slice distance of 3 mm. Each image is 512 × 512 × 12 bits. The 3D wavelet, 2D wavelet, and JPEG compression were applied to

each data set. The 2D wavelet compression was implemented with the 9/7 filter bank in x and y, applied to each slice. Figures 9a and 9b compare the performance of 3D wavelet and JPEG algorithms, and Figs 9c and 9d compare the 3D and 2D wavelet compression. In these curves, the compression ratio is given as a function of equivalent peak signal-to-noise ratio (EPSNR), defined as

$$EPSNR = 20 \log \frac{f_{win}}{\left\{ \frac{\sum [(x,y,z) - f_c(x,y,z)]^2}{N} \right\}^{1/2}}, \quad (13)$$

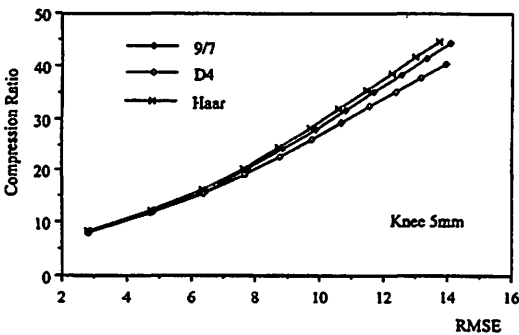
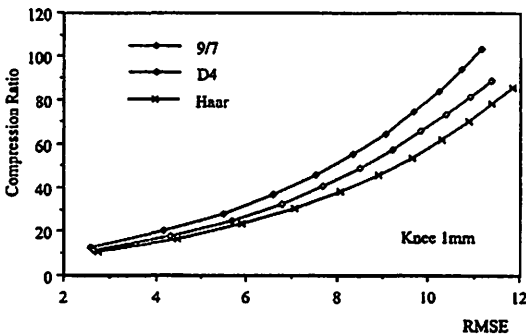
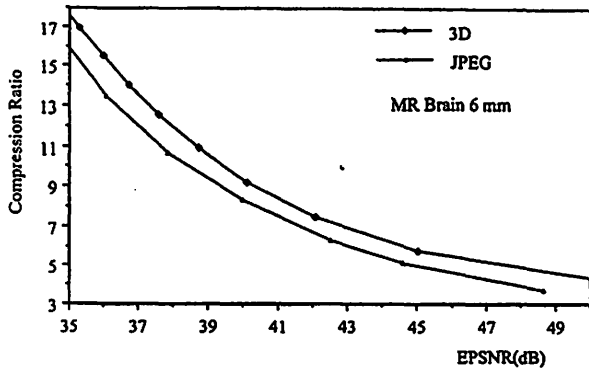


FIGURE 8 Compression ratio versus RMSE for three different filter banks in the slice direction. (a) CT knee image set with 1-mm slice distance. (b) CT knee image set with 5-mm slice distance.

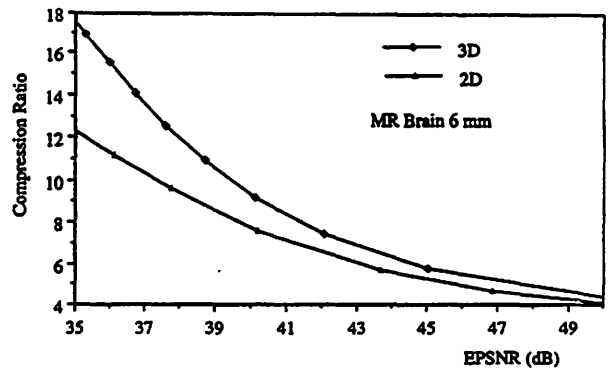
where  $f_{win}$  is the display window width of the image that depends on its modality and type of image.

Figure 10 shows the original and decompressed images of the CT spine compressed at a 20:1 ratio using the 3D wavelet, the 2D wavelet, and JPEG methods. Figures 11a, 11b, and 11c show the difference images between the original and the decompressed images for the 3D wavelet, 2D wavelet, and JPEG, respectively. In order to emphasize the differences, a window in the spine region is used (Fig. 10a). The difference images shown here have been processed by adding a gray level of 128 and multiplying by 5. The 3D difference image has the smallest visual discrepancy. The 2D difference image (Fig. 11b) shows granular noise similar to that in the 3D difference image, but with larger granules and higher amplitude. The JPEG difference image (Fig. 11c) has larger errors in high frequency regions (spine regions) than the 3D wavelet difference image. Also, the JPEG difference image clearly shows block artifacts that are typical at relatively high compression ratios with JPEG.

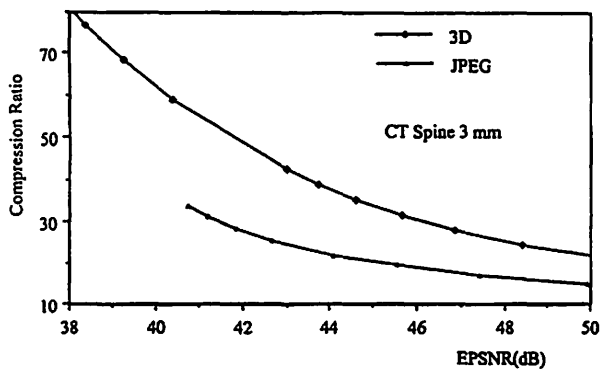
In general, the difference image of a wavelet-compressed image has uniform error in all regions. This is due to the fact that wavelets operate at multiple resolutions and the filters can accommodate the representation of small textural elements, edges as well as homogeneous regions. The 3D wavelet compression has better performance than the 2D wavelet compression because the former utilizes information in three orientations and can take advantage of the data structure and redundancies in the z direction as well.



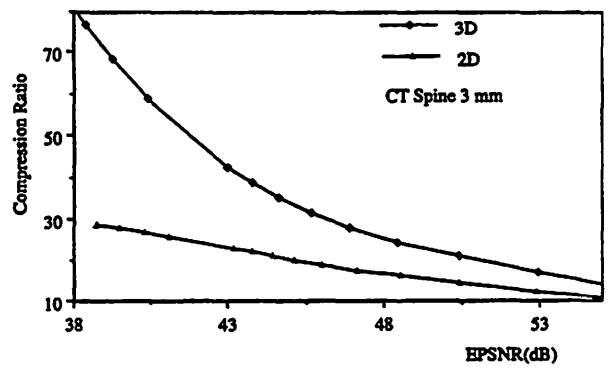
(a)



(c)



(b)



(d)

FIGURE 9 3D wavelet compression vs JPEG: (a) MR brain image set with 6-mm slice distance, (b) CT spine image set with 3-mm slice distance. 3D wavelet compression vs 2D wavelet compression: (c) MR brain image set, (d) CT spine image set.

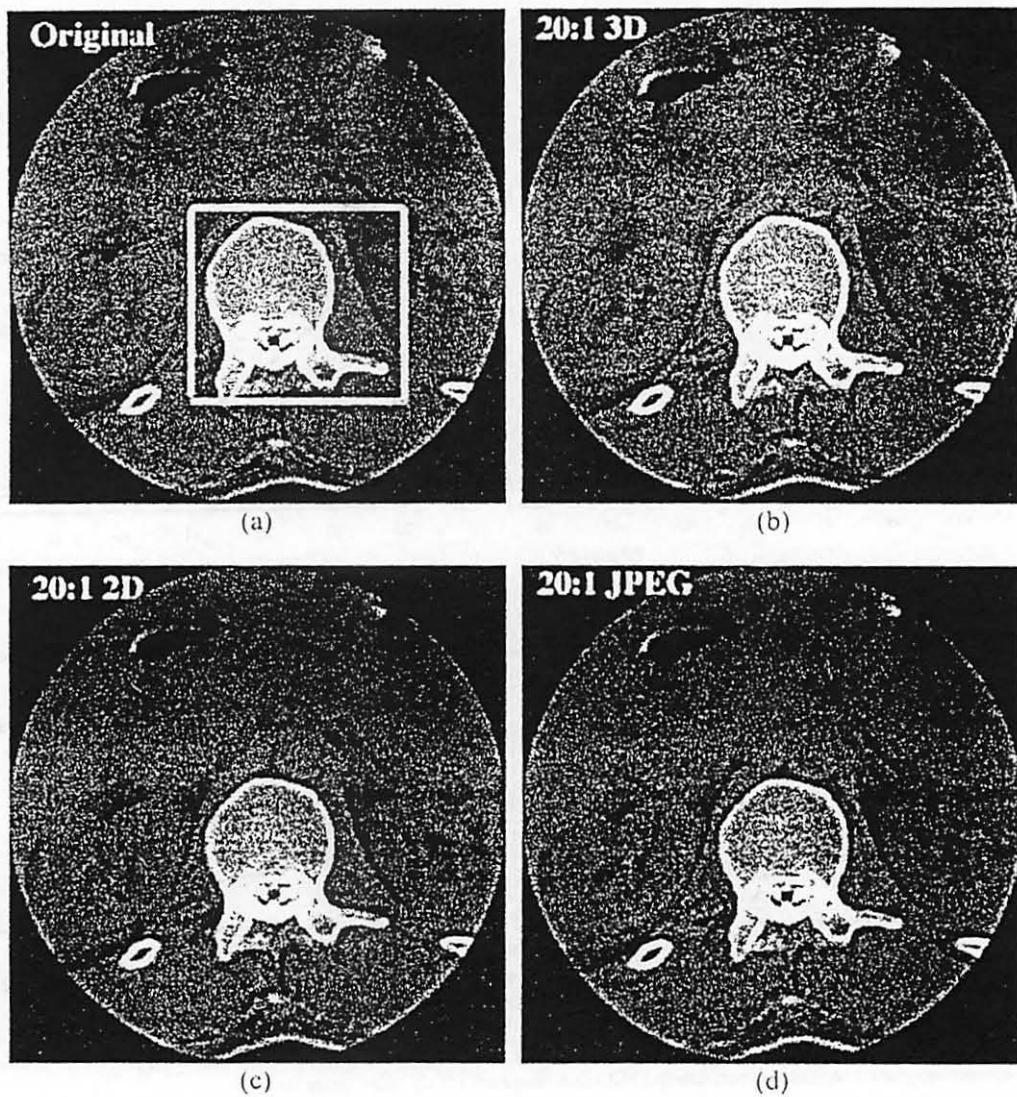


FIGURE 10 One slice of a CT image set compressed at ratio of 20:1 using the 3D and 2D wavelet algorithms and JPEG. (a) Original image, (b) compressed with the 3D wavelet method, (c) compressed with the 2D wavelet method, (d) compressed with JPEG.

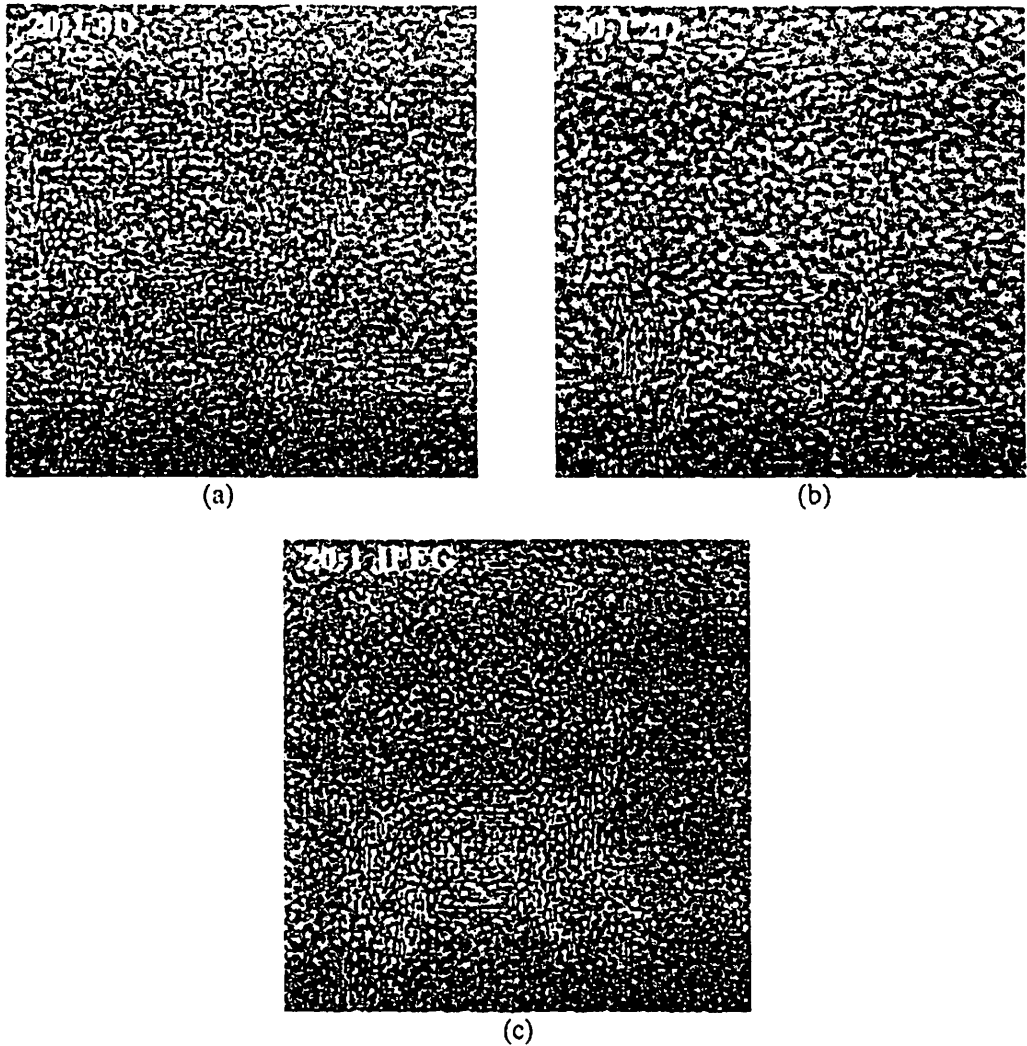


FIGURE 11 The spinal column portion of the difference images obtained after compression using (a) the 3D wavelet method, (b) the 2D wavelet method, (c) JPEG. The original image is shown in Fig. 10a within the rectangle.

## References

1. Daubechies I., "Orthonormal bases of compactly supported wavelets," *Comm. Pure Appl. Math.*, Vol. 41, pp. 909–996, 1988.
2. Mallat S. G. "A theory for multiresolution signal decomposition: the wavelet representation," *IEEE Trans. on Pattern Analysis and Machine Intelligence*, Vol. 11, No. 7, pp. 674–693, 1989.
3. Wang J., Huang H. K., "Three-dimensional medical image compression using wavelet transformation," *IEEE Trans. on Medical Imaging*, Vol. 15, No. 4, pp. 547–554, 1996.
4. Wang J., "Three-Dimensional Medical Imaging Compression Using Wavelet Transformation with Parallel Computing", Ph.D. Dissertation, UCLA, 1997.
5. Cohen A., Daubechies I., Feauveau J. C., "Biorthogonal bases of compactly supported wavelets," *Communication on Pure and Applied Mathematics*, Vol. XLV, pp. 485–560, 1992.
6. Antonini M., Barlaud M., Mathieu P., Daubechies I., "Image coding using wavelet transform," *IEEE Trans. on Image Processing*, Vol. 1, pp. 205–220, 1992.
7. Villasenor J. D., Belzer B., Liao J., "Wavelet filter evaluation for image compression," *IEEE Trans. on Image Processing*, Vol. 4, No. 8, pp. 1053–1060, 1995.

8. Lightstone M., Majani E., "Low bit-rate design considerations for wavelet-based image coding," *Proceeding of the SPIE*, Vol. 2308, pp. 501–512, 1994.
9. Gonzalez, R. C., Woods, R. E., *Digital Image Processing*, Addison-Wesley, 1992.
10. Strang G., Nguyen T., *Wavelets and Filter Banks*, Wellesley-Cambridge Press, 1995.
11. Albanesi M. G., Lotto D. I. , "Image compression by the wavelet decomposition," *Signal Processing*, Vol. 3, No. 3, pp. 265–274, 1992.

# Computer-Assisted Bone Age Assessment: Image Preprocessing and Epiphyseal/Metaphyseal ROI Extraction

Ewa Pietka, Arkadiusz Gertych, Sylwia Pospiech, Fei Cao, H. K. Huang\*, Senior Member, IEEE, and V. Gilsanz

**Abstract**—Clinical assessment of skeletal maturity is based on a visual comparison of a left-hand wrist radiograph with atlas patterns. Using a new digital hand atlas an image analysis methodology is being developed. To assist radiologists in bone age estimation. The analysis starts with a preprocessing function yielding epiphyseal/metaphyseal regions of interest (EMROIs). Then, these regions are subjected to a feature extraction function. Accuracy has been measured independently at three stages of the image analysis: detection of phalangeal tip, extraction of the EMROIs, and location of diameters and lower edge of the EMROIs. Extracted features describe the stage of skeletal development more objectively than visual comparison.

**Index Terms**—Bone age assessment, carpal bones region of interest, computer-assisted diagnosis, epiphyseal/metaphyseal region of interest, hand image processing.

## I. INTRODUCTION

**B**ONE age assessment is a procedure frequently performed in pediatric radiology. Based on a radiological examination of skeletal development of a left-hand wrist, the bone age is assessed and then compared with the chronological age. A discrepancy between these two values indicates abnormalities in skeletal development. This examination is universally used due to its simplicity, minimal radiation exposure, and the availability of multiple ossification centers for evaluation of maturity. It is an important procedure in the diagnosis and management of endocrine disorders serving as one index of therapeutic effect [1]. Being a useful procedure in the diagnostic evaluation of metabolic and growth abnormalities [2], it indicates acceleration or decrease of maturation in a variety of syndromes, malformations, and bone dysplasias [3]. Bone age assessment procedure is used for patients with gonadal dysgenesis [4] or when metacarpal sign occurs [5]. It is also applied in planning for an orthopedic procedure for correction of angular deformities or abnormalities of length involving the vertebral column or long bones.

Manuscript received June 28, 1999; revised May 10, 2001. This work was supported by the National Institutes of Health (NIH) under Grant R01-LM06270. The Associate Editor responsible for coordinating the review of this paper and recommending its publication was A. Manduca. Asterisk indicates corresponding author.

E. Pietka, A. Gertych, and S. Pospiech are with the Silesian University of Technology, Institute of Electronics, Division of Biomedical Electronics, PL -44 100 Gliwice, Poland.

F. Cao and V. Gilsanz are with the Childrens Hospital of Los Angeles, Department of Radiology, Los Angeles, CA 90027 USA.

\*H. K. Huang is with the Childrens Hospital of Los Angeles, Department of Radiology, 4650 Sunset Blvd., Los Angeles, CA 90027 USA.

Publisher Item Identifier S 0278-0062(01)06581-8.

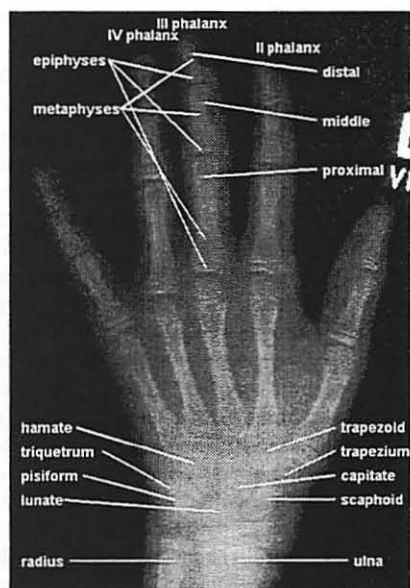


Fig. 1. Hand wrist radiograph.

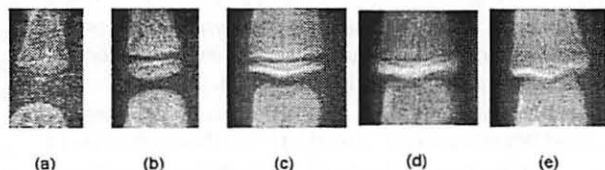


Fig. 2. Ossification centers at different stage of development.

Bone age assessment is based on an analysis of ossification centers in the carpal bones and epiphyses of tubular bones including distal, middle, and proximal phalanges as well as radius and ulna (Fig. 1). Epiphyses usually ossify after birth. With increasing age, the bony penetration advances from the initial focus [Fig. 2(a)] in all directions [Fig. 2(b)]. Penetration continues until the edges of metaphyses are reached [Fig. 2(c)]. The strip between the shaft and the ossification center diminishes progressively [Fig. 2(d)] in thickness until it disappears completely at the completion of growth [Fig. 2(e)], when the epiphysis and metaphysis fuse into one adult bone.

Carpal bones are another potential information source. In the early stage of development, they appear as a dense pin point on a radiograph. While developing, they increase in size until finally

they reach their adult size and characteristic shape. In the developmental order of appearance, [6] capitate (Fig. 1) and hamate is followed by triquetrum and lunate. Then, scaphoid, trapezoid, and trapezium occur. Finally, pisiform overlaps the already existing triquetrum and hamate. The girl's development is noticeably more advanced and may differ from boy's development as many as three years.

Medical studies [7] indicate that, due to the carpal bones nature of maturity, their analysis does not provide accurate and significant information for patients older than 9–12 years of age. In this stage of development, the phalangeal analysis yields more reliable results. Besides, more reliable results can be obtained while analyzing the most distal hand area [3].

Numerous Roentgen methods have been proposed for assessing the bone age according to the time of appearance, size, and differentiation of the ossification centers. Different time schedules of skeletal maturation from fetal until adult life have been developed. The most commonly used method (76%) [8] is the atlas matching method by Greulich and Pyle [9]. Based on this method, a left-hand wrist radiograph is compared with the series of radiographs grouped in the atlas according to age and sex. The atlas pattern which superficially appears to resemble the clinical image is selected. Since each atlas pattern is assigned to a certain year of age, the selection assesses the bone age. However, there is still concern about the variability in estimating the age that leads to a high rate of misclassification [10]. The disadvantage of this method is a subjective nature of the analysis performed by various observers with different levels of training. Studies have shown [11] interobserver difference ranging from 0.37 to 0.6 years, whereas the intraobserver differences ranging from 0.25 to 0.47 years. The reason that atlas-matching methods feature such high discrepancies, results from a general comparison of the radiograph to the atlas pattern. By a more detailed comparison of individual bones, ambiguous results may be obtained. As an example, the development of carpal bones may lead to one result, whereas, the epiphyseal development may yield another. This causes the measures to vary from person to person and from observation to observation.

Another technique relies on a trained observer applying the Tanner and Whitehouse (TW2) method [12]. This method uses a detailed analysis of each individual bone (epiphysis-metaphysis complex of each tubular bone and carpal bones). Each complex is assigned to one of eight classes reflecting the following developmental stage [12]:

- Stage B) single deposit of calcium;
- Stage C) center is distinct in appearance;
- Stage D) maximum diameter is half or more the width of metaphysis;
- Stage E) border of the epiphysis is concave;
- Stage F) epiphysis is as wide as the metaphysis;
- Stage G) epiphysis caps the metaphysis;
- Stage H) fusion of epiphysis and metaphysis has begun;
- Stage I) epiphyseal fusion completed.

This leads to the description of each bone in terms of scores. The sum of all scores assesses the bone age. This method yields the most reliable results [10], [13]. Unfortunately, the complexity of this method prevents the rate of its application from exceeding 20% [4], [10].

A number of algorithms for hand wrist analysis exist in the literature [14]–[17]. They all deal with the problem of segmentation of certain regions within the radiograph. A rather low accuracy rate of the region detection may be caused by the lack of image preprocessing functions. First, a nonuniformity of the image background should be suppressed prior to the image analysis. This would increase the hand-to-background ratio. Another preprocessing function not being considered is the hand orientation. Rather, authors define very carefully a standard (for their approach) hand position within the image. Sometimes [17] it varies from the medically accepted standard position. Another approach [18] to the computerized bone age assessment is based on the Tanner–Whitehouse method (TW). An operator positions each epiphysis beneath a video camera, views the image on the computer screen and corrects the position of the radiographs by matching it to the template of the TW stages displayed on the screen. A Fourier transform yields coefficients that are compared with those generated by each stage of the TW standards and the closest match is sought. Manual region matching replaces computerized extraction of the region of interest (ROI).

Currently developed computer-assisted bone age assessment is to be implemented in everyday clinical routine in order to aid radiologists in performing a more objective and accurate analysis. The system is based on experiences gained during a pilot study carried out on 120 clinical images. Certain approaches to the computer-aided bone age assessment have been tested. First, the accuracy of the phalangeal length has been tested [19]. Being implemented in the standard phalangeal length table [20] this measure does not appear to be a sufficient indicator of skeletal maturity and can only be used (if necessary) as a rough estimate in an early stage of the hand analysis. The measure is influenced by the length of fingers and the overall length of tubular bones. Then, the analysis has turned to extraction of diameters of the bony structures. In order not to make them sensitive to hand size, a ratio of epiphyseal diameter to metaphyseal diameter has been considered. All age groups have been examined and it turned out the ratio yields good results for children in whom the epiphyseal fusion has not started yet [21]. In older children, a wavelet transform distinguishes four stages of fusion [22]. Besides, a carpal bone region has also been considered [23]. Segmentation of carpal bones and extraction of various measures have shown a good correlation with the bone maturity for children under 6–7 years. Afterwards, the carpal bones overlap making the analysis very difficult without offering any clinically important information. A classification comparison has shown [24] that phalangeal analysis is more sensitive to the skeletal development than carpal bones analysis particularly in pathological cases.

A review of the pilot study considers three issues: 1) type of images subjected to the computer analysis; 2) accuracy of extracted features; and 3) accuracy of the overall bone age assessment. In various stages of the analysis, the accuracy ranged between 75% and 90%.

In the pilot study, only selected computer radiograph (CR) images were applied. It was assumed that neither labels nor markers were used. Technicians were trained how to place patient hand on the cassette in order to reduce the stage of image alignment. The preprocessing stage was limited to the 90° or 180° rotation or flip. Furthermore, no scanned images were considered. Goal

of the pilot study was to indicate, whether a more objective, computer-assisted analysis is possible. Thus, we concentrated our effort on finding features of high discrimination power able to describe certain stages of skeletal development and apply them to find the skeletal age. Due to the lack of preprocessing functions, the algorithm could only be used for images acquired according to a strictly defined protocol. Clustering techniques roughly eliminated features of no discrimination power and selected those which could serve as input to the fuzzy classifier.

Gained experiences permit image analysis stages of a clinical computer-assisted bone age assessment system to be designed. The currently developed system opens the analysis up to all images. This means that we deal with CR or scanned images. Image preprocessing functions should make the analysis insensitive to the lack of standardization at the image acquisition stage. The cassette is often not closed very tightly causing background nonuniformity. Various labels, markers or clips might be placed within the radiation field. The hand is often lacking the alignment toward the cassette edges. This requires a very robust image preprocessing stage with background removal and hand wrist extraction. At the stage of feature extraction the hand alignment has to be examined. Dealing with blurred image, the edge detection has to be more robust and a study on distance measurement accuracy has to be implemented. Additional (with respect to the previous study) features are to be extracted in order to increase the overall accuracy of the skeletal age assessment.

This paper discusses the first part of a computer-aided bone age assessment project, i.e., image preprocessing functions including the image standardization and background removal as well as extraction of epiphyseal/metaphyseal regions of interest (EMROIs) which include structures very sensitive to the stage of skeletal maturity. In Section II, the database is described. Then, Section III discusses some image processing issues including orientation correction and background removal. Procedures, presented in Section IV, restrict the image to be analyzed to the phalangeal area. Applying more robust image processing techniques, Section V discusses extractions of global size and distance measures.

Papers in preparation will discuss the time- and frequency-domain analysis of the EMROIs and classification issues leading to the bone age assessment. Finally, the image analysis functions will be linked to the user interface under development [25], [26].

## II. DATA BASE

The analysis is performed on left-hand wrist radiograms selected from a normal population and organized into four blocks: black male and female and white male and female. Based on preliminary result [27], for pre-pubertal children (0 to 9-years-old) 5 images for each age group are collected, whereas, for children during puberty (10 to 18-year-old) ten images for each age group are collected. This gives 135 images per block and a total of 540 images. These images are being acquired at the USC Children's Hospital in Los Angeles.

A separate group of 1000 clinical images (normal and pathological) were collected for evaluation. These images were being acquired at the University of California, San Francisco. A Fuji FCR-9000 computed radiography (CR) system is used to acquire

full resolution CR images ( $2KB \times 2KB \times 10$  bits) in a DICOM 3.0 standard. When analog technology is used, films are digitized with a Lumiscan 200 digitizer to  $2KB \times 2KB \times 10$  bits.

## III. IMAGE PREPROCESSING

Preprocessing functions are implemented in order to standardize images to be read by radiologists and/or processed on diagnostic workstations. In both cases, the correction is performed as a computerized analysis. In the first case, it precedes the film printing for hard copy reading, in the second case is included as a package within the computer-aided diagnostic system. Depending on the application, various preprocessing functions have already been implemented. They may be related to the file format [28], as well as to the information field including [29] correction of image orientation, window/level values, look-up-tables in order to enhance the brightness and contrast.

Computer-aided bone age assessment has to handle two types of images (Section II): CR images and digitized images. Set of preprocessing functions implemented in both types may vary. Processing of CR images requires orientation correction and image content standardization. Digitized images may require a file format conversion, window/level adjustment, whereas an image orientation procedure should not be necessary.

Clinical implementation of the computer-assisted bone age assessment requires four conditions to be met by the system: 1) remain open to all images acquired at CR systems and scanned images; 2) correctly extract features of high discrimination power; 3) reliably assess the bone maturation; and 4) provide a user-friendly interface. On the other hand, while developing the image analysis system, one has to keep the overall response time within a reasonable time frame. This means that time consuming procedures performed on the entire image should be avoided.

In order to fulfill the first condition and prepare an image to the computerized analysis, two preprocessing steps are performed. First, the image orientation correction ensures a standard hand position within the image. Second, a background removal increases the hand-to-background ratio increasing the accuracy of the ROI segmentation.

### A. Orientation Correction

As a standard orientation the position viewed by radiologists is considered (anterioposterior, up-right, left-hand wrist). While using phosphor plates the cassette can be placed in various positions to accommodate the examination conditions. A survey in the radiology department [29] has shown that between 35% to 40% of procedures have not been performed with the conventional image orientation. Therefore, it is necessary to develop a computerized algorithm to orient these images before further analysis (computerized or radiological) is performed. Separate algorithms have been developed for each anatomy including hand wrist images [29].

### B. Background Removal

Various definitions of background have already been introduced. It is referred to as an area outside the radiation field, caused by blocking of the collimator and resulting in white borders

surrounding the radiation field. Its removal reduces the amount of unwanted light in images during the soft copy display as well as almost transparent borders on the film. Moreover, the removed background without delivering any pertinent information, adversely affects observer performance and/or computerized image analysis [30]. Algorithms, which turn to black the unexposed background [29], [31], have already been implemented in clinical picture archiving and communication system (PACS) [32] particularly in chest imaging and pediatric radiology.

In image processing systems, background is often referred to as an area outside the patient body (within the radiation field). In this area, landmarks or labels with patient demographic data (name, birthday, ID number, etc.) may also be found. In this section, the latter background definition is considered.

Extraction of phalanges requires an increase of the hand-to-background ratio. This is of particular importance when an under- or overexposed images is subjected to the computer analysis. Moreover, significant background nonuniformity, caused by the not tightly closed cassette, makes often the future image analysis very inaccurate. Background suppression is employed in order to obtain the goal.

The removal is based on dynamic thresholding. The dynamically adjusted threshold value depends on the local background value and is performed in horizontal and vertical direction. In the first stage, a window of fixed size (estimated on the basis of an average phalangeal width) is sliding in vertical direction on the top of the image. Statistical parameters (mean, variance, maximum gradient, and maximum value) are found. Two windows of low mean value and variance located on both sides of the central image axis mark the background area. Mean values of these windows increased by their variances define the threshold values in the corresponding rows.

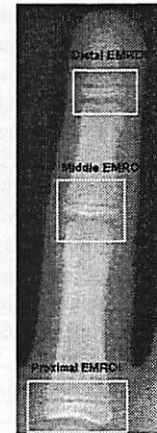
The lower part of the image is searched for another pair of windows and another threshold value is calculated. Once being found, a linear interpolation in vertical direction yields the threshold value for each row. The interpolation is also performed in the horizontal direction yielding the threshold value for each column.

The thresholding procedure, performed separately in both direction, turns to zero values lower than the threshold value without changing pixel values larger than the current threshold. Landmarks and labels remain. They are ignored in further image processing which is based on searching for a predefined pattern describing the hand wrist.

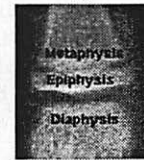
In order to remove all small noisy elements in the background, particularly between phalanges, a mathematical morphology procedure is applied [33]. An erosion function uses a  $3 \times 3$  pixel structuring element. The transformation turns to zero all elements equal to or smaller than the structuring element.

#### IV. EPIPHYSEAL/METAPHYSEAL ROI EXTRACTION

Medical observations [9], [12] as well as our pilot studies [22], [24], [27] indicate certain regions to be sensitive to the skeletal development. Size and shape of epiphyses reflect the stage of maturation until it reaches the edge of metaphyses. Then, the gap between both bones diminishes and fusion progresses until both epiphysis and metaphysis become one adult bone.



(a)



(b)



(c)

Fig. 3. (a) Epi/metaphyseal ROIs marked on the III phalanx (b) bones included in EMROI. (c) Separation lines to be located within the EMROI.

Though, image analysis begins with the location of EMROIs. Within each phalanx three EMROIs are extracted [Fig. 3(a)]. They include [Fig. 3(b)] the metaphysis, epiphysis, and upper part of diaphysis of distal and middle phalanges or metaphysis, epiphysis, and upper part of metacarpals of proximal phalanges. Within each EMROI three lines are extracted. They mark [Fig. 3(c)] diameters of metaphyses and epiphyses, and the top edge of diaphyses. Various combinations of two of them allow certain areas of the EMROI to be extracted and subjected to the feature extraction phase. Moreover, the separation lines yield two features, which roughly indicate the stage of development: 1) ratio of epiphyseal diameter divided by metaphyseal diameter and 2) epiphyseal diameter divided by width of the gap between metaphysis and diaphysis.

Four steps are performed in order to select predefined lines: 1) extraction of phalangeal tip; 2) rough extraction of phalanx long axis; 3) detection of selection lines between metaphyses and diaphyses; and 4) detailed EMROI analysis yielding location of three lines defined above.

##### A. Extraction of Phalangeal Tip

At this step a grid pattern covers the thresholded image. Within each grid window a mean value of pixels is found. This forms a matrix. In order to reduce low value matrix elements

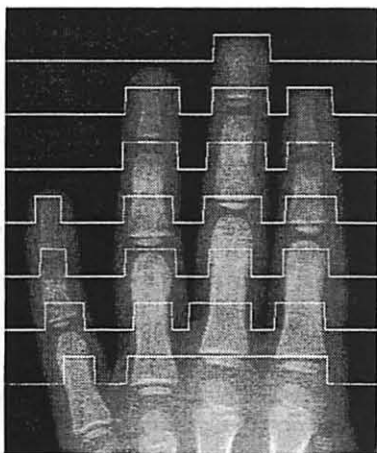


Fig. 4. Extraction of phalangeal tip, hand region step-wedge functions superimposed over the hand image.

related to structures (i.e., label, markers) not removed by the background removal procedure (described in Section III-B), the matrix is thresholded (using the value found at the background removal stage). This yields a binary matrix which is transformed into a set of step-wedge functions. Each function refers to one row of the matrix. High-value level corresponds to the area of phalanges, whereas the low-value level refers to the gap between them (Fig. 4). The width of each wave depends on a size of the hand, the age of the child, distances between fingers during the examination procedure. Therefore, no limits can be chosen to define or verify these parameters.

The set of functions is searched for a three-wave pattern related to three phalanges within the image (second step-wedge function in Fig. 4). The verification of the choice is based on two conditions. 1) Since there is no significant increase in the width while measuring a phalanx toward forearm, corresponding wave widths are equal. Due to a random location of grid windows at the soft tissue-background border, a tolerance of two grid elements is allowed. 2) Since the interphalangeal gap does not increase while measuring it downward, widths of valleys measured downward cannot increase. The latest condition is imposed by the shape of a hand and its possible location on the radiological cassette during the examination procedure.

Once the location of the three-wave pattern is confirmed, the matrix column reflecting the phalanx under consideration is searched (upward) for the last nonzero element which marks the tip of the phalanx (first step-wedge function in Fig. 4). A rescaling procedure maps it onto the original image.

### B. Extraction of Phalangeal Long Axis

Once the tip of the phalanx is marked, edges of the phalanx need to be enhanced. Two sharp variation edges are included in this area: 1) bone edges and 2) soft tissue edges. An edge enhancement function extracting the phalanx has to fulfill two conditions. First, it cannot enhance the high-frequency components related to the structure of bones and soft tissue. At this point those structures deliver no diagnostically significant information. Second, since no ROIs have been extracted and the

analysis is performed on the entire image, a no time-consuming procedure has to be implemented.

In order to locate the vertical phalanx edges, a gradient technique to be implemented has to fulfill three conditions: 1) smooth the bony edges; 2) suppress high variation pixels within the soft and bony structures; and 3) enhance soft tissue edges. Thresholding procedure, removing the hand wrist background, enhances significantly the soft tissue edges. In a 12-bit image the threshold value falls between  $2^{10}$  and  $2^{11}$ . Thus, a gradient technique based on the first order derivative yields good results. Due to the required simplicity, a Sobel gradient operator [34] is implemented.

The histogram of a gradient image [Fig. 5(a)] shows three areas. The first area (the most left-hand side peak in Fig. 5(b)) is related to the background (not being analyzed), second one reflects the bone edges as well as the nonuniformity caused by the bony structure, and the third area (the most right-hand side peak in Fig. 5(b)) is related to the sharp edges between the background and the hand region. A thresholding function cuts the third area off.

Starting from the already extracted phalanx tip, coordinates of phalangeal edges located on both sides are found. Using the median filter [34] and the third-order polynomial fit [35] the axis is smoothed [Fig. 5(c)].

### C. Extraction of EMROI

In order to roughly locate the EMROI, a vector  $P$  whose elements correspond to an average of neighbor pixels on both sides of the axis is defined as

$$p_j = \sum_{k=-n}^{k=n} x_{r_j, c_j+k} \quad (1)$$

where

- $p_j$   $j$ th element of the profile vector  $P$ ;
- $r_j, c_j$  row and column number of a  $j$ th pixel of the axis;
- $x_{k,l}$  intensity of a pixel at location  $k, l$ ;
- $n$  size of a neighborhood ( $2n + 1$  is a distance corresponding to about 0.5 cm in the image).

The size of the neighborhood has to be large enough to smooth the vector, yet it should not exceed the width of the phalanx. On average, the width is of about 0.5 cm. Then, the vector is smoothed using a moving average filter [top profile in Fig. 5(d)] and its first-order derivative [bottom function in Fig. 5(d)] is subjected to a detailed search for the EMROI.

The epiphyseal region is marked at the derivative function as a sharp variation area. Within this area a separation line is selected. It serves as a fiducial level for the EMROI border location. Since the separation line is defined as a low value row between epiphysis and top of lower diaphysis [Fig. 3(c)], a local minimum has to be found. Yet, a simple detection algorithm would fail because in over 50% of images two low gray-scale value gaps appear, one between metaphysis and epiphysis and the other one between epiphysis and diaphysis. (One gap will appear when the epiphysis is at least partially fused with the metaphysis.) Therefore, the derivative function is divided into sectors. Within each sector only one local minimum is marked. The length of sectors is related to the height of EMROIs.

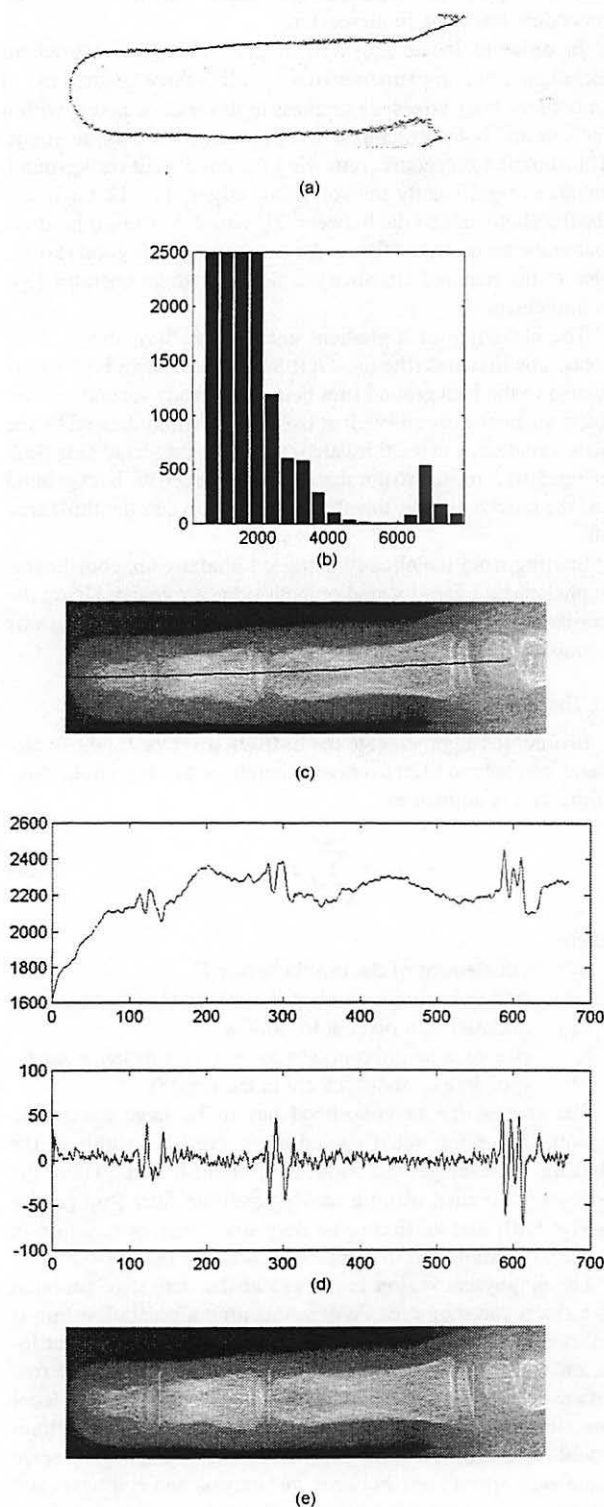


Fig. 5. Extraction of separation lines. (a) Sobel gradient images. (b) Histogram of the Sobel gradient image. (c) Axis superimposed onto a phalanx (the left-most axis pixel marks the phalangeal tip detected). (d) Pixel values in the averaged axis shown in a (top function), its derivative (bottom function). (e) Separation lines superimposed onto phalanx.

Since the distance between phalanges (the height of the EMROI) depends on the length of fingers, the sector size assessment is based on the axis length. A correlation of the long axis length and distance between two neighbor bones in 100 images of normally developed children has shown that the ratio of both values ranges between 0.02 and 0.2. The smallest values appear when epiphyseal fusion is completed, the largest ones refer to distances between proximals and metacarpals in very young children. On the other hand, the ratio of length of middles and axis length ranges between 0.16 in small children to 0.26 in teenagers.

Based on the analysis a sector length has been set to 0.15 of the axis length. Although, the sector length corresponds to anatomical distance between phalanges in children with epiphyses not fused, it does not cause a wrong extraction of separation lines in hand images with only one minimum (i.e., epiphysis fused) and can be applied independently of the chronological age.

Having roughly found the EMROI, a search for the exact location of the separation line is performed. Two local minima found within a sector corresponding to one EMROI are compared. If their values differ less than 50%, the minimum located further from the phalangeal tip marks the selection line [Fig. 5(e)].

In preparation for an unsupervised implementation, a control statement is introduced. Based on the location of separation lines, distances between the middle and distal lines and between the proximal and middle lines are calculated. If their ratio is out of the anatomical range, estimated on the basis of entire database, a warning message is generated. The test prevents misextracted ROIs from being subjected to following steps of the image analysis.

Based on the separation lines, a rough extraction of the region is performed. Its goal is to restrict the area for a detailed analysis in the following phase. The region includes the metaphysis, epiphysis, and upper part of the diaphysis. The width of each region equal to the width of the phalanx is set in the tip extraction phase. The height of regions is defined on the basis of distances between separation lines.

Three distances are defined:  $d$ , between tip of phalanx and distal separation line;  $m$ , between distal and middle separation lines; and  $p$ , between middle and proximal separation line. The distal separation lines shifted by  $0.6 \times d$  upward and  $0.2 \times m$  downward, mark upper and lower edges of distal regions, respectively. The middle separation line shifted by  $0.4 \times m$  upward and  $0.15 \times p$  downward mark upper and lower edges of middle regions. The proximal separation line shifted by  $0.3 \times p$  upward and  $0.15 \times p$  downward mark upper and lower edges of proximal regions.

## V. EXTRACTION OF GLOBAL SIZE AND DISTANCE MEASURES

Since a rough extraction of the epiphyseal ROI has limited the area to be analyzed, a more robust method can be implemented. It leads to detection of three lines to be used as edges of very precisely defined areas within the hand image. They mark diameters of metaphyses and epiphyses, and upper edge of the diaphysis below. A methodology of the extraction of edges is shown in Fig. 6 and described in the following section.

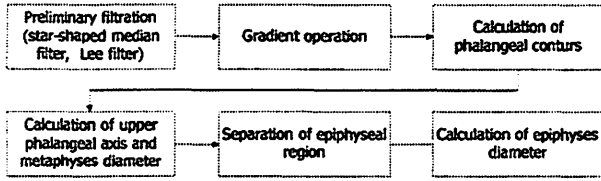


Fig. 6. Methodology yielding diameters of epiphyses and metaphyses.

### A. Filtration Procedure

A detailed hand image analysis requires a suppression of texture related to the soft tissue and bony structures. Two filtration techniques are implemented at this step. The star-shaped median filter suppresses “the salt and pepper noise,” preserving step discontinuity within the region [36]. Then, a smoothing procedure is applied in order to increase the gray-scale ratio between soft tissue and bones. The procedure should also enhance the edges. At this point, an adaptive filtering technique is more selective than a comparable linear filter. It suppresses the structural noise preserving edges and other high-frequency parts of the image. Good results are yielded by the adaptive Lee filter [36].

The model of an image corrupted by additive noise is defined as

$$g(i, j) = f(i, j) + v(i, j) \quad (2)$$

where

- $f(i, j)$  noise-free image;
- $v(i, j)$  signal-independent additive noise;
- $g(i, j)$  corrupted image (input image).

In our application, additive noise is related to the soft tissue and bony structures. In order to assess the mean value of structural noise, the overall image trend has been cut off. Since the mean values of bony and soft tissue regions is smaller than 0.05, the Lee filter can be implemented with a zero-mean value of structural noise. Thus, the processed image is given by

$$p(i, j) = m_f(i, j) + \frac{\sigma_f^2(i, j)}{\sigma_f^2(i, j) + \sigma_v^2} (g(i, j) - m_f(i, j)) \quad (3)$$

where

- $p(i, j)$  processed image (output image);
- $g(i, j)$  corrupted image (input image);
- $m_f(i, j), \sigma_f(i, j)$  local mean and standard deviation of the input image;
- $\sigma_v^2$  noise variance;
- $i, j$  pixel coordinates.

Filtration procedure requires that the variance of noise— $\sigma_v^2$ —has to be known. The noise variance is found as an average of all locally estimated variances. Other parameters such as  $m_f(i, j)$  and  $\sigma_f(i, j)$  are estimated from  $g(i, j)$  and delimited by a  $3 \times 3$  mask. A larger mask smoothes the edges. This is particularly important in images registered with optimally chosen exposure parameters yielding sharp variation edges.

Subjecting an original region [Fig. 7(a)] to the filtration procedure (star-shaped median filter and Lee filter) a smoothed region with enhanced edges is received [Fig. 7(b)].

### B. Metaphyseal Diameter Detection

Since diameters of epiphyses and metaphyses as well as ROIs to be extracted have to be defined perpendicularly to the phalangeal axis, following steps require enhancement of bone edges as a basis for the extraction of the axis. Although, the region has been significantly smoothed, the nonuniformity of both anatomical structures (soft tissue and bones) remains.

At the current stage a Sobel gradient method is implemented Fig. 7(c). The mask to be used is assessed on the basis of the system modulation transfer function (MTF). In order to obtain the MTF, bone edge is subjected to the following analysis. A trace perpendicular to the edges yields a step function (SF) defined as

$$SF = \begin{cases} L & x < x_0 \\ H & x > x_0 \end{cases} \quad (4)$$

where

- $x$  line perpendicular to the edge;
- $x_0$  location of the edge;
- $L$  low-value level;
- $H$  high-value level.

Then, the line spread function (LSF) being the derivative of the SF is given by

$$LSF(x) = \frac{d(SF(x))}{dx} \quad (5)$$

Next, a one-dimensional Fourier transform applied to the LSF is obtained. Its magnitude is the MTF [32]. Multiplying it with a spatial frequency spectrum of a perfect trace of the step edge function yields an output frequency spectrum of an edge SF. Superimposing the perfect and real traces, the blurring of edge can be estimated yielding the mask size. The mask size (set in this stage to  $9 \times 9$ ) allows the nonuniformities to be suppressed [Fig. 7(c)].

In the filtered EMROI [Fig. 7(b)], two structures appear: enhanced bone edges and suppressed soft tissue and bony texture. Gray scale levels of both structures differ significantly and appear on a histogram (or probability of gray scale distribution) as two waveforms (Fig. 8). A separation of this waveform is based on a statistical approach [37]. The separation value is calculated as maximum of discrimination function  $\eta$  defined as

$$\eta = \frac{\sigma_B^2}{\sigma_T^2} \quad (6)$$

where  $\sigma_B^2$  is a variance between classes and  $\sigma_T^2$  is a total variance of gray level. The maximum of  $\eta$  corresponds to the maximum of  $\sigma_B^2$

$$\sigma_B^2 = \omega_0(\mu_0 - \mu_T)^2 + \omega_1(\mu_1 - \mu_T)^2 \quad (7)$$

where

- $\omega_0$  probability of first class occurrence;
- $\omega_1$  probability of second class occurrence;
- $\mu_0$  mean of first class;
- $\mu_1$  mean of second class;
- $\mu_T$  total mean of the EMROI.

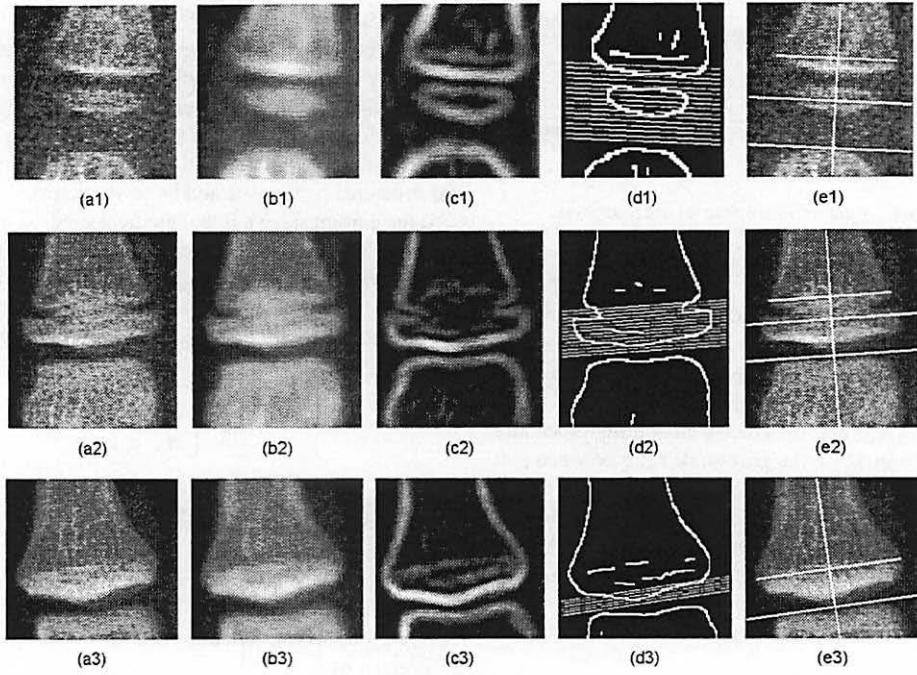


Fig. 7. Processing of EMROI. (a) Original regions. (b) Regions after star-shaped median filter and Lee filtering. (c) Gradient images. (d) Profiles marking the gap between metaphyses and diaphyses (if applied), and bottom of the EMROI. Three groups of regions are extracted from hand radiographs of 4-year-old patient, 12-year-old patients, and 16-year-old patient, respectively.

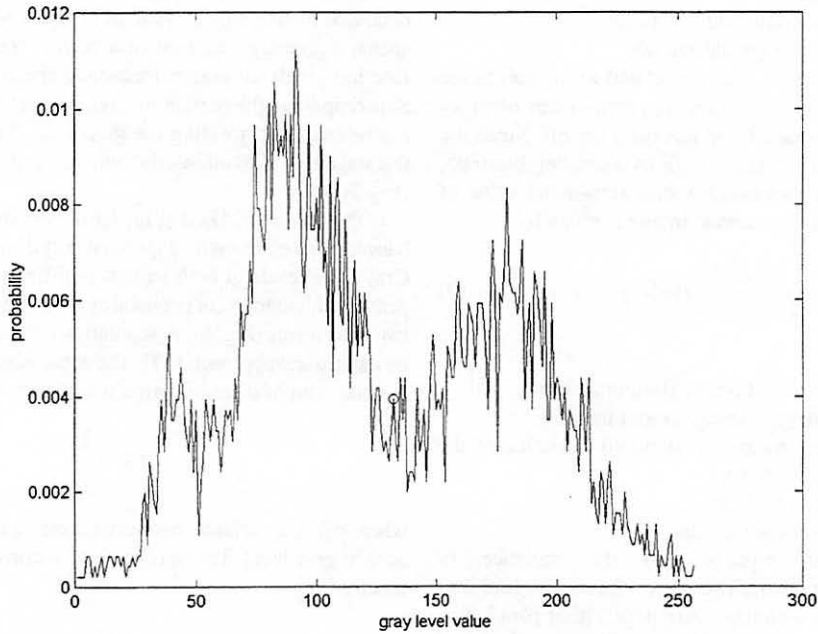


Fig. 8. Probability of gray scale distribution of a filtered EMROI.

Transformation of (7) yields, for each  $k$  gray level

$$\sigma_B^2(k) = \frac{[\mu_T \omega(k) - \mu(k)]^2}{\omega(k)(1 - \omega(k))}$$

where

$$\begin{aligned} \omega(k) &= \sum_{i=1}^k p_i; \\ \mu(k) &= \sum_{i=1}^k i p_i; \\ \mu_T &= \sum_{i=1}^L i p_i; \end{aligned} \quad (8)$$

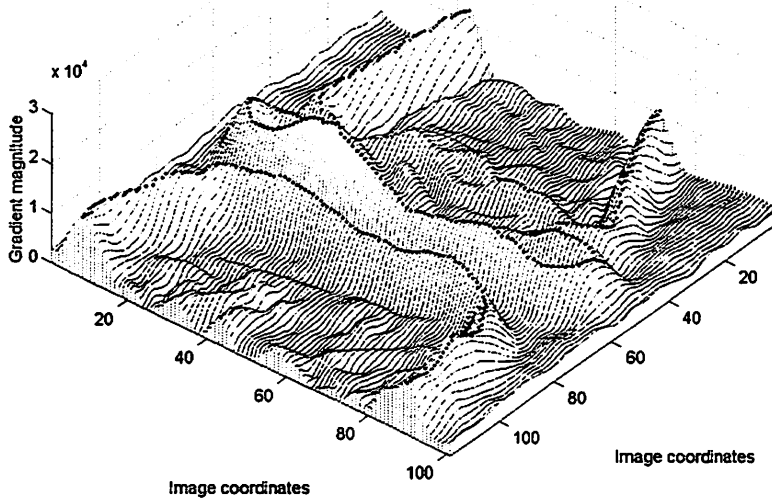


Fig. 9. Magnitude of gradient function versus profile lines in ROI. Dots mark two maxima on each profile.

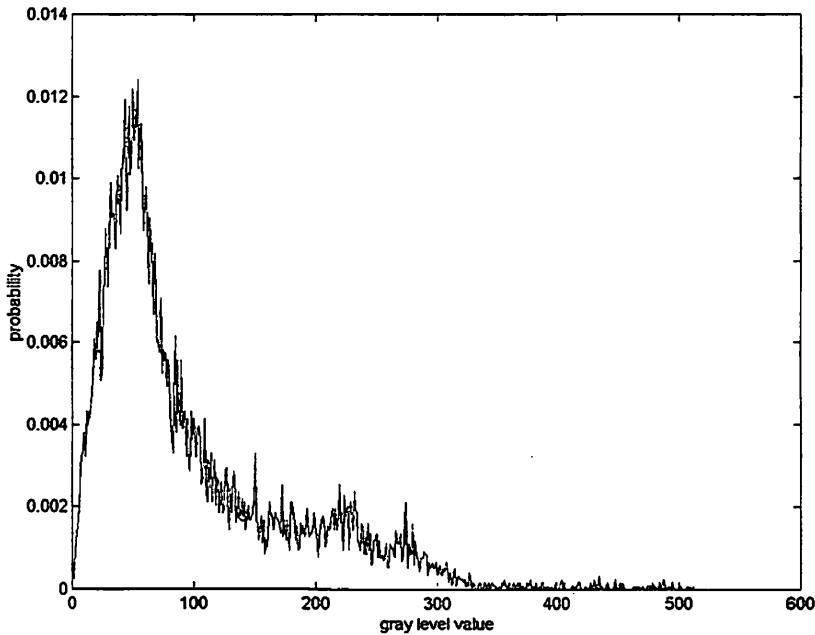


Fig. 10. Probability of gray scale distribution of a gradient image.

- $p_i$  =  $n_i/N$ ;
- $n_i$   $i$ th gray image level;
- $N$  total number of pixel;
- $L$  total number of gray levels.

After the soft tissue and bony texture have been separated, the remaining bone edges are subjected to a detection procedure based on analysis of vertical profiles scanned first from

top of the region downward (for metaphyses) and then from its bottom upward (for the upper diaphysis). Two local maxima (Fig. 9) on each profile mark the edge points. A sudden decrease of the distance between them showing the bottom phalanx edge (or epi-/metaphyseal joint space if fusion started) terminates the edge detection. Distances between edge points found horizontally mark a rough longitudinal axis smoothed by a linear regression function.

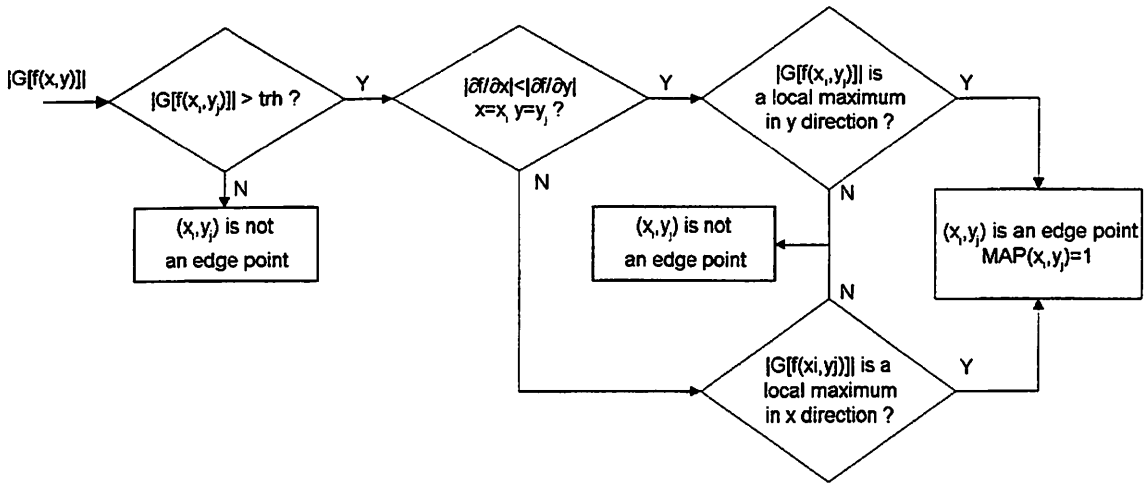


Fig. 11. Edge extraction procedure.

Detection of epiphyseal diameters requires a more precise definition of edge points. First, in order to separate the edges, a gradient image [Fig. 7(c)] is thresholded (threshold value is found from the histogram (Fig. 10) as described above) and a two-dimensional gradient analysis is performed (Fig. 11). As a result a binary image [Fig. 7(d)] is obtained, where detected edges are turned to one, other components are blacked out. Then, morphological operators [33] (diagonal fill, bridge, cleaning isolated pixels, and closing, described in the Appendix) close the edges and remove isolated pixels. Next, binary EMROI is scanned perpendicular to the phalangeal axis [Fig. 7(d)]. Distances between edge points along profiles are plot versus their location within the region [Fig. 12(a) and (b)]. A maximum distance found in each EMROI [marked by arrows in Fig. 12(a) and (b)] locates the epiphyseal diameter.

## VI. RESULTS AND DISCUSSION

Image analysis was applied to 200 clinical hand wrist radiographs selected from the normally developed population. In boys, the age was limited to 14; in girls, to 12. All of them are in the upright position. Accuracy has been measured independently at three stages of the image analysis: 1) detection of phalangeal tip yielding a rough axis; 2) extraction of EMROIs; and 3) location of diameters and lower edge of EMROIs.

Detection of phalangeal tip has failed in 4% of radiographs. Two reasons of failures have been observed. First, markers next to the phalanges, then strong background nonuniformities and low hand-to-background ratio as a result of over- or underexposure. Since then, we have mandated the quality assurance during the X-ray procedure.

Extraction of EMROI is based on location of lines separating the epiphyses from the upper edges of diaphyses (or metacarpals). Only in one case the gap has been detected incorrectly and the region could not be subjected to further analysis. In 4% of cases (24 out of 588), the gap between epiphyses and metaphyses has not been marked. Although the location of the separation line failed, the EMROI being marked as a region in

the neighborhood of selected line has been extracted correctly and can be subjected to the following steps of image analysis. Its location correction is performed in next stages.

Accuracy of diameters extraction has been performed by evaluating their intersection with bones (evaluation of location) and location of end points (evaluation of distance measures). The diameter location has been examined by three independent observers and all evaluations have had to be positive in order to accept the location. Results are shown in Table I. Due to a nonstandardized hand location during the radiological procedure (bent fingers causing overlapping of epiphyses and metaphyses or rotated fingers), ten EMROIs have been rejected. The decrease of accuracy of proximal EMROIs is caused by the presence of soft tissue resulting in the decrease of the hand-to-background ratio.

Finally, for each of the three EMROI selected features have been extracted: epiphyseal diameter (ed), metaphyseal diameter (md), distance between lower diaphysis (or metacarpal) and epiphyseal diameter (dist). In order to make final features independent from the hand size and length of fingers, ratios of distance measures are considered. Thus, three ratios have been tested: ed/md, ed/dist, and md/dist, yet only the first two of them have shown sufficient discrimination power evaluated on the basis of mean and variances of clustered features. Thus, Table II shows the evaluation results of ed/md and ed/dist.

A rough assessment of the discrimination power of each feature has been performed. The analysis is based on clinical hand wrist radiographs of male and female patients. Their endocrinological examinations have shown no developmental disorders. Thus, these images are assumed to be normal. Within one class (year of age) a mean and variance have been found and plotted versus the year of age.

A plot of features versus patients chronological age (equal to bone age since images of normal population are considered) roughly assess their discrimination power. The ratio of epiphyseal diameter divided by metaphyseal diameter (ed/md) (Fig. 13) shows high discrimination power between 4 and 10 years-of-age in female patients and between 4 and 13 years in male patients. A comparison of average measures for distals,

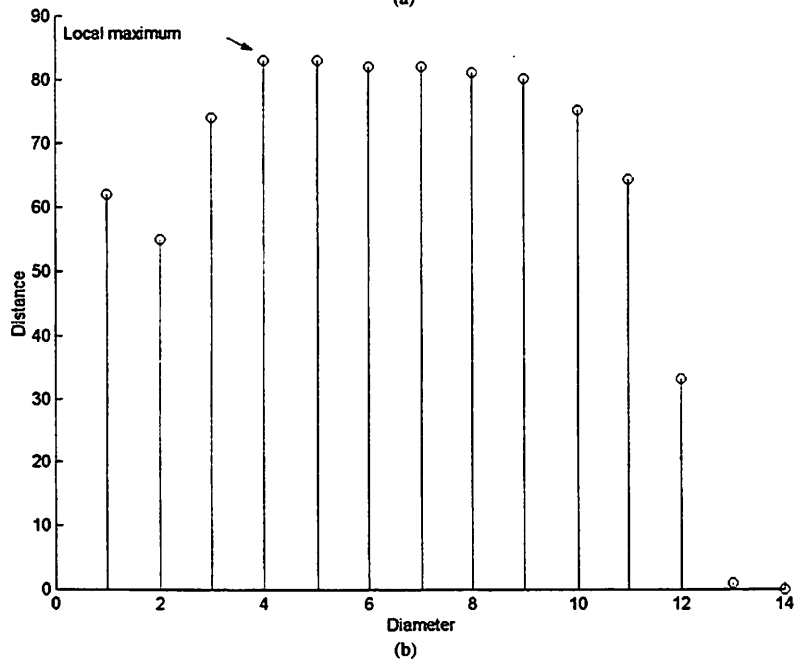
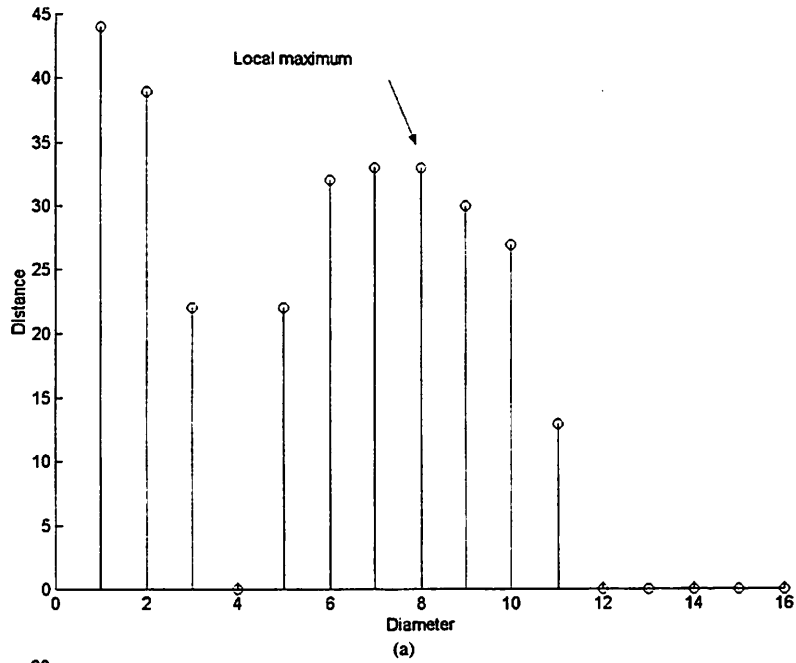


Fig. 12. Detection of epiphyseal diameter (a) for region in Fig. 7(d), (b) for region in Fig. 7(d). Arrow marks a local maximum referred to the epiphyseal diameter.

TABLE I  
ACCURACY OF MEASURES

Parameters / ROI	distal	middle	proximal
metaphyseal diameter	93%	87%	92%
epiphyseal diameter	96%	88%	77%
distance between metaphyseal line and tip of lower diaphysis	95%	84%	85%

TABLE II  
FEATURES EXTRACTION ACCURACY

Parameters / ROI	distal	middle	proximal
diameter of epiphyses / diameter of metaphyses	92%	83%	72%
diameter of epiphyses / distance between metaphyseal line and tip of lower diaphysis	90%	82%	78%

middles, and proximals show a more rapid increase of its value in distals at the early stage of development (between 2 and

7 years-of-age in males and 2 and 5 years-of-age in females) and a slowdown afterwards. In middle and proximal phalanges,

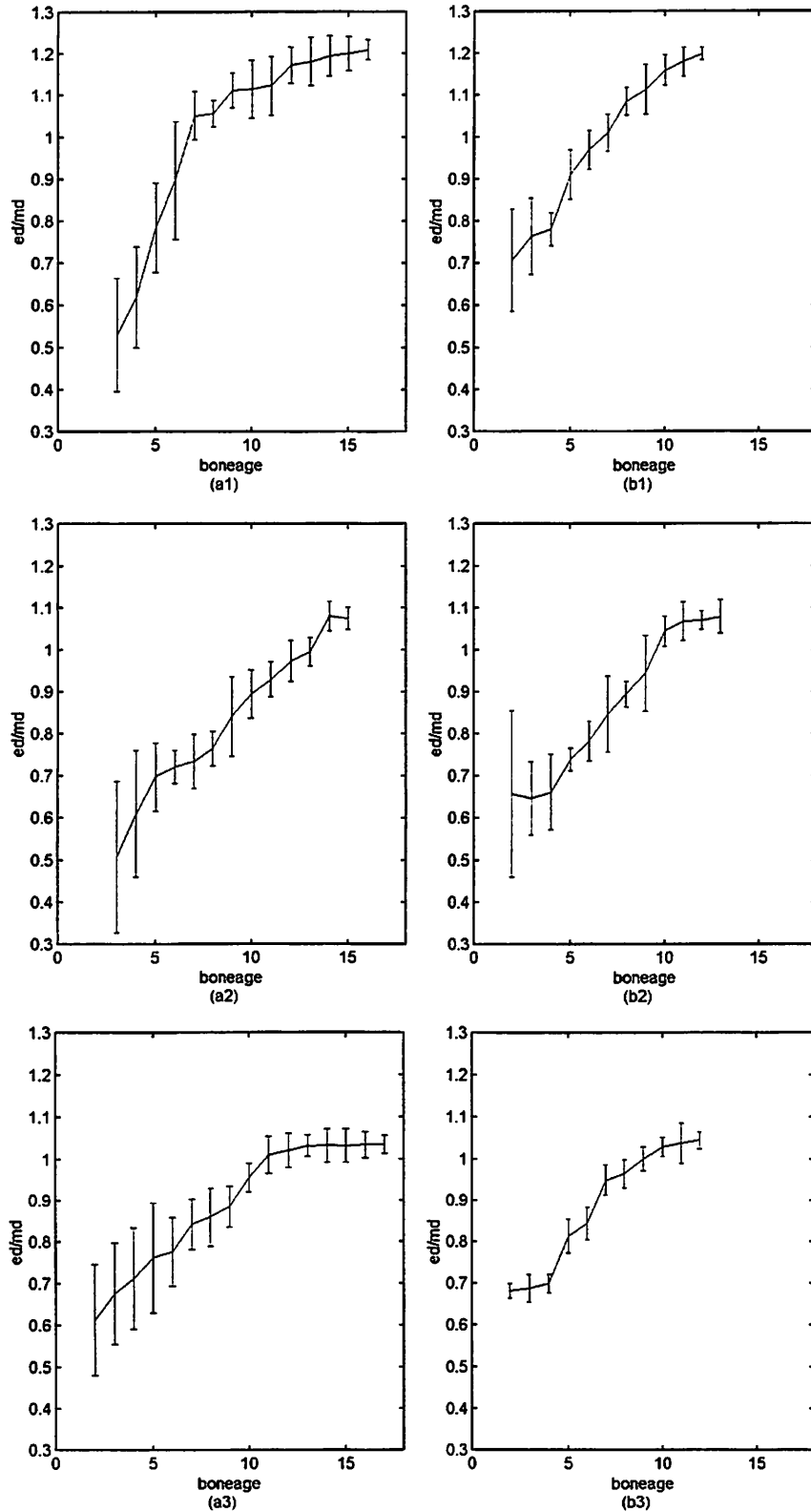


Fig. 13. Features  $ed/md$  in male patients extracted from: (a1) distal, (a2) middle, and (a3) proximal EMROI, and features in female patients extracted from (b1) distal, (b2) middle, and (b3) proximal EMROI.

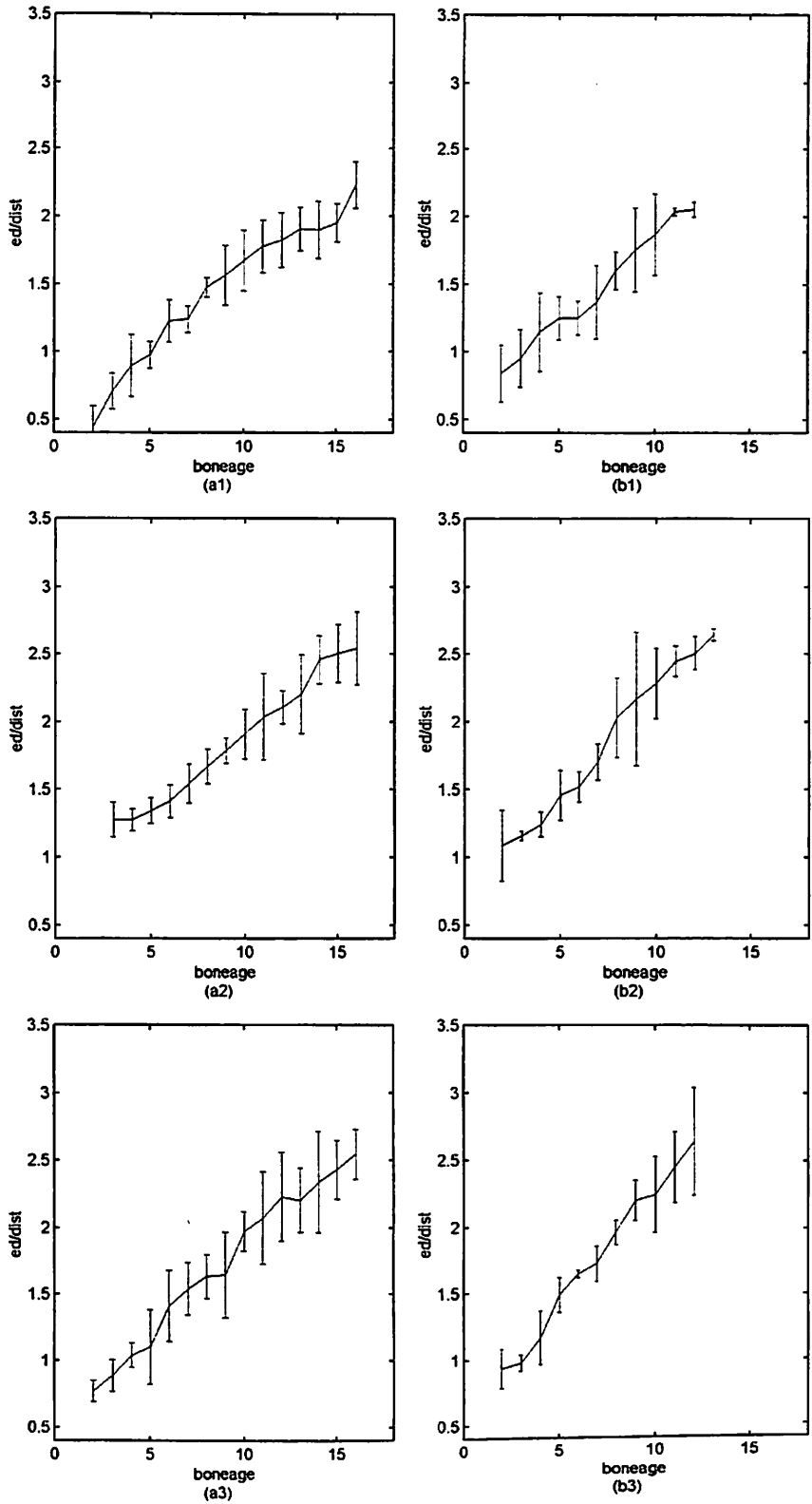


Fig. 14. Features  $ed/dist$  in male patients extracted from: (a1) distal, (a2) middle, and (a3) proximal EMROI, and features in female patients extracted from (b1) distal, (b2) middle, and (b3) proximal EMROI.

a strong increase of the average ed/md starts two years later, yet remains until the epiphyseal fusion begins.

Epiphyseal diameter divided by distance between lower diaphysis (or metacarpal) and epiphyseal diameter (Fig. 14) features similar relations at the early stage of development. Values of both parameters depend strongly on the rapid grows of epiphyseal diameter. However, the ed/dist feature keeps increasing continuously in the later stage of development, even after the ed/md feature does not change significantly. In male patients, average ed/dist increases until 16 years of age, whereas in female patients it changes until the age of 13. Afterwards a time-frequency domain analysis is performed as a separate study.

Large variances of features in very young children (1-3 years-of-age) indicate a rapid grows of epiphyses which should not be combined in one class. The Greulich and Pyle atlas separates them in more than one class as well. This will also be included in future studies.

#### APPENDIX

##### Star-Shaped Median Filter:

$$y(i, j) = \text{median}$$

$$[x(i, j), x(i, j + 1), x(i, j - 1), x(i, -1, j), x(i, +1, j)]$$

where:

- $x(i, j)$  input image;
- $y(i, j)$  output image;
- $i, j$  pixel coordinates.

**Morphological Operator Definitions:** Consider the following  $(3 \times 3)$  neighborhood pixel pattern in binary image, where  $X = 1$  (white) or  $X = 0$  (black)

$$\begin{array}{ccc} X3 & X2 & X1 \\ X4 & X & X0 \\ X5 & X6 & X7 \end{array}$$

where

- $X = I(i, j)$ ;
- $X0 = X(i, j + 1)$ ;
- $X1 = I(i - 1, j + 1)$ ;
- $X2 = I(i - 1, j)$ ;
- $X3 = X(i - 1, j - 1)$ ;
- $X4 = X(i, j - 1)$ ;
- $X5 = X(i + 1, j - 1)$ ;
- $X6 = X(i + 1, j)$ ;
- $X7 = X(i + 1, j + 1)$ .

**Four-neighbor erode (erosion):** Erase white pixel if at least one four-connected neighbor pixel is black

$$E(i, j) = X \cap X2 \cap X4 \cap X0 \cap X6.$$

**Four-neighbor dilate (dilation):** Create a white pixel if at least one four-connected neighbor pixel is white

$$D(i, j) = X \cup X2 \cup X4 \cup X0 \cup X6.$$

**Diagonal fill:** create a white pixel if creation eliminates eight connectivity of the background

$$DF(i, j) = X \cup (P1 \cup P2 \cup P3 \cup P4)$$

where

$$P1 = \bar{X} \cap X0 \cap \bar{X}1 \cap X2;$$

$$P2 = \bar{X} \cap X2 \cap \bar{X}3 \cap X4;$$

$$P3 = \bar{X} \cap X4 \cap \bar{X}5 \cap X6;$$

$$P4 = \bar{X} \cap X6 \cap \bar{X}7 \cap X0.$$

**Cleaning isolated pixel:** erase a white pixel with eight black neighborhood

$$CP(i, j) = X \cap (X0 \cup X1 \cup \dots \cup X7).$$

**Bridge:** bridge previously unconnected pixels

$$B(i, j) = X \cup (P1 \cup P2 \cup \dots \cup P6).$$

where

$$P1 = \bar{X}2 \cap \bar{X}6 \cap (X3 \cup X4 \cup X5) \cap (X0 \cap X1 \cap X7) \cap PQ;$$

$$P2 = \bar{X}0 \cap \bar{X}4 \cap (X1 \cup X2 \cup X3) \cap (X5 \cap X6 \cap X7) \cap PQ;$$

$$P3 = \bar{X}0 \cap \bar{X}6 \cap X7 \cap (X2 \cap X3 \cap X4);$$

$$P4 = \bar{X}0 \cap \bar{X}2 \cap X1 \cap (X4 \cap X5 \cap X6);$$

$$P5 = \bar{X}2 \cap \bar{X}4 \cap X3 \cap (X0 \cap X6 \cap X7);$$

$$P6 = \bar{X}4 \cap \bar{X}6 \cap X5 \cap (X0 \cap X1 \cap X2).$$

$$PQ = L1 \cup L2 \cup L3 \cup L4$$

where

$$L1 = \bar{X} \cap \bar{X}0 \cap X1 \cap \bar{X}2 \cap X3 \cap \bar{X}4 \cap \bar{X}5 \cap \bar{X}6 \cap \bar{X}7;$$

$$L2 = \bar{X} \cap \bar{X}0 \cap \bar{X}1 \cap \bar{X}2 \cap X3 \cap \bar{X}4 \cap X5 \cap \bar{X}6 \cap \bar{X}7;$$

$$L3 = \bar{X} \cap \bar{X}0 \cap \bar{X}1 \cap \bar{X}2 \cap \bar{X}3 \cap \bar{X}4 \cap X5 \cap \bar{X}6 \cap X7;$$

$$L4 = \bar{X} \cap \bar{X}0 \cap X1 \cap \bar{X}2 \cap \bar{X}3 \cap \bar{X}4 \cap \bar{X}5 \cap \bar{X}6 \cap X7.$$

**Closing:** smoothes contours of object, eliminates small holes in objects, and fuses short gaps between objects. It often is obtained by dilating and eroding the image

$$C(i, j) = X \cup (P1 \cup P2 \cup \dots \cup P6).$$

#### REFERENCES

- [1] D. B. Darling, *Radiography of Infants and Children*. 1st ed. Springfield, IL: Charles C Thomas, 1979, ch. 6, pp. 370-372.
- [2] A. Poznanski, S. M. Garn, J. M. Nagy, and J. C. Gall. "Metacarpophalangeal pattern profiles in the evaluation of skeletal malformations." *Radiology*, vol. 104, pp. 1-11, 1972.
- [3] D. R. Kirks, *Practical Pediatric Imaging. Diagnostic Radiology of Infants and Children*. 1st ed. Boston, MA: Little, Brown & Co., 1984, ch. 6, pp. 198-201.
- [4] J. Kosowicz. "The Roentgen appearance of the hand and wrist in gonadal dysgenesis." *Radiology*, vol. 93, pp. 354-361, 1965.
- [5] R. M. Archibald, N. Finby, and F. de Vito, "Endocrine significance of short metacarpals," *J.Clin.Endocr.*, vol. 19, pp. 1312-1322, 1959.
- [6] J. W. Pryor. "Time of ossification of the bones of the hand of the male and female and union of epiphyses with the diaphyses," *Amer. J. Phys. Anthropol.*, pp. 401-410, 1975.
- [7] F. E. Johnston and S. B. Jahina. "The contribution of the carpal bones to the assessment of skeletal age," *Amer. J. Phys. Anthropol.*, vol. 23, pp. 349-354, 1965.
- [8] G. R. Miller, R. K. Levick, and R. Kay. "Assessment of bone age: A comparison of the Greulich and Pyle and the Tanner and Whitehouse methods." *Clin. Radiol.*, vol. 37, pp. 119-121, 1986.
- [9] W. W. Greulich and S. I. Pyle. *Radiographic Atlas of Skeletal Development of Hand Wrist*. 2nd ed. Stanford, CA: Stanford Univ. Press, 1971.
- [10] J. M. H. Buckler. "How to make the most of bone ages." *Arch. Disease Childhood*, vol. 58, pp. 761-763, 1983.
- [11] A. F. Roch, C. G. Rohmann, and G. H. Davila. "Effect of training on replicability of assessment of skeletal maturity (Greulich — Pyle)." *Amer. J. Roentgenol.*, vol. 108, pp. 511-515, 1970.

- [12] J. M. Tanner and R. H. Whitehouse, *Assessment of Skeletal Maturity and Prediction of Adult Height (TW2 Method)*. London, U.K.: Academic, 1975.
- [13] A. L. J. Cole, L. Webb, and T. J. Cole, "Bone age estimation: A comparison of methods." *Brit. J. Radiol.*, vol. 108, pp. 683–686, 1988.
- [14] D. J. Michael and A. C. Nelson, "HANDX: A model-based system for automatic segmentation of bones from digital hand radiographs." *IEEE Trans. Med. Imag.*, vol. 8, pp. 64–69, 1989.
- [15] S. N. C. Cheng, H. Chan, L. T. Niklason, and R. S. Alder, "Automated segmentation of regions on hand radiographs." *Med. Phys.*, vol. 21, pp. 1293–1200, 1994.
- [16] G. K. Manos, A. Y. Cains, I. W. Rickets, and D. Sinclair, "Segmenting radiographs of the hand and wrist." *Comput. Methods Programs Biomed.*, vol. 43, pp. 227–237, 1994.
- [17] J. Duryea, Y. Jiang, P. Countryman, and H. K. Genant, "Automated algorithm for the identification of joint space and phalanx margin location on digital hand radiographs." *Med. Phys.*, vol. 26, pp. 453–461, 1999.
- [18] J. M. Tanner and R. D. Gibbons, "Automatic bone age measurement using computerized image analysis," *J. Ped. Endocrinol.*, vol. 7, pp. 141–145, 1994.
- [19] E. Pietka, M. F. McNitt-Gray, and H. K. Huang, "Computer-assisted phalangeal analysis in skeletal age assessment." *IEEE Trans. Med. Imag.*, vol. 10, pp. 616–620, 1991.
- [20] S. M. Garn, K. P. Hertzog, A. K. Poznanski, and J. M. Nagy, "Metacarpophalangeal length in the evaluation of skeletal malformation," *Radiology*, vol. 105, pp. 375–381, 1972.
- [21] E. Pietka, M. F. McNitt-Gray, T. Hall, and H. K. Huang, "Computerized bone analysis of hand radiographs." *Proc. SPIE*, vol. 1652, pp. 522–528, 1992.
- [22] E. Pietka and H. K. Huang, "Epiphyseal fusion assessment based on wavelets decomposition analysis." *Computerized Med. Imag. Graph.*, vol. 19, pp. 465–472, 1995.
- [23] E. Pietka, L. Kaabi, M. L. Kuo, and H. K. Huang, "Feature extraction in carpal-bone analysis," *IEEE Trans. Med. Imag.*, vol. 12, pp. 44–49, 1993.
- [24] E. Pietka, "Computer-assisted bone age assessment based on features automatically extracted from a hand radiograph." *Computerized Med. Imag. Graph.*, vol. 19, pp. 251–259, 1995.
- [25] F. Cao, H. K. Huang, E. Pietka, V. Gilsanz, and S. Ominsky, "Diagnostic workstation for digital hand atlas in bone age assessment," in *Proc. SPIE Med. Imag.*, vol. 3335, 1998, pp. 608–614.
- [26] F. Cao, H. K. Huang, E. Pietka, and V. Gilsanz, "Digital hand atlas and computer-aided bone age assessment via Web," in *Proc. SPIE Med. Imag.*, vol. 3662, 1999, pp. 394–402.
- [27] E. Pietka and H. K. Huang, "Image Processing Techniques in Bone Age Assessment," in *Image Processing Techniques and Applications*, C. T. Leondes, Ed. New York: Gordon and Breach, 1997.
- [28] O. Ratib, R. Appel, and J. R. Scherrer, "Papyrus: A multimodality image file format for PACS and teleradiology," *Radiology*, vol. 177(P), p. 320, 1990.
- [29] M. F. McNitt-Gray, E. Pietka, and H. K. Huang, "Image preprocessing for Picture Archiving and Communication System," *Investigat. Radiol.*, vol. 7, pp. 529–535, 1992.
- [30] M. Razavi, T. Hall, D. Aberle, A. Hayreptian, M. Loloyan, and S. Eldredge, "Display conditions and lesion detectability: Effect of background light," in *Proc. SPIE*, vol. 1234, 1990, pp. 776–782.
- [31] J. Zhang and H. K. Huang, "Automatic background recognition and removal (ABRR) of Computed Radiography images," *IEEE Trans Med Imag.*, vol. 16, pp. 762–771, Dec. 1997.
- [32] H. K. Huang, *PACS: Basic Principles and Application*. New York: Wiley —Liss, 1999.
- [33] J. Serra, Ed., *Image Analysis and Mathematical Morphology*. New York: Academic, 1988, vol. 2.
- [34] R. C. Gonzalez and P. Wintz, *Digital Image Processing*, 2nd ed. Reading, MA: Addison-Wesley, 1987.
- [35] W. H. Press, S. A. Teukolsky, W. T. Vetterling, and B. P. Flannery, *Numerical Recipes in C*. Cambridge, U.K.: Cambridge Univ. Press, 1992.
- [36] J. S. Lim, *Two-Dimensional Signal & Image processing*. Englewood Cliffs, NJ: Prentice-Hall, 1990.
- [37] N. Otsu, "A threshold selection method from gray-level histograms," *IEEE Trans. Syst., Man, Cybern.*, vol. SMC-9, pp. 62–66, 1979.

# Authenticity and Integrity of Digital Mammography Images

X. Q. Zhou, H. K. Huang\*, Senior Member, IEEE, and S. L. Lou

**Abstract**—Data security becomes more and more important in tele-mammography which uses a public high-speed wide area network connecting the examination site with the mammography expert center. Generally, security is characterized in terms of privacy, authenticity and integrity of digital data. Privacy is a network access issue and is not considered in this paper. We present a method, authenticity and integrity of digital mammography, here which can meet the requirements of authenticity and integrity for mammography image (IM) transmission.

The authenticity and integrity for mammography (AIDM) consists of the following four modules.

- 1) **Image preprocessing:** To segment breast pixels from background and extract patient information from digital imaging and communication in medicine (DICOM) image header.
- 2) **Image hashing:** To compute an image hash value of the mammogram using the MD5 hash algorithm.
- 3) **Data encryption:** To produce a digital envelope containing the encrypted image hash value (digital signature) and corresponding patient information.
- 4) **Data embedding:** To embed the digital envelope into the image. This is done by replacing the least significant bit of a random pixel of the mammogram by one bit of the digital envelope bit stream and repeating for all bits in the bit stream.

Experiments with digital IMs demonstrate the following.

- 1) In the expert center, only the user who knows the private key can open the digital envelope and read the patient information data and the digital signature of the mammogram transmitted from the examination site.
- 2) Data integrity can be verified by matching the image hash value decrypted from the digital signature with that computed from the transmitted image.
- 3) No visual quality degradation is detected in the embedded image compared with the original.

Our preliminary results demonstrate that AIDM is an effective method for image authenticity and integrity in tele-mammography application.

**Index Terms**—Data embedding and cryptography, digital mammography, image authenticity and integrity, tele-mammography.

## NOMENCLATURE

AIDM	Authenticity and integrity for mammography image.
DICOM	Digital imaging and communication in medicine.
FFDM	Full-field digital mammography.

Manuscript received September 22, 1999; revised May 6, 2001. The Associate Editor responsible for coordinating the review of this paper and recommending its publication was A. Amini. Asterisk indicates corresponding author.

X. Q. Zhou and S. L. Lou were with the Laboratory for Radiological Informatics, University of California, San Francisco, San Francisco, CA 94143-0628 USA. They are now with private industry.

\*H. K. Huang is with the Department of Radiology, Childrens Hospital, Los Angeles/University of Southern California, Mailstop #81, 4650 Sunset Boulevard, Los Angeles, CA 90027 USA (e-mail: hkhuang@aol.com).

Publisher Item Identifier S 0278-0062(01)06585-5.

LSB	Least significant bit.
MSB	Most significant bit.
ID	Image digest.
IM	Mammography image.
DS	Digital signature.
RSA <sub>E</sub>	RSA public-key encryption algorithm.
RSA <sub>D</sub>	RSA public-key decryption algorithm.
DES	Data encryption standard
DES <sub>E</sub>	The DES encryption algorithm.
DES <sub>D</sub>	The DES decryption algorithm.
P <sub>r,exam</sub>	Private key of the examination site.
P <sub>u,exam</sub>	Public key of the examination site.
P <sub>r,cen</sub>	Private key of the expert center.
P <sub>u,cen</sub>	Public key of the expert center.
ENV	Digital envelope.

## I. INTRODUCTION

**B**REAST cancer is the fourth most common cause of death among women in the United States [1]. Current attempts to control breast cancer concentrate on early detection by means of massive screening, via periodic mammography and physical examination, because ample evidence indicates that such screening indeed can be effective in lowering the death rate [2]. Today, film-screen mammography is the most common and effective technique for the detection of breast cancer. However, the film-screen image recording system of current mammography has several technical limitations that can reduce breast cancer diagnostic accuracy. Digital mammography can overcome most of the problems existing in film-screen mammography, and at the same time provide additional features not available with standard film-screen mammographic imaging such as contrast enhancement, digital archiving, and computer-aided diagnosis.

Currently, many major manufactures are developing FFDM. As an example, the characteristics of the digital mammography system used for this study include [3]: The imaging area is a rectangular of 240 × 300 mm<sup>2</sup>; The spatial resolution of a generated image is about 50 × 50 μm<sup>2</sup>/pixel which is approximately equivalent to nine line-pairs (lp)/mm; The matrix size of the image is 4096 × 5625 (4K × 5.5K) pixels. Each pixel has 12-bit information but is stored in 2 bytes with the four MSBs 16, 15, 14, 13 as zeros. Other manufacturers' digital mammography units may have different specifications, but in general, each digital mammogram is between 40 and 50 Mbytes.

Digital mammography uses the DICOM standard [4] in which the patient information including name, birth date, home address, gender, and history are included in the object classes. This information is sensitive to the patient and important for radiologist's diagnosis.

Telemammography requires the use of FFDM units at the examination site and is built on the concept of an expert center [5]. It allows radiologists with the greatest interpretive expertise to manage and read in real time all mammography examinations. Specifically, in principle, telemammography increases efficiency, facilitates consultation and second reading, improves patient compliance, facilitates operation, supports computer-aided detection and diagnosis, allows centralized archive, distributive reading, and enhances education through telemonitoring. Some of these advantages are being validated in clinical research environment [3], [5]–[7], [10] uses a high speed tele-imaging WAN connecting the examination site with the mammography expert center, so that IMs from a remote examination site can be sent to the expert center in almost real time.

Data security becomes a very important issue when mammographic images are transmitted in a public network. Fig. 1 gives an example of a digital mammogram with artificial calcifications inserted. Fig. 1(a) is the original mammogram, (b) is the mammogram with artificial calcifications added, (c) is the magnification of a region containing some added artifacts, and (d) is the subtracted images between the original and the modified mammogram. With current digital technology, it is fairly easy to make modifications in a digital image. For this reason, image data integrity becomes an important issue in a public network environment. Generally, trust in digital data is characterized in terms of privacy, authenticity and integrity of the data. Privacy refers to denial of access to information by unauthorized individuals. Authenticity refers to validating the source of a message; i.e., that it was transmitted by a properly identified sender and is not a replay of a previously transmitted message. Integrity refers to the assurance that the data was not modified accidentally or deliberately in transit, by replacement, insertion or deletion. All the above three aspects should be considered in a telemammography system.

Many techniques can be used for data protection including network firewall, data encryption, and data embedding. Various techniques are used under different situations. For a telemammography system, since data cannot be limited within a private local area network protected by a firewall, data encryption and data embedding are the most useful approaches to adopt.

Modern cryptography can use either private-key or the public-key methods [8], [17]–[21]. Private-key cryptography (symmetric cryptography) uses the same key for data encryption and decryption. It requires both the sender and the receiver agree on a key *a priori* before they can exchange message securely. Although computation speed of performing private-key cryptography is acceptable, it is difficult for key management. Public-key cryptography (asymmetric cryptography) uses two different keys (a key pair) for encryption and decryption. The keys in a key pair are mathematically related, but it is computationally infeasible to deduce one key from the other. In public-key cryptography, the public-key can be made public. Anyone can use the public-key to encrypt a message, but only the owner of the corresponding private-key can decrypt it. Public-key methods are much more convenient to use because they do not share the key management problem inherent in private-key methods. However they require longer time for

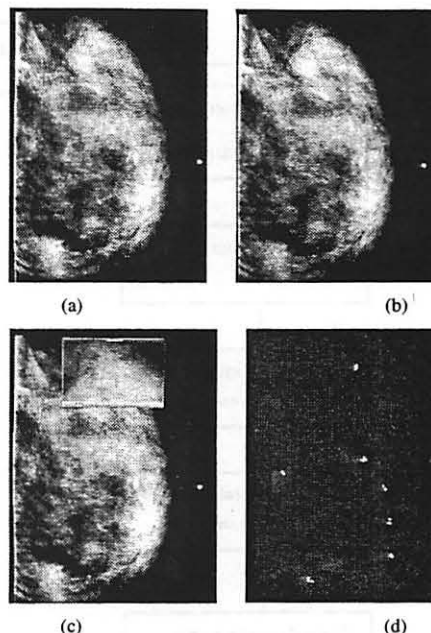


Fig. 1. An example of a digital mammogram with inserted artificial calcifications. (a) Original mammogram; (b) with artifacts; (c) magnification of some artifacts; (d) subtracted image between the original and the mammography with artifacts. The artifacts are highlighted with overexposure during photographing.

encryption and decryption. In real-world implementation, public keys are rarely used to encrypt actual messages. Instead, public-key cryptography is used to distribute symmetric keys which are used to encrypt and decrypt actual messages.

DS is a major application of public-key cryptography [9]. To generate a signature on an image, the owner of the private key first computes a condensed representation of the image known as an image hash value which is then encrypted by using the mathematical techniques specified in public-key cryptography to produce a DS. Any party with access to the owner's public key, image, and signature can verify the signature by the following procedure: first compute the image hash value with the same algorithm for the received image, decrypt the signature with the owner's public key to obtain the hash value computed by the owner, and compare the two image hash values. Since the mechanism of obtaining the hash is designed in such a way that even a slight change in the input string would cause the hash value to change drastically. If the two hash value are the same, the receiver (or any other party) has the confidence that the image had been signed off by the owner of the private key and that the image had not been altered after it was signed off.

In this paper, we discuss how to implement data security in a telemammography system by using existing cryptography techniques. Since privacy is a network access security issue and will not be discussed here, we will concentrate on IMs and related patient data authenticity and integrity.

## II. METHODS

A general description of the algorithm is shown in Fig. 2. A telemammography system generally consists of an examination site and an expert center, and images are transmitted from the

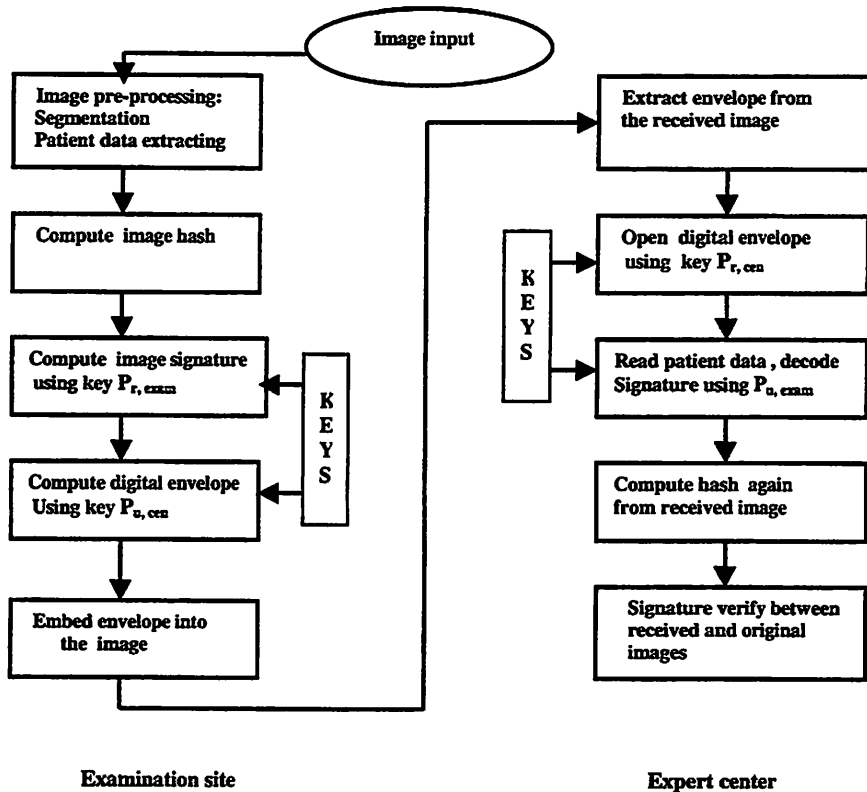


Fig. 2. The block diagram of the encryption and embedding algorithm. Left: data encryption and embedding.  $P_{r,exam}$ ,  $P_{u,cen}$  are private key of the examination site and public key of the expert center, respectively; Right: data extraction and decryption.  $P_{r,cen}$ ,  $P_{u,exam}$  are private key of the expert center and public key of the examination site, respectively.

examination site to the expert center for interpretation. Different from text files, IMs have two distinct characteristics. First, the image size is very large. Each DICOM formatted image includes a small size header file containing sensitive patient information data and a very large image pixel data file. Second, in a 16-b/pixel mammography unit the actual signal, in general, is between 12 and 14 bits, therefore, the LSB (the first bit) in each pixel is noise. This bit can be used for data embedding. Considering these characteristics, a hybrid cryptography algorithm is used to implement image authenticity and integrity in the telemammography system. When a digital mammogram is acquired at the examination site, a DS for all pixels of the image is produced and related patient data is obtained from the DICOM header. Then, both the DS and patient data are encrypted to form a digital envelope. Finally, the digital envelope is embedded into the LSB of randomly selected pixels of the image.

#### A. Data Encryption and Embedding

1) *Image Preprocessing*: This includes segmentation of breast region and acquiring patient information from the DICOM image header. A digital mammogram can be from  $4K \times 5K$  pixels to even larger sizes. By cropping large amounts of background pixels from the image, the time necessary for performing image hashing and transmission can be significantly reduced. The cropping can be done by finding the minimum rectangle covering the breast region. A method to find the

minimum rectangle is given in [10] and [11]. Extracting the boundary of breast region can guarantee that data embedding is performed within the region. If the minimum rectangle is the complete image, then embedding will be performed in the entire image. Data embedded within breast tissues would be more difficult to be decoded than embedded in the background area.

2) *Hashing (ID)*: Compute the hash value for all pixels in the image

$$ID = H(IM) \quad (1)$$

where

- ID hash value of the image;
- $H$  MD5 hashing algorithm;
- IM preprocessed mammogram.

MD5 has the characteristics of a one-way hash function [12]. It is easy to generate a hash given an image ( $H(IM) \Rightarrow ID$ ) but virtually impossible to generate the image given a hash value ( $ID \Rightarrow IM$ ). Also, MD5 is "collision-resistant". It is computationally difficult to find two images that have the same hash value. In other words, the chance of two images have the same hash value is small and it depends on the hash algorithm used [12].

Based on our experience with current FFDM units, the LSB of pixels in the mammogram is mostly noise (see Figs. 8 & 9).

It can be used for data embedding. This bit is excluded when calculating the image hash. Thus, only 11 bits in two bytes for each pixel in the image are used to compute the hash (shift the pixel "right" for 1 bit, then set bit 16, 15, 14, 13, and 12 as zero).

3) *DS*: Produce a DS based on the above image hash value

$$DS = RSA_E(P_{r,exam}, ID) \quad (2)$$

where

DS DS of the mammogram;  
 $RSA_E$  RSA public-key encryption algorithm [13];  
 $P_{r,exam}$  private key of the examination site.

4) *Digital Envelope*: Concatenate the DS, and the patient data together as a data stream, and encrypt them using the DES algorithm [14]

$$Data_{encrypted} = DES_E(key_{DES}, Data_{concat}) \quad (3)$$

where

$Data_{encrypted}$  data encrypted by DES;  
 $DES_E$  DES encryption algorithm;  
 $key_{DES}$  session key produced randomly by the cryptography library;  
 $Data_{concat}$  concatenated data stream of the DS and patient information.

The DES session key is further encrypted

$$Key_{encrypted} = RSA_E(P_{u,cen}, key_{DES}) \quad (4)$$

where  $Key_{encrypted}$  is the encrypted session key, and  $P_{u,cen}$  is the public key of the expert center.

Finally, the digital envelope is produced by concatenating the encrypted data stream and encrypted session key together

$$ENV = (Data_{encrypted})conc.(Key_{encrypted}). \quad (5)$$

5) *Data Embedding*: Replace the LSB of a random pixel in the segmented mammogram by one bit of the digital envelope bit stream and repeat for all bits in the bit stream.

First, a set of pseudorandom numbers  $X_n$  is generated by using the standard random generator shown in (6)

$$X_{n+1} = (aX_n + C) \bmod m \quad (6)$$

where

$a$  multiplier;  
 $C$  additive constant;  
 $m$  mod denoting the modulus operation.

Equation (6) represents the standard linear congruential generator, the three parameters are determined by the size of the image. In our experiment,  $a$ ,  $C$ , and  $m$  were set to be 2416, 37444, and 1771875, respectively, based on our experience with the digital mammography unit used.

To start, both the examination site and the expert center decided a random number  $X_0$ , called the seed. The seed is then the single number through which a set of random numbers is generated using (6). Unlike other computer network security problems in key-management, the number of expert sites and examination sites are limited in telemammography application, the seed-management issue can be easily handled between a mutual agreement between both sites.

Second, a random walk sequence in the whole segmented image is obtained

$$WalkAddress_n = M(X_n/m) \quad (7)$$

where

$WalkAddress_n$  location of  $n$ th randomly selected pixel in the segmented mammogram;  
 $M$  total number of pixels in the segmented mammogram;  
 $m$  mod defined in (6).

Finally, the bit stream in the envelope described in (5) is embedded into the LSB of each of these randomly selected pixels along the walk sequence.

### B. Data Extraction and Decryption

In the expert center, the digital mammogram along with the digital envelope are received. We can check the image authenticity and integrity by verifying the DS in the envelope using a series of reverse procedures. First, the same walk sequence in the image is generated by using the same seed known to the examination site, so that the embedded digital envelope can be extracted correctly from the LSBs of these randomly selected pixels. Then, the encrypted session key in the digital envelope is restored

$$key_{DES} = RSA_D(P_{r,cen}, Key_{encrypted}) \quad (8)$$

where  $RSA_D$  is the RSA public-key decryption algorithm,  $P_{r,cen}$  is the private key of the expert center. After that, the digital envelope can be opened by the recovered session key, and the DS and the patient data in (3) can be obtained

$$Data_{merged} = DES_D(key_{DES}, Data_{encrypted}) \quad (9)$$

where  $DES_D$  is the DES decryption algorithm. Finally, the ID is recovered by decrypting the DS

$$ID = RSA_D(P_{u,exam}, DS) \quad (10)$$

where  $P_{u,exam}$  is the public key of the examination site. At the same time, a second image hash value is calculated from the received image with the same hash algorithm shown in (1) used by the examination site. If the recovered image hash value from (10) and the second image hash value match, then the expert center can be assured that this image is really from the examination site, and that none of the pixels in the image had been modified. Therefore, the requirements of image authentication and integrity has been satisfied.

RSAREF toolkit (RSAREf 2.0, released by RSA Data Security, Inc.) was used to implement the data encryption part in the AIDM.

### C. Digital IMs

FFDM images including large and small breasts had been tested with the AIDM. As shown in Fig. 2, in the examination site, the input is a full-field digital mammogram (Fisher Medical Imaging Corporation, Denver, CO), and the output is the image with the digital envelop embedded. In the expert center, experts

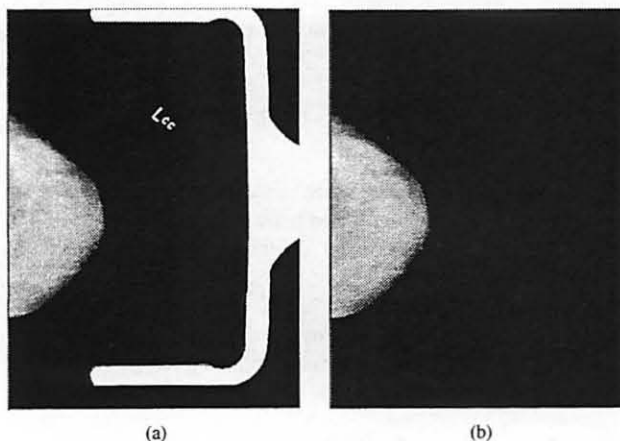


Fig. 3. (a) The original digital mammogram. (b) Mammogram with background removal.

```

c140 11be 47dc 55c8 847d 1462 9095 ac2e
(a)
478a ae44 25eb 814c 145e ea32 19ea 8a9a
e47d 153c 3bd4 b555 982a 0113 9c44 29e1
9f93 a436 a0df 7288 32cd 195e 94cf 7de7
3c8a 753d 39df 2641 a870 904c aff8 11b8
983e 2710 105f cb99 dc8f 9410 edd4 6913
261c c7e0 19e0 e740 0452 d341 4ed9 dd8b
b0dd 00ec 7e6f aacb 47f2 0acd 7b59 25a3
0557 f042 9589 5626 d4d4 cb21 d2ad 7804
(b)

```

Fig. 4. (a) The MD5 hash value of the mammogram shown in Fig. 3. (b) The corresponding DS.

can manipulate the embedded IM and verify its authenticity and integrity.

### III. RESULTS

Following results are an example obtained from one mammogram. Fig. 3(a) shows the unprocessed image, and Fig. 3(b) the image with background removed. Both images are shown to demonstrate the difference in size before and after background removed.

Fig. 4(a) and (b) shows the MD5 hash value and the DS, respectively, of the background removed mammogram in hexadecimal format.

Fig. 5(a) is the merged data file of DS and patient information. Fig. 5(b) is the digital envelope [see (5)] which is going to be embedded into the image. From this figure, we can see the digital envelope is totally incomprehensible.

Fig. 6, from left to right, represents the original mammogram, the mammogram in which the digital envelope has been embedded, and the subtracted image between the original and embedded mammogram, respectively. By comparing the original  $4K \times 4K$  image and the embedded image from two adjacent DICOM Gray Scale Standard  $2K \times 2K$  monitors, using a magnifying glass tool for a true  $4K$  resolution image, we found the embedded image has no visual quality degradation based on results from three random image sets. Also, from the subtracted image, we can see the pixels selected for data embedding are

fully random and within the region of breast tissues. In this example, the total pixels in which the LSBs were changed during data embedding are 3404 which accounts for 0.12% of the total pixels in breast tissue region. It is seen from Fig. 5(b) that there are 840 characters or  $840 \times 8 \text{ bits} = 6720 \text{ bits}$ . During embedding, only 3404 bits are required to be changed because 3316 bits in the bit stream are identical to the LSBs of the randomly selected pixels).

The % pixel changed can be computed by

$$\begin{aligned} \text{Total \% Pixel changed} \\ = ((\text{no. characters in envelope} \\ \times 8 \text{ bits} - \text{unaffected LSBs})/M) \times 100\% \quad (11) \end{aligned}$$

The time required to run the algorithm depends on the image size. In this case, the unsegmented image size is about 46 Mbytes, the time required is approximately 37 s total for signing the signature, sealing the envelope, and embedding data for the segmented image. For the unsegmented image, it will be about 6 times longer because the segmented image is less than 15% of the unsegmented image, and the algorithm is mostly linear search.

In the expert center, one can verify image authenticity and integrity as well as patient information by using the correct seed to extract the digital envelope; the correct private key of the expert center to open the envelope; and the correct public key of the examination site to verify the image signature. Image authenticity is confirmed if all keys used in the expert center match with their corresponding one used in the examination site. Any modifications of the image are easily detected by the signature verification in the expert center. Fig. 7 shows an example of the image hash calculated from the received mammogram in the expert center if the value of one randomly selected pixel was changed from 14 to 12. Comparing Fig. 7 with the original image hash produced in the examination site shown in Fig. 4(a) demonstrates the drastic difference of the hash value by such a slight change of one pixel value.

Table I shows the time required using the AIDM to process the mammogram shown in Fig. 3. Although results are only based on one image, nevertheless it provides a glimpse to the time required for such algorithm. The procedures of embedding data and extracting data refer to embedding data into the mammogram and extracting data from the embedded mammogram, respectively. For signing the signature and verifying the signature, most of the time is taken by computing image hash value. The purpose of this table is to show the relative time required for encryption and decryption processes. We did not make any effort to optimize the algorithm nor the programming.

### IV. DISCUSSION

DS can be used to verify image authenticity and integrity. Generally, a DS is attached to the head or the end of the image data file. In this paper, we present an algorithm, AIDM, by embedding the DS and some sensitive information such as patient ID into the image itself. Comparing to appending the DS on the head or at the end of the file, our method has several advantages. First, it does not change the file size. Second, it does

A@AABACAE@D%BAALATAE2AYBAEAUA}AU<:ouUA@\*AASAU0)AABAOB6 BAE2IAYAAOI}C<AEU=9B&A  
 "pABL\_@AQ\_A@>'APAP\_EAUUIA@PioiAS&A\CaAVac@ADROANUYAE\*YA@i-oaEEd  
 I{Y%EAEWB@OAEV&OOEIO-xADpatient information:  
 Patient Jane B. Doe, II, female, Caucasian, born on July 1, 1947, lives at 371  
 Main Avenue in San Francisco, was admitted on January 18, 1998, at 10:05 A. M.  
 by Doctor William K. Smith (#00135) for surgery. The patient has been assigned  
 to Room 345, bed 01 on nursing unit 100. The next of kin is John E. Doe,  
 husband. The ADT message 201 was sent from system STORE at the Mission site to  
 system MiME at the Laurel site on the same date two minutes after the admit.

Some other information can also be added here: This is just an example of how to  
 encrypt sensitive patient information. If necessary, radiologists can put as  
 much as information related to patient mammography here.....

(a)

```

A*x|B@F|A\AM@OIOU2AALAK@OMH\gCAASAYyBAM>7-U4AE@YebO-A@B@ANAU}ATVAAEAUg@B@0E-HAAI
3ALAUUN-AOAEAXOAO-UAV<7%eAB_I0EU;AY%0 UWaeAaOAppriAFBc^BeUo^AA^AUIA@AXU|BPTrE
YARAAAIRAWANASO@AO@EAL@A?AEAU4AT0AEU2ABAHZ*F!AG|@AUAI'/AZ*F. "kAAIHOBABeANbG;
CAE=APARAKEOACLAt110AhtO)ALonVY%EA<OXAY8xeakAO*AKWAE<IUU~<1AC(OAPXASO>O@A-AAAU.T
y$@cA[AL+CLUu AQUAS;RiAb@SiEnFSAUAWAEOHARY*O
TIj9EjOAEAAEABAM_AOQVpAAAUAbOAEAIbUAE]kIe/L^AQI[XA[2ES)IAIAO<xABAKAYAEfiWAAAE-
OAE%AOIAV+AUAS5AIXA@O408AI7Oau2+ASARA
+IYAZAIVN4ADXA'AD~EdAIA\O@MMAcA)UBi%CAE'z|O2-YA#4a5uzKziA\+mUW;#U>ACIE@
AOMA [aAE]yAD} ,AA\AE8E]34AEAO*YU+@ALANEUKAUAI"Ox%IQE&IAYMEAE@vY9UAM#eAOB'IA@U
a Os66]:Aj]_ @ADA@<AI-ABcH_@5HEXOI AUFOXAOCTGrI}AIAY
/daBAlAIjAOOUeAI&L-ME@UtOAFIJE@u@wAO>AE±@ANz]1 AVAMC(AA=dOdqAU~u]ABRUÉ` 'IAIOX
rABUUAU@O'Te2aE082J4FA}D;IAE{VA?eAF}a AVdiANAOHeA9ABP_0cAWAMH0U6X
A\~a;ANAUUuAU-FIxAU'T
ONAC-IYARZAE, zCA\ UAYUA_UN{icAA-mcm$~2ig)A#AI+AUvDCuA]v*RX<NeAF@AOAA[A~qIJ0
ARfEnEbA$Wi+TAY%MAQe'YyZTie;OEb00 08AOV_AU±0X
08aaK03AWU@O@AAAMU0+yASAFAFE@A@C@EA}|1NRFacAO|D0}EAip2hAE062MvPK
  
```

(b)

Fig. 5. (a) The combined data file of the DS and patient information. Two and half lines (until the word patient ...) data is the DS displayed in ASC II format identical to Fig. 4(b) displayed in hexadecimal format. (b) Its encrypted format using the public key of the expert center.

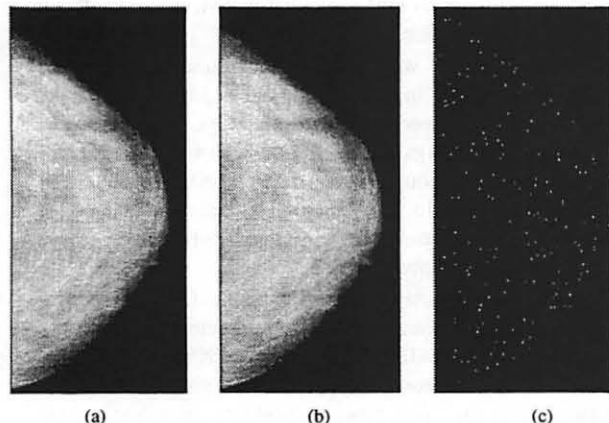


Fig. 6. (a) Original mammogram. (b) Mammogram with digital envelope embedded, and the subtracted image between the original and the imbedded mammogram.

147a a78e a5c9 db08 d2fe dd6e 2447 1621

Fig. 7. The MD5 hash value of the data embedded mammogram after the value of one randomly selected pixel in the image was changed from 14 to 12. It is totally different with the hash shown in Fig. 4(a).

not need to redefine the file format. These two advantages have  
 an add-on value that the embedded image still confirms with  
 the DICOM image format standard which is very important for  
 medical image communications. Finally, because the embedded  
 envelope in the image is invisible, it would be difficult to be  
 removed deliberately or undeliberately. Our embedding method

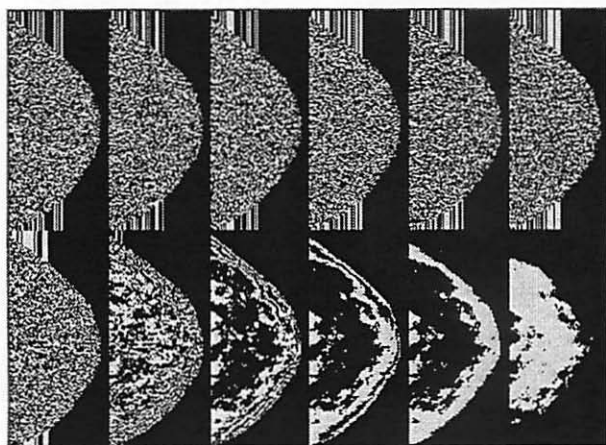
TABLE I  
TIME REQUIRED FOR THE AIDM PROCESSING ON THE MAMMOGRAM  
SHOWN IN FIG. 3(a)

Procedures in examination site	Time (s)	Procedures in expert center	Time (s)
Signing the signature	20	Extracting data	19
Sealing the envelope	< 1	Opening the envelope	< 1
Embedding data	17	Verifying the signature	17
Total	< 38	Total	< 37

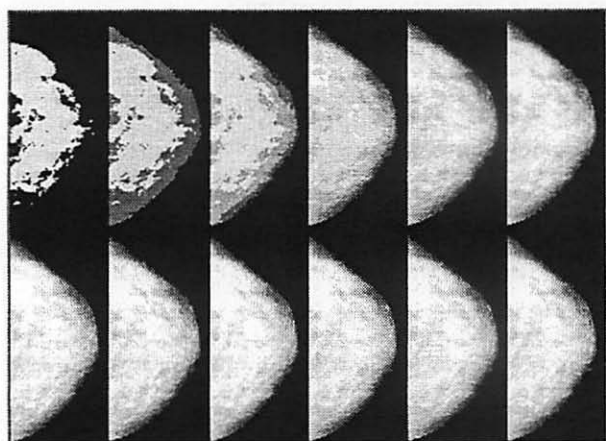
is suitable for medical images because they have 12–14 b signals/pixel in a 16b/pixel storage allocation allowing the LSB for data embedding.

Using public-key cryptography allows a better key-management. Both the examination site and the expert center can publish their public key and keep their private key secretly by themselves. Since in the examination site the image data file is encrypted by using its own private key and the public key of the expert center, and in the expert center the image file is decrypted by using its own private key and the public key of the examination site, there is no need to use a secure channel to exchange keys. However, the security of public-key cryptography depends on the validation of public key certificate which has not been considered in our method right now. With the development of the public key infrastructure (PKI), it would become easier to get and validate public key certificate from a certificate authority.

Many of the less-significant bits in live "natural" images are noise caused by the imaging acquisition device. From a visual standpoint, the noise at this bit level is entirely masked by the complexity of the scene [15]. Digital mammography is not an exception. Fig. 8(a) and (b) depicts the visual aspect of the in-



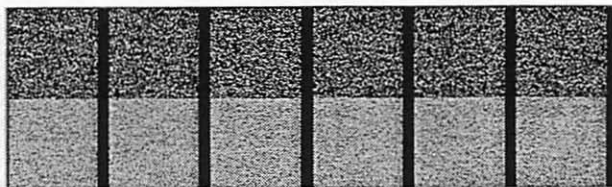
(a)



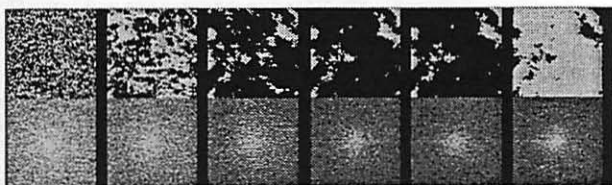
(b)

Fig. 8. (a) Individual bit planes of the mammogram. From left to right, top to bottom, individual bit plane images of bit 1 (LSB), 2, 3, 4, 5, 6, ..., and 12 (MSB). (b) Accumulative bit planes of the mammogram. From left to right, top to bottom, accumulative bit plane images of bit 12,  $12 + 11$ ,  $12 + 11 + 10$ , ...,  $12 + 11 + 10 + 9 + 8 + 7 + 6 + 5 + 4 + 3 + 2 + 1$  (the original mammogram).

dividual bit planes and the accumulative bit planes [16] of the digital mammogram shown in Fig. 3, respectively. In Fig. 8(a), the right-most in the bottom row displays the MSB (bit 12). Moving from right to left, bottom to top row, the next MSBs are 11, 10, 9, 8, 7, 6, 5, 4, 3, 2, 1, respectively. Individual bit planes demonstrate whether image information is presented at each bit. It can be seen that the more close to bit 1, the less useful information the bit contains. For the LSB (bit 1), no noticeable structural information can be observed. In Fig. 8(b), the top left image displays the MSB. Moving from left to right, and top to bottom, the next MSB is added to the previous one:  $12 + 11$ ,  $12 + 11 + 10$ ,  $12 + 11 + 10 + 9$ , ... The last image in the second row is the original. Accumulative bit planes shows the contribution of those bit planes to the image. No visual differences between the original and the image next to the original in the second row are observed. This means that the LSB has nearly no contribution to the whole image. The first row of Fig. 9(a) and (b), from left to right, is a region of  $800 \times$



(a)



(b)

Fig. 9. (a) Top row, from left to right, the randomly selected regions of  $800 \times 800$  pixels, then fixed for every bit plane, 1, 2, 3, 4, 5, and 6. The bottom row, from left to right, the corresponding frequency spectrum of the Fourier transform for the above images. (b) Top row, from left to right, bit planes, 7, 8, 9, 10, 11, and 12. The bottom row, from left to right, the corresponding frequency spectrum of the Fourier transform for the above images. The Fourier spectrum of bit 1 demonstrates random noise.

$800$  pixels randomly selected, then fixed from individual bit planes of bit 1, 2, 3, 4, ..., 11, and 12. The second row of (a) and (b) are the frequency spectrum of the Fourier transform of corresponding regional images, respectively. The spectrum of the LSB image is nearly uniformly distributed, signifying that it represents random noise.

The AIDM works well in digital mammograms for two reasons. First, pixels in a mammogram is highly correlated. Second, the LSB of each pixel in the image is mostly noise as demonstrated in Figs. 8 and 9. Although only 12 bits of 2 bytes are used in mammograms, data embedding should not be performed on the 13, 14, 15, or 16 bit because some image compression algorithms may clip these bits during image acquisition and/or archive.

Currently, we are using RSAREF toolkit (RSaref 2.0, released by RSA Data Security, Inc.) to implement the data encryption part in the AIDM. At the research stage, RSAREF toolkit is an appropriate cryptographic tool since it is free for noncommercial use. Two aspects should be considered in the future work: the speed of the algorithm both in encryption and decryption, and the key management.

Our results demonstrate that embedding DS into a mammogram using standard data encryption technique is an effective method for verifying image authenticity and integrity in teleradiology. We are in the process of implementing the AIDM method in our teleradiology system which consists of two FFDM units, three digital mammogram workstations, one archive server connecting to the department clinical picture archiving and communication systems. These components located in two UCSF campuses are linked together by an asynchronous transfer mode OC-12 (622 Mb/s) Sonet ring with an OC-3 (155 Mb/s) drop at each connection. The AIDM can be extended to other teleradiology applications. In these cases, both the noise bit and the pixel correlation of the imaging modality under consideration need to be investigated *a priori*.

## REFERENCES

- [1] C. C. Boring, T. S. Squires, and T. Tong, *Cancer Statistics*, vol. 42, pp. 19–38, 1992.
- [2] S. A. Feig, "Decreased breast cancer mortality through mammographic screening: Results of clinical trials," *Radiology*, vol. 167, pp. 659–665, 1988.
- [3] M. Yaffe, Digital mammography, in *RSNA Categorical Course in Physics*, pp. 271–282, 1993.
- [4] *Digital Imaging and Communications in Medicine (DICOM)*. Rosslyn, VA: National Electrical Manufacturers' Association, 1996, PS3.1-1996-3.
- [5] S. L. Lou, E. A. Sickles, and H. K. Huang *et al.*, "Full-field direct digital mammograms: Technical components, study protocols, and preliminary results," *IEEE Trans. Inform. Technol. Biomed.*, vol. 1, pp. 270–278, June 1997.
- [6] E. A. Sickles, Physics aspects of breast imaging—Current and future considerations: Computer-aided diagnosis and telemammography: Clinical perspective telemammography, in *RSNA Categorical Course in Breast Imaging*, pp. 283–285, 1999.
- [7] ———, Physics aspects of breast imaging—Current and future considerations: Computer-aided diagnosis and telemammography: Clinical perspective telemammography, in *RSNA Refresher Course*, 2000.
- [8] S. Garfinkel and G. Spafford, *Practical Unix and Internet Security*, Devon, U.K.: O'Reilly & Associates, Inc., 1996, pp. 139–190.
- [9] R. Rivest, A. Shamir, and L. Adleman, "A method for obtaining digital signatures and public-key cryptosystems," *Commun. ACM*, vol. 21, no. 2, pp. 120–126, 1978.
- [10] H. K. Huang and S. L. Lou, Telemammography: A technical overview, in *RSNA Categorical Course in Breast Imaging*, pp. 273–281, 1999.
- [11] S. L. Lou, "Optimization of Soft Copy Display Parameters for Digital Mammograms," Final Report Federal Technology Transfer Program to Advance Novel Breast Imaging Technologies, HHS Contract no. 282-97-0079, U.S. Department Health & Human Services, Sept. 30–Dec. 31 1999, Mar., 2000.
- [12] R. Rivest. (1992) The MD5 Message-Digest Algorithm. Document of MIT Laboratory for computer Science and RSA Data Security, Inc. [Online]. Available: <ftp://ftp.funet.fi/pub/crypt/hash/papers/md5.txt>
- [13] B. S. Kaliski Jr., "An Overview of the PKCS Standards," 1993. An RSA Laboratories Tech. Note.
- [14] B. Schneier, *Applied Cryptography: Protocols, Algorithms, and Source Code in C*, N. Y.: Wiley, 1995, pp. 250–259.
- [15] S. Walton, "Image authentication for a slippery new age," *Dr. Dobb's J.*, Apr. 1995.
- [16] H. K. Huang, *PACS—Basic Principles and Applications*. New York: Wiley, 1999, pp. 116–119.
- [17] M. M. Yeung, "Digital watermarking," *Commun. ACM*, vol. 41, no. 7, pp. 31–33, 1998.
- [18] N. Memon and P. W. Wong, "Protecting digital media content," *Commun. ACM*, vol. 41, no. 7, pp. 35–43, 1998.
- [19] S. Craver and B. L. Yeo, "Technical trials and legal tribulation," *Commun. ACM*, vol. 41, no. 7, pp. 45–54, 1998.
- [20] J. Zhao, E. Koch, and C. Luo, "In business today and tomorrow," *Commun. ACM*, vol. 41, no. 7, pp. 67–72, 1998.
- [21] J. M. Acken, "How watermarking adds value to digital content," *Commun. ACM*, vol. 41, no. 7, pp. 75–77, 1998.

# Professional Issue

## Radiography and information technology (IT)

HK Huang

Childrens Hospital of Los Angeles/University of Southern California

### Background

I was honoured to be invited by the International Hospital Federation (IHF) Congress to participate as a Panelist to discuss on "Transforming Healthcare in the Internet Era", and to co-chair a session on "Information System" during the 32nd IHF Congress in Hong Kong, May 15-18, 2001.<sup>1, 2, 3, 4</sup> After the Congress I was invited by the Hong Kong Hospital Authority (HA) to participate in an Information Technology (IT) five-year Strategic Planning Workshop and to present a topic on "High Tech Futures". As a result, I had the opportunity to learn and to observe trends of information technology (IT) development related to healthcare, radiology, and radiography, both in the international scale as well as in Hong Kong [4]. Many of the lessons learned, in my opinion, are pertinent to the future development and trend of radiography profession in Asia. I thought I would like to share some of these with you.

### Transforming healthcare in the internet era

During the Panel discussion on "Transforming Healthcare in the Internet Era", Dr. Don Detmer, Dennis Gillings Professor of Health Management, University of Cambridge, United Kingdom opened the panel discussion with his thought on the impact of Internet to healthcare delivery:

*"Healthcare services will be transformed in the Internet Era by developments in biotechnology, bioinformatics, health informatics, assimilation of modern business processes, and changing policy expectations. Discoveries in biology and communications technology offer the potential for improvements in health status of individuals and populations. Improved access to information about health and disease will typify early progress. Care in hospitals will shift toward palliation and end-of-life care; curing and prevention will increase in outpatient settings and/or within the home or workplace. Barriers include resistance to change and a lack of a global health information infrastructure that includes financing, standards, and coherent policy."<sup>5</sup>*

Dr. Bernie HK HUANG, Professor & Director of Informatics, Department of Radiology, Childrens Hospital Los Angeles/ University of Southern California, USA, and Chair Professor, Medical Informatics, The Hong Kong Polytechnic University, Hong Kong discussed the infrastructure of Internet 2 and its implication to future health care delivery.<sup>5,6</sup>

Dr TSE Chun-hing, Chief of Service, Pathology, Queen Elizabeth Hospital, Hong Kong presented the current thought on using Internet for healthcare delivery in Hong Kong.<sup>5</sup>

Points to take home in their presentations are that:

1. Healthcare delivery system has gone through substantial changes during the past five years due to the advance of computer and communication technologies.
2. Paper-based and film-based operation is gradually changed to electronic-based.
3. Internet technology allows for a more efficient clinical operation, and has become an indispensable tool in clinical environments.
4. Internet creates the issue of data security in public networks, which includes privacy, authenticity, and integrity.
5. One drawback of current Internet is its slow speed for image transmission. The new wave is the Internet 2, or the Next Generation Internet (NGI), which provides 1,000 time faster transmission rates.

### Computerized patient record (CPR), electronic patient record (EPR), and electronic medical record (EMR)

Modern hospitals require hospital information system (HIS), or clinical management system (CMS) to streamline the operation. In the Western world, the term HIS is used more often, whereas in Hong Kong, CMS is preferred.<sup>7,8</sup> These systems are hospital operation oriented and are not patient friendly in the sense that it is not portable for patient. A patient transferring from one hospital to the next may find difficulty to transfer his/her established file from the previous hospital due

to incompatible ID No. and/or data format. The current trend is to revamp the data structure toward patient-oriented so that data can go with the patient. In this new data structure, terms like EPR, EMR, and CPR emerge. In the Western world, the EPR or EMR are used, whereas in the Hospital Authority (HA) in Hong Kong, CPR is preferred. The latter term is used to distinguish it from the method of electronically scanning a paper record.

The HA is at the decision point of developing CPR to support the current and future patient-oriented data requirements of the 44 hospitals under its auspices. The one-day post Congress Workshop is for the purpose of brain storming on a five-year IT strategic planning within HA.

Data available in the current HA CMS include:<sup>4</sup>

- Discharge Summary
- Diagnoses and procedures
- Clinical data framework
- Clinical notes
- Rehabilitation outcomes
- CPR-information Retrieval
- CMS enquiry functions
- Patient administration
- Laboratory/Radiology/Pharmacy systems
- Medication Order Entry
- OT Record System
- Endoscopy Record System
- Generic Clinical Requests
- Generic Result Reporting
- Allergies and alerts
- Common dosages
- Drug-drug interaction
- E-knowledge

Among these data, the new CPR should consider two major issues:

1. What are the areas of improvement in the current available systems?
2. How is it helping us in improving patient care delivery and outcomes?

It will take many years for HA to develop such a comprehensive CPR system to serve the majority of Hong Kong patients effectively and efficiently. The keys issues are:

1. To have enough resources and supports from the Hong Kong government to embark on such large scale comprehensive data repository system,
2. To have dynamic leadership and enough expertise to lead the project to its fruitful completion,
3. To provide enough education for the healthcare providers to fully utilize such system.

## **Impact to the radiography profession**

Without the current advance in computer and communication technologies, it would be difficult to develop the CPR, which is a very large-scale medical informatics system. In the radiography profession, how can one take advantage of this full CPR development cycle, from incubation, to maturity, and to appreciation. I would like to offer the following suggestions:

### **1. Participation**

Radiographers have to be involved in the CPR development. The majority of radiographers in Hong Kong are employees of the HA, and they are therefore entitled to be involved. Take a look at the allied health science professions, who is more qualified to participate? Radiographers, of course. The profession has the training in medical imaging and informatics, with direct patient contact, and plays an important role in determining the patient outcome. The system developed will eventually affect radiographer's daily operation and professional life. Why not then participate in its development, and treat it as your system.

### **2. Continuing education**

Radiographer's traditional training is in imaging. To fully appreciate the CPR requires some IT knowledge. I encourage you to select some IT courses during your training or in your professional career development path. Courses like concept and usage of computer and communication technologies, database, graphic user interface would enrich your professional development. Courses like how to use certain computer software are good to know, but those only allow you to be proficient in your job, and not necessarily enrich your career development path related to CPR.

### **3. Ownership**

One has to take ownership of the CPR in its developmental stage as well as during its deployment and operation. Ownership does not mean to own the IT system, but to have the pride to claim that it is "your" system because you have contributed to its success. Once one claims the ownership of the CPR, one feels responsible. It is the responsibility that drives one's desire to improve, to master, and to flourish.

### **4. Leadership**

Prerequisites of leadership are participation, enough education, and after the claim of ownership of the CPR in your hospital or within HA. A senior radiographer in charge of a large hospital or medical center IT operation is common in the US, especially relating to imaging area and radiology operation like PACS (Picture Archiving and Communication System) and RIS (Radiology Information System). Leadership in IT would

eventually elevate the prestige and position of the radiography profession among the allied health sciences and medical profession.

## Conclusion

Maria Law wrote an Editorial: "Opportunity or Threat" in 1999,<sup>8</sup> I followed her lead and wrote: "Emerging Opportunity in Digital Imaging and Informatics for Radiographers in the New Millennium"<sup>9</sup> to encourage you to consider this emerging opportunity to enrich your profession. Now that the window of opportunity will be open up in Hong Kong and Asia soon, are you ready to accept this challenge?

## References

1. Yeoh EK. Developing a holistic view and approach to healthcare. Proceedings of the 32nd IHF Congress, Hong Kong. 26.
2. William H. Organizational reform in Hong Kong public hospitals. Proceedings of the 32nd IHF Congress, Hong Kong. 8.
3. Fung H. Clinical reform in Hong Kong. Proceedings of the 32nd IHF Congress, Hong Kong. 10.
4. Tse N. Infrastructure reforms in Hong Kong public hospitals. Proceedings of the 32nd IHF Congress, Hong Kong. 9.
5. Detmer DE. Transforming healthcare in the internet era. Proceedings of the 32nd IHF Congress, Hong Kong. 53.
6. Yu F, Hwang K, Gill M, Huang HK, 2000. Some connectivity and security issues of NGI in medical imaging applications. J High Speed Networks. 9, 3-13.
7. Huang HK. PACS: Basic principles and applications. N.Y. John Wiley & Sons, 1999: 521.
8. Law M. Opportunity or threat? HK Rad J. 1999; 3:1.
9. Huang HK. Emerging opportunity in digital imaging and informatics for radiographers in the new millennium. HK Rad J. 1999; 3:2.

magnitude estimates, and a mathematical framework.

A brief summary might alert the reader to the book's contents: The first three, introductory, chapters are followed by the basic theory of single-point statistics arising from the equations of motion (chapter 4) and examples of classical engineering flows (chapter 5). Chapter 6 is a description of spectral (and multipoint) analysis, and chapter 7 deals with Andrei Nikolaevich Kolmogorov's ideas (in both 1941 and 1962). The book ends with a description in chapter 8 of numerical simulation of turbulent flows; direct numerical simulations, large eddy simulations, and engineering closure schemes are described briefly. The material is more or less standard for a course taught in a US engineering science department to students with a moderate background in fluid dynamics.

The character of a book is determined at least partly by the care with which the material is presented, and this one amply demonstrates the care that the authors have invested. For instance, their treatment, in chapter 3, of length and time scales is lively and refreshing, and their description of the physics of shear flows, without much use of mathematical equations, though somewhat longish, makes rewarding reading. The authors have succeeded in the task they set out to do, and I recommend the book to all students of turbulence, no matter what their persuasion. Patient students who work their way through the authors' arguments will be rewarded by an improved intuition for the subject.

What, then, are its shortcomings? One could say that some details of the analysis of the turbulent boundary layers are slightly unconventional (and the appendix A to chapter 5 is hard to penetrate); the references are sometimes idiosyncratic and incomplete; the book avoids mention of such controversies as logarithmic versus power laws in the intermediate layer of the boundary layer and the existence or otherwise of power laws in the inertial range; and so forth. These issues and more modern developments will perhaps receive their due share of attention in the second volume the authors have promised. And, for a book aimed essentially at students, it would have been better had it included some exercises on which students could test their understanding and mastery.

KATEPALLI R. SREENIVASAN  
Yale University  
New Haven, Connecticut

## Handbook of Medical Imaging. Volumes 1-3

### ► Volume 1: Physics and Psychophysics

Edited by Jacob Beutel, Harold L. Kundel, and Richard L. Van Metter  
\$110.00 (949 pp.).  
ISBN 0-8194-3621-6

### ► Volume 2: Medical Image Processing and Analysis

Edited by Milan Sonka and J. Michael Fitzpatrick  
\$130.00 (1218 pp.).  
ISBN 0-8194-3622-4

### ► Volume 3: Display and PACS

Edited by Yongmin Kim and Steven C. Horii  
\$110.00 (512 pp.).  
ISBN 0-8194-3623-2  
SPIE, Bellingham, Wash., 2000.  
\$315.00 set (2679 pp.).  
Set no. PM81Z

*Handbook of Medical Imaging*, published by SPIE (The International Society for Optical Engineering) Press, is a three-volume edited reference providing a comprehensive overview of the theory and current practice of medical imaging.

*Volume 1: Physics and Psychophysics*, edited by Jacob Beutel, Harold L. Kundel, and Richard L. Van Metter, contains 20 chapters. Part I consists of 8 chapters devoted to the physics principles of medical imaging, and Part II covers psychophysics. *Volume 2: Medical Image Processing and Analysis*, edited by Milan Sonka and J. Michael Fitzpatrick, contains 19 chapters presenting the ideas and the methods of image processing and analysis that are at work in the field of medical imaging. *Volume 3: Display and PACS*, edited by Yongmin Kim and Steven C. Horii contains 13 chapters, with the first 7 on image display technology and the rest on PACS (Picture Archiving and Communication Systems).

These three volumes are probably one of the most comprehensive collections of topics in medical imaging available today, both in theory and practice. Each chapter is written by researchers in medical imaging who have participated frequently in the annual SPIE conference in medical imaging in southern California; for this reason, the chapters reflect the respective authors' accumulated knowledge, gained through years of interaction with colleagues in their field of expertise. Each chapter in these three volumes is self-contained and can be understood without referring to other chapters. The volumes can be used as a reference for

the professional or as a textbook in medical imaging.

For educational purposes, chapters can be selected to form senior or graduate courses; the prerequisite would be a one-year course in image processing. The instructor can select different chapters according to the medical imaging curriculum and supplement with outside readings based on references given in the chapter. In addition, the instructor may want to formulate problem sets and experiments to augment the class lectures. The descriptions in each chapter of problems remaining to be solved could provide excellent ideas for dissertation research.

Medical imaging is physics, engineering, technology, and human acceptance and interaction. Although physics principles are the driving force in medical imaging, the roles of engineering and technology evolve through time and are dictated by user requirements and demand. The readers are cautioned that today's prevailing medical imaging technology may render itself obsolete in a very short time, because of technological advancement, human, and social factors. Medical imaging is not just the practice of science, but also the practice of art.

H. K. HUANG  
Childrens Hospital of Los Angeles  
University of Southern California  
Los Angeles

## Shoemaker by Levy: The Man Who Made an Impact

► David H. Levy  
Princeton U. Press, Princeton,  
N.J., 2000. \$27.95 (303 pp.).  
ISBN 0-691-00225-8

David H. Levy's *Shoemaker by Levy* is a love story. It is the story of Eugene M. "Gene" Shoemaker's love of geology, the story of the loving relationship between Gene and his remarkable wife, Carolyn, and it is the story of Carolyn's midlife discovery of a passion for comet and asteroid hunting alongside her husband and scientific colleague, Gene.

Levy is an astronomer well known for his comet discoveries. He met Gene and Carolyn in 1988, and developed a unique friendship and collaboration with them. The trio's mutual interest and complementary experience in comet observing quickly melded them into an observing team.

This is a book for anyone interested in modern planetary sciences, in the progression and expansion of classical

# PACS, informatics, and the neurosurgery command module

H. K. HUANG, D.Sc., F.R.C.R.(Honorary)

*Childrens Hospital, Los Angeles, University of Southern California, Los Angeles, California*

**Abstract:** Picture archiving and communication system or PACS is an imaging management system. combining both imaging modalities and related patient information systems. PACS integrates images of a patient from magnetic resonance, computed tomography, ultrasonic, computed radiography, digital subtraction angiography, nuclear medicine, and endoscopy, archives them all into a database, and distributes selective information to designated workstations for review and diagnosis. PACS has been integrated into daily clinical operation by many medical centers and clinics since 1992.

Imaging informatics is the computer software technology, which extracts pertinent information from the PACS database to facilitate various medical applications. The infrastructure in medical imaging informatics includes PACS database, patient relevant information, high-speed network, images visualization and presentation.

An application using imaging informatics and PACS application for lower back spinal surgery is the concept of the Neurosurgery Command Module (NCM). The NCM is a very small version of the electronic patient record (EPR), a database system manages patients scheduled for and/or have gone through lower back spinal surgery. Before the surgery, NCM collects patient's CT and MR and other pertinent images including 3-D rendering from the spinal surgery server connected to PACS. The NCM can be located at the surgical suite or preparation area for the surgeons and healthcare providers to preview the patient folder. During pre-surgery, the NCM is wheeled to the surgical suite to connect with the C-arm X-ray and endoscopy. This will allow for on-line imaging examination and real-time image display of all types of images during the surgery. After the surgery, the informatics software in the NCM can combine all relevant images, related patient's information, and surgical procedure and results systematically into the patient soft folder for future review and use. This paper reviews PACS and medical informatics related to neurosurgery and outlines the concept of the neurosurgery command module.

**Key Words.** picture archiving, communication system, command module, imaging informatics, electronic patient record, image workstation

There are many advantages of introducing digital and communication technologies to replace the conventional paper and film-based operation used in healthcare delivery. For example, through the computer, it is possible to manipulate digital diagnostic images for value-added diagnosis like in image-guided surgery. High-speed digital and communication technologies can speed up healthcare delivery and reduce operation costs. Minimally invasive spinal medicine and surgery can benefit from taking advantage of these already existing and emerging technologies.

Modern hospitals or clinics use Hospital Information System (HIS) or Clinical Management System (CMS) to manage their operations. HIS or CMS collect patient related information including demographic, test results, diagnostic results from imaging examinations, and hospital/clinic management data and distribute them strategically to facilitate the hospital/clinic operation. Neither HIS nor CMS consists of an imaging subsystem. Both HIS and CMS are hospital- or clinic-based, not designed for an individual patient. A recent trend is to replace HIS/CMS by the Electronic Patient Record (EPR) or Electronic Medical Record (EMR)

system, a more patient centric database system.<sup>1</sup>

In addition to HIS or CMS, a digital operation in a hospital or clinic requires an imaging management and communication system (IMAC), or Picture Archiving and Communication System (PACS). PACS was originally developed to integrate and to manage image acquisitions, their storage, processing, distribution, and display for the radiology department. Its operation augments with a radiology information management system (RIS), a subset of HIS or CMS, for managing radiological examination scheduling and diagnostic reports. The combination of HIS or EPR and PACS is referred to as hospital integrated PACS (HI-PACS).<sup>2</sup> Recent development in PACS is in imaging-guided diagnosis and imaging-guided surgery.

Imaging informatics is the computer software technology, which extracts pertinent information from the PACS database to facilitate various medical applications. The infrastructure in medical imaging informatics includes PACS database, patient relevant information, high-speed network, images visualization and presentation. In subsequent sections, we will develop the concept of

## Generic PACS Components & Data Flow

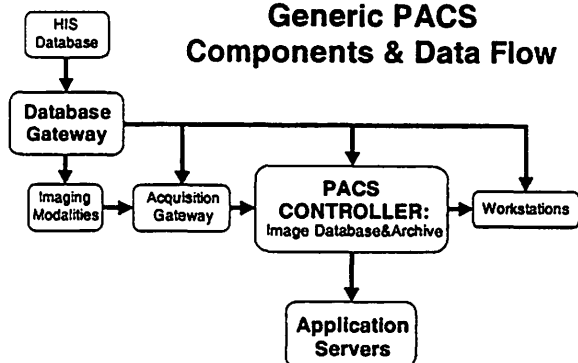


Figure 1. Generic PACS Components and Data Flow. Application servers are normally not included in a commercial PACS. The PACS manufacturer or the user can develop these servers according to needs.

the Neurosurgery Command Module (NCM) based on existing and emerging PACS and medical informatics technologies.

### Picture Archiving and Communication System (PACS)

The PACS infrastructure is physically composed of several components connected by computer networks. These components include HIS, radiological imaging acquisition devices, database and device gateway computers, PACS controller with image database and archive, display workstations, and application servers. Fig. 1 shows the PACS basic components and data flow.<sup>2</sup> The application servers can be tailored to different radiology applications like neuroradiology, body imaging, pediatric, chest, etc. Also, the application server can be customized for surgical applications such as neurosurgery.

Use PACS in a hospital or clinic operation has many benefits compared with a paper- and film-based operation system. Among them are:

- No loss of films
- Multiple copies available instantaneously
- Easy image prefetch
- Streamline and efficient operation environment
- Quicker turn around time for radiological diagnosis
- Save man power and space for archive
- Allow teleradiology, teleconferencing, and teleconsultation<sup>3</sup>
- Remote learning
- Better image management
- Expert Center concept in diagnosis
- Image guided surgery
- Image-guided therapy treatment
- Image-guided detection and diagnosis

Many large and small PAC systems have been in clinical operation since 1990, mostly restricted in diagnostic applications. It was not until in late 1990s that PACS was extended to image-guided applications.

### Medical Informatics and Electronic Patient Record

#### Medical Image Informatics Infrastructure

Concept of MIII: Medical image informatics infrastructure (MIII) is an application server designed to take advantage of existing PACS resources and its image and related data for special purpose applications. The goal of the MIII is the utilization of PACS data for customized applications in addition to daily clinical service.<sup>4</sup>

MIII Architecture and Components: Medical image informatics infrastructure (MIII) is comprised of the following components: medical images and associated data (including PACS database), image processing, data/knowledge base management, visualization, graphic user interface, communication networking, and application oriented software. These components are logically related as shown in Fig. 2 and their functions are summarized in the following subsections. The concept of the neurosurgery command module discussed in the next Section requires the support of such an infrastructure.

#### Medical Image Informatics Infrastructure (MIII) components and their logical relationship for Spinal Surgery

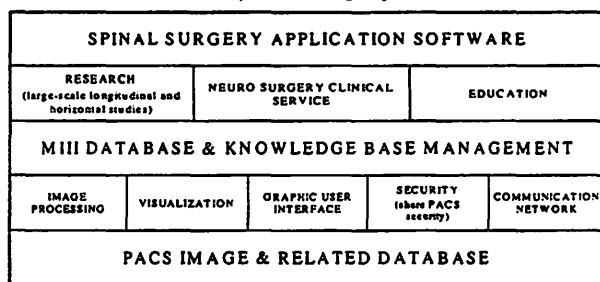


Figure 2. Medical image informatics infrastructure (MIII) components and their logical relationship as used in spinal surgery.

PACS and Related Data: PACS databases and other related health information systems containing patient demographic data, case history, medical images and corresponding diagnostic reports, and laboratory test results constitute the data source in the MIII. This data is organized and archived with standard data formats and protocols, such as DICOM (Digital Imaging and Communication in Medicine)<sup>8</sup> for image and HL7 (Health Level) for text.<sup>11</sup> In addition, controlled health vocabulary can be based on standards for medical identifiers, codes, and messages proposed by the American Medical Informatics Association.

Image Processing: Image processing software allows for set-

ting up the image content indexing and retrieval mechanism. Its functions include segmentation, region of interest determination, texture analysis, content analysis, morphological operations, and image registration. The output from image processing can be a new image or some features describing some characteristics of the image. Segmented three-Dimensional (3-D) volumetric imaging from CT and MRI are typical image processing tools for neurosurgery applications. Image processing functions can be performed automatically or interactively on image data acquired from the PACS database. Data extracted by the image processing functions can be appended to the image data file.

**Database and Knowledge Base Management:** The database and knowledge base management component software has several functions. First, it integrates and organizes PACS images and related data, extracts image features and keywords from image processing, and derives medical heuristics rules and guidelines into a coherent multimedia data model. Second, it supports on-line database management, content-based indexing and retrieval, formatting and distribution for visualization and manipulation. This component can be developed on top of a commercial database engine with add-on application software.

**Visualization and Graphic User Interface:** Visualization and graphic user interface are output components. Both components are related to workstation design. Visualization includes 3-D rendering, image data fusion, static and dynamic imaging display. Visualization utilizes extracted data from image processing (i.e., segmentation, enhancement, and shading) for output rendering.

**Graphic user interface (GUI)** considers optimization of workstation design for information retrieval and data visualization with minimal effort from the user. A well-designed GUI is essential for effective real-time visualization and image content retrieval. GUI can also be used for extraction of additional parameters for non-standard interactive image analysis.

**Communication Networks:** Communication networks include network hardware and communication software protocols required to connect MIII components together. The MIII communication networks can have two architectures: a network of its own with a connection to the PACS networks, or it can share the communication networks with the PACS. In the former, the connection between the MIII and the PACS networks should be transparent to the users and provide the necessary high speed input for the MIII to request PACS images and related data and to distribute results to a user's workstation. In the latter, the MIII should have a logical segment isolated from the PACS networks so that it would not interfere with the PACS daily clinical functions.

**System Integration:** System integration includes system interface, and shared data and workspace software. System interface software utilizes existing communication networks and protocols to connect all infrastructure components into an integrated information system. Shared data and workspace software allocates and distributes resources including data, storage space, and workstation to the on-line users.

**Security:** Security includes data integrity and data access. The former considers image authenticity and completeness of data. After

PACS images have been processed, some validation mechanisms are needed to assure accuracy, completeness, and authenticity. Data access considers who can access what type of data and when.

Once the aforementioned components are implemented in the MIII, application oriented software can be designed and developed to integrate necessary components for a specific clinical, research, or education application. This provides rapid prototyping and reduces costs required for the development of every application. It is in this application layer component that users encounter the advantages and power of the MIII. The concept of a neurosurgery command module relies heavily on the knowledge of MIII.

### Electronic Patient Record (EPR)

EPR is an emerging concept to replace or supplement the hospital- or clinic-based healthcare information system. The major functions are:

- Accept direct digital input of patient data.
- Analyze across patients and providers
- Provide clinical support and suggest course of treatment
- Perform outcome analysis, patient and physician profiling
- Distribute information across different platforms and systems

### Concept of a Neurosurgery Command Module (NCM)

NCM is a module designed for neurosurgery based on the concept of EPR taking advantage of the existing knowledge of PACS and MIII. We use the minimally invasive spinal technique as an example in developing this concept.

### PACS Workflow and Spinal Surgery Server

The spinal surgery server can be considered as one application server shown in Figure 1. Following the dataflow in Figure 1, the spinal surgery server supports both on-site and remote surgery workstations called neurosurgery command modules (NCMs)<sup>5</sup> shown in Figure 3. The EPR design concept allows the image and

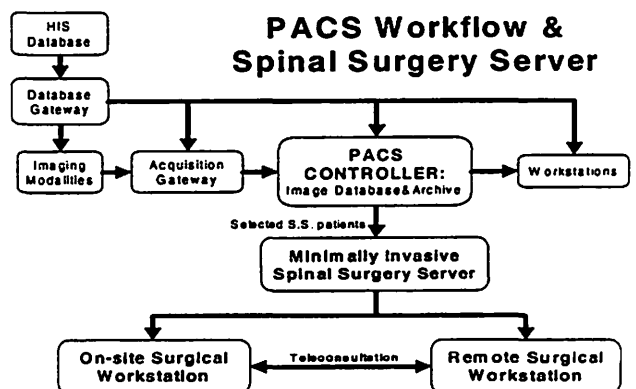


Figure 3. PACS workflow and the spinal surgery server. The on-site and remote surgical workstations (bottom) lead to the concept of neurosurgery command module (NCM).

data of a patient to be operated or being operated be staged at the server and delivered to the NCM for review before, during, or after surgery. The remote NCM can be connected to the on-site NCM by a high-speed network where second opinion and remote teaching can take place.

### Minimally Invasive Spinal Surgery Workflow

Fig. 4 shows the minimally invasive spinal surgery workflow from before surgery, at the surgical site, during surgery, and post surgery (Personal Communication, Chiu JC, December 10, 2000). The two rectangular boxes at the bottom right represent the NCMs shown in Fig. 3.

## Minimally Invasive Spinal Surgery Work Flow

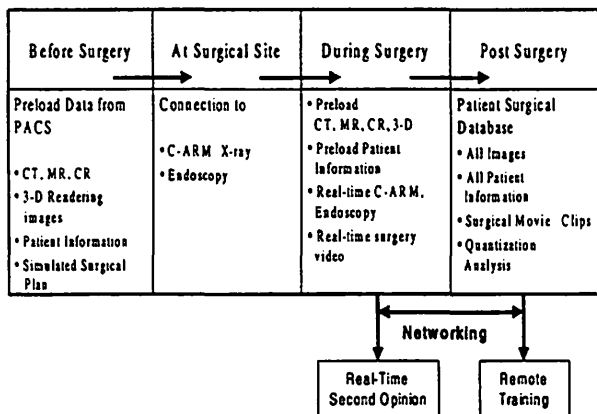


Figure 4. Minimally invasive spinal surgery workflow: before surgery, at the surgical suite, during surgery, and post surgery.

### Definition and Functionality of NCM

**Definition:** The neurosurgery command module (NCM) is a mobile workstation, connected to the minimally invasive spinal surgery server. The stand-alone NCM can be used to support neurosurgery operation and neurosurgery documentation. A pair of them can be connected via either intranet or Internet to support teleconsultation, and remote teaching during neurosurgery.<sup>6,7</sup>

**Functionality:** 1. CT/MR/US/CR and pre-reconstructed 3-D images along with pertinent clinical data of a surgical patient can be preloaded through PACS or from DICOM compliant imaging modalities to the spinal surgery server (Fig. 3). These images and data can be pushed from the server to the NCM for viewing before, during, or after surgery.<sup>6,7</sup>

2. Digital C-arm radiography and endoscopy can be connected to the NCM, and images from these modalities can be transmitted in real-time during surgery to the NCM using DICOM standard. These images can be appended to the patient's worklist in the NCM for viewing during surgery and for archive to the database in the spinal surgery server after surgery.

3. The NCM has a CCD video camera with associated software for surgical documentation and for teleconferencing.

4. Use as a stand-alone surgical workstation, the surgeon can document the surgical procedure via voice and video recorders.

5. The NCM has a dual-cursor teleconsultation package for expert opinion at a remote site during surgery. Or it can be used for surgical training or continuing education.<sup>6,7</sup>

6. Teleconsultation can be performed by using a pair of NCMs connected via either Intranet or Internet.<sup>6,7</sup>

7. Before teleconsultation, relevant data and images described in Items 1 and 2 can be preloaded to the NCM from the spinal surgery server through an authoring session provided by a consultation software package. The authoring session is prepared by personnel either from the surgical or the expert site providing that a site has access to the spinal surgery server.<sup>6,7</sup>

8. During a teleconsultation session, images described in Items 1 and 2 can be synchronized and displayed in real-time at both NCMs. A dual-cursor mechanism can be used to discuss images by the surgeon and the expert in real-time. In addition, the teleconferencing software can be used for visual and voice communication.<sup>6,7</sup>

9. The database in the NCM automatically manages the surgical document and teleconsultation transaction.

### NCM System Architecture

The NCM system architecture consists of four components: hardware, software, network, and industrial standards. Fig. 5A shows the components of the NCM, and Fig. 5B depicts the NCM prototype design sketch.

#### NCM Hardware Components

- PC NT workstation(s)
- Video Camera and recorder
- Voice phone and recorder
- Power supply and UPS
- Ethernet port and MODEM
- Mobile cart
- Flat panel display (from 2 to 4)

#### NCM Software Modules

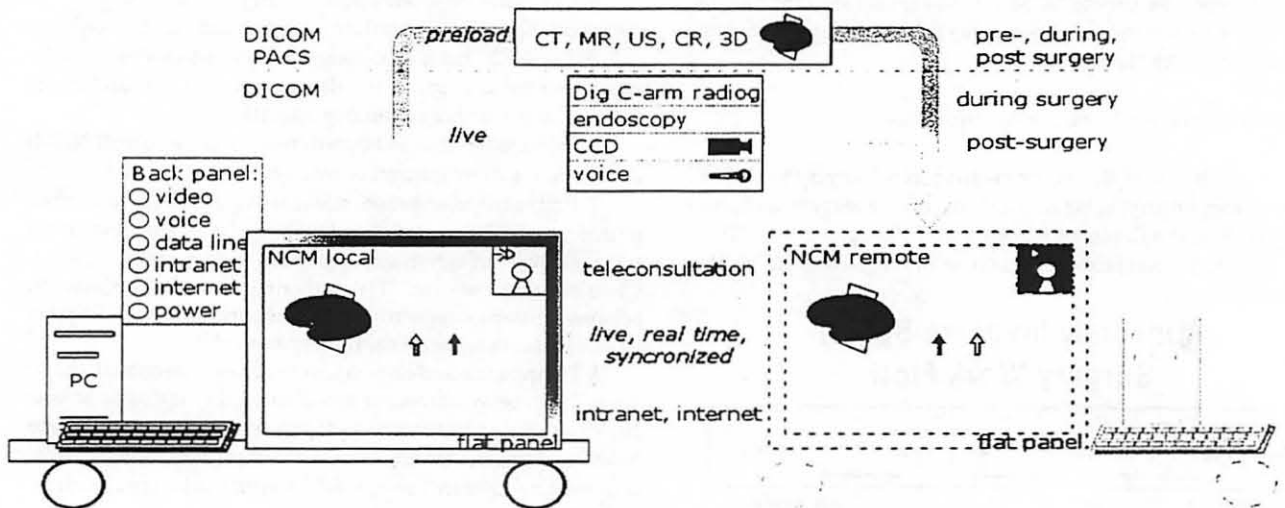
- Standard PACS workstation display functions (commercially available)
- Standard Teleconferencing software (commercially available)
- Dual-cursor Teleconsultation Software Package (available in research lab)<sup>6,7</sup>
- DCIOM acquisition gateway software (commercially available)<sup>8</sup>

#### Communication Network Connection

- Local Area Network (LAN) - Fast Ethernet or ATM (asynchronous transfer mode) Technology
- Wide Area Network (WAN) - MODEM via voice line or data line
  - ISDN
  - T1 to T3
  - ATM
  - Internet 2<sup>9</sup>

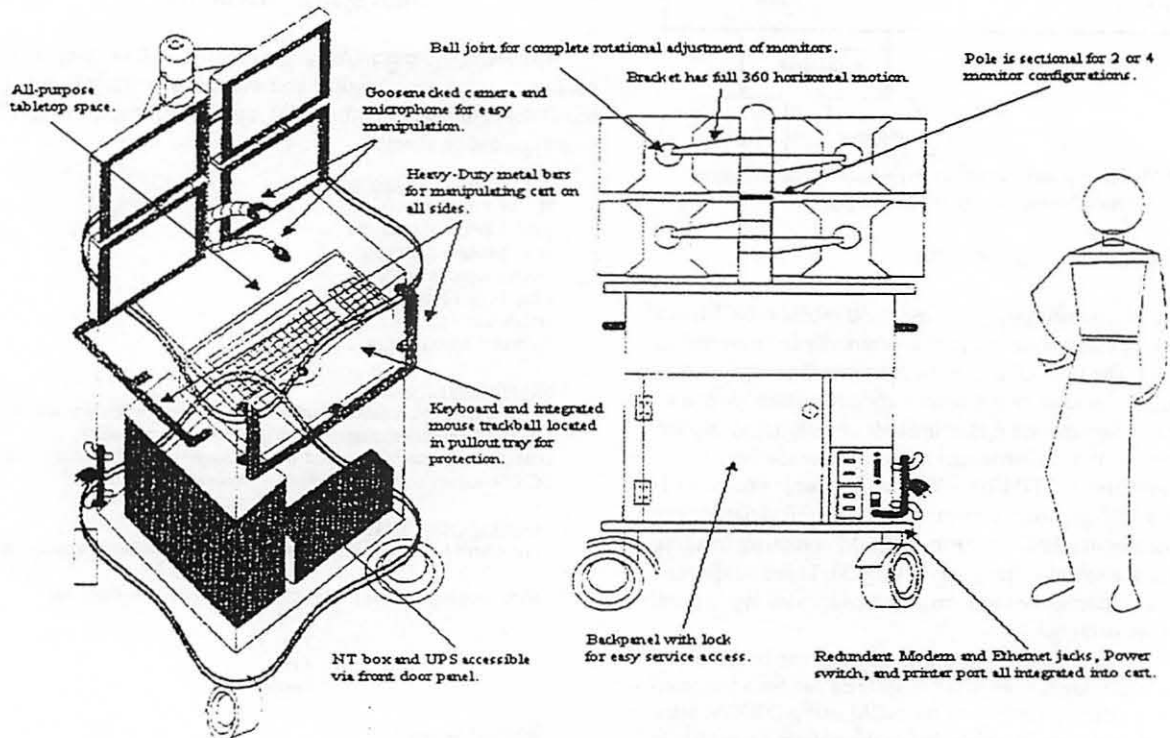
#### Industrial Standards

- Images: DICOM
- Patient information: HL-7<sup>11</sup>



- surgical documentation to database
- images
  - consultation
  - annotations (voice, text)

5A. Components in a Neurosurgery Command Module (NCM).



5B. NCM prototype design sketch.

## Discussion

PACS and imaging informatics are two emerging technologies, which can facilitate the practice of minimally invasive spinal surgery. PACS provides the collection and distribution of required medical images and related data, and imaging informatics allows this information to be used efficiently in spinal surgery.

We propose the concept of the neurosurgery command module (NCM) based on these two technologies as an aid for spinal surgery. NCM can be used as a stand-alone, image-guided, or post surgery apparatus. Many components in the NCM are available technologies, although the system integration still requires implementation.

## Acknowledgement

Clinical study partially supported by the National Library of Medicine contract No. N01-LM-6-3547, and the US Army Medical Research and Development, TARTC contract No. DAMD 17-99-P-3732. Dr. Cammy Huang contributed Fig. 5A. Dr. Brent Liu and Grace Liu contributed Fig. 5B.

## References

1. McDonald CJ: The barrier to electronic medical record systems and how to overcome them. *J Amer Med Informatics Assoc* 4:213-221, 1997
2. Huang HK: *Picture Archiving and Communication Systems: Principles and Applications*. Wiley & Sons, New York, NY, 1999, p.521
3. Huang HK, Lou SL, Dillon WP: Neuroradiology workstation reading in an inter-hospital environment: A nineteen month study. *J Comp Med Imag Graphics* 21:309-317, 1997
4. Huang HK, Wong STC, Pietka E: Medical image informatics infrastructure design and applications. *Med Informatics* 22: 279-289, 1997
5. Huang HK: Imaging informatics and PACS: What is it? Why do I need it? Presented at 1st World Congress Minimally Invasive Spinal Surgery and Medicine, December 8, 2000
6. Stahl JN, Zhang J, Zeller C, et al.: Tele-conferencing with dynamic medical images. *IEEE Trans Inform Tech Biom* 4:88-96, 2000
7. Zhang J, Stahl JN, Huang HK, et al.: Real-time teleconsultation with high resolution and large volume medical images for collaborative health care. *IEEE Trans Inform Tech Biom* 4: 178-185, 2000
8. DICOM: *Digital Imaging and Communication in Medicine*. National Electrical Manufacturers' Association, Rosslyn, VA: NEMA, 1996

9. Huang HK, Wong AWK, Zhu X: Performance of asynchronous transfer mode (ATM) local area and wide area networks for medical image transmission in clinical environment. *J Comp Med Imag Graphics* 21:165-173, 1997
10. Yu F, Hwang K, Gill M, et al.: Some connectivity and security issues of NGI in medical imaging applications. *J High Speed Networks* 9: 3-13, 2000
11. HL7: Health Level Seven. *An Application Protocol for Electronic Data Exchange in Health Care Environments*. Version 2.1. Ann Harbor, MI: health Level Seven, Inc., 1991

## ACRONYMS

ATM	Asynchronous Transfer Mode
CMS	Clinical Management System
DICOM	Digital Imaging and Communication in Medicine
EMR	Electronic Medical Record
EPR	Electronic Patient Record
GUI	Graphic User Interface
HIS	Hospital Information System
HI-PACS	Hospital Integrated PACS
HL7	Health Level Seven
IMAC	Imaging Management and Communication System
LAN	Local Area Network
MIII	Medical image informatics infrastructure
NCM	Neurosurgery Command Module
PACS	Picture archiving and communication system
RIS	Radiology Information Management System
UPS	Uninterrupted Power Supply
WAN	Wide Area Network

*corresponding author for reprints:* H. K. Huang, D.Sc., CHLA Mailstop 81, 4651 Sunset Blvd, Los Angeles, CA 90027

## COMMENTS

Dr. Huang has contributed more than 100 papers to the medical literature on computer communication networks, hospital information systems, and radiology information systems. The concept of a neurosurgery command nodule for minimally invasive spinal surgery is based upon picture archiving and communication system plus imaging informatics. Continuous rapid intraoperative imaging of the patient undergoing a spinal operation will allow the surgeon to track his instrumentation in relation to deep organs and surface anatomy with monitoring already available through endoscopic technology. The editors await reports of full implementation of the system integration needed to complete the neurosurgery command module.

John C. Chiu

# Serving up Integrated Therapy

*Key to system integration, DICOM has led diagnostic imaging to a new zone of efficiency benefits. What will it take for radiation therapy to step up to the plate?*

If you know anything about radiation therapy, you're well-aware that it's an image-intensive treatment. Images are not only required from diagnostic modalities but also from treatment equipment. On top of that, RT treatment still relies mostly on tedious manual image and data transfer methods because the community as a whole has not championed integration. Yet, system integration could greatly benefit the field in several ways—lowering equipment and operational costs, streamlining treatment procedures and improving patient care.

So, the question remains: How can you integrate diverse health care information systems, imaging modalities and RT equipment into one seamless treatment system? The key lies in picture archiving and communications systems (PACS) and an imaging informatics-based server. With these, you can determine the workflow and dataflow from various pieces of equipment to the server, using the DICOM standard and DICOM RT. Also at your service is the Integrating the Healthcare Enterprise (IHE) initiative, which defines protocols for scheduled workflow and is a must if the RT community wants to offer more effective treatment.

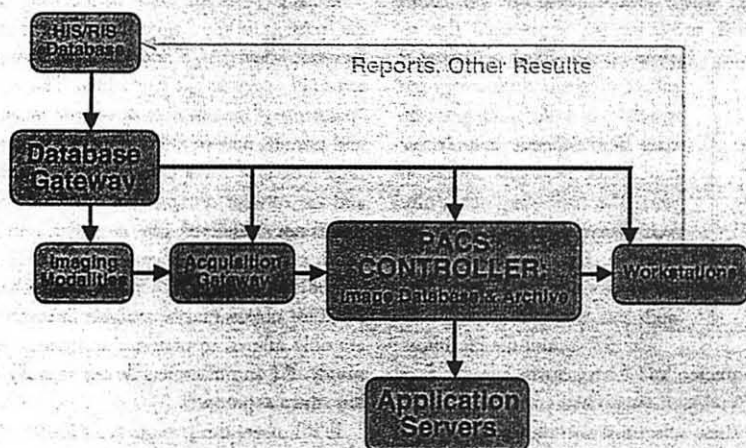
## **Building blocks to integration**

Achieving these goals starts with a brief review of RT, PACS and imaging informatics basics. As

you know, radiation therapy requires images from projection X-rays, computed tomography (CT), magnetic resonance (MR), and positron emission tomography (PET) for tumor localization, treatment planning and treatment verification. Treatment planning requires several components: patient information; image registration to identify treatable regions, and markers to align images; image fusion to delineate pathological structures from imaging modalities; anatomy to identify the shape, size, and location of the targets and radiosensitive vital organs; and dose computation to ensure uniform high-dose delivery to the target while avoiding sensitive structures. In addition, carefully monitoring treatment optimization and dose calculation is essential for successful patient outcomes.<sup>1,2</sup> But while PACS and imaging informatics technologies are used extensively in these processes, they aren't integrated with these technologies as a complete radiation treatment system.

Integrated by many centers since 1992, PACS was developed for diagnostic purposes, although it hasn't formally been stated as such. (See Figure 1 for the generic PACS architecture and its connection to different application servers.) PACS also uses DICOM as an image format and communication standard, and HL-7 as a textual information standard.<sup>3</sup>

Imaging informatics is the computer software technology that extracts pertinent information ►



from the PACS database to facilitate medical applications. The infrastructure in medical imaging informatics includes a PACS database, patient information, a high-speed network, image visualization and presentation, and a disease-related knowledge base.<sup>4</sup>

RT processes can use PACS and imaging informatics technologies more extensively and be integrated as a total RT PACS and imaging informatics-based system. Two recent RT technologies, intensity modulated radiation therapy (IMRT)<sup>2,5</sup> and image-guided radiotherapy, rely on images from PACS and data derived from imaging informatics.<sup>6</sup> In the former, a networked computerized workflow of

the patient image and informatics information can provide more efficient planning and treatment procedures. The latter is based on a linear accelerator mounted on an image-guided robotic arm for delivering optimal uniform dose to targets.

### DICOM standard and RT DICOM

RT uses radiological images and images from the simulator and linear accelerator for planning, treatment and verification. It's therefore advantageous to use DICOM RT's image and data communication standard.<sup>7</sup> As of 1999, seven RT-specific DICOM objects were ratified:<sup>8</sup>

1. RT structure set ('97): contains information related to patient structures, markers, isocenter and related data;

2. RT plan ('97): refers to information contained in a treatment plan such as beam angles, collimator openings and beam modifiers;

3. RT image ('97): includes all images taken using radiotherapy equipment such as conventional simulators, digitizers for simulator films or electronic portal imagers;

4. RT dose ('97): contains dose data such as dose distribution generated by the treatment planning system, dose volume histogram, dose points, etc.;

5. RT beams treatment record ('99);

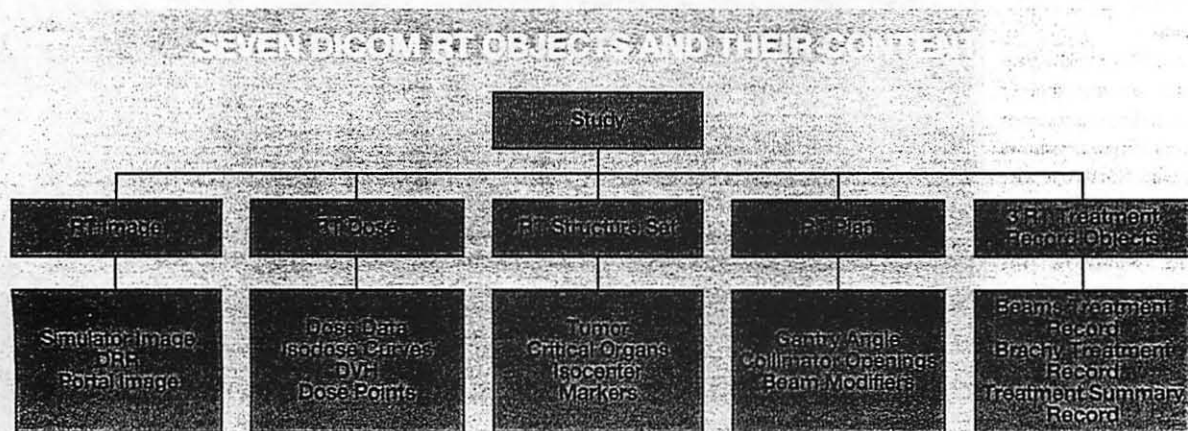
6. RT brachy treatment record ('99); and

7. RT treatment summary record ('99).

Most RT vendors are at various stages of implementing these objects; in particular, the '97 ratified objects and the RT structure set, plan, image and dose. The three '99 record objects are in preliminary stages of vendor implementation. Figure 2 categorizes these objects and their contents.

The advantages of having these DICOM objects in RT are obvious. First, information and images within an object can be transferred across different RT vendors with minimum effort. Second, it allows the total integration of RT components from various vendors. Third, you can closely monitor and analyze RT treatment workflow, improving patient care. And fourth, you can integrate a patient's RT treatment under the scheme of the electronic patient record (EPR), a current trend of patient-oriented health care delivery. The individual RT treatment EPR can be combined with

Figure 2. Seven DICOM RT Objects and their contents.





## WORKFLOW OF THE PACS AND IMAGING INFORMATICS-BASED RT SERVER.\*

### STEP 1

#### Images from PACS

- Acquire images for diagnosis or treatment planning from modalities before treatment as well as images for evaluating treatment results.
- Store images in PACS server.
- Select relevant images and send them to the RT Server.

### STEP 2

#### Treatment Planning

- Retrieve acquired CT images from the PACS server at the virtual simulation (VS) workstation or treatment planning system (TPS).
- Generate digital reconstructed radiographs (DRR) from VS workstation or TPS.
- Perform treatment field planning.
- Send treatment plans from VS workstation to TPS for dose computation if required.
- Send resultant RT plans together with DRR to RT server. Each treatment plan consists of the following files: CT image file, structure set file, plan setup file and dose file (from TPS only).

### STEP 3A

#### Using a VS Workstation without an Isodose Plan

- Retrieve CT simulator images at the VS workstation.
- Reconstruct DRR images from the CT simulator images.
- Perform field planning on VS workstation.
- Follow bullets two to five in Step 2.

### STEP 3B

#### When an Isodose Plan Is Required

- Retrieve CT simulator images at the TPS.
- Perform field planning and dose computation at the TPS.
- Forward plans to the TPS for dose com-

putation when VS is available and field planning has been done in the VS workstation.

- Follow bullets two to five in Step 2.

### STEP 4

#### Define Treatment Fields

- Acquire conventional simulator treatment planning film images for cases that do not require CT for planning.
- Draw treatment fields manually on hard copy simulator film, then digitize them.
- Send digitized image to RT server.

### STEP 5

#### Portal Image Acquisition

- Acquire portal image from linear accelerator either manually or using the EPI.
- Send digitized or digital portal image to the RT server.

### STEP 6

#### Verify the Image

- Retrieve the relevant images from the RT server at the RT workstations for evaluation of treatment plans or for verification.
- Either have the radiation oncologist confirm a treatment plan, or compare the simulator image (reference image) of a patient with the portal image from the linear accelerator, whereby verification is confirmed or modification is ordered.

### STEP 7

#### Route Confirmation

- Send the written confirmation or comments about the treatment plan or the radiation oncologist's treatment verification to the RT server.
- Generate an EPR at the RT server.

### STEP 8

#### Modify If Necessary

- Request to modify or redo the plan if it isn't satisfactory.

\* See figure 3

manufacturers won't automatically offer it—a classic example we witnessed in diagnostic imaging. But eventually, the consumers and manufacturers were educated, and as customers began demanding DICOM, manufacturers delivered. As a result, the DICOM standard has pushed diagnostic imaging forward, with widespread benefits for end users and manufacturers. The same transition must occur in radiation therapy; without DICOM RT, the efficiencies that come with system integration will remain one step out of reach. ■

### References

1. Hendee, W.R. (2000). Medical imaging for the 21st century. In N.Z. Xie (Ed.), *Medical Imaging and Precision Radiotherapy*, (pp. 24-30). Guangzhou, China: The Foundation of International Scientific Exchange.
2. Sternick, E.S. (2000). Intensity modulated radiation therapy. In N.Z. Xie (Ed.), *Medical Imaging and Precision Radiotherapy*, (pp.38-52). Guangzhou, China: The Foundation of International Scientific Exchange.
3. Huang, H.K. (1999). Picture archiving and communication systems: Principles and applications. (pp. 521). N.Y.: Wiley & Sons.
4. Huang, H.K., Wong, S.T.C., & Pietka, E. (1997). Medical image informatics infrastructure design and applications. *Medical Informatics*, 22, (4), 279-89.
5. Cheung, K.Y. (2000). Precision radiotherapy in nasopharyngeal carcinoma treatment. In N.Z. Xie (Ed.), *Medical Imaging and Precision Radiotherapy*, (pp. 69-83). Guangzhou, China: The Foundation of International Scientific Exchange.
6. Adler, J.R., Chang, S.D., Murphy, M.J., Doty, J., Ceis, P., & Hancock, S.L. (1997). The Cyberknife: A frameless robotic system for radiosurgery. *Stereotactic & Functional Neurosurgery*, 69 (1-4 Pt. 2): 124-8.
7. Borras, C. (2000). Automation in precision radiotherapy: From image acquisition to dose computation—existing and needed standards. In N.Z. Xie (Ed.), *Medical Imaging and Precision Radiotherapy*, (pp. 168-69). Guangzhou, China: The Foundation of International Scientific Exchange.
8. Neumann, M. The Impact of DICOM in Radiotherapy. Lecture 5th Biennial ESTRO Meeting on Physics for Clinical Radiotherapy, Gottingen, April 8, 1999. <http://www.sgmp.ch/full983b.htm>.
9. [www.rma.org/IHE](http://www.rma.org/IHE)



Maria Y.Y. Law is an assistant professor of the department of opometry and radiography in the Hong Kong Polytechnic University, where she leads the radiation therapy track of the bachelor of science radiography program. H.K. Huang, DSc, FRCR (Hon.), is professor and director of informatics, department of radiology at the Childrens Hospital Los Angeles/University of Southern California. He is also the chair professor of medical informatics at The Hong Kong Polytechnic University.

---

## Advance in radiological informatics\*

HK Huang

Department of Radiology, Children's Hospital of Los Angeles/University of Southern California, Los Angeles, USA.

### ABSTRACT

*Radiological informatics is the study of information related to radiology. In this paper, hospital information system (HIS), radiology information system (RIS), and picture archiving and communication system (PACS) are first introduced. The integration of these three systems is the hospital integrated HI-PACS. The idea of multimedia including HI-PACS in the radiology environment is presented followed by the description of electronic patient record (EPR). The concept of using the interfacing engine for the ultimate information system integration is illustrated. The integrating of the healthcare enterprise (IHE) initiative identifying the technical framework in information system integration is the first step to realize such a systematic approach. Finally, medical imaging informatics infrastructure design based on information and knowledge derived from HI-PACS is described which allows for large scale horizontal and longitudinal clinical, research, and education applications.*

*Key Words: Radiological informatics, Imaging informatics, HIS, RIS, PACS, DICOM, HL7, Healthcare System Integration.*

### HIS, RIS AND PACS

Three basic clinical tools in radiology informatics (RI) are the hospital information system (HIS), radiology information system (RIS), and picture archiving and communication system (PACS). If these systems are properly integrated, they form the Hospital integrated (HI) PACS (1). RI is the branch of radiology utilizing HI-PACS for large scale horizontal and longitudinal research to facilitate clinical services, and improve staff and patient education.

#### Hospital Information System

A Hospital Information System (HIS, in Hong Kong it is called CMS, Clinical Management System) is a computerized management system for handling three categories of tasks in a healthcare environment:

1. Support clinical and medical patient care activities in the hospital.
2. Administration of the hospital's daily business transactions including financial, personnel, payroll, bed census, etc.

\*Most materials are extracted from Reference 1.

---

Correspondence: Professor HK Huang, Professor and Director of Informatics, Department of Radiology, Children's Hospital of Los Angeles/University of Southern California, Mailstop #81, 4650 Sunset Boulevard, Los Angeles, CA 90027, USA.  
E-mail: hkh Huang@aol.com

3. Evaluation of hospital performances and costs, and project the long term forecast.

Radiology, pathology, pharmacy, clinical laboratories, and other clinical departments in a healthcare center have their own specific operational requirements, which differ from those of general hospital operation. For this reason, special information systems may be needed in some health centers. Often, these subsystems are under the umbrella of the HIS, which maintains their operations. Others may have their own separate information systems, and some interface mechanisms are built to transfer data between these systems and the HIS. For example, radiology information systems (RIS) were originally a component of HIS. Later, independent RIS was developed because of the limited support offered by HIS to handle special information required by the radiology operation.

#### Radiology Information System

RIS is designed to support both the administrative and the clinical operation of a radiology department, to reduce administrative overhead, and to improve the quality of radiological examination delivery. The major functions of a RIS include:

1. Process patient and film folder records.
2. Monitor the status of patients, examinations, and examination resources.
3. Schedule examinations.

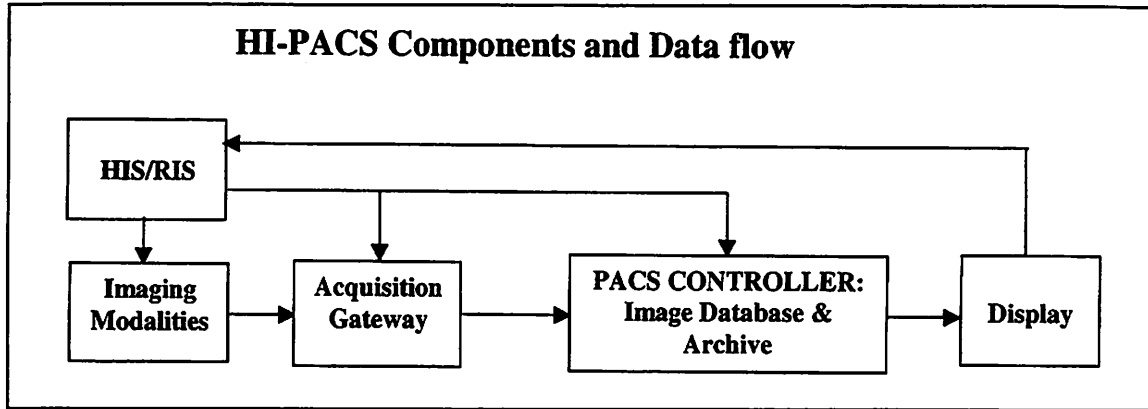


Figure 1 Hospital integrated PACS components and data flow.

4. Create, format, and store diagnostic reports with digital signatures.
5. Track film folders and digitally archived images.
6. Maintain timely billing information.
7. Perform profile and statistics analysis.

The RIS (system organization and configuration) is very similar to the HIS except it is on a smaller scale. RIS equipment consists of a computer system with peripheral devices such as workstations, alpha-numeric terminals, printers, and bar code readers. The RIS software controls this equipment to perform functions described previously. In most cases, an independent RIS is autonomous with limited access to HIS. However, some HI systems offer embedded RIS subsystems with a higher degree of integration, like the CMS in Hong Kong.

**PACS**

A picture archiving and communication system (PACS) consists of image and data acquisition, storage, and display subsystems integrated by various digital networks. It can be as simple as a film digitizer connected to a display workstation with a small image data base, or as complex as a total hospital image management system. In general, PACS consists of an infrastructure design including features such as standardization, open architecture, expandability for future growth, connectivity, and reliability.

The infrastructure itself consists of a basic skeleton of hardware components (imaging modality interfaces, storage devices, computers, communication networks, display workstations) integrated by standardized, flexible software subsystems for image and related data communication, database management, storage manage-

ment, job scheduling, interprocessor communication, error handling, and network monitoring. The infrastructure as a whole is versatile and can incorporate rules to reliably perform not only basic PACS management operations but also more complex research jobs and clinical service requests. The software modules of the infrastructure embody sufficient understanding and cooperation at a system level to permit the components to work together as a system rather than as individual networked computers. Figure 1 shows the PACS components and data flow.

**INFORMATION TRANSFER BETWEEN HIS, RIS, AND PACS**

**Reasons for Interfacing PACS with HIS and RIS**

In a hospital environment, interfacing the PACS, RIS, and HIS has become necessary in order to streamline patient scheduling and examination, diagnostic and reporting process, PACS image management, RIS administration, as well as to enhance research and education.

**Streamline Patient Scheduling and Examination**

After the patient is registered at the hospital HIS, if radiological examinations are required, RIS is used to schedule the patient and to locate resources for the examinations. Patient information from HIS and RIS are routed directly to the imaging modalities to avoid human errors due to reentering the data.

**Diagnostic and Reporting Process**

The diagnostic and reporting process at the PACS workstation includes the retrieval of images of interest

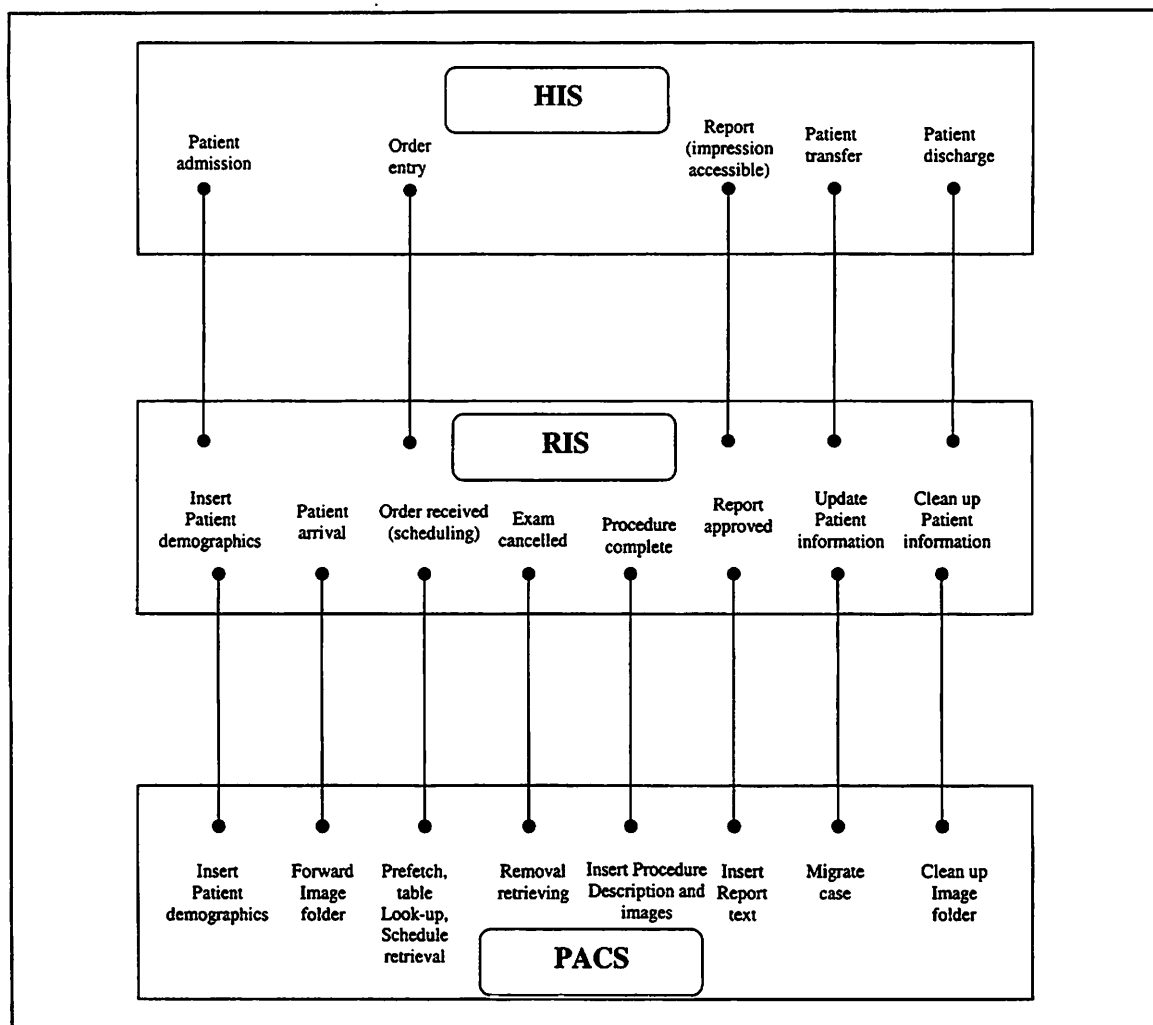


Figure 2 Information transfer between HIS, RIS, and PACS.

and pertinent textual information describing patient history and study reports. Along with the image data and the image description, a PACS also provides all related text information acquired and managed by the RIS and the HIS in a way that is useful to a radiologist during the diagnostic and reporting process. RIS and HIS information such as clinical diagnosis, radiological reports, and patient history are necessary at the PACS workstation to complement the images of the cases being reviewed.

### PACS Image Management

Some information provided by the RIS can be integrated into PACS image management algorithms to optimize the grouping and routing of image data on the network

to requesting locations. In the PACS database, which archives huge volumes of images, a sophisticated image management system is required to handle the depository and distribution of this image data.

### RIS Administration

In a digital radiology operation, it may require the reorganization of some administrative operations. The reorganization can be carried out by the RIS. For example, the PACS can provide the image archive status and the image data file information to the RIS. RIS administration operations would also benefit from the HIS by gaining knowledge about patient admission, discharge, and transfer (ADT). Together this information can be used to facilitate the operation of the department.

## Research and Training

Much research and teaching in radiology involves screening of clinical cases and determining what constitutes a normal versus an abnormal condition for a given patient population. The corresponding knowledge included diverse types of information that need to be correlated, such as image data, results from analyzed images, medical diagnosis, patient demographics, study description, and various patient conditions. Some mechanisms are needed to access and to retrieve data from HIS and RIS during a search for detailed medical and patient information related to image data. Cooperation between diverse medical database systems such as HIS, RIS, and PACS is therefore critical to the successful management of research and teaching in radiology. Figure 2 illustrates information transfer between HIS, RIS, and PACS.

## MULTIMEDIA MEDICAL DATA

The many consultation functions of a radiology specialist in a large medical center include consulting with primary and referring physicians on the proper radiological procedures for patients, performing the procedures, reading images from the procedures, and dictating and confirming reports. Referring physicians review images with the radiologists and receive consultation. Based on these radiological images, reports, and consultations, the requesting physicians prescribe the proper treatment plan for their patients. The radiologists also use the images from the procedures and the corresponding reports to train fellows, residents, and medical students.

In their practice, the radiologists often request from medical records other necessary patient information (e.g., demographic data, laboratory tests and consultation reports from other medical specialists). Radiologists also review literature from the library information systems and give formal rounds to educate colleagues on radiological procedures and new radiological techniques. Thus, the practice of radiology requires integrating various types of information—voice, text, medical records, images, and video recordings—into proper files. These various types of information exist on different media and are stored in data systems of different types. The advance of computer and communication technologies allows the possibility of integration of these various types of information to facilitate the practice of radiology.

## Multimedia in the Radiology Environment

“Multimedia” has different meanings depending on the context. In the radiology environment, the term refers

to the integration of medical information related to radiology practice. This information is stored in various databases and multimedia. Patient demographic information, clinical laboratory test results, pharmacy information, and pathological reports are stored in the HIS. The radiological images are stored in the PACS archive system, and its corresponding reports are stored in RIS. The electronic mail and files are stored in the personal computer system database. The digital learning files are categorized in the learning laboratory or the library in the department of radiology. Some of these databases may exist in a primitive way in the sense that the digital and communication technology used is primitive; others — PACS, for example — can be very advanced. Thus, the challenge of developing multimedia in the radiology environment is to establish an infrastructure for the seamless integration of this medical information by means of blending different technologies, while providing an acceptable data transmission rate to various parts of the department and to various sites in the hospital. Once the multimedia infrastructure is established, various units of medical information can exist as modules and be interfaced to this infrastructure. In the multimedia environment, radiologists (or their medical colleagues) can access this information through a user-friendly, inexpensive, efficient, and reliable interactive workstation or a client connected to a Web server.

RIS, HIS, electronic mail and files involve textual information requiring from 1K to 2K bytes per transaction. For such a small data file size, although developing an interface to each information system is tedious, the technology involved is manageable. On the other hand, PACS contains image files that can be in the neighborhood of 20–40 Mbytes. The transmission and storage requirements for PACS are manifold those of text information. For this reason, HI-PACS becomes central in developing multimedia in the radiology environment.

## ELECTRONIC MEDICAL RECORD, INTERFACE ENGINE, AND INTEGRATED HEALTHCARE ENTERPRISE

### Electronic Medical Record

Electronic medical record (EMR) or electronic patient record (EPR) is the ultimate information system in a healthcare enterprise. One can consider EPR as the big picture of the future healthcare information system. Although the development of a universal EPR as a commercial product is still years away, its eventual impact to the healthcare delivery system should not be underestimated. An EPR consists of five major functions:

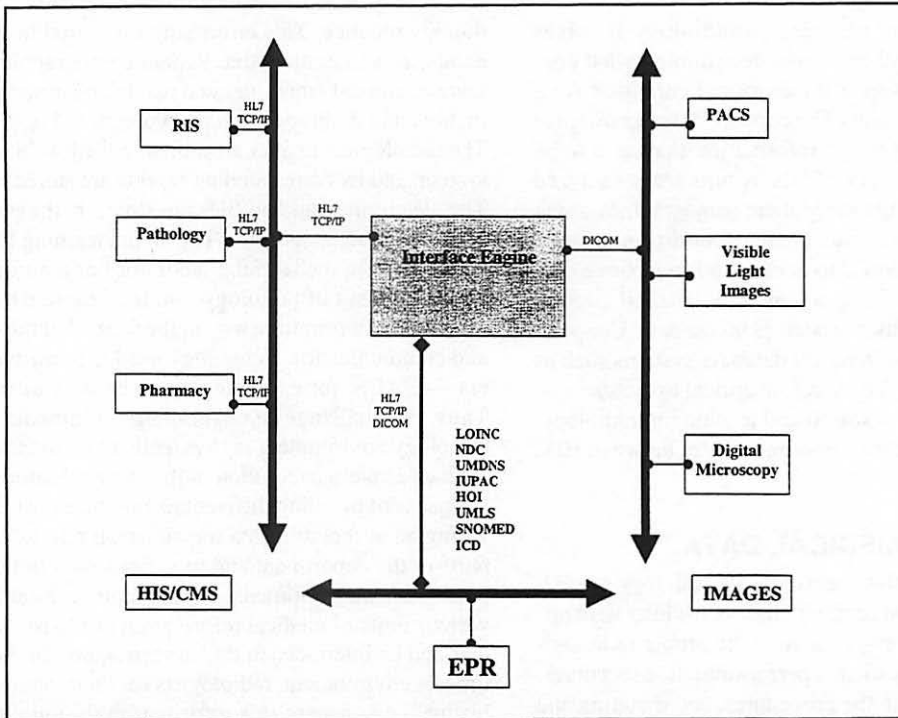


**Figure 3** The concept of using an interface engine as a possible connection of the HI-PACS to EPR. TCP/IP = Transport control protocol/ internet protocol; LOINC = Logical observation identifier names and codes; NDC = National drug codes; UMDNS = Universal medical device nomenclature system; IUPAC = International union of pure and applied chemistry; HOI = Health outcomes institute; UMLS = Unified medical language system; SNOMED = Systemized nomenclature of medicine; ICD = International classification of diseases

1. Accepts direct digital input of patient data.
2. Analyzes across patients and providers.
3. Provides clinical decision support and suggests courses of treatment.
4. Performs outcome analysis, and patient and physician profiling.
5. Distributes information across different platforms and health information systems.

HIS and RIS, which deal with patient non-imaging data management and hospital operation, can be considered a subset of EPR. An integrated HIS-RIS-PACS system, which extends the patient data to include imaging, forms the corner stone of EPR. Existing EPRs have certain commonalties. They have large data dictionaries with time stamped in their contents, and can query and display data flexibly.

Just like any other medical information system, however, EPR also faces several obstacles to its development: lack of a method to input patient examination and related data to the system, need to develop of an across-the-board data and communication standard, need to

assure buy-in from manufacturers to adopt the standards, and need to gain acceptance by healthcare providers. A HI-PACS system provides solutions for some of these obstacles. First, it has adopted DICOM (digital imaging and communication in medicine) and HL7 (Health Level) standards for imaging and text, respectively. Second, images and patient related data are entered to the system almost automatically. Third, the majority of imaging manufacturers has adopted DICOM and HL7 as de facto industrial standards. For these reasons, one can consider HI-PACS as a subsystem of EPR. Figure 3 illustrates the concept of using an interface engine as a possible connection of the HI-PACS to EPR.

### Interface Engine

The interface engine provides a single interface and language to access distributed data in networked heterogeneous information systems. In operation, it appears as if the user is operating on a single integrated database from his or her workstation. In the interface engine, a query protocol is responsible for analyzing the requested information, identifying the required databases, fetching the data, assembling the results in a standard for-

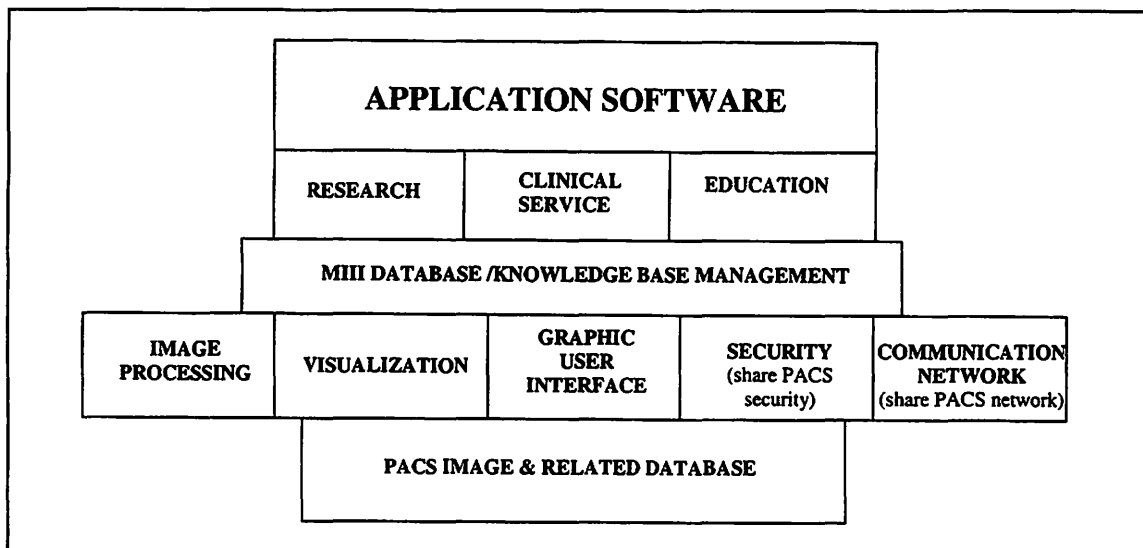


Figure 4 Medical image informatics infrastructure (MIII) components and their logical relationship. The bottom layer is image and related data from PACS and other databases. The middle two layers are described in Section 5. The top layer software is application specific.

mat, and presenting this information at the workstation. Ideally, all this processing is transparent to the user, and at the same time does not affect the autonomy of any database system. To build a universal interface engine is not a simple task. Most currently available commercial interface engines are only tailored to certain information systems.

### Integrating the Healthcare Enterprise (2,3)

The interface engine is a concept of system interoperability and system integration. It will be years before it would be materialized. As a first step towards its realization, HIMSS (Healthcare Information Management System Society) and RSNA (Radiological Society of North America) introduced the Integrating the Healthcare Enterprise (IHE) initiative to encourage manufacturers to consider the interoperability between various HL7 and DICOM conformance information systems. However, it is noted that IHE is a Technical Framework based on existing HL7 and DICOM and not a new standard. Both HIMSS and RSNA sponsor public demonstrations of some basic interoperability and systems integration with participation of many healthcare information and imaging manufacturers. The first two demonstrations had taken place at the annual conferences of the RSNA in 1999 and HIMSS in 2000. These demonstrations with progressing interoperability will continue during the next several years.

The IHE Year 1 demonstration was based upon a system design that integrates relevant “building blocks”

from the HL7 and DICOM standards. The Technical Framework defines five IHE Workflow-integrated modules:

1. ADT (Admission, Discharge, Transfer) Patient Registration System
2. Order Placer
3. Order Filler/Departmental Database System/Performance Procedure Step (PPS) Manager
4. Acquisition Modality Devices
5. Image Manager/Image Archive/PPS Manager

Successful demonstrations of the IHE and the willingness from manufacturers to abide to the IHE Technical Framework will facilitate the radiological information exchange and utilization for the future.

## MEDICAL IMAGE INFORMATICS INFRASTRUCTURE DESIGN

### Concept of MIII

Medical image informatics infrastructure (MIII) is a server designed to take advantage of existing HI-PACS resources and its image and related data for large scale horizontal and longitudinal clinical, research, and education applications which could not be performed before due to insufficient data and knowledge.

### MIII Architecture and Components

Medical image informatics infrastructure design (MIII) is comprised of the following components: medical images and associated data (including HI-PACS data-

base), image processing, data/knowledge base management, visualization, graphic user interface, communication networking, and application oriented software. These components are logically related as shown in Figure 4 and their functions are as follows.

### **HI-PACS and Related Data**

HI-PACS database and other related health information systems containing patient demographic data, case history, medical images and corresponding diagnostic reports, and laboratory test results constitute the data source in the MIII. This data is organized and archived in compliance with DICOM for image and HL7 for text. In addition, controlled health vocabulary can be based on standards for medical identifiers, codes, and messages proposed by the American Medical Informatics Association.

### **Image Processing**

Image processing software allows for setting up the image content indexing and retrieval mechanism. Its functions include segmentation, region of interest determination, texture analysis, content analysis, morphological operations, and image registration. The output from image processing can be a new image or some features describing some characteristics of the image. Image processing functions can be performed automatically or interactively on image data from the HI-PACS database by an input server. Data extracted by the image processing functions can be appended to the image data file.

### **Database and Knowledge Base Management**

The database and knowledge base management component software has several functions. First, it integrates and organizes PACS images and related data, extracts image features and keywords from image processing, and derives medical heuristics rules and guidelines into a coherent multimedia data model. Second, it supports on-line database management, content-based indexing and retrieval, formatting and distribution for visualization and manipulation. This component can be developed on top of a commercial database engine with additional application software.

### **Visualization and Graphic User Interface**

Visualization and graphic user interface are output components. Both components are related to workstation design. Visualization includes 3-D rendering, image data fusion, static and dynamic imaging display. Visualization utilizes extracted data from image processing (i.e., segmentation, enhancement, and shading) for output

rendering. Visualization can be performed on a standard workstation (WS) or with high performance graphic engines. For low performance WS, the final visualization can be pre-computed and packaged at the WS; with high performance graphic engines, the rendering can be in real-time at the WS.

Graphic user interface (GUI) considers optimization of workstation design for information retrieval and data visualization with minimal effort from the user. A well-designed GUI is essential for effective real-time visualization and image content retrieval. GUI can also be used for extraction of additional parameters for non-standard interactive image analysis.

### **Communication Networks**

Communication networks include network hardware and communication protocols required to connect MIII components together. The MIII communication networks can have two architectures: a network of its own with a connection to the HI-PACS's networks, or it can share the communication networks with the HI-PACS. In the former, the connection between the MIII and the PACS networks should be transparent to the users and provide the necessary high speed throughput for the MIII to request PACS images and related data and to distribute results to a user's workstation. In the latter, the MIII should have a logical segment isolated from the PACS networks so that it would not interfere with the PACS daily clinical functions.

### **System Integration**

System integration includes system interface, and shared data and workspace software. System interface software utilizes existing communication networks and protocols to connect all infrastructure components into an integrated information system. Shared data and workspace software allocates and distributes resources including data, storage space, and workstation to the on-line users.

### **Security**

Security includes data integrity and data access. The former considers image authenticity and the completeness of data. After PACS images have been processed, some validation mechanisms are needed to assure its accuracy, completeness, and authenticity. Data access considers who can access what type of data and when.

### **Application Software**

Once the aforementioned components are implemented in the MIII, application oriented software can be de-

signed and developed to integrate necessary components for a specific clinical, research, or education application. This provides rapid prototyping and reduces costs required for the development of every application. It is in this application layer component that the user encounters the advantages and power of the MIII.

### **Current Status**

There are hundreds of HI-PACS in operation. However the research and development of MIII is still in its infancy.

### **SUMMARY**

The method of practicing radiology has changed tremendously during the past five years. Instead of the traditional paper and film based operating method, digital based operation has gradually taken over. In this process, utilizing radiological informatics becomes increasingly critical in facilitating the image diagnostic and reporting procedures. In this respect, HI-PACS plays an important role. In addition to HI-PACS radiologists also rely on other information systems normally not in-

cluded in HI-PACS to perform their daily clinical duties. This leads to the concept of multimedia in the radiology environment. The ultimate information system in a healthcare enterprise is the Electronic Medical (Patient) Record (EMR, EPR) in which HI-PACS is a major component. In order to realize EPR, the concept of an interface engine is vital. The integrating of the healthcare enterprise (IHE) initiative is a first step towards its realization. Medical imaging informatics infrastructure design is the current concept of utilizing HI-PACS and EPR for large scale horizontal and longitudinal clinical, research, and education applications which could not be performed before due to insufficient data and knowledge. We predict that the field of radiological informatics will advance tremendously in the next several years and its derivatives will benefit the patient healthcare delivery system.

### **REFERENCES**

1. Huang HK. PACS - Basic Principles and Applications. NY: Wiley & Sons, 1999.
2. ihe@rsna.org
3. ihe@himss.org

**RSNA 2001 PRESENTATION, NOVEMBER 25-30, 2001  
Chicago, Illinois**

*Image Processing and Informatics Lab (IPI), CHLA/USC,  
Los Angeles, CA and Collaborators from St. John's Health Center;  
Santa Monica; Hong Kong; Shanghai; Poland; and Germany*

*Childrens Hospital Los Angeles  
4650 Sunset Boulevard  
Los Angeles, California 90027  
323-671-3898  
323-671-1588 FAX*

**RSNA 2001**

SUPPLEMENT TO RADIOLOGY - NOVEMBER 2001 - VOLUME 221 (P)

# SCIENTIFIC PROGRAM

THE RADIOLOGICAL SOCIETY OF NORTH AMERICA

87<sup>th</sup> SCIENTIFIC ASSEMBLY AND ANNUAL MEETING

NOVEMBER 25 - 30, 2001

MCCORMICK PLACE, CHICAGO, ILLINOIS

from  
Science

to  
Patient Care

**RSNA 2001**

RSNA



AMERICAN ASSOCIATION  
OF PHYSICISTS IN MEDICINE

## ***REFRESHER COURSES (1)***

***Course N. 525 – 8:30-10:00 am, Wednesday***

**Update Course in Diagnostic Radiology Physics: Physical Aspects of Breast Imaging-Current and Future Considerations.**

**B. Telemammography: A Technical Overview**

H. K. Huang, DSc, Los Angeles, CA (hkuang@aol.com)

**Objective:** 1) To learn the basic terminology and state-of-the-art technology used in telemammography. 2) To understand how a telemammography system works. 3) To review the image quality in telemammography. 4) To update "How to Use the Internet 2" for telemammography application.

## **SCIENTIFIC PAPERS (4)**

### **Oral Presentations (3)**

**Tuesday Morning – Room S404AB**

**622 • 11:06AM**

**PACS Simulator: A Standalone Educational Tool**

G.T. Mogel, MD, Los Angeles, CA (xrad2@alltel.net) • H.K. Huang, DSc • F. Cao, PhD • B.J. Liu, PhD • M.Z. Zhou, MD • J. Zhang, PhD

**PURPOSE:** Many educational courses have been designed for training radiologists and allied healthcare providers in learning how to operate PACS workstations. There are yet tools available for training of PACS concept and workflow analysis. We have designed and implemented a PACS Simulator for this purpose.

**METHOD AND MATERIALS:** The PACS Simulator consists of five key components simulating a typical clinical PACS: acquisition modality Simulator (AMS), DICOM gateway, PACS server (UNIX-based), two clinical viewing workstations, and network infrastructure with a 100 mbits/sec Ethernet switch connecting to all these components. A generic PACS DICOM compliant software package is used to run on these components simulating normal clinical data flow.

**RESULTS:** We have successfully used this Simulator as a standalone PACS training tool 24 hours/day, 7 days/week for four months to simulate clinical PACS operation. The AMS (Acquisition Modality Simulator) is connected to a clinical PACS and contains thousands of CT, MRI, US, CR, and digitized films examinations. These images are replenished continu-

ously through the clinical PACS connection. Image examinations are fed from AMS to the DICOM gateway continuously in loop simulating the continuous clinical environment. From there they are pushed to the PACS server for archive and workstations for review. Using this simulator, trainees can: 1. Observe clinical PACS operation, component by component, 2. Trace image flow through each component, 3. Query and retreat images from workstations and observe the image flow, 4. Review images from workstations, and 5. Induce failure in a component to observe its impact on PACS operation.

**CONCLUSIONS:** We have developed a PACS Simulator as a stand-alone tool for trainees to understand the overall PACS concept and image dataflow. It is a valuable tool for participants to appreciate the complexity of PACS data flow with hand-on experience. The next version of the PACS Simulator will be an addition of a HIS Simulator connected to the AMS and PACS server for simulating input of patient related information.

## Scientific Papers (4)

### Oral Presentations (3)

Tuesday Morning – Rm. S404AB

---

623 • 11:15AM

**Parallel Cluster for Image Processing in PACS: Clinical Experience and Research Evaluation with Functional MRI Analysis**

*S.G. Erberich, MS, Aachen, Germany (stephan.erberich@izkf.rwth-aachen.de) • M. Hoppe, MD • T. Schmidt, BSc • A. Thron, MD • W. Oberschelp, PhD*

**PURPOSE:** PACS has become a standard facility for clinical routine diagnostic. With the emerging of Computer Aided Diagnosis into the diagnostic process the demand for image processing increases. Image processing becomes unacceptable slow when very large case numbers from PACS are to be processed. Not only for clinical routine diagnostics, but as well as for research applications, one would like to have enough image processing capabilities in the PACS. We introduce a parallel cluster of standard distributed systems and its software components for large-scale image processing and how such a system can be integrated into a hospital environment. To demonstrate the cluster technique we present our clinical experience with the crucial but computational intensive motion correction of functional brain MRI (fMRI) data, as it is processed in our Lab on a daily basis.

**METHOD AND MATERIALS:** Currently we have examined over 1000 fMRI cases (~120MB per case). The 4D fMRI data (brain volumes in time) were acquired on 1.5 T Philips Gyroscan NT systems, having either 64x64 or 128x128 slice matrices from Gradient Echo Planar Imaging sequences (TR500-4000, FA60-90, RFOV 192-256, 15-45 slices). The parallel cluster consists of a 48 processor distributed system (24 dual 500 MHz Pentium-III PCs running Linux connected in an isolated 100Mbits switched network). Parallel execution is carried out by motion correction of one volume per processor. We used PVM library for load balancing and client communications. Run-time of 200 randomly selected cases was compared with a 64Bit 450 MHz SUN Ultra80 Solaris8.0 workstation.

**RESULTS:** Using the cluster the average overall runtime for the motion correction dropped by the factor of 41,3 (91% linearity). A single fMRI case which needs 20 hours on a single workstation is processed in only 30 minutes on the cluster. We observed, that the optimal load/cost ratio depends on the problems dimensions - higher dimensions results in a better performance, because of the finer granularity of the cluster's processor mesh.

**CONCLUSIONS:** We introduced a cluster technique for the PACS to solve large scale image processing problems in only a fraction of the usual run-time. The design of the parallel cluster is hot-swappable and fault-tolerant due to massive redundancy. Each single system of the cluster can take over a failed system which can be replaced while the cluster is online. Also the cluster is cost-efficient and scalable compared to workstations. Common clinical data processing, like image processing or data mining can be implemented.

Scientific Papers (4)  
Oral Presentations (3)

---

Wednesday

Rm. 2401AB

1156 • 2:39PM

Model Independent Analysis of Functional MRI Time-series by Self-organizing Map Neural Network

S.G. Erberich, MS, Aachen, Germany (stephan.erberich@izk.rwth-aachen.de) • M. Liebert, Dipl Phys • K. Willmes, PhD • A. Thron, MD • W. Oderschelp, PhD

**PURPOSE:** Functional MRI has become a common method to study task induced brain activation. Using rapid Echo Planar Imaging one can obtain a higher MR-Signal under a task condition close by activated regions as a result of susceptibility changes in blood oxygenation (BOLD effect). The purpose of this paper is to introduce a new model independent method, based on an artificial neural network - the self-organizing map (SOM) - to distinguish between brain regions of activation, deactivation and baseline. Features from the hemodynamic response functions (HRF) for each voxel are learned by their similarity. The pattern-to-voxel mapping is superimposed on an anatomical or EPI image of the subject for task evaluation.

**METHOD AND MATERIALS:** We used 30 fMRI epochs and event-related experiments including motor, sensory, visual and language tasks of subjects (age 20-40). Imaging was done on a Philips ACS NT 1.5T MR covering the whole brain using single-shot EPI. After motion correction and segmenting the brain tissue, the brain tissue voxels were spatially and temporal smoothed with a Gauss filter. To reduce the number of baseline voxel, we selected voxels being affected by the task using auto-correlation and F-test statistics. The selected voxel time-series were used for the training of the SOM. Event-related data was temporally sorted for each event and fitted to the theoretical HRF averaging all event samplings. 4x6 neuron maps for whole brain and 4x3 neuron maps for slice training was used. The results were compared with SPM99 general linear model approach.

**RESULTS:** The SOM separated activation, deactivation and baseline in adjacent neurons of map. Differentiation of task induced voxels could be accomplished from the neuron pattern reference vectors, build through the data-driven learning process. Besides patterns with strong correlation to the box-car paradigm or for event-related data with the HRF function, we found neurons carrying information of the fading BOLD effect in the surrounding of region of activation or deactivation.

**CONCLUSIONS:** Box-car or temporally sorted and fitted event-related responses can be differentiated by the neural net SOM method. The mechanism of feature separation based on the pattern of the time-series can be achieved without using a hemodynamic response model. The advantage of the data-driven SOM approach is, that it can not only depict activation or deactivation patterns, but although gives additional information of the intensity, the temporal shape and the regional extend of the hemodynamic response for a certain region.

## **Poster Sessions (1)**

---

### **Scientific Poster Viewing Hours**

**Lakeside Center, Level 3, Hall D**

**Sunday, 8:00 am-6:00 pm**

**Monday-Thursday, 7:00 am -10:00 pm**

**Friday, 7:00 am-12:45 pm**

#### **076GM-p • Tuesday • 12:00 PM**

##### **A PACS and Image Informatics Training**

*M.Y. Law, MPhil, Kowloon, Hong Kong • F.H. Tang, MPhil • F. Cao, PhD*

**PURPOSE:** Hong Kong healthcare delivery system is 92 % public with 44 hospitals and 8 % private. The former is under the auspices of the Hong Kong Hospital Authority (HKHA). HKHA is in the process of designing and implementing EPR (electronic patient record) and PACS to all its hospitals during the next five years. The Hong Kong Polytechnic University is the only education entity in Hong Kong providing training for radiological technologists and radiation therapists to supply the required human resource. For this reason, we have designed and implemented a PACS with image informatics infrastructure to educate the professionals and the trainees alike to prepare for the arrival of this new technology era. The implementation of the infrastructure is made possible through the support from the University resources, collaboration with laboratories in the world, and contributions from manufacturers. The purpose of this presentation is to describe our experience in establishing this training.

**METHOD AND MATERIALS:** The infrastructure consists of three laboratories: Radiology Modality Lab, PACS Lab, and Image Management Lab; connected by a 100 mbits/s intranet. The Modality Lab has 3 US scanners, one Mammography unit, one CR, and two film digitizers; all are connected to the PACS Lab with DICOM acquisition gateways. The PACS Lab has one PACS consisting of a UNIX PACS Controller and archive server, and multi-monitor workstations. The PACS controller distributes images to eight workstations in the Image Management Lab for hands-on training. The PACS Lab also connects to the University Clinic for case review and a nearby 1,800-bed public hospital for CT and MR examination input.

**RESULTS:** This infrastructure has been open for training since December 2000. It provides an environment for a basic understanding of PACS and informatics, workflow and dataflow studies and hands-on live on-site debugging and service training. The trainees can observe and play step-by-step with the PACS operation in vivo. This presentation will detail the architecture of the infrastructure, training protocols, and preliminary training experience learned.

**CONCLUSIONS:** We have developed a laboratory PACS with imaging informatics infrastructure in a laboratory environment. We believe that hands-on experience without the fear of interrupting clinical PACS operation will enhance trainee's understanding during the training process. (M.L. Research received support from TEDPC Corp., Shanghai Institute of Technical Physics, Chinese Academy of Sciences, Array Corporation, Children Hospital Los Angeles/University of SC, Hong Kong Polytechnic University.)

## **EDUCATION EXHIBITS (4)**

---

**Lakeside Center, Level 3, Hall D**

**Sunday, 8:00 am -6:00 pm**

**Monday through Thursday 7:00 am – 10:00 pm**

**Friday, 7:00 am – 12:45 pm**

### **0664PH-e**

**PACS Archive Upgrade and Data Migration: Clinical Experiences**

*B.J. Liu, PhD, Torrance, CA (Brent.Liu@stjohns.org) • L. Documet • D.A. Sarti, MD • H.K. Huang, DSc • J. Donnelly*

**LEARNING OBJECTIVES:** Report on a clinical and technical process template for upgrading/expanding the PACS archive, migrating current PACS image data to the new archive, and providing a secondary backup for disaster recovery. In addition, report on the pitfalls involved during the process. (Siemens provides support for PACS Implementation.)

### **0529PD-e**

**Digital Hand Atlas and Web-based Bone Age Assessment**

*F. Cao, PhD, Los Angeles, CA (fcao@pacbell.net) • H.K. Huang, DSc • E. Pieltka, PhD • V. Gilsanz, MD, PhD • P.S. Day, BS*

**LEARNING OBJECTIVES:** • Learn the design and implementation methods for the digital hand atlas. • Assess current technologies and their applications in hand image database, display and processing. • Understand Web-based bone age assessment.

### **0681PH-e**

**Building a Teaching Server Out of the PACS**

*M.Y. Law, MPhil, Kowloon, Hong Kong (ormaria@polyu.edu.hk) • F.H. Tang, MPhil • F. Cao, PhD*

**LEARNING OBJECTIVES:** 1. PACS and Informatics Infrastructure for education. 2. Technicality in building teaching servers. 3. Categorization of teaching files. (Equipment was provided by TEDPC Corp, Taiwan, ROC. Software was provided by the Shanghai Institute of Technical Physics, Chinese Academy of Sciences.)

### **0644PH-e**

**PACS Simulator: A Standalone Educational Tool**

*H.K. Huang, DSc, Los Angeles, CA (hkuang@aol.com) • F. Cao, PhD • B.J. Liu, PhD • M.Z. Zhou, MD • J. Zhang, PhD • G.T. Mogel, MD*

**LEARNING OBJECTIVES:** 1. To understand the basic architecture of a PACS system. 2. To learn the connectivity of PACS components. 3. To see all basic PACS components in one exhibit. 4. To observe PACS dataflow. 5. To get hands-on experience of DICOM Query/Retrieve and observe image movement through PACS components.

## **InfoRAD EXHIBITS (4)**

---

**Demonstration Area: Lakeside Center, Level 3, Hall D**

**Sunday through Thursday, 8:00 am-5:00 pm**

**Friday, 8:00 am-12:45 pm**

### **9114DS-I**

**Computer-assisted Atlas Matching Assessment of Skeletal Maturity**  
*E. Pietka, PhD, Gliwice, Poland • A. Gertych, MS • S. Kurkowska-Pospiech, MS  
• F. Cao, PhD • H.K. Huang, DSc • V. Gilsanz, MD, PhD*

Assessment of skeletal development is frequently performed in pediatric patients to evaluate their growth. The most common assessment method is the image (or region) matching by visually comparing a hand radiograph with a film-based hand atlas. We have developed a computer-assisted method to automatically match a patient image with a digital hand atlas. The digital method is based on bony features extracted from hand radiographs. The extracted features include the size of epiphyses and metaphyses, the shape at the bone periphery, and the parameters describing the stage of epiphyseal fusion. The standard images of normal children along with their extracted features are organized into a hand atlas database. When a clinical image is analyzed, its features are extracted and then compared with the atlas database to find the closest matched image for a radiologist approval. This exhibit will demonstrate various stages of the computer-assisted image analysis and matching process.

**LEARNING OBJECTIVES:** Interactive hand image analysis and manipulation · Interactive extraction of quantitative features describing developmental stage of bones · Automatic matching of a hand image with atlas database

### **9617PACS-I**

**A Fault-tolerant Back-up Archive Using an ASP Model for Disaster Recovery**

*B.J. Liu, PhD, Torrance, CA • H.K. Huang, DSc • F. Cao, PhD • L. Documet • D.A. Sarti, MD*

A single point of failure in PACS during a disaster scenario is the main archive storage and server. When a major disaster occurs, it is possible to lose an entire hospital's PACS data. Some current PACS systems do have a minimal disaster recovery design with limitations in terms of how frequent a back-up is performed and the operational costs associated to maintain the back-up. A novel approach towards providing a short-term, automatic, fault-tolerant solution for disaster recovery of PACS data based on the Application Service Provider model is demonstrated. A fault-tolerant back-up archive server and storage device is implemented offsite from the main PACS archive. Clinical data from a hospital PACS is sent to this ASP storage server in parallel to the exams being archived in the main server. A disaster scenario was simulated and the PACS exams were sent from the offsite ASP storage server back to the main PACS for recovery. Initially, connectivity between the main archive and the ASP storage server is established via a T-1 connection. In the future, other more cost-effective means of connectivity will be researched such as the Next Generation Internet (NGI).

**LEARNING OBJECTIVES:** 1. Investigate an offsite PACS archive storage solution that can be used for instantaneous back-up and retrieval of clinical PACS exams during a disaster scenario. 2. Learn how to perform a disaster recovery procedure for PACS image data.

## ***InfoRAD EXHIBITS (4)***

***Demonstration Area: Lakeside Center, Level 3, Hall D***

***Sunday through Thursday, 8:00 am-5:00 pm***

***Friday, 8:00 am-12:45 pm***

### **9504NT-1**

#### **Fault-tolerant PACS Server**

***F. Cao, PhD, Los Angeles, CA • H.K. Huang, DSc • B.J. Liu, PhD • M.Z. Zhou, MD • J. Zhang, PhD • G.T. Mogel, MD***

Failure of PACS archive server would cripple the entire PACS operation. Last year we demonstrated in infoRAD that it was possible to design a fault-tolerant (FT) server with 99.999% up time. The FT design was based on a triple modular redundancy with a simple majority vote to automatically detect and mask a faulty module. The FT server runs uninterrupted with no downtime or data loss should any hardware component fail. The purpose of this presentation is to report on its continuous development. A FT PACS Simulator with generic PACS software will be used for the demonstration. The PACS Simulator consists of an acquisition modality simulator (AMS), a DICOM acquisition gateway, a FT PACS server, and two workstations. The AMS has over 2,000 image examinations looping continuously to the DICOM gateway to simulate image acquisition. To simulate PACS clinical operation image examinations are transmitted continuously from the AMS to the DICOM gateway then to both the FT server and workstations. Participants will be allowed to manually induce failures to Ethernet, CPU module, and hard disk, and observe the failover recovery of the FT PACS to resume its normal data flow.

**LEARNING OBJECTIVES:** 1. Fault-tolerant concept of the PACS server 2. How the entire PACS fails when a component is down 3. Failover stages of the FT server during system fail 4. How the system recovers during failover 5. How PACS data flow resumes after failover recovery

### **9503NT-1**

#### **Automatic Monitoring System for PACS Operation**

***J. Zhang, PhD, Shanghai, People's Rep of China • R. Han, MS • D. Wu • X. Zhang • J. Zhuang • H.K. Huang, DSc***

Many interrelated processes are running simultaneously in PACS components. Chances of any of these processes failing at any given period of time are high. When it happens, immediate attention and service is required for the PACS to resume its normal operation. Current PACS application software has only limited monitoring functions to alert the PACS manager should any of these processes fail. For this reason, a large team is required to maintain a smooth PACS operation resulting in increasing the total cost of ownership (TCO). We have developed an automatic PACS operation monitoring system (OMS) based on the concept of API (Application Programming Interface) to alert the manager timely of any process failure in the PACS operation. The PACS OMS consists of two parts: monitoring agents and a Monitor Server. Monitoring agents are connected to all PACS processes running in each PACS component. The Monitor Server monitors each agent that allows the server to track the status of individual PACS process. We have installed the OMS on top of an existing PACS in a 800 bed hospital. The PACS manager can monitor the entire PACS operation from the remote Monitor Server.

**LEARNING OBJECTIVES:** 1. Concept of API 2. Concept of automatic PACS operation monitoring 3. Monitor and control the entire PACS

**A Fault-Tolerant Back-up Archive Using an ASP Model for Disaster Recovery**

*Brent J. Liu, Torrance, CA • Dennis Sarti • Luis Documet • Fei Cao • H.K. Huang*

**Learning Objectives:**

Investigate an offsite PACS archive storage solution that can be used for instantaneous back-up and retrieval of clinical PACS exams during a disaster scenario

**Abstract:** A single point of failure in PACS during a disaster scenario is the main archive storage and server. When a major disaster occurs, it is possible to lose an entire hospital's PACS data. Some current PAC systems do have a minimal disaster recovery design with limitations in terms of how frequent a back-up is performed and the operational costs associated to maintain the back-up. A novel approach towards providing a short-term, automatic, fault-tolerant solution for disaster recovery of PACS data based on the Application Service Provider model is demonstrated. A fault-tolerant back-up archive server and storage device is implemented offsite from the main PACS archive. Clinical data from a hospital PACS is sent to this ASP storage server in parallel to the exams being archived in the main server. A disaster scenario was simulated and the PACS exams were sent from the offsite ASP storage server back to the main PACS for recovery. Initially, connectivity between the main archive and the ASP storage server is established via a T-1 connection. In the future, other more cost-effective means of connectivity will be researched such as the Next Generation Internet (NGI).

## Info RAD Theater schedules (4):

---

- **November 25, Theater 2** **12:30pm**  
**Computer-assisted Atlas matching Assessment of Skeletal Maturity**  
*Arkadiusz Gertych, M.S.*
- **November 28, Theater 2** **10:30am**  
**A Fault-Tolerant Back-up Archive Using an ASP Model for Disaster Recovery**  
*Brent Liu, Ph.D.*
- **November 29, Theater 1** **8:00am**  
**Fault Tolerance PACS Server**  
*F. Cao, Ph.D. and Brent Liu, Ph.D.*
- **November 29, Theater 2** **8:00am**  
**Automatic Monitoring System for PACS Operation**  
*Jianguo Zhang, Ph.D.*